Assessments for Arterial Toxicity in Patients Receiving Systemic Anti-Cancer Therapies

Dr Stephen Henry Rankin

BMSc (Hons), MBChB, MRCP(UK)

Submitted in fulfilment of the requirements of the degree of Doctor of Philosophy

School of Cardiovascular and Medical Health,
College of Medical, Veterinary and Life Sciences

Faculty of Medicine

University of Glasgow

August 2025

Abstract

Cardiovascular (CV) toxicity is a recognised complication of numerous anticancer treatment regimens. Many cancer therapies may be associated with arterial injury. The mechanism underlying arterial toxicity from cancer treatment is not well understood and the risk may be underappreciated. Immune checkpoint inhibitors (ICI) are an effective anticancer therapy that may be associated with atherothrombotic events such as myocardial infarction (MI) and ischaemic stroke. It is proposed that ICIs induce T-cell infiltration into plaque leading to inflammatory atheroma and plaque rupture. ICIs are used in combination with vascular endothelial growth factor inhibitors (VEGFI). VEGFI alone are associated with hypertension, heart failure and MI. It is unclear if the combination of drug classes has an additive effect on atherothrombosis and ischaemic events. ICI-associated atherothrombosis is supported by basic science and observational retrospective studies. This association has not been observed in randomised clinical trials. Trial design within oncological studies may not be suitable to adequately capture CV events and trial participants may not be representative of the population seen in clinical practice. The true risk, if any, of ischaemic events with ICI is not yet known.

Inflammation plays a role in the development of numerous CV conditions and may be relevant in arterial toxicity from anticancer treatments. While cardiotoxicity is a well-known side effect of anthracyclines, they are also associated with arterial injury. Inflammation is implicated in development of anthracycline cardiotoxicity but the role of inflammation in anthracycline associated arterial injury is not yet known.

Fluorodeoxyglucose positron emission tomography computed tomography [^{18}F]FDG-PETCT is a metabolic imaging technique used for assessment of arterial inflammation and is a surrogate marker of inflammatory atheroma. Quantitative assessment of arterial uptake is performed using the maximal tissue-to-background ratio (TBRmax). Inflammation assessment should be performed using specific imaging parameters. The European Association of Nuclear Medicine (EANM) provided recommendations on how PET protocols should be performed in 2016. However, these recommendations may be out of date with the advances in PET technology, such as the advent of digital PET scanners. The optimal

parameters for assessment of arterial inflammation by contemporary digital PET scanners are not well-defined, nor are methods for comparing one PET-CT protocol to another.

[^{18}F]FDG-PETCT may offer mechanistic insight into the possible association of ICI and ischaemic events. [^{18}F]FDG-PETCT assessment of ICI associated arterial inflammation has been previously assessed in small retrospective studies with conflicting results. There have been no prospective studies. No study has assessed the potential additive effect of VEGFI combined with ICI on arterial inflammation.

Aims

The aims of my thesis were: 1) to assess how trial eligibility criteria and CV adverse event (CVAE) reporting may impair the ability to capture CV safety data in ICI+VEGFI combination therapy trials; 2) to assess whether anthracycline exposure is associated with large artery inflammation, measured by [^{18}F]FDG-PETCT, in a retrospective analysis of a cohort of patients with lymphoma; 3) to compare current international recommendations for imaging protocols for arterial assessment by [^{18}F]FDG-PETCT in comparison to a locally optimised protocol; 4) to make a prospective assessment of the effect of ICI on arterial inflammatory activity, and; 5) to compare arterial inflammatory effects in patients receiving ICI+VEGFI versus ICI monotherapy and VEGFI monotherapy.

Methods

A systematic review of randomised controlled trials of combination ICI+VEGFI therapy was performed. I assessed data relating to trial eligibility criteria and CVAE reporting. I subsequently performed a retrospective analysis of clinically indicated [^{18}F]FDG-PETCT scans to compare large artery inflammation before and after completion of anthracycline-based chemotherapy. A locally optimised PET imaging protocol was designed and compared with EANM recommendations for arterial inflammation assessment in order to inform the design of my prospective PET-CT study. Novel metrics to quantifiably compare imaging protocols were used for assessment, such as mean contrast recovery (MCR), coefficient of variation (CoV), and error. A prospective observational study of

patients with cancer receiving either VEGFI, ICI or ICI+VEGFI was performed. Arterial inflammation was assessed using [^{18}F]FDG-PETCT before and after 24-weeks of therapy. The primary outcome was the change in TBRmax at 24-weeks from baseline in ICI+VEGFI vs monotherapy. Biomarker analyses were also performed.

Results

In the review of 17 trials with 10,313 participants, there was broad CV eligibility criteria using heterogenous definitions of CV disease. No trial published baseline CV characteristics of participants. Reporting of CVAE was inconsistent and subject to incidence thresholds. No trial reported the absence of CVAEs. In 16 trials, AEs were investigator reported without centralised adjudication.

I observed no change in arterial [^{18}F]FDG uptake in patients with lymphoma treated with anthracycline chemotherapy, compared with pre-treatment scans.

Current international recommendations for arterial inflammation assessment by [^{18}F]FDG-PETCT are not applicable to modern digital PETCT scanners. Fewer reconstruction parameters (iterations and subsets) are required for optimal imaging, than recommended by EANM.

In the first prospective study of ICI and large artery inflammation, 55 patients were enrolled (VEGF: n=15; ICI: n=20; VEGFI+ICI: n=20), mean age was 66±10 years, 29% female. CV risk factors were highly prevalent and comparable in all groups. Compared to pre-treatment, at 24 weeks TBRmax had not increased in any group (baseline vs 24 weeks, VEGFI: 1.72±0.2 vs 1.72+0.2; ICI: 1.71±0.1 vs 1.67±0.1; VEGFI+ICI: 1.74±0.2 vs 1.64±0.2). There was no difference in the change of TBRmax over time between groups (p=0.13). The results were consistent when accounting for potential heterogeneity, including clinical characteristics (such as pre-existing CV disease) and arterial characteristics (such as calcification vs none).

Conclusion

Arterial toxicity from anticancer therapies is poorly understood and limitations within oncological efficacy trials impairs accurate capture and quantification of CV toxicity in ICI+VEGFI regimens. The heterogeneity in defining and reporting CVAE, in a population where prevalence of CV disease is unknown, limits understanding of the incidence and severity of events relating to these combinations. [^{18}F]FDG-PETCT analysis did not reveal an association between anthracycline exposure and large artery inflammation. If anthracyclines are associated with arterial injury, this could occur through a non-inflammatory process. Current international recommendations for assessment of large artery inflammation by [^{18}F]FDG-PETCT are not applicable to modern digital PET scanners but metrics, such as MCR, CoV and error, are valuable methods to quantifiably compare imaging protocols. When assessed in a prospective study, ICI exposure was not associated with large artery inflammation, when assessed by [^{18}F]FDG-PETCT, compared to baseline, when used alone or in combination with VEGFI.

Standardisation within the design and reporting of randomised clinical trials and mechanistic PET research are required to truly elucidate the potential association, between ICIs and atherothrombotic events before risk stratification and therapeutic strategies can be developed.

Table of Contents

List of Tables

List of Figures

Publications relating to this work

Rankin S, Gemmell AJ, McClure J, Venugopal B, Slomka PJ, Petrie MC, et al. Image reconstruction and analysis of atherosclerosis imaging by [18F]FDG PETCT using digital PET technology. Eur J Nucl Med Mol Imaging. 2025 Jun 14;

Rankin S, Fountain C, Gemmell AJ, Quinn D, Henderson A, McClure J, et al. Arterial effects of anthracycline: structural and inflammatory assessments in non-human primates and lymphoma patients. Clin Sci (Lond). 2025 Jan 15;139(1):29–41.

Rankin S, Elyan B, Jones R, Venugopal B, Mark PB, Lees JS, et al. Cardiovascular Eligibility Criteria and Adverse Event Reporting in Combined Immune Checkpoint and VEGF Inhibitor Trials. JACC: CardioOncology. 2024;6(2):267–79.

Henriksen PA, **Rankin S**, Lang NN. Cardioprotection in Patients at High Risk of Anthracycline-Induced Cardiotoxicity. JACC: CardioOncology. 2023 Jun;5(3):292–7.

Elyan BMP, **Rankin S**, Jones R, Lang NN, Mark PB, Lees JS. Kidney Disease Patient Representation in Trials of Combination Therapy With VEGF-Signaling Pathway Inhibitors and Immune Checkpoint Inhibitors: A Systematic Review. Kidney Medicine. 2023 Jul;5(7):100672.

Presentations relating to this work

Young Investigator Award (Finalist) at Global Cardio Oncology Summit 2025, Cape Town, October 2025.

Biomarker and Imaging Characterisation of Inflammatory Atheroma in Patients Receiving Immunotherapy and Angiogenesis Inhibitors (BIOCAPRI Study). ESC Congress 2025. Madrid. August 2025

Image reconstruction and analysis of atherosclerosis imaging by [18F]FDG PETCT using digital PET technology. British Nuclear Medical Society. Glasgow, UK, May 2025

Arterial effects of anthracycline: structural and inflammatory assessments in non-human primates and lymphoma patients. ESC Congress 2024. London, August 2024

Case Based Discussion: Use of Dexrazoxane" Presented at the Cardio-oncology MDT at BCS 2024. Manchester. June 2024

Oral presentation: 'Inflammatory Atheroma in patients receiving cancer treatment'. DC Academy International Summit on Clinical Research in Heart Failure. April 2024.

Case Based Discussion: 'ICI-myocarditis' : CV disease & multimorbidity. Royal College of Physicians of Glasgow's Interactive Cardiology Conference, Glasgow. March 2023

Cardiovascular Eligibility Criteria and adverse event reporting in cancer therapy of combined immune checkpoint and VEGF inhibitors. GCOS, Madrid, September 2023

Acknowledgement

I would like to thank my supervisors, Professor Ninian Lang, Professor Mark Petrie and Dr Balaji Venugopal for their constant unwavering support throughout this period in my life. They have given me inspiration and drive throughout the project and without each of their contributions, I would not have been able to complete this thesis. Their guidance and support have extended beyond just academic work and for that I am forever grateful.

I would like to thank Roche Diagnostics for funding this project and my role as a Clinical Research Fellow with The University of Glasgow. I would also like to thank them for the collaborative attitude relating to this project.

I am extremely grateful to the staff and team within the Beatson West of Scotland Cancer Centre, including all the staff in the Clinical Research Unit, Anthony Cunningham in the echocardiography department and the support staff in clinic areas including Fiona, Victoria and Christine. I would also like to thank the team in Glasgow Biomarker laboratory, particularly Paul Welsh and Elaine Butler, for their help and hard work.

Success in completing these clinical studies would not be possible without the enthusiastic involvement by the medical oncology staff, particularly Dr Balaji Venugopal, Dr Manreet Randhawa, Dr Sarah Slater, Prof Rob Jones, Professor Jeff Evans, Dr Gregory Naylor, Prof Richard Wilson, Dr Kathryn Graham, Dr Sharon Armstrong, Dr Ashita Waterston and Dr Pavlina Spiliopoulou. I am extremely grateful to them for supporting me and this project with recruitment. I would like to thank Dr Pam McKay and Dr Giselle Melendez for their support and guidance through the additional projects carried out in this thesis. I would like to extend this thanks to the clinical nurse specialists, Nicola Thomson and Megan Wilson, and pharmacists in the renal team, Gillian Barmack and Jennifer Laskey.

This thesis would not be possible without the hard work, support and enthusiasm from the team at the West of Scotland PET Centre. Prof Dave Colville, Dr Sandy Small and Mr Alastair Gemmell were instrumental in this project being a success and helped me all the way through the steep learning curve of PET imaging. I am

extremely grateful for everything they have taught me and supported me through. I would also like to thank the rest of the staff in the PET Centre, particularly Ana Matos and Nick Gulliver, PET imaging Service managers, and Carole Maxfield, Emily Routamaa and Mairi Bending.

I would like to thank the participants of the study, without whom, this thesis would not be possible. They selflessly gave me, and this study, their precious time and energy. For that, I am forever indebted.

This thesis is dedicated to my family. I would not have been able to complete this thesis without the unwavering support and strength from my wife, Sarah, whose patience, kindness and support was ever-present. Finally, I would like to thank my two boys, Calum and Dougie, for the patience during the weekends and evenings with 'Working Dad' and without whom, working from home would have been a lot more productive, but a lot less fun.

Author's Declaration

The work presented in this thesis was performed during my employment as a Clinical Research Fellow in the School of Cardiometabolic Health at the BHF Glasgow Cardiovascular Research Centre, University of Glasgow. I was supervised by Professor Ninian Lang, Professor Mark Petrie and Dr Balaji Venugopal.

I helped develop the study protocol and obtained regulatory and ethical approval. I performed the screening and recruitment, including obtaining informed consent of all patients in the study. I performed all the study visits.

I organised all investigations in the study. A clinical report for the PET scans were provided by Prof Dave Colville. I was responsible for the results of these clinical reports and organised a management plan, in conjunction with the clinical team, for any clinical relevant finding. Analysis of these scans were performed blinded by myself under supervision of Prof Dave Colville. Echocardiography was performed by myself and the echocardiography team, mainly by Anthony Cunningham. Biomarker analysis was performed by the Staff of the Glasgow Biomarker Laboratory in the Institute of Cardiovascular and medical Sciences at the BHF Glasgow Cardiovascular Research Centre, University of Glasgow under the supervision of Paul Welsh and Elaine Butler. Statistical analyses were performed by me under supervision of Dr John McClure and Dr Alasdair Henderson. PET phantom analysis was performed by Mr Alastair Gemmell under supervision of Dr Sandy Small. Histopathological analysis was performed by Miss Caitlin Fountain, under the supervision of Dr Giselle Melendez.

I confirm that this thesis has been composed solely by me and that is has not been submitted for any other degree at the University of Glasgow or any other institution. The writing of this thesis is entirely my own work, and all sources of information within this thesis have been specifically acknowledged.

Abbreviations

ACE – angiotensin converting enzyme
ACS – acute coronary syndrome
AE – adverse event
AEOSI – adverse event of special interest
AGM – African Green monkey
ANOVA – analysis of variance
ApoA – apolipoprotein A
ApoB - apolipoprotein B
ARB – angiotensin receptor blocker
ARSAC – Administration of Radioactive Substance Advisory Committee
ASCVD – atherosclerotic cardiovascular disease.
BP – blood pressure
BSA – body surface area
BWoSCC – Beatson West of Scotland Cancer Centre
BMI – body mass index
BNF – Biritish National Formulery
CABG – coronary artery bypass grafting
CAD – coronary artery disease
CCB – calcium channel blocker
CD – cluster of differentiation
CI – confidence interval
CKD – chronic kidney disease
CRF – case report form
CTCAE - Common terminology criteria for adverse events
CTL – control
CoV – coefficient of variation
CV – cardiovascular
CVF – Collagen volume fraction
CV-AEOSI – cardiovascular adverse event of special interest
CVA – cerebrovascular accident
CVAE – cardiovascular adverse event
CVD – cardiovascular disease
CT – computed tomography
CTLA4 – cytotoxic T-lymphocyte associated protein-4
DLBCL – diffuse large B-cell lymphoma
Dox – doxorubicin
DOAC – direct oral anticoagulant
DVT – deep vein thrombosis
EANM – European Association of Nuclear Medicine
ECG - electrocardiogram
Echo - echocardiogram
ELISA – enzyme-linked immunosorbent assay
ESC – European Society of Cardiology

ET1 – endothelin-1
FAERS – Food & Drug Administration adverse event reporting system
FAPI – fibroblast activation protein inhibitor
FRS – Framingham risk score
FDA – Food & Drug Administration
[^{18}F] – 18-fluorine
[^{18}F]FDG - fluorodeoxyglucose
[^{18}F]FDGPETCT – fluorodeoxyglucose positron emission tomography
GDPR – General Data Protection regulation
GLUT – glucose transporter
GDF15 – growth differentiation factor 15
HDL c – high density lipoprotein cholesterol
H&E – haematoxylin and eosin
HF – heart failure
HIV – human immunodeficiency virus
HTN - hypertension
HR – hazard ratio
hsTnT – high sensitivity troponin T
hsCRP – high sensitivity C-reactive protein
i – iterations
ID – identification
ICC – interclass correlation coefficient
ICD – Internation Classification of Disease
ICI – immune checkpoint inhibitor
ICAM-1 – intracellular adhesion molecule 1
IHD – ischaemic heart disease
IL – interleukin
irAE – immune related adverse event
ICOS – International Cardio-oncology Society
IN – innominate vein
IJ – internal jugular vein
IQR – interquartile range
IVC – inferior vena cava
LAG3 – lymphocyte activator gene 3
LDLR – low density lipoprotein receptor
LDL – low density lipoprotein
Lp(a) – lipoprotein(a)
LV – left ventricle
LVEF – left ventricular systolic dysfunction
LOA – limits of agreement
mAB – monoclonal antibody
MACE – major adverse cardiovascular event
MCR – mean contrast recovery
MDS – most diseased segment
MHC – major histocompatibility complex
MPO - myeloperioxidase

MI – myocardial infarction
NaF – sodium fluoride
NIH – National Institute of health
NHS – National Health Service
NHP – non-human primate
NTproBNP – N-terminal pro-B-type natriuretic peptide
NO – nitric oxide
NYHA – New York Health Association
OR – odds ratio
OSEM – ordered subset expectation maximisation
PAI-1- plasminogen activator inhibitor-1
PD1 – programmed death-1
PDL1 – programmed death ligand 1
PE – pulmonary embolism
PET – positron emission tomography
PICO – Population, Intervention, Comparison, Outcome
PPES – palmar-plantar erythrodysaesthesia
PRES – posterior reversible encephalopathy syndrome
PRISMA – Preferred Reporting Items for Systematic Reviews and Meta-analyses
PSF – point spread function
PSCK9 – proprotein convertase subtilisin/kexin 9
PVE – partial volume error
REC – regional ethics committee
ROI – region of interest
s - subsets
SACT – systemic anticancer therapy
SiPM – silicone photomultiplier
R-CHOP – rituximab, cyclophosphamide, doxorubicin, vincristine, prednisolone
R-CODOC-M – rituximab, cyclophosphamide, cytarabine, vincristine, doxorubicin, methotrexate, ifosfamide, etoposide, cytarabine
RC – recovery coefficient
RCC – renal cell carcinoma
RCT – randomised controlled trial
RR – relative risk
SD – standard deviation
SUV – standardised uptake value
SVC – superior vena cava
TBR – tissue to background ratio
TCR – T-cell receptor
TGFβ - tissue growth factor β
TIA – transient ischaemic attack
TK – tyrosine kinase
TKI – tyrosine kinase inhibitor
TNF α - tumour necrosis factor α
TOF – time of flight
tPA - tissue plasminogen activator

trAE – treatment related adverse event
VAP – vascular access port
VCAM1 – vascular cell adhesion molecule-1
VEGF – vascular endothelial growth factor
VEGFI – vascular endothelial growth factor inhibitor
VEGFR – vascular endothelial growth factor receptor
VOI – volume of interest
VTE – venous thromboembolism
WHO – World Health Organisation

Chapter 1 Introduction

1.1 Cardio-Oncology

Cardio-oncology is a sub-speciality of cardiology which focuses on the assessment and management of patients with both cancer and cardiovascular (CV) disease (CVD). This encompasses both the management of pre-existing CVD and of CV toxic effects of anticancer therapy[1].

The sub-speciality of cardio-oncology originated from the management of patients who developed heart failure (HF) as a result of anthracycline chemotherapy, a common systemic anticancer therapy (SACT). Thirty years ago, CV toxicity and HF were considered an accepted risk with anthracycline use, when the outlook from a cancer perspective was so poor. With advances in cancer management and improvements in cancer survival, the accepted level of CV risk from cancer therapies has changed. Approximately 50% of patients with a diagnosis of cancer of all types will now survive at least ten years[2], so identifying and minimising CV burden in patients with cancer is of extreme importance.

Cardio-oncology has moved from dealing with CV consequences of SACT, years after it was given, to focussing on early recognition and treatment of CV consequences, as well as prevention strategies. This has been possible as our understanding of CV toxicity has increased. While HF and left ventricular systolic dysfunction (LVSD) was previously the focus, there is now an appreciation that CV toxicity extends to all aspects of cardiology, including hypertension, arrhythmias and ischaemic events, Table 1-1. Understanding how CV toxicity occurs allows clinicians to identify those at risk and develop preventative, surveillance and treatment strategies.

Table 1-1 CV adverse events associated with SACT, adapted from the European Society of Cardiology Cardio-Oncology guidelines[1]

Drug class	Example	HTN	HF	QTc	Arrhythmia	VTE	Ischaemia	Other
Alkylating agents	Cisplatin, cyclophosphamide, mephalan	+++	++		+++	++	++++	nephrotoxicity
Alk inhibitors	Alectinib, lorlatinib	++++		+++	++			dyslipidaemia
GnRH agonist	Goserelin	+	+++	+			+++	
GnRH antagonist	Degarelix	++	+		++		+	
Androgen deprivation therapy	Apalutamide	++++	+++	+				
Androgen inhibitor	Abiraterone	++++	+++	+	+++		+++	
Anthracyclines	Doxorubicin, epirubicin		+++					
Antimetabolites	5-Fluorouracil						++++	vasospasm
Aromatase inhibitors	Letrozole, exemestane	++	+				+++	dyslipidaemia
BCR-ABL TKI	Ponatinib, Dasatinib, bosutinib	++++	++		++++		+++	Pleural effusion, pulmonary hypertension, dyslipidaemia
BRAF/MEK inhibitors	Dabrafenib, encorafenib, binimetinib, trametinib	++++	+++	+++	+++	+++		bleeding
EGFR inhibitors	Osimertinib		+++	++	++	+++		
HER2-targeted therapies	Trastuzumab		++++					
Immune checkpoint inhibitors	Pembrolizumab, ipilimumab, nivolumab							myocarditis
Immuno-modulatory drugs	Lenalidomide, pomalidomide, thalidomide	++	+++	+++	+++	++++	+++	

Myeloma mAb	Daratumumab, elotuzumab	++++			+++	++		
Proteasome inhibitors	Bortezomib, carfilzomib	++++	+++	+++			++	Pulmonary hypertension
VEGFI (mAb)	Aflibercept	++++	+++			++++	++	
VEGFI (TKI)	Axitinib, lenvatinib, sunitinib	++++	+++	+++		+++	++	
+ rare (<0.1% incidence) ; ++ uncommon (0.1 to <1% incidence) ; +++ common (1 to 10% incidence) ; ++++ very common (≥10% incidence)								
Abbreviations: Alk – anaplastic lymphoma kinase; EGFR – epidermal growth factor receptor; GnRH – gonadotropin-releasing hormone; HER2 – human epidermal growth factor receptor 2; HF – heart failure; HTN – hypertension; MEK – mitogen-activated protein kinase; mAb – monoclonal antibody; TKI – tyrosine kinase inhibitor; VEGFI – vascular endothelial growth factor inhibitor; VTE – venous thromboembolism								

My main area of interest is cancer related arterial toxicity, particularly atherothrombotic toxicity. Atherothrombotic complications of cancer treatment are an under-appreciated risk, particularly in association with novel therapies.

Immune checkpoint inhibitors (ICI) are a drug class that have revolutionised cancer outcomes in many cancer types. As such, there has been an exponential rise in the number of cancer types that ICIs are licensed for. While these drugs can have substantial anticancer effects, they are also associated with multiple adverse events (AE). ICI cause T cell activation and as such have an extensive immune mediated side effect profile, including myocarditis. ICI may also result in an increased risk of ischaemic events, such as myocardial infarction (MI) and ischaemic stroke, due to T-cell mediated inflammation within atheroma. Inflammation is a key pathophysiological process in atherosclerosis and atherothrombotic plaque rupture, leading to ischaemic events. Metabolic imaging using ^{18}F-fluorodexoyglucose positron emission tomography computed tomography ([^{18}F]FDG-PETCT) is a valuable tool to investigate the pathophysiological process of ICI associated atherothrombosis by assessing glucose uptake, a surrogate marker of inflammation, within the arterial wall.

ICI are increasingly used in combination with other drugs, such as vascular endothelial growth factor inhibitors (VEGFI). VEGFI have substantial CV adverse events (CVAEs) associated with them when used alone. It is not yet known if combination therapy of ICI+VEGFI has a higher atherothrombotic risk than monotherapy. In order to assess if ICI+VEGFI has a synergistic effect of atherothrombosis, it is necessary first to understand how the process of ICI-associated atherothrombosis occurs and the complex interaction between cancer, CVD and inflammation.

1.2 Cancer & cardiovascular disease

The co-existence of cancer and CVD occurs for many reasons. There are numerous shared risk factors for both conditions, such as smoking and obesity. There is a bidirectional relationship with cancer and CVD: both cause substantial metabolic alterations in cellular homeostasis, metabolic remodelling, changes to extracellular matrix and clonal haematopoiesis[3]. These alterations result in a change in normal physiology and potentiate the development of both cancer and

atherothrombosis. It is also vital to consider CVD as a consequence of cancer therapy.

It is important to improve understanding of additional CV risk from novel anticancer treatments as the burden of CVD in patients with cancer is already substantial, impacting morbidity and mortality[4-7]. CV death is the most frequent non-cancer cause of death in patients with malignancy [8,9]. A population-based retrospective analysis of 4.5 million adults in Canada observed participants with cancer had a higher risk of CV mortality than those without cancer over 12 years of follow up [10]. This risk is enhanced further in patients with pre-existing CVD[11].

If ICIs do cause inflammation of atheroma and plaque instability from T-cell activation, then the amount of pre-existing atheroma in patients receiving ICI is an important factor to consider. The incidence of atherosclerotic CVD (ASCVD), such as MI and ischaemic stroke, was 3-fold higher in people with cancer than matched controls in a multi-centre registry analysis 279719 patients in America between 2002 to 2011[12]. This data was collected prior to the widespread use of ICI and therefore the risk of ASCVD may be higher than the data reported.

1.2.1 Assessing toxicity of anticancer therapies

SACT is an umbrella term for all anticancer treatments given systemically (rather than surgery or radiotherapy). The term was adopted to encompass both older therapeutics, such as anthracyclines and platinum-based treatments (typically referred to as chemotherapy), and novel therapies, such as ICI and VEGFI.

AEs from SACT are common. There are numerous ways that AEs are defined and categorised. The most common definition, used in oncological trials, is the common terminology criteria for adverse events (CTCAE). This encompasses all systems. Each AE has its own definition based on clinical presentation and clinical features. Each CTCAE definition is graded for severity on a scale of 1-5. CTCAE grade 1 represents a mild/asymptomatic event and grade 5 is death as a result of the AE. Grade 3-4 are classed as ‘high grade,’ often requiring temporary cessation of SACT, hospitalisation and medical intervention[13].

While expansive, there is heterogeneity and ambiguity in the definitions and severity grading used in CTCAE. This is especially the case for CVAEs. For instance, while CTCAE includes definitions for MI and HF, it also includes separate listings of 'chest pain' and 'dyspnoea'[13]. Due to the complexity in diagnosis and investigation of CV toxicity, these toxicities require their own classification and definitions. The International Cardio-Oncology Society (ICOS) has provided definitions and severity gradings of CVAEs. These are specific and reflect individual cardiological conditions[14]. It is currently unknown to what extent the CTCAE reporting process affects accuracy and capture of CV events in clinical trials. While oncological efficacy trials have rigorous protocols for patient safety and AE reporting, these trials are designed with a primary focus upon the capture of cancer outcomes. This is confounded by tools used in these trials for adverse event reporting, such as CTCAE, which may not be optimal to capture CVAEs. The current lack of clear capture of CV events in an accurate and quantifiable manner limits knowledge of CV toxicity in clinical trials.

1.3 Anthracycline-associated cardiovascular toxicity

Anthracyclines are effective anti-cancer drugs used in a number of cancers including breast cancer, sarcoma and haematological malignancies. Anthracyclines have a substantial cardiotoxic profile, principally manifesting as LVSD and HF[15]. Anthracycline causes free radical formation and mitochondrial dysfunction leading to myofibrillar disarray and necrosis[16]. Although not fully understood, proposed mechanisms for anthracycline cardiotoxicity include inhibition of macromolecule synthesis, myofibril degeneration, oxidative stress and lipid peroxidation, as well as inhibition of topoisomerase and induction of apoptosis.[15]

While there is major focus on their myocardial toxic effects, anthracyclines are also associated with arterial injury. In patients treated with anthracyclines, there is evidence of endothelial dysfunction within large arteries, suggesting that anthracyclines have a direct arterial toxic effect. In a meta-analysis of 19 longitudinal and cross-sectional studies evaluating arterial stiffness in people treated with chemotherapy (14 of which examined the effects of anthracycline exposure) there were statistically significant increases in arterial stiffness both from baseline to follow up assessment, as well as when comparing those with

cancer treated with chemotherapy and matched healthy controls[17]. Anthracycline exposure (n= 635) was associated with greater arterial stiffness compared to healthy controls (n=701) and in comparison to those who had been treated with non-anthracycline chemotherapy (n=310). It should be noted, however, that a high risk of bias was noted in these studies. A systematic review and meta-analysis of nine studies specifically anthracycline-associated effects reported similar findings[18].

The impact of anthracycline-associated arterial toxicity on clinical outcomes has largely been unexplored. Some studies observe a modest increased risk of ischaemic events with anthracyclines compared to patients without cancer[19-24], while others do not[25-27]. Peripheral arterial endothelial dysfunction may contribute to the development of anthracycline-related left ventricular dysfunction through changes in peripheral vascular resistance and ventriculo-arterial uncoupling[28]. While anthracycline arterial toxicity may lead to an increased risk of hypertension and atherothrombotic events, the data are conflicting.

Studies assessing the association of anthracyclines and arterial disease are often based upon data that do not reflect contemporary practice (1960s to 1980s [25-27]), with small sample sizes and heterogenous study designs impacting the interpretability of the body of evidence as a whole. Patients with cancer are compared with either case matched controls or siblings, employ questionnaire surveys to collect data, and use different ways to define CVD, such as both CTCAE[20,22] and International Classification of Diseases (ICD)[23,24]. There is also a challenge in extrapolating the association of anthracyclines and CVD in a population that is already at a high risk of CV events and in making comparisons with other chemotherapy regimens that are also associated with greater events than controls, such as platinum-based therapies[29].

The largest and most robust registry study assessing CVD in patients with cancer (including patients treated with anthracyclines) was a Danish cohort study of 45152 patients aged 15-39 years who had survived at least 1-year following a cancer diagnosis. This study examined rates of hospitalisation from a CV cause. CVD was defined by ICD-10 classifications of 26 CV conditions ranging from hypertension to cardiac arrest and compared to matched controls (n=255513)[23].

This study reported a modestly increased risk of MI (RR 1.2, 95% CI 1.13 to 1.27), cerebral infarction (RR 1.26, 95% CI 1.16 to 1.36) and 'arterial disease' (ICD-10 definition: atherosclerosis, aneurysm and arterial thrombosis; RR 1.55, 95% CI 1.47 to 1.64). There was a similar increase in hypertension (RR 1.20, 95% CI 1.16 to 1.25) and even higher increase in hypertension with complications (RR 1.53, 95% CI 1.36 to 1.73) compared to matched controls[23].

Another large, more recent registry from Washington and Colorado included 10211 women with surgically-treated breast cancer and compared these to women treated with anthracycline (and/or trastuzumab), other chemotherapies and no chemotherapy. In this older cohort (mean age 62) there was an increased risk of ischaemic heart disease (IHD) after 5 years from treatment in those treated with anthracyclines (HR 1.51 95% CI=1.06 to 2.14) which increased further after 10 years (HR=1.86, 95% CI=1.18 to 2.92) in comparison to women who did not receive chemotherapy. After adjusting for multiple covariables, only the combination of anthracycline with trastuzumab was associated with an increased risk of MI[21]. The risk of stroke was also increased (HR 1.33, 95% CI=1.05 to 1.69)[21]. Further studies are required to explore the impact of anthracyclines and arterial toxicity.

The mechanism of anthracycline associated arterial toxicity has not yet been elucidated. Inflammation has been implicated in anthracycline cardiotoxicity and may therefore play a role in anthracycline associated arterial toxicity[30-33]. The role of inflammation in vascular dysfunction is well established[34,35]. Both anthracycline toxicity and vascular dysfunction share common pathophysiological pathways where inflammation is implicated[30–35]. While this supports the hypothesis that inflammation contributes to anthracycline associated artery toxicity, this has not yet been established.

1.4 Atherosclerotic disease, cancer and inflammation

Within the complex relationship between cancer and CVD, inflammation is a common theme. Inflammation, and the role of the immune system, in both cancer and CVD are discussed below.

1.4.1 Basic principles of immunity

There are two principal forms of immunity: innate immunity and adaptive immunity. Both innate and adaptive immune system are involved in the development of cancer and CVD.

Innate immunity is the 'general' immune system and the body's first line of defence, actioned mainly by neutrophils and macrophages. It acts quickly, but also in a non-specific manner. The adaptive immune system is activated by a series of triggers, either by recognition of a previously identified threat (via antigen presentation) or by release of inflammatory and immune-system-stimulating-proteins and signalling pathways, such as cytokines[36].

Adaptive immunity is mediated by T cells, B cells, and antibodies. In all inflammatory responses, there is a complex interaction and involvement with the innate and adaptive immune system. ICI manipulate the adaptive immune system by reversing the inhibition of highly differentiated effector T cells. 'Cytotoxic' T cells (CD8+ T cells) kill bacteria and tumour cells by attaching to the surface of the bacteria through their anchoring system, the T cell receptor (TCR), and cytokine release[37]. In order for activation of the adaptive immune system to begin, an antigen must be presented to the T cells by dendritic cells using major-histocompatibility complex (MHC). Once the antigen is attached, T cell multiplication occurs, invoking an inflammatory response[37]. T helper cells (CD4+ T cells) augment the inflammatory response and recruit other principal components of the immune system. Regulatory T cells regulate the inflammatory properties of the T cells and promote 'immune tolerance' to prevent over-activation of the adaptive immune system through inhibitory cytokines, such as tissue growth factors-β (TGFβ) and interleukin-35 (IL-35)[38]. This promotes 'T cell exhaustion' where effector cytotoxic T cells become less effective. Whether antigen presentation results in a large inflammatory response or is simply stored as part of the adaptive immune system's future defence depends on a balance of cytotoxic T cells and regulatory T cells[39]. Maintaining this balance occurs through many mechanisms which occur simultaneously, including activation of immune checkpoints.

1.4.2 Immune checkpoints

In order for the immune system to invoke an inflammatory response, multiple stimulatory signals are required. To maintain homeostasis and prevent overactivation of this process, there are built in immune checkpoints to keep the immune system quiescent when the stimulus has gone. The two main checkpoints pathways for lymphocytes are programmed cell death-1 (PD-1) and cytotoxic T-lymphocyte-associated protein 4 (CTLA-4)[40]. PD-1 is expressed early in antigen-mediated activation. It is activated by interaction with its two ligands, PDL-1 and PDL-2, which inhibits TCR and CD28 (a crucial costimulatory receptor on T cells) by downstream signalling pathways[40]. This results in a series of inhibitory effects: T cell exhaustion, reduced effector function (cytotoxicity and cytokine production), reduced response to stimuli, and altered transcriptional and epigenetic states[41].

CLTA-4 has a more proximal role in immune activation. Upon activation of T-cells, the intracellular CTLA-4 translocates to the surface and antagonises CD28 as well as reducing TCR activity and susceptibility to antigen presentation. This limits the extent of T cell activation at the priming stage. CTLA-4 also enhances the function of regulatory T cells, and promotes regulatory T-cell expansion[41].

1.4.2.1 Cancer and immune checkpoints

The immune system is an integral part of the body's defence against cancer. Surface receptors and immune checkpoints are manipulated by cancer cells to evade the immune system. Cancer cells express PD-L1 in several tumours, which exploits the co-inhibitory pathway to evade the immune system and promote cancer growth[42]. ICIs inhibit these checkpoints to invoke a substantial anticancer effect through an inflammatory response.

1.5 Immune checkpoint inhibitors

ICIs have been a massive advance in cancer therapy and are approved for 17 different malignancies[41]. ICIs inhibit the two main checkpoint pathways, PD1 and CTLA4. LAG3 inhibitors represent another ICI class which is licensed for use in melanoma. By inhibiting these pathways, ICIs can rescue tumour-specific progenitor exhausted T-cells to highly active effector T-cells.

Previously incurable cancers, such as lung cancer and melanoma, have seen particularly impressive improvements in cancer outcomes[43]. Ipilimumab was the first anti-CTLA-4 monoclonal antibody (mAb) assessed in metastatic melanoma, a condition previously associated with a median life expectancy of months. Ipilimumab yielded 19% survival at ten years. This survival benefit was increased to 43% when used in combination with a PD-1 inhibitor, nivolumab[44]. Similar outcomes have been observed in other cancers such as lung cancer and renal cell carcinoma (RCC) which were previously associated with poor prognosis[45,46]. While this is a dramatic improvement in outcomes, long-term survival, despite ICI, remains poor.

Due to their impressive anticancer effects, the indications for ICI have increased from three licensed indications to more than fifty between 2014 and 2020. The percentage of patients eligible for ICI has increased from 1.5% in 2011 to >43.6% in 2018[47,48].

Table 1-2 lists ICIs and their licensed indication within the United Kingdom (UK).

Table 1-2 Immune checkpoint inhibitors & their indication for use

ICI	Licensed for use in:
PD-1	
Pembrolizumab	Melanoma (palliative and adjuvant: stage II and III) Non-small cell lung cancer (palliative, neoadjuvant and adjuvant) Urothelial carcinoma Classical Hodgkin lymphoma Head and neck squamous cell carcinoma Renal cell carcinoma (palliative and adjuvant) Colorectal carcinoma Oesophageal carcinoma Breast cancer (palliative, adjuvant and neo-adjuvant) Endometrial cancer Cervical cancer Gastric & bilary cancer Small intestine cancer
Nivolumab	Melanoma (palliative and adjuvant, for completely resected metastatic/lymph node involvement) Renal cell carcinoma (1st and 2nd line) Non-small cell lung cancer (palliative and adjuvant) Malignant pleural mesothelioma Urothelial carcinoma (palliative and adjuvant) Squamous cell cancer of head and neck Classical Hodgkin lymphoma Gastrointestinal cancer Oesophageal cancer (palliative and adjuvant)
Cemiplimab	Cutaneous squamous cell carcinoma
PD-L1	
Atezolizumab	Urothelial carcinoma Non-small cell lung cancer (palliative and adjuvant) Small cell lung cancer Breast cancer Hepatocellular carcinoma
Avelumab	Merkel cell carcinoma Renal cell carcinoma Urothelial carcinoma
Durvalumab	Non-small cell lung cancer (palliative and adjuvant) Small cell lung cancer Bilary tract cancer
CTLA-4	
Ipilimumab	Melanoma Renal cell carcinoma Non-small cell lung cancer Malignant pleural mesothelioma Colorectal cancer
Tremelimumab	Hepatocellular carcinoma
LAG3	
Relatlimab	Metastatic melanoma (in combination with nivolumab)
Abbreviations: PD-1, Programmed cell death protein-1; PD-L1, Programmed death ligand-1; CTLA-4, Cytotoxic T-lymphocyte protein-4; LAG3. Data extracted from the British National Formulary (BNF) in April 2025[49].	

1.5.1 Immune related adverse events

Immune related adverse events (irAE) are common in patients treated with ICI[50]. Overall, high grade CTCAE toxicities occur in 38.6% and 57.9% of metastatic melanoma patients receiving ipilimumab 3mg and 10mg, respectively[51]. ICI also cause CVAEs. ICI-associated myocarditis is a rare but serious irAE with a mortality of up to 50%[52]. The reported incidence of ICI myocarditis varies, ranging from 0.03-0.5%[53,54]. In pooled-trial data of 59 trials submitted to the FDA, the reported incidence is 0.03% for all ICI and 0.13% for dual ICI[54] compared with 0.4-1.5% in registry data[55-58]. The pathophysiology of ICI myocarditis is not fully understood. Histopathological assessment of endomyocardial biopsy (EMB) in ICI myocarditis reveal interstitial fibrosis, lymphocyte infiltration (predominantly CD8+ T-cells) and macrophages[59,60]. A suggested mechanism of ICI myocarditis is T-cell activation resulting in an autoimmune reaction to release of cardiac antigens, such as troponin. In the first two reported cases of ICI myocarditis, autopsy studies observed high levels of troponin within tumour tissue and increased PD1 expression in the myocytes[52].

Patients with higher circulating troponin, such as those with CVD, may have increased risk of myocardial sensitisation and T-cell activation. The risk of ICI-myocarditis appears to be higher in patients with pre-existing CVD compared to those without CVD, in both trial data and registry data[56,57,61]. Both ICI-myocarditis and acute coronary syndromes (ACS) have been observed to occur at once[61]. A large pharmacovigilance study utilising the WHO's global individual-case-safety-report database to identify AE secondary to ICI reported that 4% of patients with myocarditis had concurrent MI[55]. This data may suggest that there is a similar pathophysiological occurring in ICI-myocarditis and ischaemic events, but the validity and accuracy of these data must be considered when assessing the association of ICI and ischaemic events. In a large pooled analysis of 59 papers from the Food and Drug Administration (FDA), the rates of ischaemia were higher with ICI (particularly dual ICI) compared to non-ICI therapies[54] suggesting that ICI are associated with ASCVD, with a RR of 1.35-2.56 for ICI and dual ICI respectively.

1.5.2 ICI and atherosclerosis

1.5.2.1 The immune system & atherosclerosis

Atherosclerosis is a leading cause of death worldwide. Inflammation and instability within atheromatous plaque results in sudden rupture leading to MI and stroke. Ischaemic events, such as ACS and stroke, occur predominantly by two mechanisms: plaque rupture and plaque erosion. Inflammation plays a key role in these processes[62]. The role of inflammation in atherosclerosis and ischaemic events summarised in Figure 1-1.

Figure 1-1 The pathogenesis of fatty streaks leading to atheroma and plaque rupture and the role of the immune system

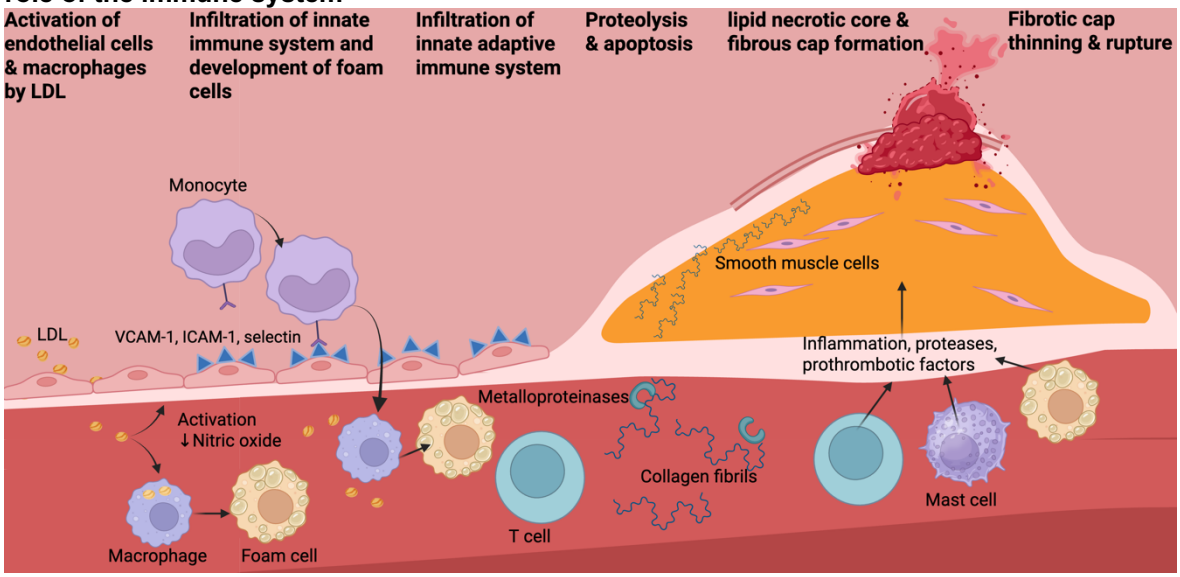

Created in BioRender. Rankin, S. (2025) https://BioRender.com/ebxl1ee *Adapted from Hannson[63] & Orbay et al, 2013* [64]

Atherosclerotic lesions, also known as atheroma, are asymmetric focal thickening of the intima, the innermost layer of arteries[63]. This consists of vascular endothelial cells, smooth muscle cells, as well as lipids. The first step in the development of atheroma is accumulation of fat and lipid deposition. Low density lipoprotein (LDL) cholesterol (LDL-C) infiltrates the artery and is retained within the intima. In an attempt to clear the fatty streak, macrophages consume lipid and become foam cells. Oxidative and enzymatic modifications lead to inflammatory lipid modification that induce endothelial activation[65]. These activated endothelial cells express surface anchoring proteins, such as vascular-cell adhesion molecule 1 (VCAM-1) and intracellular adhesion molecule-1 (ICAM-1), which promote adhesion of monocytes and lymphocytes, as well as platelet adhesion [63]. Monocytes then differentiate into macrophages through

release of growth factors, cytokines and macrophage colony-stimulating factor by the inflamed endothelium [66].

These macrophages, foam cells, inflammatory cells and lipid deposition form a core region, which is surrounded by a cap of smooth-muscle and collagen-rich matrix[63]. This process invokes an inflammatory response, with infiltration of more macrophages, T cells and mast cells and activate inflammatory pathways[63,67]. The activation of the T cells primed against the oxidised LDL-C results in a cascade of cytokine release including interferon-γ, IL-1, tumour necrosing factor, as well as release of IL-6 which promotes systemic inflammation and production of C-reactive protein[63]. As atheroma progresses, the fibrous cap thins and is filled with proteases, proteolytic enzymes and prothrombotic factors released by macrophages and mast cells which weaken the cap, promote instability leading to plaque rupture and erosion[63,68].

It is hypothesised that the increased risk of ischaemic events associated with ICI is secondary to accelerated atherosclerosis and plaque instability, Figure 1-2. In understanding the inflammatory process involved in atheroma development and plaque rupture, it is clear to see a plausible mechanism in which T cell activation from ICI could increase the risk of ischaemic events. Alternatively, ICIs could cause a direct coronary vasculitis in a T-cell mediated pathway[69]. Large vessel vasculitis including giant cell arteritis, aortitis and primary angiitis of the nervous system have been reported[70]. A pharmacovigilance study of 31321 AEs reported to the WHO database, assessed incidence of CV toxicity in those treated with ICI specifically, compared to the rest of the AE database. The reported incidence of vasculitis was higher in those treated with ICI compared to the entire AE database. 6% of patients who developed vasculitis died. However, the absolute number of events for such a large database was small with only 82 cases of vasculitis were reported[55].

Figure 1-2 ICI and VEGFI: mechanisms of anticancer effect and CV adverse effects

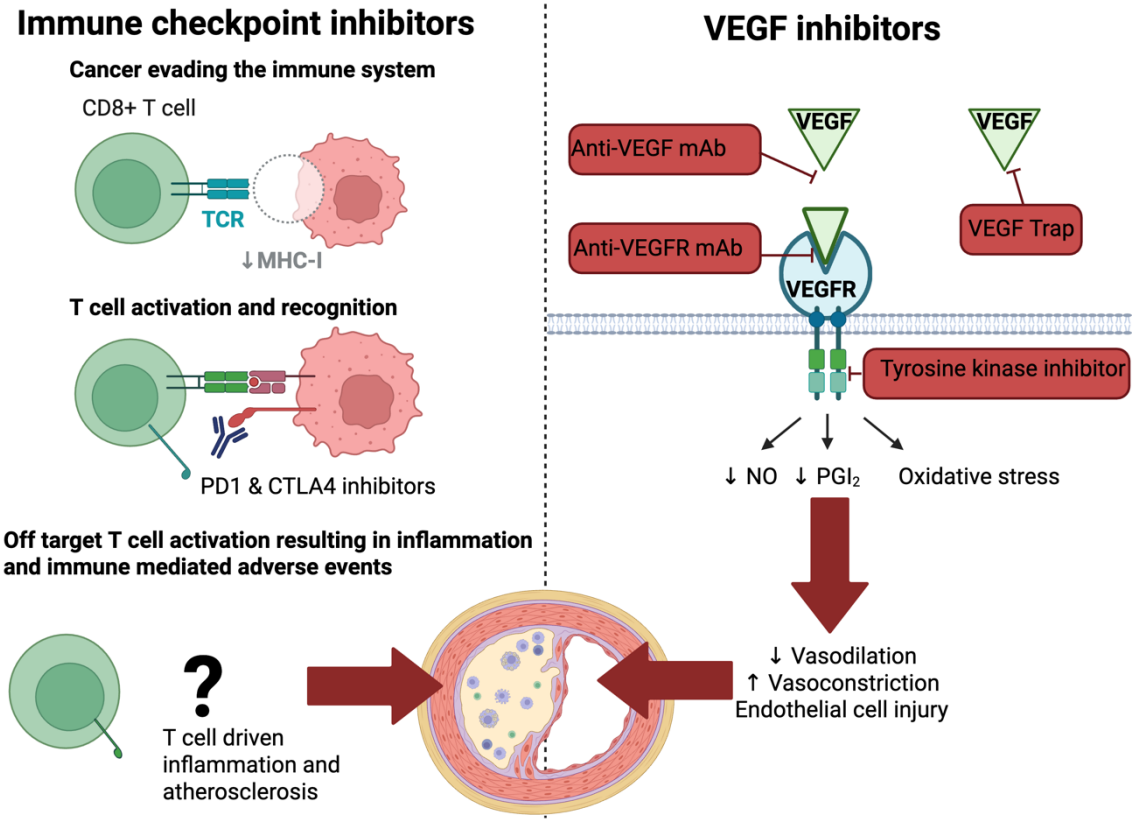

Adapted from Johnson et al 2022 & Dobbin et al 2021[41,71].Created in BioRender. Rankin, S. (2025) https://BioRender.com/ n89zp2x.

1.5.2.2 Clinical & observational data supporting ICI & atherosclerosis

Clinical data suggest an association between ICI and ischaemic events. In case reports, ACS, MI due to coronary spasm [72], pericarditis, Takotsubo-like syndromes and other MI mimics, such as vasculitis presenting with ischaemic symptoms, have been presented in case reports[73-76]. MI is reported in the FDA label for safety information for both pembrolizumab and atezolizumab [77]. An autopsy analysis performed on 11 patients on ICI revealed that there was an increased ratio of CD3+ lymphocytes to CD68+ macrophages (and a trend towards increased CD8+ to CD68+ ratio which was not significant) but no change in absolute number of inflammatory cells when compared to 11 cancer controls who were not treated with ICI[78].

Data from clinical trials is limited. In a meta-analysis of 22 trials of PD-1 and PD-L1 inhibitors used in the treatment of patients with non-small cell lung cancer, only two trials reported the occurrence of MI or stroke. This meta-analysis reported an incidence of 1% for MI and 2% for stroke in patients on ICI with fewer

events occurring in these groups than in comparator groups. It is unclear if the absence of reporting reflects absence of events. In addition, the comparator group was composed of patients treated with platinum-based chemotherapy, which is itself associated with a clinically relevant increased risk for ischaemic events[79]. In a similar meta-analysis of 26 studies (n=4633), incidence of MI was only 0.4% (95% CI 0 to 0.7%) with only six studies reporting events[53]. Another meta-analysis of 66 studies (n=34664) observed no difference in CVAEs (including myocarditis, MI, arrhythmia, heart failure, valvular disease, cardiac arrest and cardiac death) compared to non-ICI groups[80]. In this analysis, seventeen studies (n=10241) reported on the number of cardiac AEs compared to non-ICI group. Only nine studies compared against placebo, the remainder compared against standard of care, often VEGFI or platinum therapy. Out of 34664 patients, MI was reported in a total of 39 patients (ICI: 27 vs non-ICI: 12, RR 1.19, 95% CI 0.63 to 2.23)[80]. It is important to note that this meta-analysis was performed with inclusion of trials with no events occurring. If these trials are removed, in accordance with the Cochrane Handbook, higher rates of CVAE are observed[81].

Only one meta-analysis of clinical trials suggested higher rates of CVAEs than the control arm. A meta-analysis of 48 randomised clinical trial (RCT) of 29592 patients compared ICI with control arm event rates[82]. In this, they used differently methodology to the previous meta-analysis, using clinicaltrials.gov register. In this meta-analysis, in addition to myocarditis, other CV complications were associated with ICI. Dyslipidaemia (Peto odds ratio (OR) 3.68, 95% CI: 1.89 to 7.19, p <0.01), HF (Peto OR 1.98, 95% CI 1.36 to 2.88, p <0.01), cerebral artery ischaemia (Peto OR 1.56, 95% CI 1.10 to 2.20, p=0.01) and MI (Peto OR 1.51, 95% CI 1.01 to 2.26, p=0.047) were higher in the ICI arm compared to the control arms. Absolute number of events were low: 70 MI (0.6%, n=12698 patients) occurred in the ICI arm in the 31 trials that reported MI. Only 4 trials reported dyslipidaemia, with 39 events occurring (2%, n=2047); cerebral arterial ischaemia occurred in 98 patients in the ICI arm (0.8%, n=12366)[82].

In larger cohort studies, the association between ICI and atherothrombosis is observed. Observational data from registries and single centre studies have shown an absolute risk of CV events in ICI therapy at 1-year of between 7-10% [57,83,84]. This is in contrast to MI being reported in 0.6% of patients in a meta-analysis of trials sponsored by the National Cancer Institute[85]. In a retrospective

cohort study of 646 patients with melanoma, the rate of major adverse cardiovascular events (MACE) was 3.6 events per 100-person years compared to 0.9 in those treated with targeted therapies or no systemic treatment[86]. This has been replicated in another single centre retrospective study with higher rates of MACE in patients on ICI with both cancer patients not treated with ICI and non-cancer controls. This was mainly driven by HF and myocarditis. Incidence of ACS in the ICI group was higher than the non-cancer control group: ICI - 1.57 (95% CI 0.88 to 2.58) events per 100 subject years vs control - 0.80 (95% CI 0.6 to 1.06), p <0.01. However, the number of events were similar to the matched cohort of cancer patients not treated with ICI (non ICI group event rate 1.44 per 100 subject years, 95% CI 0.66 to 2.73)[87]. Event rates in this study were low (15 events in the ICI group). In the largest single centre retrospective analysis of 5684 patients, there was a 4-fold higher risk for cardiovascular events (MI, coronary revascularisation and ischaemic stroke) after starting ICI compared to matched controls (HR 4.7, 3.5-6.2) and increased risk of MI (HR 7.2, 95%CI 4.5-11.5) [47]. They also observed a 4-fold higher risk for CV events in the two years post ICI treatment compared to the two years pre-treatment.

Not all observational data support the hypothesis that ICI are associated with ischaemic events. A large observational pharmacovigilance study of the World Health Organisation's (WHO) global database of individual case safety reports of 31321 ICI AEs, there was no greater reporting of MI than the entire database of all AE[55].

1.5.2.3 Pre-clinical data relating to ICI & atherosclerosis

The mechanism by which ICI might cause ischaemic events has been investigated in pre-clinical animal models and in imaging studies in humans observing changes in the size of existing plaque and morphological changes within the plaque.

Immune checkpoints play a critical role in the prevention of atherosclerosis progression by inhibiting T-cell driving inflammation in plaque[88]. Blockade of PD-L1 increases inflammation and accelerates atherosclerosis in mouse models[88]. $PD1^{-/-}$ and $LDLR^{-/-}$ mice have larger atherosclerotic lesions with more abundant CD4+ T cells, CD8+ T cells and macrophage infiltration with higher levels of TNFα, compared to controls[89].

TNFα is a pro-inflammatory cytokine that has a proximal role in inflammation and antigen presentation[90]. Its downstream cascade activates not only T cells but also plays a key role in macrophage activation. TNFα is upregulated with inhibition of PD1[91]. TNFα promotes accumulation of intracellular lipids[91] and also is involved in endothelial dysfunction and development of atherosclerosis[92,93]. Animals support that TNFα contributes to the development of atherosclerosis and observe higher levels of TNFα in PD1 knockout studies[94].

In humans, exhausted T cells expressing PD1 are present in atherosclerotic plaques from patients who have had a recent stroke [95]. PD-1 is expressed on macrophages and dendritic cells in atherosclerotic plaques and PD-1 expression is reduced in circulating T cells for patients with ACS[88]. ICI may activate these T cells and accelerate atherosclerosis. In mice treated with ICI, arterial plaques demonstrated an inflammatory process with infiltration of T cells and increased in the size of plaque necrotic core compared to controls. Administration of a CTLA4 agonist decreased this inflammation and reduced atherosclerosis in mouse models treated with ICI[96].

Two retrospective studies have shown that patients exposed to ICI have a 3-fold greater increase in atheroma volume on CT imaging compared to case-matched controls[47,97]. There was a progressive increase in both calcified and non-calcified plaque compared to pretreatment with a 3-fold increase in size per year[47]. This observation was attenuated with concomitant use of statin or steroids, with a 50% reduction in plaque progression compared with those not on as statin.

The above observational data supports the hypothesis that ICI are associated with accelerated atherosclerosis and ischaemic events. The underlying mechanism of this process and the role of inflammation within this process has not been established in humans. It is crucial to understand the true risk of ischaemic events from ICI and its underlying mechanism given the exponential use of ICIs and their increasing use in combination regimens with other anticancer therapies, such as VEGFI.

1.6 VEGF inhibitors

VEGFI are targeted anti-cancer therapies and have effective anti-cancer treatment effects in a range of tumour types. Their main mechanism of action is via the prevention of growth of new blood vessels (angiogenesis). This is achieved by inhibition of the endogenous protein, VEGF, that is crucial for vascular growth and vascular physiology, Figure 1-2.VEGF also plays a critical role in the maintenance of vascular homeostasis and in cardiac development and function[98]. VEGFI block the transduction of intracellular signals through a variety of mediators impairing angiogenesis, lymphangiogenesis, vascular permeability, and vascular homeostasis which inhibit growth of cancer cells[98,99].

Bevacizumab (anti-VEGF mAb) was the first VEGFI to be approved and was initially used in the treatment of metastatic colorectal cancer in 2004[100]. Since then, further VEGFIs have been developed and approved in different cancer types, all in the non-curative (palliative) setting. There are four principal types of VEGFI: anti-VEGF mAb; VEGF soluble decoy receptors capturing free VEGF; anti-VEGFR mAb; and tyrosine kinase inhibitors (TKI) of the VEGF receptor, Figure 1-2. Most TKIs are multi-targeted and affect other tyrosine kinase (TK) receptors[98]. A list of VEGFI and their licensed use for cancer in the United Kingdom is provided in Table 1-3.

Table 1-3 VEGFI approved in the UK

VEGF inhibitors	Licensed for use in:
Tyrosine kinase Inhibitor	
Axitinib	Renal cell carcinoma
Cabozantinib	Hepatocellular carcinoma Renal cell carcinoma Thyroid cancer (differentiated & medullary)
Lenvatinib	Differentiated thyroid carcinoma Endometrial carcinoma Hepatocellular carcinoma Renal cell carcinoma
Nintedanib	Non-small cell lung cancer
Pazopanib	Renal cell carcinoma Soft-tissue sarcoma
Regorafenib	Colorectal cancer Gastrointestinal stromal tumours Hepatocellular carcinoma
Sorafenib	Differentiated thyroid carcinoma Hepatocellular carcinoma Renal cell carcinoma
Sunitinib	Gastrointestinal stromal tumours Pancreatic neuroendocrine tumours Renal cell carcinoma
Tivozinib	Renal cell carcinoma
Vandetanib	Medullary thyroid cancer
Monoclonal antibodies (anti-VEGF and anti-VEGFR)	
Bevacizumab	Breast cancer Cervical carcinoma Colorectal cancer Epithelial ovarian cancer Fallopian tube cancer Non-small cell lung cancer Peritoneal cancer Renal cell carcinoma
Ramucirumab	Colorectal cancer Gastric cancer Hepatocellular carcinoma Non-small cell lung cancer
VEGF-Trap mediators	
Aflibercept	Colorectal cancer
Abbreviations: VEGF, Vascular endothelial growth factor. Data extracted from British National Formulary on 15/04/2025 [49]	

1.6.1 VEGFI associated cardiovascular toxicity

VEGFI are associated with a range of CVAEs, including hypertension, LVSD, HF and atherothrombotic sequelae including MI, stroke and electrocardiographic QT interval prolongation [8,101-103]. VEGFI interrupt homeostasis of vasoconstrictor and vasodilator factors, resulting in increased endothelin-1 (ET1), decreased nitric oxide (NO) and prostacyclin and decreased endothelial cell survival. VEGFI are also associated with induction of oxidative stress and release of reactive oxygen species[98,104]. These pathways result in endothelial dysfunction, reduced coronary perfusion and increased peripheral vascular resistance. Microvascular rarefraction, which is the reduction in microvessel density, has also been proposed to contribute to VEGFI-induced hypertension by increasing peripheral vascular resistance[98]. In a recent prospective observational cohort study in Glasgow, 19% of patients treated with VEGFI developed cancer treatment related cardiac dysfunction and 77% developed hypertension[105].

1.6.2 Thrombotic events with VEGFI

1.6.2.1 Pre-clinical data

VEGFI are also associated with thrombotic events. Early case reports described atherosclerotic plaque rupture and consequent MI, development of coronary artery disease (CAD) and arterial vasospasm secondary to VEGFI[106-108]. In both animal models and in humans, VEGFI has been shown to be directly associated with atherosclerotic progression[104,109,110]. This may be due to increased mitochondrial superoxide and free radical formation as well as reduced NO bioavailability [104]. VEGFI's disruption of regulators of vascular homeostasis and downstream mediators, such as NO and prostacyclin (potent vasodilators and inhibitors of platelet activation) may further contribute to thrombotic events[98]. Endothelial cell-derived microparticles, which are biomarkers for endothelial injury, are increased in cancer patients during VEGFI therapy[111]. Exposing platelets to subendothelial extracellular matrix components promotes platelet activation[112].

1.6.2.2 Clinical data

Clinical observations support the pre-clinical observations that VEGFI are associated with thrombotic events. Meta-analyses of clinical trials show an association with VEGFI and atherosclerotic risk. This is also reflected in real world data. The incidence of arterial thromboembolic events ranges from 1.4-3.3% in trials, with a 3-fold increased risk compared to controls[102,113-116]. It is important to note however, that data from trials remain limited by factors already outlined.

A meta-analysis of 72 VEGFI randomised controlled trials (n=38078) revealed that VEGFI treatment was associated with an increased risk of MI, hypertension, arterial thromboembolism and proteinuria compared to control patients with cancer[112]. In this meta-analysis, fatal and non-fatal MI were reported in 7 trials (n=4613). Although there was a significant increased risk of MI compared with controls (RR 3.54) the absolute risk of MI was 0.8%. In another meta-analysis of 77 randomised control trials involving VEGFI therapy, there was an increased risk of cardiac ischaemia (odds ratio 2.83,95% CI: 1.72-4.65) compared to routine care[115]. Only 8 trials (n=3891) adequately reported events to allow comparison between the VEGFI and control arms. The incidence of cardiac ischaemia was 1.7%.

Despite a documented increased risk of ischaemic events in trial data, the overall incidence reported is low. A meta-analysis of bevacizumab trials including 4617 patients reported increased IHD (defined as MI, unstable angina, coronary revascularisation, CAD, arrhythmias, sudden death of CV death) compared with controls. VEGFI were associated with a 2.5-fold higher risk of major adverse cardiovascular event (MACE) compared with controls [102]. The incidence of IHD was only 1.0%. The lack of adequate definitions of events and reporting of events limits the interpretation of these trials and understanding the true ischaemic risk with VEGFI.

The fact that a signal suggesting risk of ischaemia with VEGFI is observed in trial populations, despite the limitations of clinical trials, may imply that the true impact of VEGFI on ischaemic events is even greater in the general population compared to the trial populations. The mechanisms for this include exacerbating

underlying risk factors such as hypertension, accelerated atherosclerosis, coronary vasospasm, acute arterial thrombosis and endothelial dysfunction.

1.7 ICI+VEGFI combination therapy

The use of ICI and VEGFI in combination is now a common treatment regimen for various cancers, including hepatic, renal, cervical, and endometrial cancer[100]. In a number of cancer types, combination therapy is superior to monotherapy[117–120]. More than ninety clinical trials of combinations of ICI+VEGFI have been conducted over the last five years[99,121]. ICI+VEGFI treatments are currently approved by the FDA[100] for 17 different malignancies and this number may increase in the coming years[41]. In the UK, six ICI+VEGFI regimens are approved for use, Table 1-4. While ICI+VEGFI are associated with greater cancer benefits than monotherapy, it is unclear whether or how combination therapy might modify the CV adverse effect profile.

Table 1-4 ICI+VEGFI combination regimens approved in the UK

ICI+VEGFI	Licensed for use in:
Pembrolizumab / bevacizumab	Cervical cancer
Nivolumab / cabozantinib	Renal cell carcinoma
Atezolizumab / bevacizumab	Hepatocellular carcinoma
Pembrolizumab / lenvatinib	Renal cell carcinoma Endometrial cancer
Avelumab / axitinib	Renal cell carcinoma
Pembrolizumab / axitinib	Renal cell carcinoma
Abbreviations: ICI – immune checkpoint inhibitor; VEGFI – vascular endothelial growth factor inhibitor. Data extracted on 15/04/2025[49]	

1.7.1 Lack of CV safety data from clinical trials

At present, there are no robust long-term CV safety data on ICI+VEGFI combination therapy. Two meta-analyses of therapies for metastatic RCC (n=13,893) and lung cancer (n=2313) patients reported that combination therapies are effective and with a similar incidence of AE to monotherapy[121,122]. The number of CVAEs are infrequent and often not reported. Despite the infrequent events, treatment-associated deaths were largely due to bleeding and CVAEs, demonstrating that CVAEs are still an important clinical issue even in the trial population[122].

There have been two meta-analysis comparing CV toxicity rates in ICI+VEGFI vs VEGFI monotherapy[123,124] in nine and twelve clinical trials each. In the more recent and larger meta-analysis (12 studies, n=8124), predictably myocarditis occurred more in the ICI+VEGFI arm compared to the VEGFI arm. ICI+VEGFI was associated with a marginally higher rate of severe hypertension in both meta-analyses (19% vs 16%, odd ratio (OR) 1.24, 94% CI 1.01-1.53, p=0.04) but not 'all grade' hypertension[123]. Only three trials reported acute vascular events with only 50 events occurring, the majority of which were pulmonary embolism. The incidence of MI and stroke was 0.2% and 0.4% in each arm[123].

The discrepancy between trial CV safety data and real-world observational data has already been discussed in relation to ICI and VEGFI monotherapy trials[47,57]. The issue of non-representative trial populations and heterogenous reporting is likely to impact ICI+VEGFI safety data in the same manner as monotherapy trials. A secondary analysis of one ICI+VEGFI combination trial which reported the prevalence of baseline CV risk factors[125]. In that report, the prevalence of CV risk factors was low. Only 4% of people in the ICI+VEGFI arm had dyslipidaemia, 9.5% had diabetes and 3.2% had cerebrovascular disease. Prior MI was not reported in baseline characteristics.

1.7.2 Observational data supporting the association of ICI+VEGFI combination therapy and atherothrombotic events

Registry data suggests that there is an increased risk associated with ICI+VEGFI compared to other treatment strategies. A retrospective study of 252 lung cancer patients treated with ICI revealed an increased risk of major CVAE in patients pre-treated with VEGFI or receiving combination ICI+VEGFI (HR: 2.2; 95% CI: 1.05 to 4.37) in comparison to those treated with ICI alone, although it was inadequately powered to draw firm conclusions[126]. In another single centre retrospective study of 672 patients receiving ICI, prior VEGFI was associated with increased MACE compared to those without prior VEGFI therapy[87]. Prior VEGFI and smoking history were independent risk factors for ACS in this study, although events were low (15 ACS events in the ICI group)[87]. A pharmacovigilance study of ICI+VEGFI combination therapy using real world safety reporting from FDA AE reporting system (FAERS) database assessing CVAEs found that ICI+VEGFI had a greater risk of CVAEs than ICI alone, mainly driven by embolic and thrombotic

events[127]. Combination therapy was associated with a lower frequency of all cause death and life-threatening CVAEs, but a higher number of deaths from thrombotic and embolic events. The number of patients on ICI+VEGFI, and number of CVAEs, were lower than the monotherapy-treated group. This reflects the fact that ICI+VEGFI is the most recently approved regimen. There was a rapid rise in ICI+VEGFI combination therapy use form 2019 (in the last 3 years of the study period). Longer term safety follow up for ICI+VEGFI is required.

In a similar pharmacovigilance study assessing the drug-drug interactions of ICI+VEGFI between 2015 to 2023, PD-1/PDL-1 inhibitors combined with VEGFI was associated with vascular disorders, defined by the MedDRA system organ class classification, but CTLA-4 inhibitors with VEGFI were not[128]. The effect on vascular disorders of PD-1/PDL-1 inhibitors and VEGFI was greater than the effect of PD1/PDL-1 inhibitor monotherapy and VEGFI monotherapy[128].

A major limitation of the data accruing from AE reporting databases is that it is predicated upon clinicians not only making an association between ischaemic events and ICI+VEGFI treatment but also reporting it. Both of these studies use unclear and broad definitions of ‘vascular’ and ‘thrombotic’ events, based on standardised MedDRA Query codes which do not delineate between arterial and venous thrombotic and embolic events.

1.7.3 Mechanisms that support VEGFI may exacerbate ICI-atherosclerosis

ICI+VEGFI combination therapy may lead to an increased risk for CVAEs and worse CV outcomes for different reasons. Firstly, with improved survival outcomes, there is increased risk of CVD simple through survivor bias. As ICI+VEGFI are associated with increased survival, the long-term CV and atherosclerotic consequences of the regimen are potentially more relevant than monotherapies. Secondly, with two drug classes, there is double exposure to drug class specific CVAEs. ICI-associated CVAE and VEGFI-associated CVAE may occur concurrently resulting in a more severe clinical presentation, such as the co-existence of ICI myocarditis and VEGFI-induced myocardial dysfunction. Thirdly, the CV toxicity profile of VEGFI may exacerbate ICI AEs. Pre-existing hypertension is associated with vascular toxicity in patients on ICI compared to

those without[84]. Given the high incidence of VEGFI-induced hypertension, VEGFI may exacerbate ICI associated vascular toxicity.

VEGFI CVAEs such as hypertension and LVSD may exacerbate pre-existing CVD and increase the risk of atherosclerotic events induced by ICI. Hypertension and endothelial dysfunction contribute to the development of atherosclerosis and atherothrombosis[129]. In a single centre data of 1215 patients receiving ICI, pre-existing CVD increased the risk of acute vascular events, and the presence of vascular toxicity was associated with poorer survival than those without[84].

Finally, both drugs appear independently to be associated with an increased risk for atherothrombotic events. It is not known if this associated risk is mediated by two independent pathways or whether concomitant ICI+VEGFI will have a synergistic effect on the same pathophysiological process. Pre-clinical data supports the hypothesis that combination ICI+VEGFI have a greater effect on development of and instability within atherosclerosis compared to monotherapy. However, the underlying mechanism, and the question of how inflammation plays a role is still unanswered.

1.7.3.1 Synergistic immunomodulatory effects

It has been proposed that the additional anticancer benefit of combination ICI+VEGFI over monotherapy may lie in the immunomodulatory effects of VEGFI. VEGF has direct and indirect effects on the immune system and the immunomodulatory effect of VEGFI may occur through different mechanisms.

VEGFI may augment the infiltration of ICI activated T cells into tumours and to enhance its function[130]. Cancer cells can upregulate the expression of PD-1 within the tumour microclimate through VEGF mediated pathways, which can contribute to cancer immune evasion[42]. Inhibiting VEGF reduces the expression of PD-1 and enhances immune system's detection of cancer cells. In animal models, bevacizumab has been shown to increase activation of dendritic cells, cytotoxic T cells and reduce T cell exhaustion[131,132]. Sunitinib decreases the amount of regulatory T cells[133]. It has also been proposed that VEGFI stimulates immune cell infiltration by increasing expression of adhesion molecules, such as ICAM-1 and VCAM-1[99].

By enhancing the adaptive immune system, decreasing immune checkpoints and regulatory T cells, and enhancing adhesion and infiltration of immune cells, VEGFI can enhance the immune response mediated by ICI[99]. While all of the mechanisms have a beneficial role in anticancer effect, these same mechanisms are seen in the development of atheroma and plaque instability. These factors, plus the prothrombotic changes observed with VEGFI may lead to increased arterial injury, increased arterial inflammatory, plaque instability and plaque rupture[39].

While the above data suggests that ICI cause plaque inflammation within atheroma, and the concomitant administration of VEGFI may enhance the atherothrombotic process, this mechanism has not yet been elucidated in humans.

1.8 The role of PETCT imaging in assessment of vascular inflammation

^{18}Fluoride-Fluorodeoxyglucose positron emission tomography/computed tomography ([^{18}F]FDG-PETCT) is a molecular imaging technique that is highly sensitive to metabolically active processes which use glucose as a fuel. PETCT scanning combines positron emission tomography (PET) with computed tomography (CT). The CT component gives a detailed 3D image of the body and organs. PET imaging uses radioactive tracers attached to molecules designed to give unique insights into metabolic activity. PET scanners construct images via the detection of radioactivity released from the radiotracer. The most commonly used radiotracer is ^{18}Fluoride-Fluorodeoxyglucose, [^{18}F]FDG.

Radiotracers are made in cyclotrons. To produce [^{18}F]FDG, ^{18}Oxygen-enriched water is bombarded with protons. The bombardment of protons converts the stable isotope ^{18}O into the unstable ^{18}F by adding an extra proton to the F nucleus. This unstable isotope decays to turn the proton into a neutron. In doing so it releases a positron (a 'positive electron') [134]. When a positron collides with an electron, an 'annihilation reaction' occurs releasing two γ photons. These photons have two unique qualities: each γ ray has a charge of 511 keV (kiloelectron volt) and both travel 180 degrees apart. With this knowledge, the PET scanners detects the radioactivity of two 511keV charges and by following

the 'line of response', determine where the annihilation reaction has occurred, and create a PET image[134,135], Figure 1-3.

Figure 1-3 Radioactive decay resulting in positron release and the annihilation reaction, producing γ rays used for detection in PET imaging

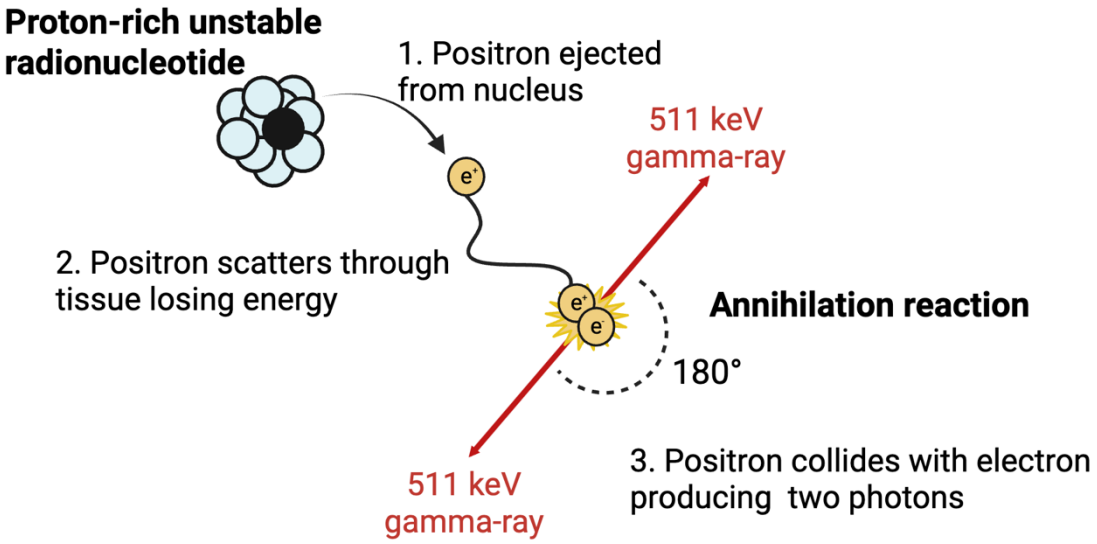

Created in BioRender. Rankin, S. (2025) https://BioRender.com/6pyss7o. Adapted From Cherry et al. [135]

[^{18}F]FDG has the same structure as glucose and enters cells in the same manner, via the glucose transporter (GLUT) system. [^{18}F]FDG lacks a hydroxyl group because this is replaced by the radiotracer, ^{18}F. Intracellular phosphorylation of [^{18}F]FDG produces FDG-6-phosphate which cannot be metabolised via the glycolytic pathway. Therefore, the cellular accumulation of FDG is in direct proportion to their metabolic activity and is known a metabolic trapping[136]. Only once ^{18}F is changed back to ^{18}O through positron decay can FDG be metabolised[136].

As inflammatory cells and malignant cells have a high rate of glucose uptake, [^{18}F]FDG-PETCT is frequently used in the staging of cancers and assessing response to treatment[136]. It is also the gold standard method for the identification and quantification of inflammatory activity and in the assessment of large vessel inflammation[136-138].

1.8.1 FDG-PETCT & atherosclerotic imaging

[^{18}F]FDG can be used as a biomarker of metabolic activity within atherosclerosis[136,138,139], and therefore, may give valuable insights into the association between ICI and atherosclerosis. Atherosclerotic PETCT assessment was first assessed alongside histopathological assessment of patients with recent stroke undergoing endarctectomy[139]. High [^{18}F]FDG uptake was seen in macrophage rich areas of plaque in carotid arterial specimens, predominantly in the lipid core/fibrous cap border of the lesion. [^{18}F]FDG is a suitable radiotracer for atherosclerosis assessment as there is high metabolic uptake of macrophages infiltrating plaque. Furthermore, the anaerobic conditions within the necrotic core prevent macrophages using free fatty acid metabolism and promotes glucose metabolism.

[^{18}F]FDG can identify culprit atherosclerotic lesions and phenotypically high-risk carotid plaque in patients with TIA and minor stroke at an atherosclerotic lesion level[140]. Culprit coronary artery lesions following ACS have higher [^{18}F]FDG uptake than non-culprit lesions. Assessment of the artery as whole, in contrast to the assessment of individual atherosclerotic lesions, is also predictive of ASCVD. Even in larger arteries, arterial [^{18}F]FDG uptake of the ascending aorta is higher in patients with ACS, and those with high CV risk, than it is in controls[141]. This suggests that even in the absence of atheroma, larger artery [^{18}F]FDG uptake can be used as a surrogate for inflammatory atheroma.

[^{18}F]FDG uptake is measured by a semi-quantifiable assessment of radioactivity within the tissue, using standardised uptake values (SUV). Both the maximal and mean SUV can be reported. SUV is a dose uptake ratio that is mathematically calculated using the concentration of activity the time a specific region corrected to the injected dose of FDG and the patient's body weight[142]. Arterial inflammation can be quantitatively assessed by measuring arterial FDG uptake, corrected to blood pool activity, creating the tissue-to-background ratio (TBR)[134,138,143,144]. There are different metrics via which TBR can be reported, including TBRmax, TBRmean, TBRmax of 'active segments' and the most-diseased segment (MDS, calculated by taking the segment with the highest TBR and taking the average of the segment with the highest TBRmax and the segment above and below it). The most commonly used that is validated in the

most clinical settings is TBRmax, which is the most accurate measurement for atherosclerosis inflammatory assessment.

By convention, arterial segments are defined as 'active' or inflamed if TBRmax is ≥1.6. The TBRmax threshold of 1.6 to determine 'active segments' originates from a study of PETCT in patients undergoing endarctectomy. In this study of seventeen patients, a TBR value <1.6 was associated with <5% inflammation (CD68+ staining) on histopathological assessment[145]. Although this threshold was derived from a small cohort from relatively historic data, it has since been validated in numerous clinical settings for assessment of both atherosclerotic lesions and whole vessel inflammation, and has been used as a clinical endpoints in therapeutic trials[141,144,146,147]. Statins are effective at reducing arterial inflammation[143] and steroids may also have an effect[47].

In order to perform optimal PETCT imaging for atherosclerosis assessment, the recommended acquisition and reconstruction parameters are different to those used for oncological assessment. The European Association of Nuclear Medicine (EANM) provide recommendations on reconstruction parameters for atherosclerosis assessment[138]. One recommendation is for a longer circulation time (from injection to scanning) to allow for clearance of [^{18}F]FDG from the bloodstream in order to improve arterial imaging. Oncological assessments use 60 minute circulation times while EANM recommend 120 minute circulation time for atherosclerotic assessment. Different reconstruction parameters and PETCT scanners used can markedly influence the results of arterial assessment[148]. This poses a challenge as there have been numerous advances in PETCT imaging since the EANM recommendations were published in 2016. One example of this is the introduction of digital scanners in place of analogue scanners, improving sensitivity and spatial resolution[149]. A study comparing digital versus non-digital scanners for carotid arterial assessment observed that the threshold of 1.6 may not be applicable to digital scanners[150]. It is not currently established what effect modern digital scanners have on atherosclerotic imaging and what the optimal reconstruction parameters are for digital scanners.

1.8.2 Use of PETCT in assessment of CVD and SACT toxicity

[^{18}F]FDG-PETCT is highly correlated with atherosclerotic disease both at an individual atherosclerotic lesion level, and assessment of whole vessels as a surrogate for atherosclerotic disease. [^{18}F]FDG may provide valuable insights into the pathophysiological process underlying ICI-associated atherothrombosis. [^{18}F]FDG-PETCT is most commonly associated with macrophage activity, due to their high metabolic state. This has raised concern that [^{18}F]FDG-PETCT may not be suitable for T cell mediated inflammation within atheroma. [^{18}F]FDG-PETCT is used commonly in inflammation where T cells mediated inflammation occurs, such as T-cell driven vasculitic diseases. In histopathological assessment of high risk plaque by [^{18}F]FDG-PETCT observed both macrophage and lymphocyte infiltration[136]. T cell mediated irAE associated with ICIs have been observed by [^{18}F]FDG-PETCT[151]. These data would support the use of [^{18}F]FDG-PETCT for T cell mediated inflammation within atheroma.

1.8.3 PET assessment of ICI associated arterial inflammation

To date, there have been six observational studies that have assessed ICI large artery inflammation by [^{18}F]FDG-PETCT. Their time frames have been between 6 weeks from ICI initiation to several years after completion. Each study used different and often unclear methods to assess arterial inflammation. Frequently, study manuscripts have lacked detail in the description of the methods used for PETCT arterial assessment and it is not possible to ascertain how these scans were analysed. A summary of key results and a comparison of the study design of each is provided in Table 1-5.

The first study retrospectively assessed arterial [^{18}F]FDG uptake in ten patients receiving ICI with melanoma, alongside a mouse model, comparing pre-treatment arterial uptake and 6 weeks after therapy, including combination ICI regimens. They observed no difference in [^{18}F]FDG activity in large arteries in humans or mice, but did observe marked changes in the adaptive immune system (increased CD4+ helper and CD8+ cytotoxic T cells) and plaque progression toward a lymphoid-based inflammatory phenotype in mice with a 2.7-fold increase in CD8+ cells, 4-fold increase in necrotic core size and 1.6-2.2 fold

increase in vascular adhesion molecules, such as VCAM-1 and ICAM-1. This was performed on a non-digital scanners using a 60 minute circulation time[96].

There have been three retrospective studies from the same centre using [^{18}F]FDG-PETCT in patients with melanoma (20 patients)[152], lymphoma (12 patients) [153] and lung cancer(47 patients) [154].

The first assessed 20 patients with melanoma receiving ICI[152]. PETCT was assessed before starting ICI and 4.4±1.6 months after initiation of ICI. They assessed only active segments (TBR ≥1.6) by analysing 1cm^3 volumes of interest (VOI) in 6 arterial segments (aorta and iliac arteries) and observed an increase arterial TBR in all segments (1.76±0.06 to 2.05±0.06, $p<0.001$). No details about how the PET scans were performed was given. The method of how arteries analysed is unclear. The study also observed that this signal was only present in non-calcified or mildly calcified lesions, but not in moderate-severely calcified lesions. The presence of calcification is proposed to be a represent late stage, established 'burnt out' atherosclerotic disease[155]. As such, it is proposed that calcified lesions have less soft atheromatous plaque and therefore have less of an active inflammatory process. The existing data around this matter, however, is conflicting. Research has observed that [^{18}F]FDG uptake is both lower in calcified lesions and also that calcification and inflammation coexist[146,156].

The same group published similar findings in twelve patients under 50 years of age receiving ICI, assessing arterial TBR before treatment and 9.6±3.9 months after ICI[153]. In this cohort of twelve patients, 117 arterial lesions over 6 arterial segments in twelve patients were analysed. There is no explanation as to how these 117 lesions were identified or what a 'lesion' was defined as. This study observed an increased inflammatory activity in all arterial lesions assessed. This inflammatory signal was only present in lesions without pre-existing arterial inflammation. For this study, pre-existing inflammation was defined as a TBR≥1.48 instead of 1.6. No explanation or justification was given for the lower threshold used in this study compared to the previous study, or EANM recommendations. A potential risk of selecting only lesions with low baseline values, labelled as 'cold lesions without pre-existing inflammation,' is that an

observed regression to the mean may be construed as a significant positive result.

This study also categorised these lesions based on their baseline calcification and pre-existing inflammation. In contrast to their previous work, they observed a significant increase in TBR in calcified lesions, but not in non-calcified lesions.

More recently, this centre published assessment of arterial [^{18}F]FDG-PETCT in 47 patients with lung cancer treated with ICI[154]. Patients were scanned prior to ICI treatment and 2.5±1 month after ICI. 761 lesions were examined from scans of 47 patients. The mean TBRmax of all arterial segments that were not included was not reported, nor was the number of segments per scan that were not analysed. They again observed a change only in lesions with a baseline TBR <1.6 but not in those ≥1.6. In this study, this change was present in lesions with and without prior calcification. They also only observed a change in patients without CV risk factors but not those with CV risk factors; however the numbers were small.

In the last two years, two larger retrospective studies have been performed with different methodologies. The CHECK-FLAME I study assessed 132 patients with advanced melanoma retrospectively with [^{18}F]FDG-PETCT scans prior to treatment, at 6 months and at 18 months[157]. The median follow up time was 2.3 years and CV events were reported. This study also included patients who were not treated with ICI (27% of the cohort) which act as a control group. Two PETCT scanners were used, one digital and one non-digital, with a 60-minute circulation time. 1cm^2 2-dimensional regions of interest (ROI), rather than 3D which is more contemporary, were drawn over the whole vessel for smaller arteries (carotids and iliacs). For the aorta 1cm^2 ROI were drawn around one side of the vessel wall and part of the lumen. There is no description of where the aorta was assessed, and how the side that was chosen was analysed. 'Total TBR,' the sum of all TBRs over the eight segments was reported. Mean TBR was calculated by dividing the total TBR by eight, given eight segments, rather than the conventional EANM recommended assessment of the mean TBR of all arterial segments analysed. This study reported a significant increase in mean TBRmax between 18 months (p=0.046) and baseline but not at 6 months. The absolute

values for both time points being the same (baseline to 6 months TBR: 1.29±0.12 to 1.32±0.12, p=0.07; baseline to 18 months TBR: 1.29±0.12 to 1.32±0.14, p=0.046). No difference in the change of mean TBR over time was observed between ICI and control group. A sensitivity analysis excluding patients on statins or steroids found an increase in ICI compared to control at 6 months. There was again an increase in patients without pre-existing inflammation (TBR <1.6). This was not observed in the control group. Strengths of this study are its larger numbers, serial PET imaging, and use of a control group. The method of analysis is unclear. The fact that only sections of the arterial wall were included raises the possibility of selection bias. It is also important to note that there is no comment if patients were scanned on different scanners on serial imaging, and no sensitivity analysis was performed to compare those who were scanned on a digital vs non-digital scanner, or in those who were scanned on different scanners over time.

The most recent paper to address this area assessed 156 patients over 4 sequential scans within a 30-month period in patients receiving ICI and those without ICI, using TBRmax of the carotids, iliacs, thoracic aorta and abdominal aorta. Fifty patients received ICI, 106 received no ICI. Scans were performed on two non-digital scanners and one digital scanner, with 60-minute circulation time. Because of the retrospective nature and long study period (over 13 years), sensitivity analyses and statistical methods to adjust for variation in PET scanner used over time were performed. In addition, their analysis was performed at 8 specific locations within each arterial segment, predominantly at points of bifurcation, rather than looking at the whole vessel. Overall, there was no association between ICI use and arterial [^{18}F]FDG uptake ratios. For this analysis, TBRs were corrected to the TBR of the baseline scan to create an arterial uptake ratio. Over time, there was a 2.5% increase in FDG uptake ratio in those on ICI compared to 0.8% in non-ICI patients.

The above studies have provided conflicting evidence on the role of inflammation in ICI accelerated atherosclerosis using [^{18}F]FDG-PETCT. The heterogeneity in imaging protocols, methods of assessment and methods of reporting, and their retrospective nature with opportunistic use of clinical scans

contributes to this. Prospective assessment of ICI arterial inflammation is required with transparent and robust methodology.

Table 1-5. Arterial assessment of ICI large artery inflammation studies to date

	Cancer type	N	Comparator group	PET scanner	Follow up (months)	Key methods	Key results
Poels 2020	Melanoma	10	No	Non-digital	1.5	TBRmax of carotid and thoracic aorta, spleen and bone marrow Whole artery analysed	TBR ↔
Calabretta 2020	Melanoma	20	No	Non digital	4.4±1.6	6 arterial segments (aorta and iliac arteries) analysed Only active segments (TBR ≥1.6) assessed. Unclear if whole artery or individual lesions were analysed	Active lesions (baseline TBR≥1.6): TBR ↑ Non/mildly calcified lesions: TBR ↑ Moderate-severe calcification: TBR ↔
Calabretta 2021	Lymphoma	12	No	Non digital	9.6±4	117 arterial lesions over 6 segments within 12 patients using 1cm^3 VOI No information on how lesions were identified or analysed Compared pre-existing inflammation (TBR≥1.48) vs no inflammation	All arterial lesions: TBR ↑ Pre-existing inflammation (TBR≥1.48): TBR ↔ No pre-existing arterial inflammation: ↑ Non-calcified lesions: TBR ↔ Calcified lesions: TBR ↑

Calabretta 2024	Lung	47	No	Non digital	2.5±1	761 lesions over size arterial segments in 47 patients using 1cm^3 VOI No information on how lesions were identified or analysed. Compared pre-existing inflammation (TBR≥1.6) vs no inflammation	All arterial lesions: TBR ↑ Pre-existing inflammation (TBR≥1.6): TBR ↔ No pre-existing arterial inflammation: ↑ Non-calcified lesions: TBR ↑ Calcified lesions: TBR ↑
Polomski 2024	Melanoma	132	36 Cancer controls 28% RTx 30% targeted therapy	Non-digital & digital	T1: 6 T2:18	1 ROI per arterial segment assessed. carotids and iliacs - a 1cm^2 ROI over the whole vessel aorta: 1cm^2 ROI drawn around one side of the vessel wall. No details of how this section of segment was defined 'Total TBR,' the sum of all TBR's over the eight segments reported. Mean TBR: total TBR/number of arterial segments. No adjustment for different scanners used	TBR at 6 months: ↔ TBR at 18 months: ↑ Change in TBR: ICI vs no ICI: ↔ In a sensitivity analysis excluding patients on statins or steroids found there was an increase between groups at 6 months No pre-existing inflammation (TBR <1.6): ICI ↑ No ICI ↔

Bacmeister 2025	Melanoma Lung Head/neck GI Other	156	106 (70%) cancer controls 52% received chemotherapy 14% targeted therapy 70% radiotherapy	Non-digital & digital Different scanners used per patient	30	4 sequential scans of the carotids, iliacs, thoracic and abdominal aorta 7 VOI analysed per artery at pre-specified sections of each artery Ratio of TBR at each time point, corrected to baseline TBR Statistical methods to adjust for different in PET scanners used over time between patients	TBR over 3 time points compared to baseline: ICI vs no ICI: TBR ↔ Longitudinal time dependent effects: Annual increase rate of TBR: ICI: 2.5% No ICI: 0.8%

GI: gastrointestinal ICI: immune checkpoint inhibitor ROI: 2D region of interest T1: timepoint 1; T2: timepoint 2; TBR: tissue to background ratio VOI: 3D Volume of interest; RTx: radiotherapy

1.9 Aims & Hypotheses

My aims for this thesis are:

Aims

- To assess CV eligibility criteria, CV baseline characteristic reporting and methods of CV safety reporting in ICI+VEGFI combination trials. (Chapter 3)

- To assess [^{18}F]FDG-PETCT markers of arterial inflammation in patients before and after exposure to anthracycline chemotherapy (Chapter 4)

- To assess the optimal reconstruction parameters for large artery atherosclerosis assessment by [^{18}F]FDG-PETCT using state of the art digital PETCT (Chapter 5)

- To prospectively assess large artery inflammation, using [^{18}F]FDG-PETCT, in patient before and after receiving ICI, (Chapter 6)

- To compare the effect of combination ICI+VEGFI on large artery inflammation, using [^{18}F]FDG-PETCT, with ICI alone and with VEGFI alone (Chapter 6)

My hypotheses are:

- CV eligibility criteria exclude patients with CVD from oncological ICI+VEGFI trials and the representation of these trial populations to real world patients is unknown because of lack of baseline characteristics reporting(Chapter 3)

- CVAE reporting is heterogenous and impacts on the interpretation of CV safety of ICI+VEGFI regimens (Chapter 3)

- Anthracycline exposure is associated with large artery inflammation, as assessed by [^{18}F]FDG-PETCT (Chapter 4)

- EANM recommendations for atherosclerotic assessment by [^{18}F]FDG-PETCT are not applicable to state of the art digital PETCT scanners (Chapter 5)

- Exposure to ICI is associated with increased arterial inflammatory activity, by [^{18}F]FDG-PETCT, in patients receiving ICI, compared to VEGFI (Chapter 6)

- ICI associated arterial inflammatory activity is modified by co-administration of VEGFI, as assessed by [^{18}F]FDG-PETCT (Chapter 6)

Chapter 2 Methods

The central theme of this thesis is the investigation of anti-cancer treatments by [^{18}F]FDG-PETCT and arterial inflammation. I assessed:

- arterial inflammation, by [^{18}F]FDG-PETCT, in a prospective study of patients receiving either ICI monotherapy, VEGFI monotherapy or ICI+VEGFI combination therapy.

- the quality and robustness of the CV safety data from oncology trials of ICI+VEGFI combination therapy;

- arterial inflammation in patients exposed to anthracyclines;

- EANM recommendations on how best to assess arterial inflammation by PETCT when using modern, state of the art imaging technology.

A separate scientific manuscript addressing each of these research questions is included in this thesis. Details of the methods pertaining to each chapter, is outlined in each manuscript. Here I present general principles of the methods, including technical aspects of PETCT. I provide further detail on each chapter, including the rationale for the methods used.

2.1 Research questions

This thesis addresses the following research questions:

1. To what extent do oncology drug trial study designs impede the interpretation of CV safety data in combination ICI/VEGFI efficacy trials, by their eligibility criteria and AE reporting? (Chapter 3)

2. Is anthracycline therapy associated with arterial inflammation when assessed by [^{18}F]FDG-PETCT? (Chapter 4)

3. What are the optimal parameters to assess arterial inflammation by [^{18}F]FDG-PETCT on a digital PET scanner? (Chapter 5)

4. Is ICI exposure associated with arterial inflammation, as assessed by [^{18}F]FDG-PETCT? (Chapter 6)

5. Is co-administration of VEGFI with ICI associated with more arterial inflammation than monotherapy? (Chapter 6)

2.2 General methods

2.2.1 Justification for thesis in alternate format

The distinct research studies included in this thesis are linked by the over-arching theme of arterial toxicity in cancer treatment. Given this, the compilation of separate scientific publications into one thesis is justified. All research included in this thesis was undertaken while I was registered as a post-graduate research student at the University of Glasgow. This thesis contains three published manuscripts, and one manuscript prepared for publication. All of which were published under CC-BY copyright.

2.2.2 Acknowledgement of the contributions of others

Where work is presented in this thesis that I did not directly perform myself, the contributions of others are explicitly stated within each results chapter. This primarily relates to histopathological analyses in Chapter 4 that were performed by Miss Caitlin Fountain, under the supervision and leadership of Dr Giselle Melendez. In Chapter 5, phantom data collection and analysis was performed by Mr Alastair J Gemmell. Interpretation of the phantom data was performed by myself and Mr Gemmell. The methods relating to their work are described within the relevant results chapters.

2.2.3 Consent and ethics

All of the studies described in this thesis were performed in accordance with the Declaration of Helsinki. All studies had appropriate ethical approval and Administration of radioactive Substances Advisory Committee (ARSAC) approval, where applicable.

2.2.4 Study settings

All of the clinical studies were conducted at the Beatson West of Scotland Cancer Centre (BWoSCC) and the West of Scotland PET Centre. The BWoSCC is the regional cancer centre for four different health boards covering a population of approximately 2.8 million. The PET Centre provides care for a larger region, but all PET imaging analysis was performed in patients who received care within the BWoSCC and the PET Centre, within NHS Greater Glasgow & Clyde.

2.2.5 Data handling

I was responsible for the coordination of data for each study. All data were stored in compliance with General Data Protection Regulations (GDPR) 2021. No participant personal data was stored on a personal computer or laptop. Each participant was assigned a unique study identifier and all data was analysed and processed using the pseudonymised identifier. For the prospective study (BioCAPRI), data were recorded using an online electronic case report form (eCRF) on a Good Clinical Practice approved data management system (Castor EDC, Amsterdam, Netherlands). The eCRF was developed by myself.

2.3 Arterial inflammatory assessment by PET imaging

PET scanners use radiotracers to give metabolic insights within the body. PET scanners detect the amount of radioactivity (measured in kilo-becquerels per millilitre, kBq/ml) within the scan field. The measured radioactivity can vary with the amount of FDG injected and the patient size. In order to make quantitative assessment, FDG is measured by the standardised uptake value (SUV), Equation 1[158]. This SUV can then be used to assess arterial inflammation using the tissue to background ratio (TBR).

Equation 1 Standardised uptake value (SUV)

$$Standardised\ uptake\ value\ (SUV) = \frac{radioactivity\ measured\ (kBq/ml)}{FDG\ dose\ injected(MBq/ml)\ /\ weight(kg))}$$

2.3.1 Tissue to background ratio (TBR)

TBR was been validated in numerous clinical settings for assessment of arterial inflammation. [146,159,160]. TBR analysis was performed on sequential 4mm thick 3-dimensional polygonal volumes of interest (VOI) of the artery. Within each arterial VOI, the maximal and mean SUV of [^{18}F]FDG was corrected to the blood pool activity in the superior vena cava. The most commonly used and widely validated quantitative assessment is TBR max, using the maximal SUV within the arterial VOI. TBR values of every VOI were then averaged for each arterial segment. Analysis was performed in concordance with EANM recommendation for arterial activity including TBRmax, TBRmean, activity within 'active segments' (defined as a TBRmax ≥1.6) and most diseased segment (MDS, the three consecutive VOIs centred around the VOI with the highest activity to represent the most intense lesion)[138], Figure 2-1.

Figure 2-1 Tissue-to-background ratio (TBR) for arterial analysis

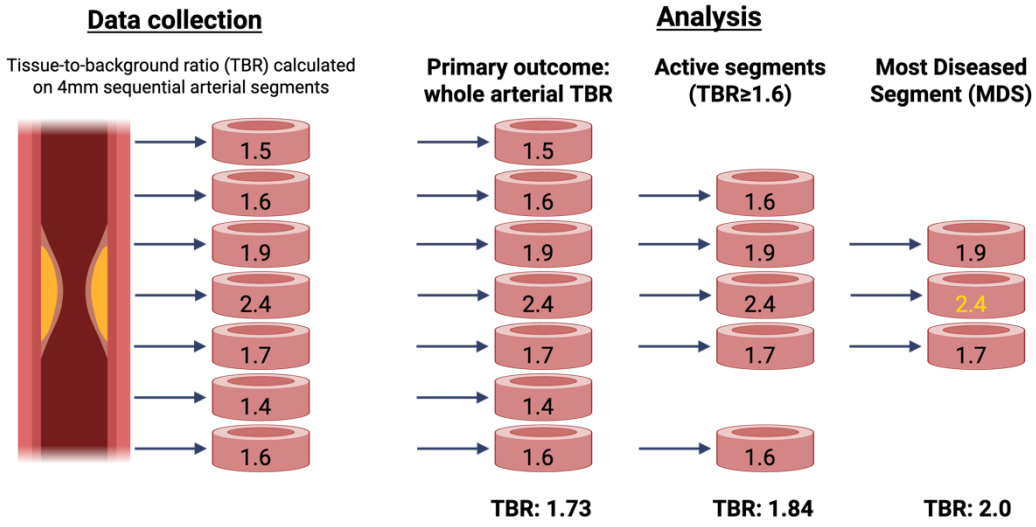

Created in BioRender. Rankin, S. (2025) https://BioRender.com/gny8pul Adapted from Tawakol et al[161].

The threshold of TBRmax ≥1.6 indicating active disease comes from historic data with small patients numbers[145]. It has been used in various clinical settings and used as endpoints for clinical trials. There are many factors within PET acquisition that can influence the TBR value, depending on parameters used[150]. These acquisition parameters are detailed below, Section 2.7. The impact of imaging protocols, particularly using digital PET scanners, on TBR values is not

established and there is no international guidance. This is discussed in Chapter 5.

As this was the first study of PETCT atherosclerotic assessment undertaken in Glasgow, intra- and inter-observer variability was important to assess. 10% of scans from Chapter 4 were randomly selected and re-analysed by two trained observers (SR, DC) for inter-observer and intra-observer agreement. To minimise recall bias, intra-observer repeatability was assessed by the same trained researcher (SR) using repeated assessments performed 3 months apart in random order. Intra- and interobserver variability was assessed by consistency intra-class correlation (ICC) coefficient.

Blood pool

For Chapter 4 and 6, blood pool activity was calculated by taking the mean SUVmean of ten sequential 4mm high cylindrical VOIs with a 3mm radius within the superior vena cava, starting at the confluence of the innominate vein moving caudally to the heart. Comparison of different blood pool regions, recommended by EANM, and their potential impact on TBR calculations is discussed in Chapter 5.

Arterial landmarks

Arterial analysis was performed using anatomical landmarks. Aortic analysis started at the ascending aorta, at the inferior aspect of the right pulmonary artery, and stopped when the descending aorta passed through the diaphragm. The abdominal aorta analysis began inferior to the renal arteries down to the aortic bifurcation. Iliac arteries were analysed from the aortic bifurcation to the femoral bifurcation. The right carotid artery was analysed from the bifurcation of brachiocephalic artery to the approximate level of the carotid bifurcation, at the cricothyroid cartilage. The left carotid artery was analysed from the aortic arch to the carotid bifurcation.

Interfering tissue

Care was taken to ensure activity from adjacent tissue, such as oesophagus or adjacent malignant tissue, was not included in the arterial analysis. Areas of

possible interference were first reviewed by visual assessment. Areas of interference were then determined semi-quantatively by assessing proximity to the vessel, maximal SUV within the area of possible interference and the SUV of the tissue immediately surrounding the artery to determine an area of interference. When an area of interference was identified, the adjacent arterial tissue was excluded from that 4mm region of interest, ensuring a clear margin. A minimum of a quarter of arterial tissue was excluded, depending on the degree of interference. If interference affected more than two thirds of the aortic ROI, the 4mm segment of aorta was not included in analysis. Any areas of dubiety were reviewed by a second reporter and consensus was made.

2.3.2 Developing a PET imaging protocol for arterial assessment

As no research in arterial PET research had been performed in Glasgow prior to my PhD, I was responsible for establishing a protocol for arterial PET imaging.

For all PET analysis, FusionQuant v1.21 software (Cedars-Sinai Medical Centre, Los Angeles) was used. FusionQuant is a research software. It was been used in numerous research studies worldwide. As FusionQuant is not a commercial software, there is no publicly available data on the quality or validation of the software. Commercial software is tested to an Image Biomarker Standardisation Initiative (IBSI) standard. Testing was performed to ensure comparative accuracy and local validation with the commercial software package, Hermes (Hermes Medical Solutions, Sweden). These data are presented in appendix 8.3. Ensuring FusionQuant performed adequately was important as the EANM has reported that different software systems can affect the PET assessment[148].

2.3.2.1 Using a digital PETCT system

All scans performed in the BioCAPRI study were performed on a digital PETCT scanner, Siemens Biograph Vision 600 (Siemens, Erlangen, Germany). A digital scanner uses silicon photomultipliers (SiPM), instead of the standard photomultiplier tubes[162]. In analogue, non-digital systems, PET images are created from photons detected by photomultiplier tube detectors linked with scintillation crystals to create a radiological image, Figure 2-2. As SiPM are smaller than photomultiplier tubes, they offer higher resolution and

sensitivity[149]. Digital PETCT can achieve better image quality, improved small lesion detectability and reduced acquisition time[163]. The Biograph Vision scanner also offers continuous bed motion scanning. Other PET scanners create their image by performing a series of scans at different bed positions (head, chest, torso etc) and merging them together to create one image, known as 'step and shoot' acquisition.

Figure 2-2 Creation of a PET image

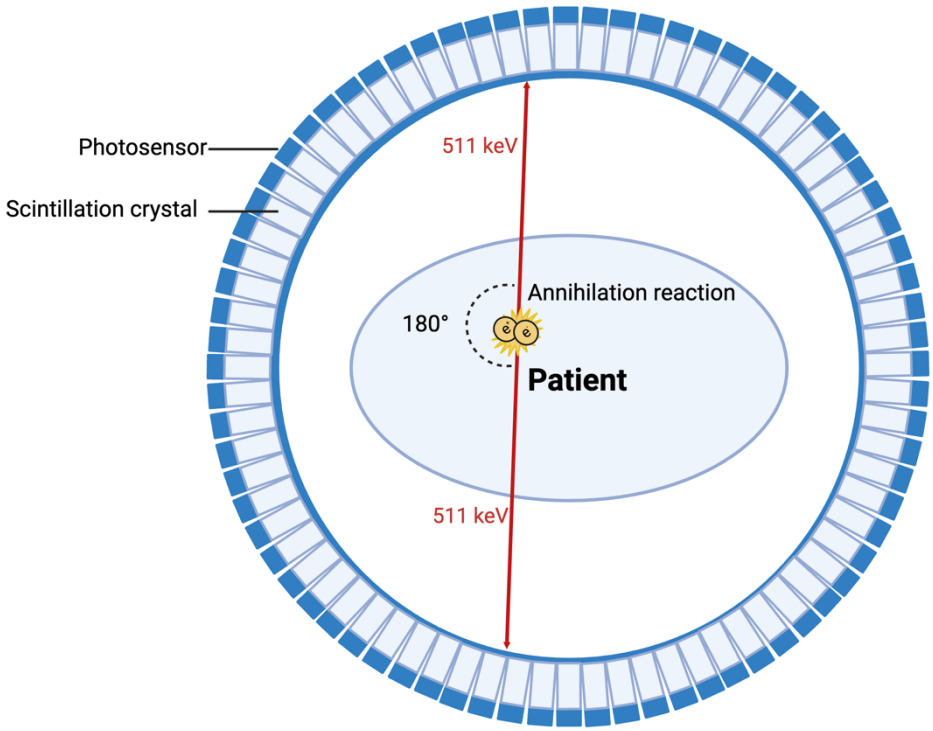

Adapted from Turkington, Introduction to PET instrumentation, 2001[164], Created in BioRender. Rankin, S. (2025) https://BioRender.com/et19kq5 .

While digital PET imaging clearly has benefits for atherosclerotic imaging, it also posed a challenge for developing my atherosclerotic PET imaging protocol in Glasgow. EANM published a position paper with recommendations on how best to optimise PET imaging protocols for atherosclerotic assessment in 2016[138]. This was used for the development of the protocol. These recommendations pre-date the advent of digital scanners and therefore may not apply to digital scanner used in my thesis and imaging protocol. Assessing the EANM recommended parameters with locally assessed and optimised parameters is the focus of Chapter 5. From doing this work, I was able to create a robust imaging protocol for the BioCAPRI study.

2.3.3 Retrospective & prospective PET arterial assessment methods

The results presented in Chapters 4-6 use [^{18}F]FDG-PETCT for assessment of large arteries. Each chapter contains detailed methods of the imaging parameters used. Many of the methods for PET acquisition and analysis was the same for all three PET imaging chapters. There were some key differences in the methods of the studies. This is mainly due to the retrospective (Chapter 4) and prospective (Chapter 6) nature of the studies. The key differences were:

- Scanners and imaging protocols used
- Circulation time
- Acquisition time

2.3.4 Scanners used & protocols used

The prospective study (Chapter 6) used only the digital scanner, Biograph Vision 600, and used a protocol optimised for atherosclerotic imaging. Chapter 4 includes analysis of both digital and non-digital scanners, and used protocols created for oncological assessment. The imaging protocols for the scanners used in Chapter 4 varied to create the most optimal image for each individual scanner. Chapter 5 compares of the accuracy of digital vs non-digital scanners.

2.3.5 Circulation time

To further enhance the PET image quality for arterial assessment in the prospective study, I used a longer circulation time (time from injection to scanning) and a longer acquisition time than used in routine clinical practice.

PETCT scans used for oncological assessment typically use a 60-minute circulation time. Longer circulation times allow for more FDG to be washed out from the blood pool and excreted in the urine. This improves contrast between arterial uptake and blood pool uptake[138,165]. For the prospective study, a 90-minute circulation time was used.

The EANM recommend a 120-minute circulation time for atherosclerotic assessment[138]. The deviation from the EANMN recommendation was to ensure the study was practically feasible. I prioritised patient comfort and to minimise the impact on the clinical service. The EANM recommendation, and the evidence to support the recommendation, predates digital scanners. The recommendation for 120-minute circulation time is supported by only two pieces of evidence[165,166]. One of these studies recommends at least 90-minutes for optimal assessment[166], which my protocol is in accordance with.

In Chapter 4, arterial assessment was performed retrospectively on clinical PETCT scans. These PET scans were acquired using a 60-minute circulation time. EANM advise that only large arteries be assessed for inflammation in retrospective studies, as the protocol is not optimised for atherosclerotic imaging[138]. Given this advice, only the thoracic aorta was analysed in Chapter 4.

2.3.5.1 Acquisition time

To maximise detection of smaller arteries, patients in the prospective study were scanned for longer than would be used in routine clinical practice. I used a 0.7mm/second scan speed using continuous bed motion. In routine clinical practice, 1-1.5mm/second scan speeds are used.

EANM recommends that, for atherosclerosis assessment, patients are scanned for 8 minutes/bed position (for 'step and shoot' acquisition)[138]. Continuous bed motion scanning had not been developed at the time of the EANM position paper. Previous comparison of shorter acquisition times vs longer acquisition times reported minimal effect on SUV, when comparing 8 mins/bed to 4 mins/bed[166]. 0.7mm/second equates to 5 minutes/bed position. A quicker scan speed was used for pragmatic reasons, such as patient comfort, to minimise impact to the clinical service and to limit the effect of artefact from respiration.

2.3.6 Calcium scoring

Arterial calcification assessment was performed on the CT component of the PETCT scan using a dedicated workstation (Vitrea Advanced, Vital Imaging, Toshiba Systems, Minnesota, USA). A density threshold of 130 Hounsfield units

with a 3-pixel threshold on 3mm slice thickness was used for defining the presence of calcium[167]. A cumulative calcium score of each arterial segment, and all arterial segments, was calculated as previously described[167]. Calcium score is created from the density of calcium, measured in Hounsfield units, and volume of calcium, measured in cm^3, but the calcium score itself has no units.

2.3.7 Statistical analysis

All statistical analyses were performed using STATA Version 17 (StataCorp 2021. Stata Statistical Software. College Station, Texas: StataCorp LLC). Statistical significance was defined as two-tailed *p* value <0.05 for all tests. R package with ggplot2 was used for additional figures. Continuous data with normal distribution are presented as mean ± standard deviation (SD), and skewed data are presented as median and interquartile range (IQR). Between groups comparisons were made using paired t tests, linear regression and ANOVA or non-parametric equivalents as appropriate. For the prospective study, a linear mixed effects model was used to account for multiple observations per patient scan.

2.4 Cardiovascular Eligibility Criteria and Adverse Event Reporting in Combined Immune Checkpoint and VEGF Inhibitors Trials (Chapter 3)

I was interested in understanding whether oncological efficacy trials of combination ICI+VEGFI trials allow meaningful insights into the potential for CV adverse events when used in clinical practice. I investigated:

- to what degree are patients with CVD excluded from these trials and how were CVD exclusions defined?
- What is reported about the trial population and their CV risk?
- Are CVAEs being reported and if so, how are they defined and by whom?

I performed a systematic review of the literature of oncological efficacy trials in patients receiving combination ICI+VEGFI therapy. A systematic search was performed on three research platforms (Embase, MEDLINE and Cochrane library) using a comprehensive search term. The protocol for my search was registered

on PROSPERO (CRD42022337942) and used the Preferred Reporting Items for Systematic reviews and Meta-Analyses (PRISMA) statement guidance[168].

I determined that reporting of patients' CV health and CVAEs was so heterogenous and inadequate that it would have been inappropriate to perform a meta-analysis. Full methods, including the search terms, are within the Chapter 3. The PICO framework is available in Appendix 8.1.

2.5 Arterial effects of anthracycline: structural & inflammatory assessments in non-human primates and lymphoma patients (Chapter 4)

This section outlines details the methods used in the study to assess arterial inflammation by [^{18}F]FDG-PETCT in patients with lymphoma receiving anthracycline chemotherapy. This was a retrospective analysis of 101 patients with diffuse large B-cell lymphoma (DLBCL). The methods section of Chapter 4 also outlines the histopathology and animal model study methods.

2.5.1 Ethical approval

Ethical approval was granted by the West of Scotland Research Ethics Committee (22/WS/0180). This was a retrospective observational study with no change in patient management and as such no written consent was required. In routine clinical practice, prior to each clinical PET scan, patients were asked to consent for images to be used in future research as part of the routine clinical pre-PET questionnaire (Appendix II). Only those who consented were included.

2.5.2 Study population

I performed a retrospective review of [^{18}F]FDG-PETCT scans of patients with DLBCL at BWoSCC between 2019 to 2023. End of treatment PETCT scans were assessed and compared to baseline staging PETCT.

Patients with DLBCL were chosen for the study cohort for a number of reasons. DLBCL typically occurs in an older population, with a median age between 60-70, and therefore is a patient cohort with high prevalence of comorbidities[169]. It was anticipated that this would enrich any potential signal for arterial inflammation.

DLBCL is commonly treated with anthracyclines and PETCT is used both for staging at baseline and to assess response to treatment. In other types of lymphoma, such as Hodgkins lymphoma, PET imaging is predominantly only used for staging but not used for follow up imaging, within the BWoSCC. These factors made patients with DLBCL a suitable cohort for the retrospective study.

The eligibility criteria were:

Inclusion criteria:

- aged 18 years and older
- treated using anthracycline regimens receiving a cumulative equivalent dose of >150mg/m^2 of doxorubicin.

Exclusion criteria:

- those treated at a hospital that was not in the NHS Greater Glasgow & Clyde catchment area
- incomplete medical records
- concurrent thoracic radiotherapy
- technically inadequate scans (such as non-diagnostic tracer uptake)
- blood glucose >11mmol/L before either scan
- patients whose arterial FDG uptake could not be quantified due to significant interference from adjacent lymphoma
- suspected or confirmed vasculitis on the baseline scan
- baseline PETCT was more than 3 months before starting chemotherapy

2.5.3 Data Collection

Data was collected using a pre-specified proforma on Microsoft Excel stored on an encrypted password protected file on an NHS computer. Detailed baseline demographic data, including past medical history, cancer history, drug history, were collected from electronic case note reviews and the electronic chemotherapy prescribing system, ChemoCare. Baseline CV risk stratification was performed using the European Society of Cardiology (ESC) baseline cardio-oncology CV risk stratification assessment tool[170]. Response to treatment was collected by the Deauville score reported on the clinical scan. As part of the clinical radiologist's report, response to treatment is reported using the five-point Deauville score (Table 2-1)[171].

Table 2-1 The Deauville score

Deauville score	Definition	Interpretation
1	No uptake above background activity	Complete metabolic response
2	Uptake at an initial site that is lower than or equal to mediastinum	
3	Uptake at an initial site that is more than the mediastinum but lower than or equal to the liver	
4	Uptake at an initial site that is moderately increased in comparison to the liver	Residual cancer activity (partial response, stable disease, progressive disease)
5	Uptake at an initial site that is markedly increased in comparison to the liver	

2.6 Biomarker and imaging characterisation of inflammatory atheroma in patients receiving immunotherapy and angiogenesis inhibitors (Chapter 6)

I performed a prospective study of patients with cancer receiving ICI, VEGFI and ICI+VEGFI combination therapy to assess large artery inflammation, measured by [^{18}F]FDG-PETCT.

The prospective study was approved by the West of Scotland Research Ethics Committee (REC) 05 in July 2022 (REC reference 22/WS/0085) and approval by ARSAC for the administration of radioactive substances (ARSAC Ref AA-4580).

The study was registered on clinicaltrials.gov (NCT06597045). An overview of the study design was shown in Figure 2-3.

Figure 2-3 Schedule of study visits and investigations

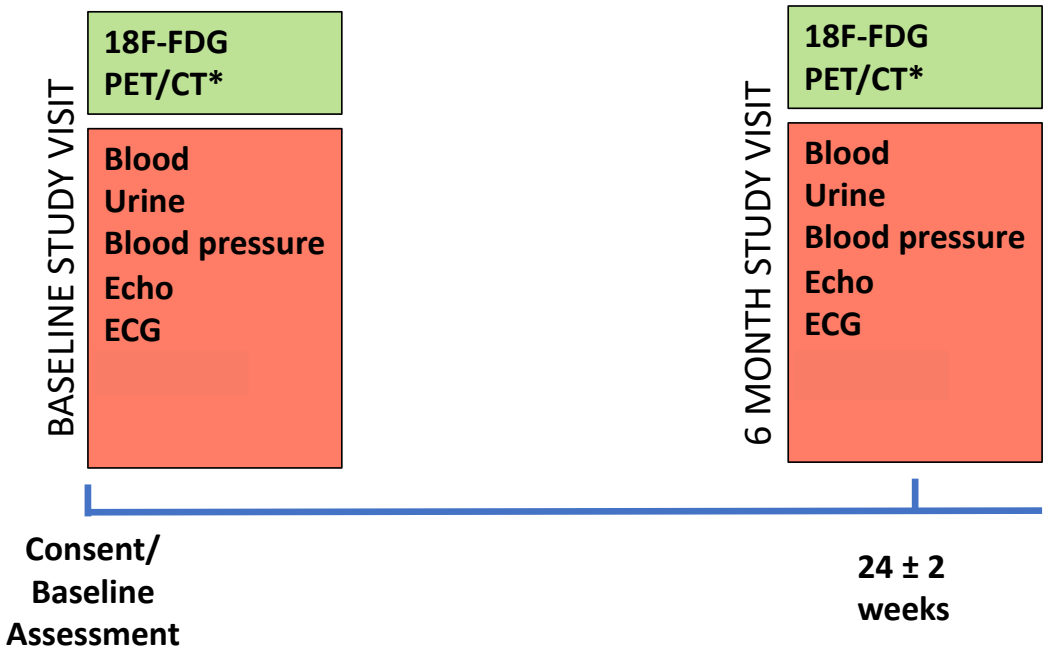

*where possible all tests were performed at the same visit however to minimise impact of patients, if required, PETCT was performed on another day. Abbreviations: Echo – echocardiography; ECG – electrocardiography; 18F-FDG-PETCT – 18F-fluorodeoxyglucose positron emission tomography computed tomography.

2.6.1 Participant identification and consent

Patients who agreed to participate in the study provided written informed consent *(*Appendix). Copies of the consent form were given to the patient and filed in their medical case notes. A letter summarising the study aims and the participant's enrolment was issued to the participant's general practitioner, as well as contact information for the research team (Appendix).

2.6.2 Study Funding

This research was sponsored by the National Health Service and funded by an investigator-initiated study grant from Roche Diagnostics, Germany.

2.6.3 Study Setting and Recruitment

All patients were recruited from BWoSCC in Glasgow, UK. A screen log was recorded using standard documentation supplied by the Glasgow Clinical Trials Unit, including those who did not participate. Patients recruited into this study

were referred to the oncology outpatient clinical service via standard referral pathways within the region from the local hospital by the relevant team. Patients were recruited over 22-month period (15th August 2022 – 13th June 2024).

2.6.4 Power calculation

Based on prior studies, using TBRmax as primary outcome, a sample size of 16 patients per group would have 80% power at 5% significance to detect a between groups difference of 10-15% [142,151,160]. Furthermore, given the paired nature of the data, within group assessments would have greater power than this. The primary outcome was the change in TBRmax of all arterial segments in patients receiving ICI+VEGFI combination therapy vs ICI alone or VEGFI alone

2.6.5 Study Population

I studied patients commencing 3 different treatment regimens: VEGFI monotherapy, ICI monotherapy, and ICI+VEGFI combination therapy. To reduce selection bias, I aimed to recruit a near-consecutive population as a truly consecutive, prospective population. I prospectively screened all patients referred to the renal and hepatocellular oncology teams. These two teams use all three treatment regimens as first line treatment and therefore all patients commencing SACT would receive one of the treatment regimens investigated in this project. Any patient who was deemed to potentially suitable for inclusion was highlighted to me by consultant oncologist in the teams: melanoma, thyroid, sarcoma, gynaecology, and colorectal.

2.6.6 Inclusion Criteria

Patients were invited to participate in the study if they met all the following criteria:

- Age ≥ 18 years
- Diagnosis of cancer and considered suitable for ICI, VEGFI or ICI+VEGFI combination therapy

2.6.7 Exclusion criteria

To ensure the study population represented a real-world cancer population, the only exclusion criteria for the study was:

- Patients who are unable or unwilling to provide valid consent for the study
- Patients with a history of diabetes on current oral treatment or insulin
- Patients with planned concurrent thoracic or abdominal radiotherapy with SACT

Patients with a history of diabetes that were not controlled with diet alone were excluded. Anti-diabetic medication can affect PETCT scanning and interpretation: insulin can alter FDG uptake and metformin causes high FDG uptake within the bowel. Patients with planned concurrent thoracic or abdominal radiotherapy were excluded as radiotherapy can cause inflammation in the radiation beam, which may include the aorta, and affect interpretation of PETCT.

2.6.8 Data collection

Detailed demographic and clinic data were collected for each patient at both visits. Data were obtained through history, clinical examination and review of medical records. Each participant was allocated a unique and anonymous study

identification number. Baseline data were recorded on the eCRF under the following headings: demographics (including past medical history, cancer history, medication history including proposed SACT, study procedures (clinical examination findings, blood pressure (BP), electrocardiography (ECG), urine and blood biomarkers, echocardiography and PETCT data). On follow up visits, all AEs (CTCAE grade 2 or above) were logged. All AEs are assessed with each prescription of SACT and completed by the oncological clinical team using a clinical assessment protocol. Clinically significant events, such as hospitalisation or new clinical diagnoses, were recorded through review of the medical health records and clinical history with the participant. Immune mediated adverse events were characterised by any of the following: tissue or imaging supportive of an immune mediated process, the initiation of immunosuppressants, and a diagnosis made and documented by a consultant physician. CVAEs were recorded using the International Cardio-Oncology Society definition of cardiovascular toxicities of cancer therapy. CVAEs were reviewed by two cardiologists.

2.6.9 Study procedures

At each visit, study procedures outlined in the study design figure (Figure 2-3) were performed. The methods of these are outlined below.

2.6.9.1 Blood pressure monitoring

BP monitoring was performed in accordance with ESC guidance[172]. BP was measured at both visits a minimum of three times. BP was initially measured in both arms. When there was a >15mmHg difference in one side, the arm with the higher BP was used for subsequent measurements. Additional measurements were performed if there was a >10mmHg difference in the first two readings. An average of the last two BP readings was taken. In addition to this, on follow up visit, review of the medical records was performed to collect data on treatment induced hypertension. VEGFI-induced hypertension was defined as a new rise in BP (either a >20mmHg increase in systolic BP or ≥140/90 mmHg or ≥130/80 mmHg if CV risk >10%, as per ICOS definition) or the initiation or escalation of anti-hypertensive therapy[14].

2.6.9.2 Echocardiography

Echocardiography allows non-invasive assessment of heart structure and function by 2D and 3D analysis and Doppler echocardiography. Patients underwent transthoracic echocardiography at baseline and follow up visits at BWoSCC. The images were obtained by myself and members of the cardiac physiology department. The study echo protocol is in Appendix VI – BioCAPRI echocardiography protocol and encompasses the British Society of Echocardiography minimum dataset. I performed analysis on all images.

Left ventricular ejection fraction (LVEF) assessment was performed by 2D Simpson's biplane method for quantification of LVEF. This test relies on accurate tracing of the endocardial borders to calculate left ventricular volume. In cases where sub-optimal image quality precluded volumetric analysis, an estimated ejection fraction was given. A clinical report for each echocardiogram was made available to the clinical team and filed in the medical records.

Echocardiographic data was collected for baseline characterisation, adverse event reporting, and to allow pooling of echocardiographic data with other studies performed in the University of Glasgow in the future.

2.6.9.3 Electrocardiography

Each patient underwent a 12-lead ECG at baseline and follow up visit using a MAC 5500 HD recorder (GE healthcare) in the Clinical Research Unit in the BWoSCC. At each visit the rate rhythm, PR, QRS and QTc intervals were recorded as well as presence or absence of bundle branch block, ST segment deviation and left ventricular hypertrophy (LVH). LVH was defined using the Sokolow-Lyon index.

2.6.9.4 Biomarkers

High sensitivity troponin T (hsTnT), N-terminal pro B-type natriuretic peptide (NT-proBNP), growth differentiation factor-15 (GDF-15), high sensitivity C-reactive protein (hsCRP), lipoprotein(a) (lp(a)), total cholesterol, triglycerides, high density lipoprotein (HDL-cholesterol), apolipoprotein A (ApoA) and apolipoprotein B (ApoB) were measured using a Roche Cobas autoanalyser

(Roche Diagnostics, Rotkreuz, Switzerland). Intracellular-adhesion molecule-1 (ICAM-1), vascular cell adhesion molecule-1 (VCAM-1), myeloperoxidase (MPO), p-selectin, interleukin-6 (IL-6), endothelin-1 (ET-1), tissue necrosing factor-α (TNF-α), VEGF, tissue plasminogen activator (tPA) and plasminogen activator inhibitor-1 (PAI-1) were measured by ELISA (BioTechne ELLA automated ELISA analyser; Minneapolis, Minnesota, United States).

2.7 Technical aspects to PET imaging (Chapter 5)

There are technical aspects of PETCT imaging that are not explained elsewhere in this thesis. As Chapter 5 was written for a nuclear medicine journal, there is a high level of assumed understanding of PET principles. Below is a summary of basic PET methods that are not detailed in the publications.

2.7.1 Phantom analysis

Various techniques and mathematical algorithms are used to reconstruct raw PET data collected into an image. Changes in reconstruction parameters can have great impact on large artery assessment. In order to quantitively assess and compare these reconstruction parameters, phantom analyses were performed.

A ‘phantom’ is a term used in medical imaging referring to objects used to simulate the human body[173]. In PET imaging, glass spheres are filled with FDG which are then scanned. As the concentration of FDG within the sphere is known and pre-determined, the true concentration of FDG can be compared to the amount of FDG measured by the scanner. This allows for calibration and evaluates performance of scanning protocols. Phantoms were used in local validation, to develop the imaging protocol, and within Chapter 5. I used two different phantoms to emulate different arterial size. The first was a National Electrical Manufacturers Association (NEMA) phantom with sphere diameters of 10-37 mm to approximate larger arteries in the abdomen and chest and a smaller custom phantom to replicate smaller arteries in the neck and legs (diameters 5-13 mm), Figure 2-4.

Figure 2-4 Body Phantoms. Left: NEMA Torso phantom. right: custom "neck" phantom. (Images supplied by Alastair Gemmell with permission)

2.7.2 Recovery coefficients

Comparison between different reconstructions can be performed with quantitative recovery coefficients (RC). The RC was calculated for each of the spheres using the formula:

Equation 2 Recovery coefficient

$$Activity\ Recovery\ Coefficient\ (ARC) = \frac{A}{a} \quad [174]$$

$A = Activity\ concentration\ measured\ in\ sphere$

$a = Known\ activity\ concentration\ in\ sphere$

For both local validation work and for the results within Chapter 5, RCs from different reconstructions were plotted against sphere diameter and a best-fit curve fitted using a logistic function[175]. This analysis was performed by Alastair Gemmell. The interpretation of these analyses and implementation of the results to develop the protocol was done by myself and Alastair Gemmell, with supervision from Dr Sandy Small.

The optimal image reconstruction is one that quickly reaches an RC equal to 1.0 (known as convergence) and stays at 1.0. Often smaller object detection is less precise, due to inherent limitations within PET scanning, resulting in lower RC values. PET scanners are typically not able to reach convergence purely from detection alone. Additional reconstructions are required to improve the image

quality and convergence. There are additional methods to quantitatively assess performance[176]. These are discussed in Chapter 5.

2.7.3 Methods to improve spatial resolution of PETCT scanning

PET imaging measures the spatial distribution of an active functional process, such as glucose metabolism using detection of radioactivity. The PET image is created from the release of two photons (γ rays) released from the annihilation reaction of a positron. These photons travel in 180 degrees of each other[134]. The two photons are detected by the scanner at almost exactly the same time, Figure 2-2. This is known as a true 'coincidence' event[177]. The PET scanner detects these photons and determines where the annihilation reaction occurred by the line of travel the two photons follow, known as the line of response. This is the basis of PET imaging. In reality, there are many confounding factors which can interfere with this process. PET technology can correct for a number of these confounding factors using a series of mathematical algorithms.

2.7.3.1 Errors in creating the PET image

There are multiple events that can occur to degrade the quality of creating the PET image, Figure 2-5. These issues can be addressed by various mathematical algorithms, Figure 2-6.

Figure 2-5 Errors in PET detection

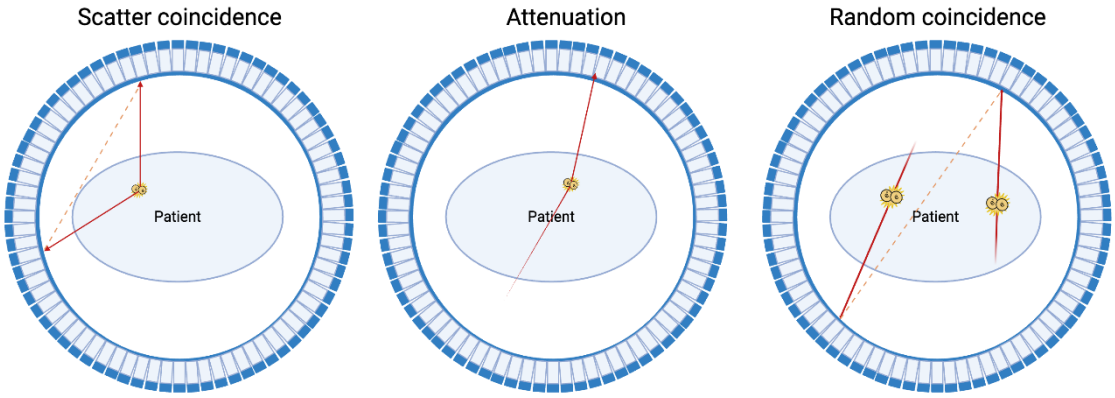

Scatter coincidence: If a photon interacts with an electron on its travel, it can alter the travel of one of the photons. This incorrect line of response is then used for creating the image. **Attenuation**: the speed and energy of photons vary, depending on the density of the tissue it is travelling through. Photons from the skin are very easily detected by the scanner. The speed, and possibly direction, of photons from deeper tissues can be attenuated, reducing image quality. **Random coincidence:** A single photon from two random annihilation reactions can incorrectly be detected as a coincidence event. Adapted from Turkington, 2001[163]. Created in BioRender. Rankin, S. (2025) https://BioRender.com/fxwifyi

2.7.3.2 Attenuation correction

Attenuation correction corrects for the fact that the energy and direction of a photon can be attenuated by the tissue it is travelling through. It performs a corrective process by creating an attenuation map from the CT image[134], Figure 2-6.

Figure 2-6 Attenuation correction & effective iterations

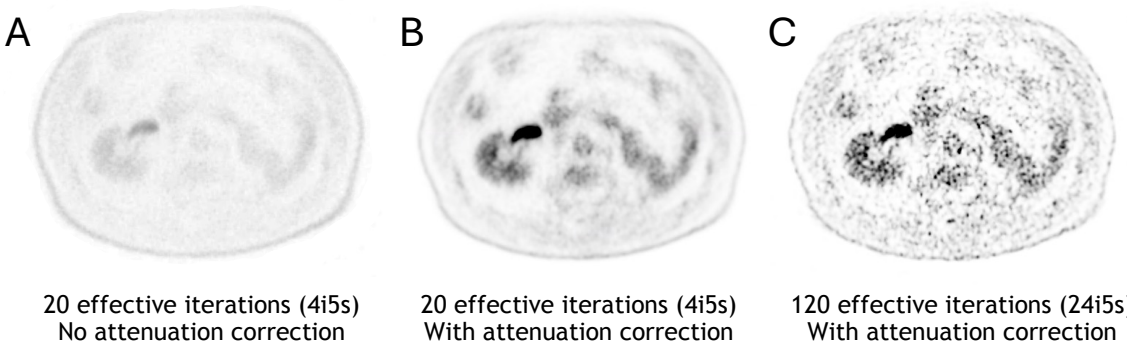

Representative images from a BioCAPRI participant and the effect of reconstruction parameters on the final image. **A**: 20 effective iterations with no attenuation correction. The high uptake from the skin and low uptake from deeper tissues is evident. **B:** 20 effective iterations with attenuation correction leads to improved uptake within the abdomen to account for the dense tissue photons must travel through to reach detection by the scanner. **C:** 120 effective iterations. Increasing the number of iterations results in increased noise in the image.

2.7.3.3 Time of Flight (TOF)

Time-of-Flight (TOF) is a corrective algorithm that improves the spatial resolution of PET imaging by measuring the subtle time differences between the two photons being detected and therefore can localise the exact location of the annihilation reaction[177].

2.7.3.4 Partial volume effects and point spread function

PET imaging is at risk of partial volume effects (PVE) and errors. This causes blurring of the image,

Figure 2-7. Smaller vessels and vessels near areas of high activity are more susceptible to PVE therefore minimising its effect is important for atherosclerotic assessment[137]. Point spread function (PSF) reduces the amount of blurring and the impact of scatter to improve spatial resolution.

Figure 2-7 Partial Volume Effect & the effect of voxel matrix and photosensor size.
A

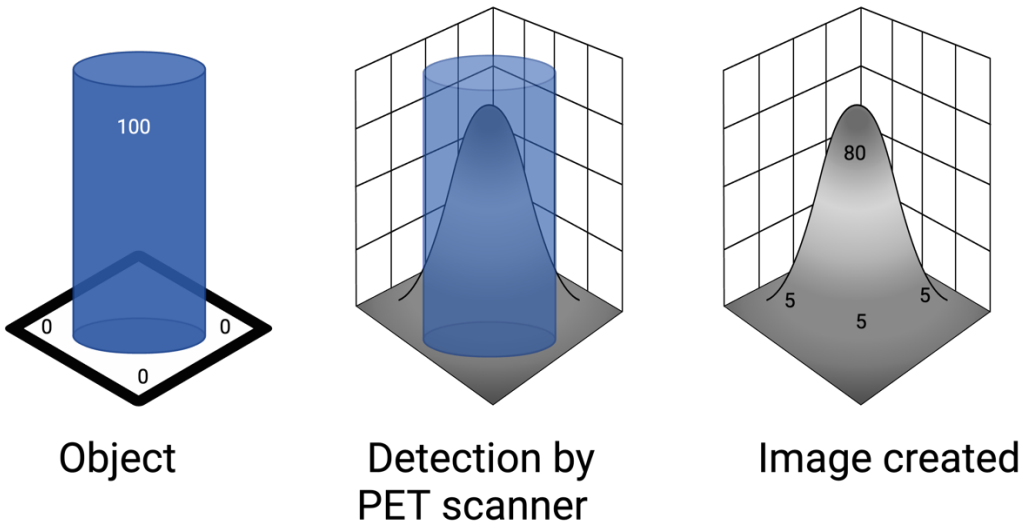

B

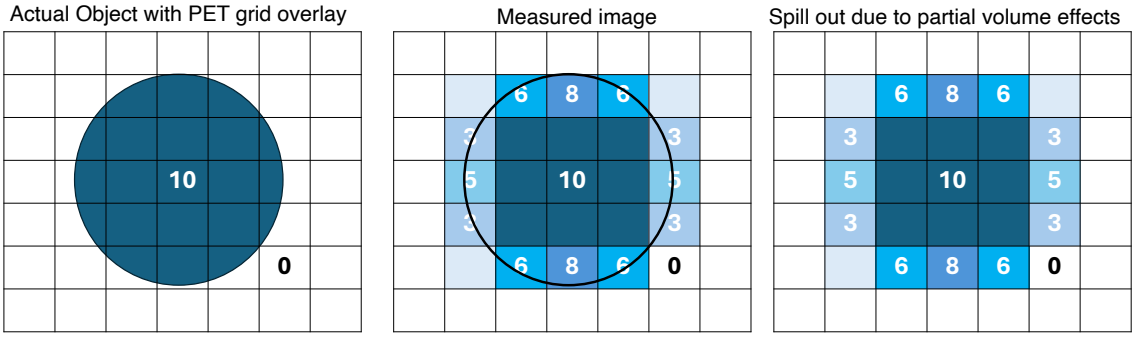

A: The left panel depicts a cylindrical object with uniform FDG activity (with 100 arbitrary units). The middle depicts the PET scanner's ability to detect the 100 units within the cylinder. It is unable to detect the full amount and the activity extends beyond the dimension of the cylinder. The right panel depicts this numerically. It also gives a visual representation of what recovery coefficients (RC) measure. In this instance, the RCmax would be 0.8 (80/100 arbitrary units). **B:** This figure shows how the PVE occur. The grid overlay represents the matrix created by photosensors to create the PET image. Here, the circle incompletely fills a square of the grid. The photosensor detects this as the activity across that whole area. This image shows 'spill out' of activity, but 'spill in' can also occur. This figure also demonstrates how smaller photosensors used in digital PET systems can improve spatial resolution and sensitivity.Created in BioRender. Rankin, S. (2025) https://BioRender.com/llh3sq3. Adapted from Soret *et al*[178].

2.7.3.5 Iterative reconstructions

A very important aspect of the reconstruction process is iterative reconstruction, most commonly using ordered subset expectation maximisation (OSEM). OSEM takes the observed raw data image and, using subsets of the raw data, creates a simulation of the image. This simulated iteration is then compared with the original observed image. This process is repeated many times using different subsets to improve accuracy and can allow imaging protocols to reach

convergence (RC equal to 1.0). Higher iterations and subsets can also increase the amount of background noise, degrade image quality (Figure 2-6) and increase variation in repeated measurements of SUV[179].

2.7.3.6 Filters

Filters can reduce background noise from iterative reconstruction. In doing so, it reduces detection by the PET scanner[180]. EANM recommend that no post-reconstruction filtering is applied to the images to optimise detection of small objects, such as carotid arteries.

2.7.3.7 Voxel and pixel size

PET images are created with voxels. The size of voxel used can be changed. It is mostly determined by the size of the photomultiplier tube, which is another way in which digital PET scanners offer better spatial resolution. The number of pixels used forms a matrix to create the PET image,

Figure 2-7B. Voxel size and matrix size can be altered to optimise imaging.

Chapter 3 Cardiovascular Eligibility Criteria and Adverse Event Reporting in Combined Immune Checkpoint and VEGF Inhibitors Trials

3.1 Introduction

There is a high prevalence of cardiovascular disease (CVD) in people with cancer[5]. The incidence of cardiovascular (CV) events, such as myocardial infarction (MI) and ischaemic stroke, is higher in people with cancer than it is in people without cancer[10]. As clinical outcomes for people diagnosed with cancer have improved considerably over the past two decades, the competing risks from cardiovascular comorbidity and mortality have gained increasing relevance[43].

Therapies such as immune checkpoint inhibitors (ICI) and vascular endothelial growth factor inhibitors (VEGFI) have improved cancer outcomes for people with a variety of tumour types[43,120]. When used alone, ICIs are associated with a range of CV adverse effects (CVAE) including myocarditis, MI and ischaemic stroke[47,52]. VEGFI are also associated with a range of cardiovascular toxicities particularly hypertension, as well as left ventricular systolic dysfunction (LVSD), heart failure (HF) and atherothrombotic sequelae including MI and stroke[8,101,181].

The use of ICI and VEGFI in combination is now a common treatment regimen licensed in various cancer types, including melanoma, renal, cervical, and endometrial cancer[100]. This is a consequence of successful trials of combinations of ICI+VEGFI conducted over the last five years with more than ninety clinical trials of ICI+VEGFI combination regimes ongoing[99,120]. Six combination ICI+VEGFI treatments are currently approved by the Food and Drug Administration (FDA)[100]. Given the CV adverse effects seen with each of these drugs in isolation, understanding the potential for an increased incidence of these effects when the drugs are combined is of major importance.

There is limited understanding of the extent to which pre-existing CVD increases the risk of ICI+VEGFI cardiovascular toxicity. To understand these issues, it is imperative to have clarity about the representation of people with or without pre-existing CVD in trials. Understanding and limiting heterogeneity between

trial populations is required for subsequent robust meta-analysis of CVAEs. Furthermore, consistency and clarity of definitions and trial publication reporting of CVAEs is fundamental to achieving these aims.

We conducted a scoping review of randomised controlled trials of ICI+VEGFI combination therapy in patients with cancer. Our primary interests were trial cardiovascular exclusion criteria and the heterogeneity of these between trials. We also examined reporting of baseline CV characteristics and methods by which adverse events (AEs) were defined, adjudicated and reported in trial results publications.

3.2 Methods

This scoping review protocol was registered on PROSPERO (CRD42022337942) and used the Preferred Reporting Items for Systematic reviews and Meta-Analyses (PRISMA) statement guidance[168]. We used the Population, Intervention, Comparison, Outcome (PICO) criteria for inclusion (Appendix 8.1). The registered protocol also included assessments relating to nephrology-related inclusions and trial reporting and these findings have been published separately[182]. As this was a review of publicly available data, no ethical approval was required.

3.2.1 Search strategy

The search was conducted on MEDLINE, Embase and Cochrane Library on 20th May 2022. All trials published in the public domain until the data of extraction were eligible for analysis. The search terms are included in Table 3-1. Duplicates were removed. Relevant articles were identified by two independent reviewers (BE and SR). Disagreements were resolved by consensus with a third reviewer (JSL).

Table 3-1 List of VEGF inhibitors and immune checkpoint inhibitors & systematic review search terms

VEGF inhibitors	
Tyrosine kinase Inhibitor	
Apatinib Axitinib Brivanib alaninate Cabozantinib Cediranib Dovitinib Lenvatinib Nintedanib	Pazopanib Regorafenib Sorafenib Sunitinib Tivozinib Vandetanib Vatalanib
Monoclonal antibodies	
Bevacizumab	Ramucirumab
VEGF-Trap mediators	
Aflibercept	
Immune checkpoint inhibitors	
PD-1	
Pembrolizumab Nivolumab	Cemiplimab
PD-L1	
Atezolizumab Avelumab	Durvalumab
CTLA-4	
Ipilimumab	Tremelimumab
Search Terms	
((“Phase II” OR “Phase 2” OR "Phase III" OR "Phase 3" OR "Phase IV" OR "Phase 4") AND (Ipilimumab OR Tremelimumab OR Atezolizumab OR Avelumab OR Durvalumab OR Pembrolizumab OR Nivolumab OR Cemiplimab) AND (Apatinib OR Axitinib OR Bevacizumab OR Aflibercept OR 'Brivanib alaninate' OR Cabozantinib OR Cediranib OR Dovitinib OR Ramucirumab OR Lenvatinib OR Nintedanib OR Pazopanib OR Regorafenib OR Sorafenib OR Sunitinib OR Tivozanib OR Vandetanib OR Vatalanib))	
Abbreviations: VEGF, Vascular endothelial growth factor; PD-1, Programmed cell death protein-1; PD-L1, Programmed death ligand-1; CTLA-4, Cytotoxic T-lymphocyte protein-4	

3.2.2 Study eligibility criteria

A systematic search of the literature was conducted to identify clinical trials of combination ICI+VEGFI therapy. We included any trial conducted in an adult population with any solid organ cancer who received combination ICI+VEGFI therapy in either the intervention or the control arm. ICIs and VEGFI that were not approved by the FDA for use as an anti-cancer treatment at the time of data

extraction were excluded. Trials using only single dosing or sequential (non-concurrent) ICI+VEGFI therapy were excluded.

3.2.3 Inclusion and exclusion criteria

We included all phase II-IV randomised controlled trial with a minimum population of 20 participants with available results published at time of extraction. Non-randomised controlled trials, meta-analyses, review articles, commentaries, subsequent therapy analyses, cost-effectiveness analyses, published abstracts, patient-reported outcomes, subgroup analyses and retrospective analyses were excluded. If two published articles reported data from the same patient group, such as subgroup analyses and extended follow-up analyses, the original article was used.

3.2.4 Outcomes

Key trial characteristics, trial eligibility criteria and exclusion criteria relating to cardiovascular disease were extracted. Trial design characteristics relating to the assessment, adjudication of CVAEs and the extent of reporting of these within the published article were recorded. Data were extracted from the original publication, supplemental material and available protocols from the journal website. Trial registration numbers, identified from the publication, were used to search relevant clinical trial platforms to ensure all relevant publicly available protocol data were identified if they were not available from the publication.

3.2.5 Cardiovascular adverse events

An AE was defined as a CVAE if it was recorded as a cardiac disorder under the Common Terminology Criteria for Adverse Event (CTCAE) criteria. CTCAE criteria grades AE severity on a scale of 1 to 5. Grade 1 events are considered ‘mild’ and Grade 2 ‘moderate’. Grade 3 events are considered to be ‘severe or medically significant but not immediately life-threatening’ while Grade 4 events reflect those with life-threatening consequences. Death is recorded as Grade 5. CVAEs were grouped in similar categories and, of note, MI and ‘acute coronary syndrome’ (ACS) were reported together under the AE ‘myocardial infarction’

category. If the AE was not recorded as a cardiac disorder by CTCAE but fulfilled any pre-specified trial criteria for cardiovascular and stroke endpoints for clinical trials, based on FDA endorsed Hicks' criteria (such as 'sudden death'), it was also classified as a CVAE[183].

3.3 Results

The search identified 4893 references which were screened (Figure 3-1). The final analysis included 17 randomised controlled trials with a total of 10313 participants, published between 2018 and 2022 (Table 3-2). Twelve were Phase III trials (9687 participants, 94%) and five were Phase II (626 participants, 6%). There were eight different combinations of ICI and VEGFI used. Atezolizumab with bevacizumab was the most common combination (Table 3-3) used in six trials, (4357 participants, 42%).

Figure 3-1. PRISMA diagram

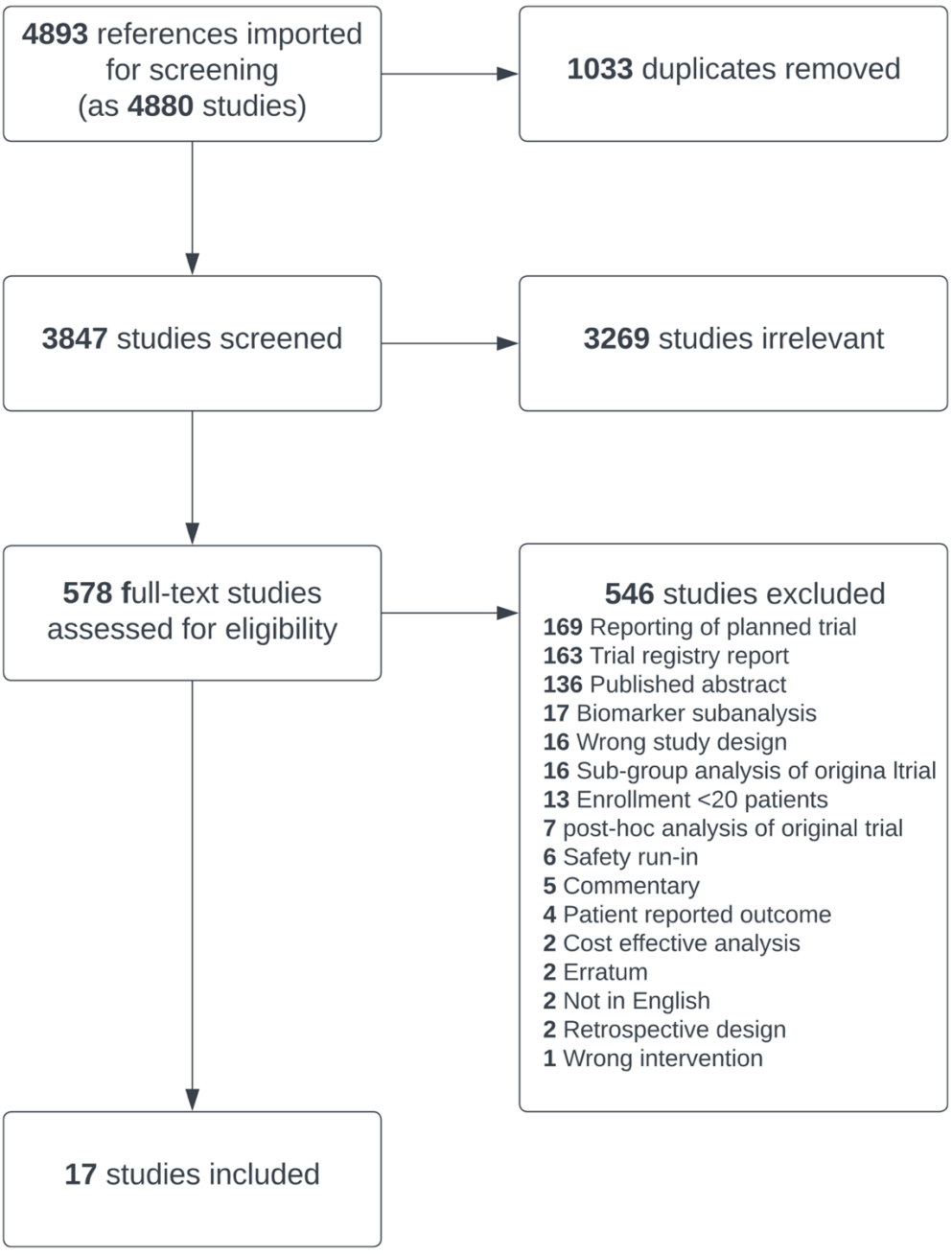

Table 3-2 Randomised Controlled Trials of ICI/VEGFI Combination Therapy - Exclusion Criteria

Study	Regimen	N	Cancer	NYHA exclusion criteria	LVEF exclusion criteria	Coronary heart disease exclusion criteria	Blood pressure exclusion criteria	Peripheral arterial disease exclusion criteria	VTE exclusion criteria	Stroke exclusion criteria	QTc exclusion criteria
Phase III RCTs											
Andre 2020[184]	Pembrolizumab / bevacizumab	307	Bowel	-	-	-	-	-	-	-	-
Choueiri 2021[185]	Nivolumab / cabozantinib	651	Renal	≥III[b]	≤50%	MI, unstable angina, CABG, cardiac angioplasty or percutaneous coronary intervention[b]	>150/90	symptomatic peripheral vascular disease	PE/DVT[b]	stroke/TIA[b]	>450/470
Colombo 2021[186]	Pembrolizumab / bevacizumab	617	Cervical	-	-	-	-	-	-	-	-
Finn 2020[119]	Atezolizumab / bevacizumab	501	Liver	≥II[c]	-	MI[c], unstable angina	≥150/100	vascular disease[b,d]	-	stroke[c]	>500
Makker 2022[187]	Pembrolizumab / lenvatinib	827	Endometrial	≥III[a]	'LLN'	MI, unstable angina[a]	≥150/90	-	-	stroke[a]	>480
Moore 2021[188]	Atezolizumab / bevacizumab	1301	Ovarian	≥II	<50%[e]	MI[c], unstable angina	>150/100	vascular disease[b,d]	CTCAE grade 4 VTE	stroke[c]	-
Motzer 2019[189]	Avelumab / axitinib	886	Renal	symptomatic[a]	'LLN'	MI, severe/unstable angina or CABG[a]	≥140/90	peripheral artery bypass grafting[a]	PE/DVT[b]	stroke/TIA[a]	>500
Motzer 2021[117]	Pembrolizumab / lenvatinib	1069	Renal	≥III[a]	'LLN'	MI, unstable angina[a]	≥150/90	-	-	stroke[a]	>480
Rini 2019[190]	Atezolizumab / bevacizumab	915	Renal	≥II [b]	<50%	MI, unstable angina[b]	>150/100	vascular disease[b,d]	-	stroke/TIA[b]	>460

Rini 2019[118]	Pembrolizumab / axitinib	861	Renal	≥III[a]	-	MI, unstable angina, CABG, cardiac angioplasty or stenting[a]	≥150/90	peripheral artery bypass grafting[a]	PE/DVT[b]	stroke/TIA[a]	≥480
Socinski 2018[191]	Atezolizumab / bevacizumab	1202	Lung	≥II[c]	<50%[e]	MI, unstable angina[c]	>150/90	vascular disease[b,d]	-	stroke[c]	-
Sugawara 2021[192]	Nivolumab / bevacizumab	550	Lung	≥III	-	MI, unstable angina[b]	≥ 150/90	-	PE/DVT[b]	stroke/TIA[b]	-
Phase II RCTs											
Lheureux 2022[193]	Nivolumab / cabozantinib	82	Endometrial	≥III	-	MI, unstable angina[b]	>140/90	thromboembolic event requiring anticoagulation[b]	thromboembolic event requiring anticoagulation[b]	stroke/TIA[b]	>500
McDermott 2018[194]	Atezolizumab / bevacizumab	305	Renal	≥II	<50%[e]	MI/unstable angina[c]	>150/100	vascular disease[b,d]	-	stroke/TIA[c]	-
Mettu 2022[195]	Atezolizumab / bevacizumab	133	Bowel	≥II	-	MI, unstable angina, stenting, angioplasty, cardiac surgery[a], "active coronary heart disease"	>150/100	arterial thrombosis[a], symptomatic PVD, vascular disease[d]	CTCAE grade 4 VTE	stroke/TIA[a]	-
Nayak 2021[196]	Pembrolizumab / bevacizumab	80	Brain	**	-	-	inadequately controlled	arterial thromboembolism[a]	thromboembolism[a]	-	-
Redman 2022[197]	Avelumab / bevacizumab	26	Bowel	≥II	-	MI[c], unstable angina	-	-	-	stroke[c]	-
a) within 12 months, b) within 6 months, c)within 3 months. d) such as aortic aneurysm, dissection or carotid stenosis that requires surgical intervention or stenting or recent peripheral arterial thrombosis. e) LVEF <50% acceptable if stabilised on optimal medical therapy in the opinion of the treating physician.											

Table 3-3 Summary of trial characteristics and exclusions

	Number of trials n (%)	Number of patients n (%)
Total (randomized controlled trials)	17	10313
Median Age*	62 (50-67)	
Male	5308 (51%)	
Female	5005 (49%)	
Overall Median safety follow-up* (months)	11 (5.1-18.0)	
Overall Median efficacy follow up* (months)	19.9 (9.9 – 48.6)	
Tumour type		
Renal	6 (35)	4687 (45)
Gynaecological (endometrial, ovarian, cervical)	4 (24)	2827 (27)
Lung	2 (12)	1752 (17)
Liver	1 (6)	501 (5)
Bowel	3 (18)	466 (5)
Brain	1 (6)	80 (1)
Trial Phase		
III	12 (71)	9687 (94)
II	5 (29)	626 (6)
ICI and VEGFi combination		
Atezolizumab & bevacizumab	6 (35)	4357 (42)
Pembrolizumab & Lenvatinib	2 (12)	1896 (18)
Pembrolizumab & bevacizumab	3 (18)	1004 (10)
Avelumab & axitinib	1 (6)	886 (9)
Pembrolizumab & axitinib	1 (6)	861 (8)
Nivolumab & cabozantinib	2 (12)	733 (7)
Nivolumab & bevacizumab	1 (6)	550 (5)
Avelumab & bevacizumab	1 (6)	26 (0.3)
*weighted by trial participants		

3.3.1 Cardiovascular Eligibility Criteria

Eligibility criteria were available for all 17 trials. CVD trial exclusion criteria were broad with heterogenous definitions (Figure 3-2). Fifteen trials (9389 participants, 91%) had multiple CV exclusion criteria. Of these, there were specific exclusion criteria for people with prior HF, MI/unstable angina, hypertension and stroke in 13 trials (9283 participants, 90%). Two of the 15 trials (106 participants) had a general exclusion criterion of ‘clinically significant cardiovascular disease or impairment’. The remaining two trials (924 participants) did not explicitly exclude people on the basis of prior CVD but had a general criterion excluding those with ‘a relevant prior condition which may affect the results of the trial’. The interpretation of these more generic criteria was left at the discretion of the investigator.

In the 12 trials reporting eligibility data prior to enrolment, 31% (3905 participants) were ineligible. Only one paper reported reasons for screen failure and in that publication, 10% of those ineligible were excluded because of cardiovascular exclusions (PE/DVT, hypertension, QTc and 'cardiovascular conditions').

3.3.1.1 Heart Failure & Left Ventricular Systolic Dysfunction (LVSD)

Of the 14 trials (9309 participants, 88%) with specific exclusions for people with heart failure, seven excluded those with New York Heart Association (NYHA) ≥II, six excluded NYHA ≥III and one trial excluded 'symptomatic' patients (Table 3-2). Eight of the trials' heart failure exclusions specified heart failure within a varying time frame prior to enrolment, ranging between 3-12 months prior to screening.

People with reduced left ventricular ejection fraction (LVEF) were excluded from eight trials (7156 participants, 69%): five excluded those with LVEF <50% (although three of these accepted LVEF <50% if the participant was 'stable on a medical regimen that was optimised in the opinion of the physician') and three excluded people with LVEF less than the 'lower limit of normal' of the 'institutional normal range.' Only four trials (3433 participants, 33%) mandated echocardiography before enrolment for all participants. Three other trials (1909 participants, 19%) mandated LVEF assessment prior to enrolment in specific circumstances (for patients with anthracycline exposure in one trial and, in if a patient had 'cardiac risk factors or an abnormal electrocardiogram (ECG)' in the remaining two).

There were exceptions to allow inclusion of participants with prior heart failure. In four trials, people with HF who did not meet pre-specified NYHA exclusion criteria, as well as people with LVEF <50%, were eligible to enrol provided they were on a stable regimen that was optimised in the opinion of the physician.

Figure 3-2 Cardiovascular exclusion criteria in ICI/VEGFi combination therapy trials. Percentage of trials with CV exclusion criteria and the definitions used across trials for: a) heart failure; b) coronary artery disease; c) blood pressure; d) vascular / rhythm exclusion criteria.

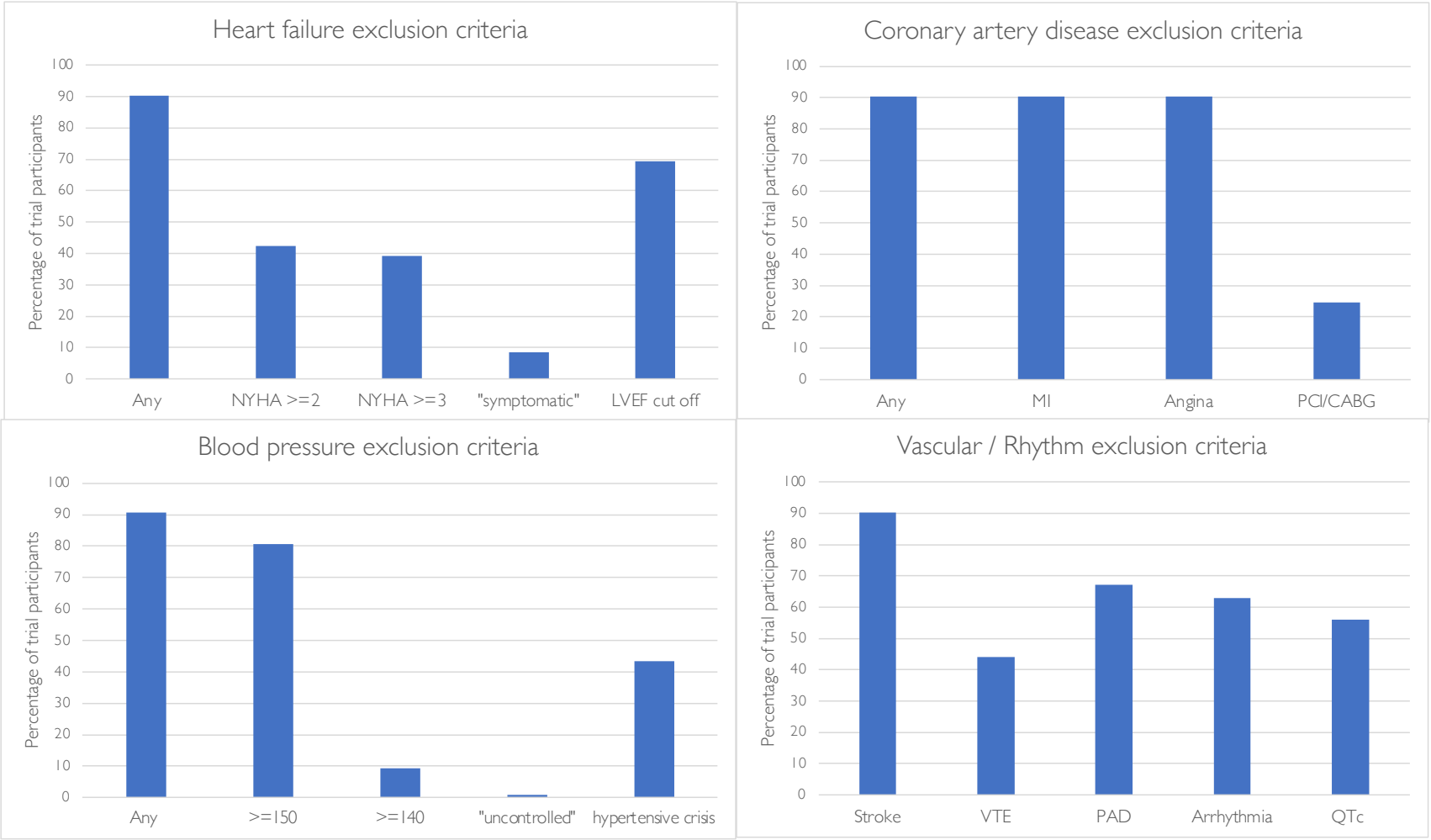

3.3.1.2 Coronary Artery Disease

The 14 trials with LVSD/heart failure exclusions also excluded patients with a history of recent MI/unstable angina (Table 3-2). The timeframe for exclusion of people with prior acute coronary syndrome varied from 3-12 months prior to screening. In addition to exclusions on the basis of acute coronary syndrome, four trials (2531 participants, 25%) also excluded people with coronary angioplasty, stenting or coronary artery bypass grafting (CABG) within 6-12 months prior to screening. In four trials, people known to have coronary artery disease (not otherwise meeting pre-specified coronary exclusions) were eligible for inclusion provided they were on a stable regimen that was optimised in the opinion of the physician.

3.3.1.3 Blood Pressure

Fifteen trials had a blood pressure (BP) or hypertension exclusion criterion (Table 3-2), most commonly excluding those with a systolic BP of 150mmHg and above (8315 participants, 81%). Two trials (106 participants) did not specify a BP cut-off but one trial excluded those with 'inadequately controlled hypertension' or a history of hypertensive encephalopathy/crisis. The second trial did not have a specific BP cut off but excluded participants randomised to receive bevacizumab if they had a previous history of hypertensive emergency or hypertensive encephalopathy. Any prior history of hypertensive encephalopathy or crisis was an exclusion in eight trials (4463 participants, 43%).

3.3.1.4 Stroke

Previous 'cerebrovascular accident' (CVA) or transient ischaemic attack within 3-12 months of screening was an exclusion criterion in 14 trials (9309 participants, 90%).

3.3.1.5 Arterial disease

Arterial vascular disease, such as aortic aneurysm requiring surgical repair, peripheral artery bypass grafting, peripheral arterial thrombosis in the 6-12 months prior to screening, was an exclusion criterion in 11 trials (6917 participants, 67%). There was heterogeneity in the definition of arterial disease, varying from those with surgical intervention (peripheral artery bypass grafting)

or those with any form of intervention or arterial thrombus in the preceding 6-12 months. Symptomatic PVD was an exclusion criterion in two trials.

3.3.1.6 Venous Thromboembolism

"Prior pulmonary embolism (PE) or deep vein thrombosis (DVT)" was an exclusion criterion in eight trials (4544 participants, 44%, Table 3-2), three of which had a time limit of exclusion to within the preceding 6 months. Venous thromboembolism (VTE) exclusion criteria were defined as either 'PE/DVT within the preceding 6 months' or a previous 'CTCAE grade 4 VTE' in two trials.

3.3.1.7 QTc & Arrhythmia

Patients with arrhythmia were excluded from ten trials (6482 participants, 63%). 'Unstable' or 'haemodynamically significant' arrhythmia was the most common exclusion terminology but 'grade ≥2,' 'uncontrolled' arrhythmias, and "clinically significant arrhythmias" were used to define this in three trials. Eight trials (5792 participants, 56%) had an upper QTc limit for enrolment, between 450-500 milliseconds. Only one trial used a different threshold for men and women.

3.3.1.8 Myocarditis

No trial specifically excluded those with previous myocarditis, however every trial excluded patients with recent or current use of corticosteroids or immunosuppression, or previous hypersensitivity to ICI.

3.3.2 Reporting of Baseline Cardiovascular Characteristics

With the exception of smoking status, which was reported in two lung cancer trials, no trial reported baseline CV characteristics, such as the prevalence of previous MI, heart failure, LVSD, diabetes, dyslipidaemia or hypertension.

3.3.3 Reporting of Adverse Events

All 17 trials reported adverse events using CTCAE definitions and severity grading. CTCAE Version 4 was used in 15 trials. AEs were reported by the site investigator with no central or CV specialist event adjudication in 14 trials and was not specified in the remaining three trials. One trial had an independent

cardiovascular events adjudication committee. AEs were either reported as treatment related (trAE) or 'AEs of any attribution.' TrAEs (adjudicated by the investigator) were reported in all trials. AEs of any attribution were less commonly reported (11 trials, 7458 participants, 72%).

3.3.3.1 Duration of Adverse Event Reporting

Follow-up for CV events was shorter than the trial duration in all trials (Table 3). Follow-up for CV events in five trials was 'the duration of treatment plus 30 days after last dose.' In nine trials follow-up for CVAEs was 'duration of treatment plus 30 days or the initiation of new anti-cancer therapy, whichever came first'. Ten trials had extended follow-up for serious AES and AE of special interest (AEOSI), including CVAEs, ranging from 90-120 days. The follow-up period was not specified in two trials.

3.3.3.2 Incidence Thresholds for Adverse Event Reporting

No phase III trial reported all CV events. Fifteen trials reported events when they reached a pre-specified incidence (Table 3-4). The most common threshold in the main paper was ≥10% in six trials (3756 participants, 36%) but higher reporting thresholds (incidence of ≥20-25%) were used in 5 trials (4307 participants, 42%). One phase II trial (26 participants, 0.25%) reported all CTCAE grade ≥2 treatment related AEs. A lower threshold specifically for reporting more severe AEs (CTCAE grade ≥3 or SAE) was used in nine trials (6565 participants, 64%) and that threshold ranged from 'all events' to 10%. Three trials (1633 participants, 16%) reported AEs under a variety of other specific circumstances with lower thresholds, such as 'AEs leading to discontinuation' (Table 3-4). Grade 5 AEs (deaths) were reported in all trials. Twelve trials (7854 participants, 76%) reported AE deaths regardless of relationship to treatment, where 5 trials (2459 participants, 24%) only reported treatment related AE deaths, adjudicated by the investigator. There was no apparent difference in reporting between trial phase, sponsorship or year published (Table 3-5).

Table 3-4 Reporting of CTCAE Grade 1-4 Adverse Events

Study	Combination	Median follow-up duration (months)		Threshold incidence for reporting AE in main paper	Other reporting thresholds for AEs in paper/supplement
		safety	efficacy		
Andre 2020[184]	Pembrolizumab / bevacizumab	12.1	32.4	≥10%	-
Choueiri 2021[185]	Nivolumab / cabozantinib	17.6	18.1	≥10%	-irAE (all events)
Colombo 2021[186]	Pembrolizumab / bevacizumab	11	22	≥20%	-Comparison of risk difference of AE occurrence between treatment groups with: - ≥10% in either arm or ≥5% for Grade≥3 AEs with an incidence ≥5% -irAEs (all events)
Finn 2020[119]	Atezolizumab / bevacizumab	9.6	-	≥10%	-trAE Grade 3/4 ≥2% -AE grade 3/4 with incidence 1% -'AE leading to withdrawal ≥1% -AEOSI (CV) – all events
Makker 2022[187]	Pembrolizumab / lenvatinib	8.6	12.2	≥25%	-trAE ≥10% -AE leading to dose reduction/interruption ≥5% -AE leading to discontinuation ≥1% -'clinically significant AE for lenvatinib (includes CV) – all events -AEOSI for pembrolizumab – all events -SAE ≥1%
Moore 2021[188]	Atezolizumab / bevacizumab	-	19.9	≥25%, 0.5% for grade ≥3	-SAE ≥2% -irAEs
Motzer 2019[189]	Avelumab / axitinib	9.6	9.9	≥10%, ≥5% for grade ≥3	-

Motzer 2021[117]	Pembrolizumab / lenvatinib	18	26.6	≥25%	-trAE ≥10% -a selection of grade ≥3 occurring >10% were reported in main text -CV-AEOSI for ICI/SACT/VEGFI - all events
Rini 2019[190]	Atezolizumab / bevacizumab	13	24	≥20%[a]	-trAE ≥10% -AEOSI (all events)
Rini 2019[118]	Pembrolizumab / axitinib	11.4	12.8	≥10%	-AEOSI (all events)
Socinski 2018[191]	Atezolizumab / bevacizumab	7.7	20	≥10%, ≥5% for grade ≥3	-trAE ≥10% or grade 3/4 trAE ≥1% -tr-SAEs – all events -tr-irAEs
Sugawara 2021[192]	Nivolumab / bevacizumab	11.5	13.7	≥10%	-
Phase II trials					
Lheureux 2022[193]	Nivolumab / cabozantinib	-	15.9	≥25%, ≥10% for grade ≥3	"rare grade 4 trAE and SAE" reported
McDermott 2018[194]	Atezolizumab / bevacizumab	10.3	20.7	≥20%[a,b]	-single most common AE leading to discontinuation for each drug was reported (proteinuria, AKI and PPES) -AEOSI (all events)
Mettu 2022[195]	Atezolizumab / bevacizumab	5.1	20.9	Unspecified[c]	-treatment related irAEs
Nayak 2021[196]	Pembrolizumab / bevacizumab	-	48.6	≥5% (grade ≥2)	trAE grade 4 – all events
Redman 2022[197]	Avelumab / bevacizumab	-	15.1	All events (grade ≥2)	-

a) or AE incidence had ≥5% difference between arms. b) from supplement – no table in main paper c) no table – selection of AEs reported in main paper Abbreviations: AE: adverse event, AEOSI: adverse event of special interest, AKI: acute kidney injury, CV: cardiovascular, CV-AEOSI: cardiovascular adverse event of special interest, PPES – palmar-plantar erythrodyesthesia syndrome, trAE: treatment related adverse event, tr-SAE – treatment related serious adverse event, VEGFI: vascular endothelial growth factor inhibitor

3.3.4 Cardiovascular events

No trial used the FDA-endorsed, standardised Hicks' criteria for reporting of cardiovascular events[183]. With the exception of hypertension, which was reported in all trials, no trial explicitly stated the absence or occurrence of CVAEs. In trial manuscripts that did not report CVAEs other than hypertension, it was not clear whether this was because of a true absence of CVAEs or because of their occurrence with an incidence beneath a reporting threshold.

3.3.4.1 CV death

'AE deaths of any attribution' were reported in 11 trials (7203 participants) and 7 of these (4734 participants) reported the mode of AE death. In six trials (3110 participants), only deaths that were considered to be treatment related (adjudicated by the investigator) were reported.

Most frequently, CVAEs were described when associated with death. No trial reported total number of CV deaths. However, ten trials (7737 participants) reported AE death that would be categorized as CV death by Hicks' Criteria (Figure 3-3).

Figure 3-3 Percentage of trials reporting cardiovascular adverse events

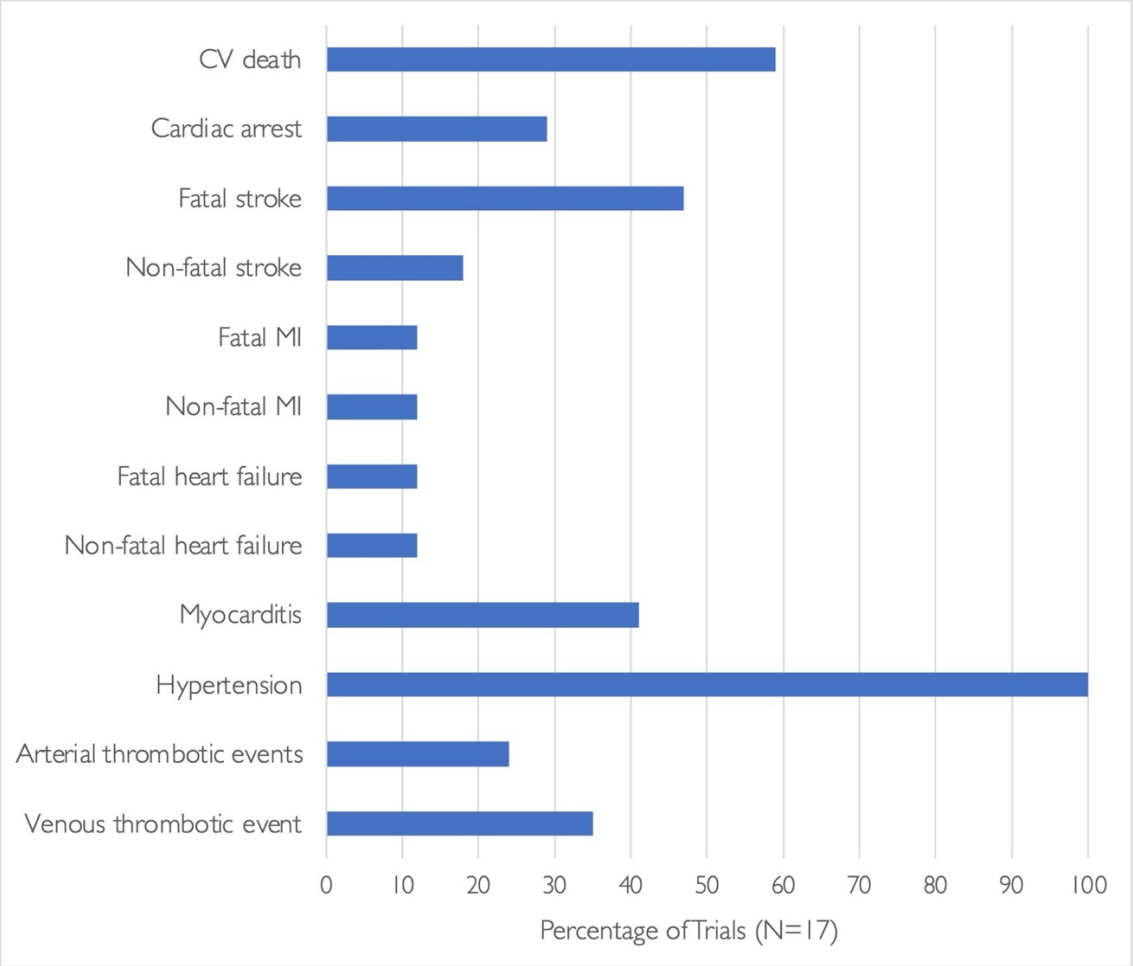

3.3.4.2 Myocardial Infarction

MI was only reported in four trials (3181 participants, 31%), two of which only reported fatal MI (Figure 3-3). No trial reported if coronary revascularisation occurred.

3.3.4.3 Heart failure & LVSD

HF was reported in three trials (2564 participants, 25%), two of which reported one fatal case of HF. One trial reported one case of fatal cardiac failure and three cases of grade 1-2 'congestive cardiac failure' defined by CTCAE Version 4. LVSD was also reported in three trials (3,098 participants, 30%). Two of the three trials that reported LVSD mandated echocardiography surveillance on treatment. Four trials (2913 participants, 28%) reported 'peripheral oedema'.

3.3.4.4 Stroke

Stroke was reported in eight trials (5782 participants, 56%). Five trials (2778 participants, 27%) only reported the occurrence of fatal stroke. Ischaemic stroke was reported in five trials (4536 participants, 44%). Fatal ischaemic stroke occurred in four of these trials, three of which were only reported in supplementary data. Haemorrhagic strokes were reported in six trials (3864 participants, 38%) and five of these trials only reported fatal haemorrhagic strokes.

3.3.4.5 Myocarditis

Myocarditis was reported in seven trials (5309 participants, 52%). Fatal myocarditis was reported in two trials. No trial reported if myocarditis did not occur.

3.3.4.6 Hypertension

Hypertension was reported in all trials, defined by CTCAE. Posterior reversible encephalopathy syndrome (PRES) was reported in two trials (2271 participants, 22%). There were two reported deaths attributed to hypertension: one secondary to PRES and another death secondary to ‘uncontrolled hypertension’ adjudicated by the investigator.

3.3.4.7 Other thrombotic events

Venous thrombotic events were reported in six trials (5309 participants, 52%) but four of these only reported thrombotic events that resulted in death. Four trials (3599 participants, 35%) reported arterial thrombotic events and three trials (1944 participants, 19%) reported unspecified thromboembolic events.

Table 3-5 CVAE reporting by trial phase, sponsorship and year published.

CV event	Number of trials (number of participants)	Trial phase		Trial Sponsorship		Year trial published	
		II	III	Industry	Academic	2018-June 2020	July 2020-2022
Total	17 (10313)	5 (626)	12 (9687)	9 (7239)	8 (3074)	7 (4977)	10 (5336)
CV death	10 (7737)	2 (385)	8 (7352)	8 (6588)	2 (1149)	6 (4670)	4 (3067)
Cardiac arrest	5 (3963)	0	5 (3963)	4 (2894)	1 (1069)	3 (2277)	2 (1686)
Fatal Stroke	8 (5782)	2 (385)	6 (5397)	7 (5702)	1 (80)	5 (3784)	3 (1998)
Non-fatal Stroke	3 (3004)	0	3 (3004)	3 (3004)	0	2 (1703)	1 (1301)
Fatal MI	2 (1478)	0	2 (1478)	2 (1478)	0	1 (861)	1 (617)
Non-fatal MI	2 (1703)	0	2 (1703)	2 (1703)	0	2 (1703)	0
Fatal HF	2 (2063)	0	2 (2063)	2 (2063)	0	2 (2063)	0
Non-fatal HF	2 (1703)	0	2 (1703)	2 (1703)	0	2 (1703)	0
Myocarditis	7 (5384)	1 (133)	6 (5251)	3 (3148)	4 (2336)	3 (2054)	4 (3330)
Hypertension	17 (10313)	5 (626)	12 (9697)	9 (7239)	8 (3074)	7 (4977)	10 (5336)
Arterial thrombotic events	4 (3599)	0	4 (3599)	2 (1703)	2 (1896)	2 (1703)	2 (1896)
Venous thrombotic events	6 (5309)	0	6 (5309)	5 (4482)	1 (827)	3 (2564)	3 (2745)

3.3.5 Adverse Events of Special Interest (AEOSI)

AEOSI were collected in 15 trials (10205 participants, 99%), all of which included the collection of immune-related AE (irAE), including myocarditis. All 15 trials

reported ir-AEOSI, with lower incidence thresholds (all ir-AEOSI events in 13 trials, >1% in the ICI arm in one trial, and unspecified in one trial).

Additional CV-AEOSI, excluding hypertension and myocarditis, were collected or reported in six trials (4717 participants, 46%). CVAEs were included in AEOSI lists in the protocol of five of these trials (3890 participants, 38%). The definition of these CV-AEOSI varied from 'grade ≥2 cardiac disorders' to more comprehensive lists detailing reporting of venous, arterial thromboembolism, LVSD, significant, arrhythmias and heart failure events. Only four trials reported CV-AEOSI, however three of these reported CV-AEOSI only in supplementary materials (Table 3-4). No trial specifically reported that an AEOSI did not occur.

3.4 Discussion

This scoping review of randomized trials of ICI+VEGFI combination therapy demonstrates heterogeneity in three key areas relevant to potential adverse cardiovascular effects of these important anti-cancer drugs (Figure 3-4, Central Illustration). First, cardiovascular trial exclusion criteria are inconsistent between trials. Second, primary trial manuscript reporting of the prevalence of cardiovascular disease and risk factors in trial participants is variable and limited. Third, there is variation in methods, thresholds and follow-up periods for reporting and publication of adverse cardiovascular events associated with ICI+VEGFI combination therapy.

Randomised trials of combined ICI+VEGFI were first reported in 2018 and therefore represent contemporary trial methodology[191,194]. A prior review of a broad range of anti-cancer agents, including conventional chemotherapeutics, examined cardiovascular adverse event reporting in cancer trials supporting FDA approval but this included trials conducted over 30 years ago and was prior to any FDA approval of combination therapy[198].

Figure 3-4 Central illustration: Heterogenous cardiovascular eligibility and event reporting in ICI/VEGFI combination trials. In contemporary trials with "state of the art" trial design, such as trials of combined immune checkpoint inhibitors (ICI) and vascular endothelial growth factor inhibitors (VEGFI) therapy, there is marked heterogeneity in definitions of cardiovascular (CV) disease for exclusion criteria and in adverse event reporting. No trial reported CV baseline characteristics or reported the absence of CV events CV adverse events were reported only when a threshold incidence within the trial population is reached, which is likely to lead to under-reporting of CV events.

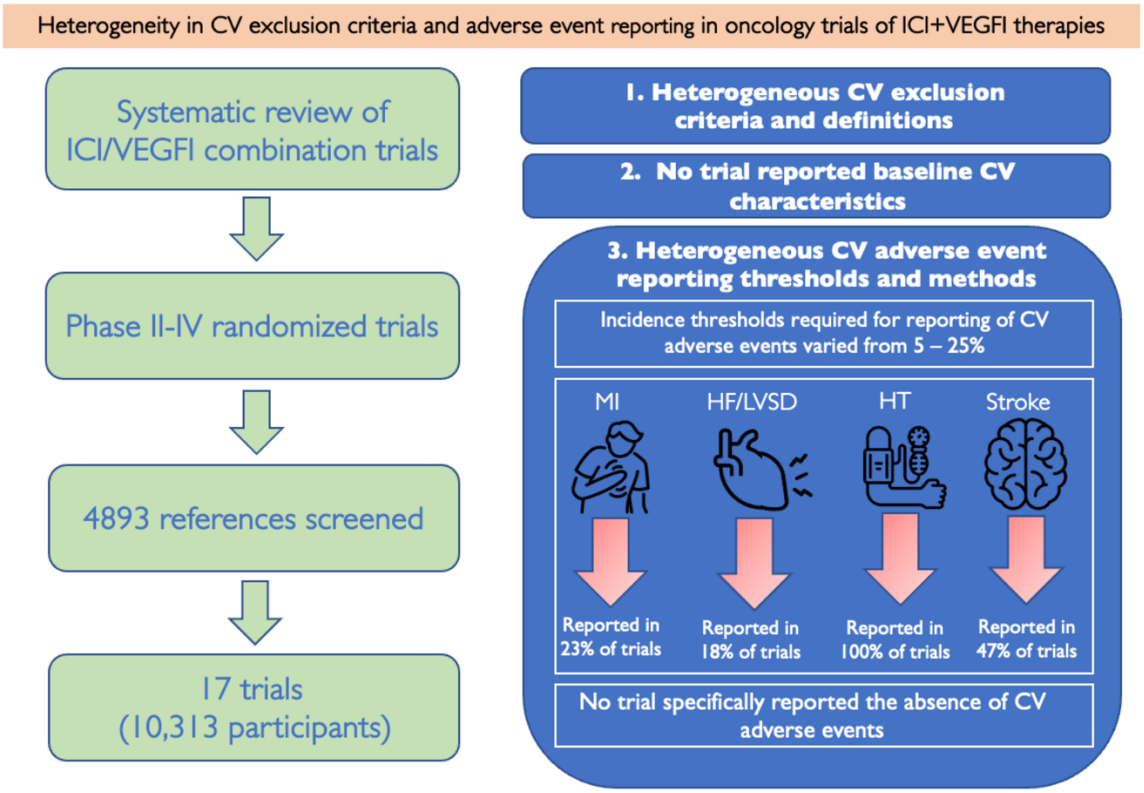

3.4.1 Cardiovascular Trial Eligibility Criteria Heterogeneity

Our review identified that cardiovascular exclusion criteria were ubiquitous in these trials. We also identified substantial heterogeneity in the nature of these exclusion criteria and the use of potentially arbitrary CV definitions and exclusion thresholds. It is of note that the FDA recommend the avoidance of 'unnecessarily restrictive eligibility criteria' to maximise the generalizability of trial results to the patient population in whom the drug may be used in subsequent routine clinical practice[199]. This recommendation is made particularly to allow trials to inform the net risk/benefit profile. While we acknowledge that it may be appropriate to include some clinically-relevant cardiovascular eligibility criteria for trial safety reasons and while these trials were designed and powered to provide information on cancer treatment effects, potential safety signals may only become apparent when trial populations are combined for meta-analysis. Those insights are currently limited by heterogeneity in eligibility criteria.

3.4.2 Baseline CVD and CVD Risk Factors in Trial Participants

Baseline prevalence of cardiovascular disease, including cardiovascular risk factors or established CVD, were not reported in any primary trial publication. However, a secondary analysis of one trial did report the prevalence of baseline CV risk factors[124]. In that report, the baseline prevalence of CV risk factors was low. Only 4% of people in the ICI/VEGFI arm had dyslipidaemia, 9.5% had diabetes and 3.2% had cerebrovascular disease[124]. In addition to potentially stringent trial eligibility criteria, trial recruitment bias toward inclusion of people with fewer comorbidities may contribute to a trial population who are not representative of the general population of patients with cancer in whom these drugs may ultimately be used. Irrespective of these issues of eligibility and potential recruitment bias, the lack of data on baseline CV characteristics means that the baseline CV risk for patients in these trials is unknown. Inclusion of those with comorbidities, when assessed in non-cancer trials, only modestly affected completion of study enrolment, meaning there could be an increase in generalisability of trial data with minimal impact on trial completion[200 20]. Without this information, it is impossible to assess the degree to which pre-existing CVD or risk factors may potentiate adverse cardiovascular effects of ICI+VEGFI therapy. It also remains possible that an interaction between pre-existing CVD and adverse effects of ICI+VEGFI therapy is lower than might otherwise be expected. These insights are critical for providing patients with the best information relating to potential risks of treatment in the context of pre-existing CVD.

3.4.3 Cardiovascular Adverse Event Description and Reporting

CVAEs were reported using CTCAE criteria in all trials and reporting of these was based upon incidence thresholds. The threshold that was required to be reached varied from 5-25% between trials. Furthermore, only four trials used a lower reporting incidence threshold for more severe (CTCAE grade ≥3). In addition to standardization of reporting methods, lowering the threshold or potentially removing this threshold for reporting in primary trial publications altogether should be considered. While the signal to noise ratio of grade 1 and 2 events may mean that reporting on the basis of incidence thresholds could be appropriate, we would argue that reporting of all of the more severe adverse events may be

justified. Irrespective, reporting of events of special interest of any severity should continue for conditions such as myocarditis, for which the most granular information is required to understand whether or not there may be a potential disconnect between initial CTCAE severity grading and outcomes.

Trial publication reporting of CVAEs, and the clarity of this, was variable. While many primary trial publications did not report the occurrence of CVAEs, they also did not explicitly state their absence. Reporting of AEs that were specifically considered to have been related to treatment (trAEs) was more frequent than reporting of AEs of any attribution. Reporting of hypertension and, to a lesser extent myocarditis, was common in the context of already well-recognised associations with VEGFi and ICI, respectively. However, without consistently robust assessment and reporting of other CVAEs, the ability to discern associations (or lack thereof) between these drugs and a broader range of potential CVAEs will remain sub-optimal. The assessment of CVAE 'treatment-relatedness' was by the local investigator and therefore this introduces bias and impedes transparent understanding of AE profiles. One trial included a pre-specified subgroup analysis of cardiovascular events in ICI+VEGFI therapy. In that analysis, the number of CV events was small but CVAE incidence was higher than reported in the primary manuscript[124].

All trials had longer follow-up for anti-cancer efficacy assessment than they did for collection of CVAEs. Given that the accrual of CVAEs might be expected to occur over a similarly more prolonged period, increasing follow-up duration for CVAEs would provide important information.

3.4.4 Limitations

This review has several limitations. We did not extract data on pre-trial safety data which may have influenced eligibility criteria. We also did not extract data on subgroup analysis and extended follow-up papers which may have provided additional information on CV comorbidities and adverse effects. However, given that original trial manuscripts frequently inform drug licensing approvals we believe that our focus on these publications is particularly relevant. It is also possible that some safety data are still to be placed in the public domain and

therefore not captured. Given that there was variable follow-up/trial inclusion time between trials and also between trial participants, reported percentage incidence of CVAEs should be considered as crude rates here rather than being time-adjusted. Data extraction occurred in May 2022. While further ICI+VEGFI combination trials have been reported since then, we believe that our findings retain relevance, particularly to currently approved combination regimens.

3.5 Conclusion

This scoping review of randomized trials of ICI+VEGFI combination therapies has identified heterogeneity in trial cardiovascular eligibility criteria, limited trial manuscript reporting of the baseline cardiovascular characteristics in participants and heterogeneity in methods used for reporting of adverse cardiovascular events. These factors may have substantial impact on the ability to make accurate assessments, including meta-analyses, of the potential for cardiovascular adverse effects of these important anti-cancer therapies. These findings should be considered carefully from the time of inception of novel cancer therapy trials. Our observations have relevance to clinical trialists and to sponsors of research. Importantly, this requires ongoing consideration by regulatory authorities, including the FDA and European Medicines Agency (EMA). Furthermore, alignment and incorporation of consensus definitions of cardiotoxicity, such as those proposed by the International Cardio-Oncology Society, should be considered in the next version of CTCAE. While it is possible that cardiovascular adverse effects are under-appreciated in cancer trials, it is also possible that they may be less frequent than feared. With the rapid rise of combination ICI+VEGFI treatment regimens there is an urgent need to standardise these components and, in particular, to inform their use in patients who frequently have pre-existing cardiovascular disease.

Chapter 4 Arterial effects of anthracycline: structural & inflammatory assessments in non-human primates and lymphoma patients

4.1 Introduction

Anthracyclines, such as doxorubicin, are effective anti-cancer drugs used as the backbone of treatment of numerous cancer types, including breast cancer, sarcoma, and lymphoma. However, these chemotherapeutic agents are associated with cardiovascular toxicities including arterial and myocardial injury[15]. It is hypothesised that coronary endothelial injury may contribute to the development of left ventricular dysfunction and heart failure while peripheral arterial injury may further amplify these risks via arterial stiffening and consequent disruption of ventriculo-arterial coupling[28]. While aortic stiffening has been observed in humans after exposure to anthracycline, assessment of the underlying pathophysiologic mechanisms has been limited to small animal and cell line studies[201,202].

The role of inflammation as a mediator of vascular dysfunction is well recognised[34,35,203]and is a notable target for the prevention or treatment of a range of arterial diseases and injurious processes.[204–206] Furthermore, in small animal models exposed to anthracyclines, inflammation-associated aortic stiffening[207] and peri-vascular inflammation have been demonstrated.[31] While these observations raise the hypothesis that anthracyclines induce inflammation-mediated arterial injury in human patients, this has not yet been established. ^{18}Fluoride-fluorodeoxyglucose positron emission tomography/computed tomography [^{18}F]FDG PETCT) is a molecular imaging technique that is highly sensitive to metabolically active processes that use glucose as a fuel. It is in routine clinical use for the staging of a range of cancers and the assessment of treatment responses. Notably, it is also the gold standard method for the identification and quantification of inflammatory activity, including in large arteries[135,137,138,143].

In this study, we examined the histopathological and inflammatory effects of exposure to doxorubicin in a non-human primate model and in patients before

and after chemotherapy for the treatment of lymphoma. We evaluated these effects in order to inform detection, prevention and treatment strategies for patients at risk of anthracycline-associated arterial toxicity.

4.2 Methods

4.2.1 Non-human Primate Study

This non-human primate study (NHP) was performed, at Wake Forest, School of Medicine, Clarkson Campus, Winston-Salem, by Miss Caitlin Fountain under supervision of Dr Giselle Meléndez. The study was performed in accordance with the National Institutes of Health's (NIH) Guide for Care and Use of Laboratory Animals with local approval by the Wake Forest School of Medicine Institutional Animal Care and Use Committee. The institution is accredited by the Association for the Assessment and Accreditation of Laboratory Animal Care International and operates in compliance with the Animal Welfare Act.

Five female pre-menopausal African Green monkeys (AGM) (*Chlorocebus aethiops sabeus*) aged 13 ± 1.3 years were used in this study. The study subjects were sourced from a multigenerational pedigreed colony of African Green monkeys (n=311, 4-27 years, lifespan ≈ 26 years), which descended from 57 founder monkeys at the Wake Forest Vervet Research Colony (P40-OD010965). Animals were fed a commercial laboratory primate chow (Laboratory Diet 5038; LabDiet, St. Louis, MO) with daily supplemental fresh fruits and vegetables and tap water ad libitum. Monkeys were housed in a climate-controlled room. As previously described [30,208], animals underwent doxorubicin treatment which consisted of two initial doses of 30 mg/m^2 and three doses of 60 mg/m^2 given via vascular access port (VAP) every 17 ± 3.5 days (total cumulative dose: 240 mg/m^2). At the experimental endpoint (15 weeks after the last dose of doxorubicin), euthanasia was induced in accordance with *American Veterinary Medical Association (AVMA)* guidelines. While under anaesthesia, a catheter was placed in a peripheral vein, and euthanasia solution was administered at a dose of sodium pentobarbital ~100 mg/kg IV. Euthanasia was achieved by exsanguination and subsequent removal of the heart. Ascending aorta cross-sections were acquired from ~1 cm above the sinotubular junction and fixed in 4% paraformaldehyde for subsequent histopathologic analysis. For non-treated control samples, archival tissues from 5 age- and sex-matched healthy animals were used for histopathological comparisons.

4.2.2 Histopathology

Histological images of the aortas were captured using a digital slide scanner (Hamamatsu HT NanoZoomer). Five μm consecutive sections from each block were stained with hematoxylin and eosin (H&E) and Masson's trichrome staining. Tunica media collagen volume fraction (CVF) and vacuoles were quantified from photomicrographs of 10 random fields from each aortic section obtained using a 20X objective[209]. Collagen volume fraction was determined from these images using Image J (NIH, Bethesda, MA) and expressed as a percentage of area. The number of vacuoles from each microphotograph was annotated and expressed as the mean of the 10 microscopy fields. The aortic medial area was measured in low magnification H&E-stained sections by tracing the circumference of the external and internal elastic lamina; the area was calculated by subtracting the area of the internal from the external circumference. Medial thickness was determined by measuring the distance from the internal to external elastic lamina from four random points across the aorta. All analysis was performed by researchers blinded to the treatment group.

4.2.3 Clinical Study in Patients with Lymphoma

Ethical approval was granted by the West of Scotland Research Ethics Committee (22/WS/0180). This was a retrospective observational study with no change in patient management. Prior to each clinical PET scan, patients were asked to consent for images to be used in future research as part of the routine clinical pre-PET questionnaire (Appendix 8.2). Those who consented were included. All aspects of this study were performed in accordance with the Declaration of Helsinki. The data underlying this article will be shared on reasonable request to the corresponding author.

We performed a retrospective review of [^{18}F]FDG-PET/CT scans of patients with diffuse large B-cell lymphoma (DLBCL) referred to the Regional PET service at Glasgow Beatson West of Scotland Cancer Centre between 2019 to 2023. This is a cancer network hub centre which receives referrals from 16 referring hospital sites. We included patients aged 18 years and older treated using anthracycline regimens receiving a cumulative dose of >150mg/m^2 of doxorubicin. We excluded patients whose arterial FDG uptake could not be quantified due to significant

interference from adjacent lymphoma. Other exclusion criteria were those treated at a hospital that was not in the NHS Greater Glasgow & Clyde catchment area, incomplete medical records, concurrent thoracic radiotherapy, technically inadequate scans (such as non-diagnostic tracer uptake), blood glucose >11mmol/L before either scan and suspected or confirmed vasculitis on the baseline scan. Patients were also excluded if their baseline PETCT was more than 3 months before starting chemotherapy.

Detailed baseline demographic data, including past medical history and cancer history, were collected from electronic case note reviews. Baseline cardiovascular risk stratification was performed using the European Society of Cardiology (ESC) baseline cardio-oncology CV risk stratification assessment tool[170]. Response to treatment was collected by the Deauville score reported on the clinical scan.

4.2.4 ^{18}F-FDG PET/CT imaging

[^{18}F]FDG-PET/CT scanning was performed in accordance with departmental standard procedures based on *European Association of Nuclear Medicine (EANM)* guidelines [136] on PET/CT scanners (Discovery-690 or 710, General Electric System, Milwaukee, WI, USA or Biograph Vision 600, Siemens, Erlangen, Germany). Patients were fasted for a minimum of 6 hours prior and blood glucose levels were checked during patient preparation. Scanning was performed one hour after intravenous administration of 4 MBq/kg [^{18}F]FDG. CT images were acquired at 120kV, with automatic mA modulation applied (Noise Index=30 or reference mAs=50, dependent on the scanner used) and covered from the base of the skull to mid-thigh, reconstructed at 1.5-2.5mm increments. PET images encompassed the same transverse field of view as the CT. PET acquisition times were 3-4 min per bed position or 1-1.5mm/second, depending on the scanner used. PET attenuation correction was based on CT, and images were corrected for the scatter, time-of-flight and point spread function, and iteratively reconstructed using local clinical reconstruction parameters.

4.2.5 PET analysis

Analysis of aortic [^{18}F]FDG uptake was performed using FusionQuant v1.21 software (Cedars-Sinai Medical Centre, Los Angeles). For all methods, co-registration between PET signal and CT images was ensured in 3 orthogonal planes. Care was taken to ensure activity from adjacent tissue, such as oesophagus or adjacent lymphoma, was not included in the aortic analysis. Background activity in the blood pool was determined as the mean standardised uptake value (SUVmean) of 10 sequential cylindrical 3-Dimensional (3D) volumes of interest (VOI) within the superior vena cava (SVC), starting at the confluence of the innominate vein. Aortic ^{18}F-FDG activity was measured using 4mm thick 3D polygonal VOIs starting at the ascending aorta to the end of the thoracic descending aorta. Aortic analysis started at the inferior aspect of the right pulmonary artery and stopped when the descending thoracic aorta passed through the diaphragm. FDG uptake of the arterial vessel compared to background uptake was used, giving a target-to-background ratio (TBR), in accordance with EANM guidelines[137].

TBR was calculated for each VOI by dividing the SUVmax and SUVmean value by the blood pool activity to give TBRmax and TBRmean, respectively. TBR values were then averaged for the thoracic aorta and each aortic segment. Analysis was performed in concordance with EANM recommendation for aortic activity including TBRmax, TBRmean, activity within 'active segments' (defined as a TBRmax $\geq$1.6) and most diseased segment (MDS, the three consecutive VOIs around the VOI with the highest activity to represent the most intense lesion), described previously[137]. 10% of scans were randomly selected and re-analysed by two trained observers (SR, DC) for inter-observer and intra-observer agreement. To minimise recall bias, intra-observer repeatability was assessed by the same trained researcher (SR) using repeated assessments performed 3 months apart in random order.

4.2.6 Calcium scoring

Aortic calcification assessment was performed on the CT of the baseline PETCT scan on a dedicated workstation (Vitrea Advanced, Vital Imaging, Toshiba Systems, Minnesota, USA). A density threshold of 130 Hounsfield units, 3-pixel

threshold on 3mm slice thickness was used and a cumulative calcium score of the whole aorta and each thoracic aortic segment was calculated as previously described[167].

4.2.7 Statistical analysis

Statistical analysis was performed using STATA software (Version 17). Continuous data with normal distribution are presented as mean ± standard deviation (SD), and skewed data are presented as median and interquartile range (IQR). Between groups comparisons were made using paired t tests and ANOVA or non-parametric equivalents as appropriate. Normal distribution was assessed by the Shapiro-Wilk test. Intra- and interobserver variability was assessed by the intra-class correlation (ICC) coefficient. Based on prior studies using change in mean TBRmax as a primary outcome, a sample size of 101 patients was needed to detect a 10-15% difference between groups with a power of 85% and significance of 5%, assuming a baseline TBRmax of 1.57 ± 0.42 and a SD of change in TBRmax of 0.4[142,152,210]. A p value <0.05 was taken to represent statistical significance.

4.3 Results

4.3.1 Non-Human Primate Study

Both groups were of similar age (control 12.5 ± 0.7 vs doxorubicin 13.1 ± 0.6y, p=0.3), weight (control: 5.4 ± 0.5 vs doxorubicin: 4.9 ± 0.3kg, p=0.2), and body surface area (BSA, control: 0.28 ± 0.01 vs doxorubicin: 0.27 ± 0.01, p=0.2). Morphometric data of the animals have been previously described [30,208].

Histopathological analysis of the structural changes within hematoxylin-eosin stained aortas of AGMs exposed to doxorubicin there was more intracellular vacuolisation in comparison to control animals (control 11.5 ± 4.2 vs doxorubicin 66.3 ± 10.1 vacuoles/field, p<0.0001, Figure 4-1).Doxorubicin treatment was associated with an increase in collagen deposition in the aortic media consistent with fibrosis (controls: 4.67 ± 0.54% vs. doxorubicin: 6.23 ± 0.88%, p=0.01;Figure 4-2). There was no difference in the medial area (controls: 10.6 ± 2.03mm^2 vs dox: 9.32 ± 2.27mm^2, p=0.3) nor medial area/BSA (control: 2200 ± 404.3 mm^2/m^2 vs doxorubicin: 2127 ± 462.2 mm^2/m^2, p=0.7) between groups and medial thickness was also not different between control animals and those exposed to doxorubicin (control: 573.2 ± 71.61μm vs doxorubicin: 519.4 ± 96.15 μm, p=0.34).

Figure 4-1 Intracellular vacuolization within the aortic media of monkeys exposed to doxorubicin compared with controls. Histopathological assessment of hematoxylin-eosin stained aortas (n=10). A: Graphical representation of the number of vacuoles present in the arterial wall in the control arm (CTL, n=5) and the doxorubicin treated arm (Dox, n=5), analysis by unpaired two tailed t test, p<0.0001. (B). Representative microphotographs of hematoxylin-eosin stained aortas at 10X and 40X magnification. Black arrows indicate cardiomyocytes with intracellular vacuolisation. All values are mean ± SEM.

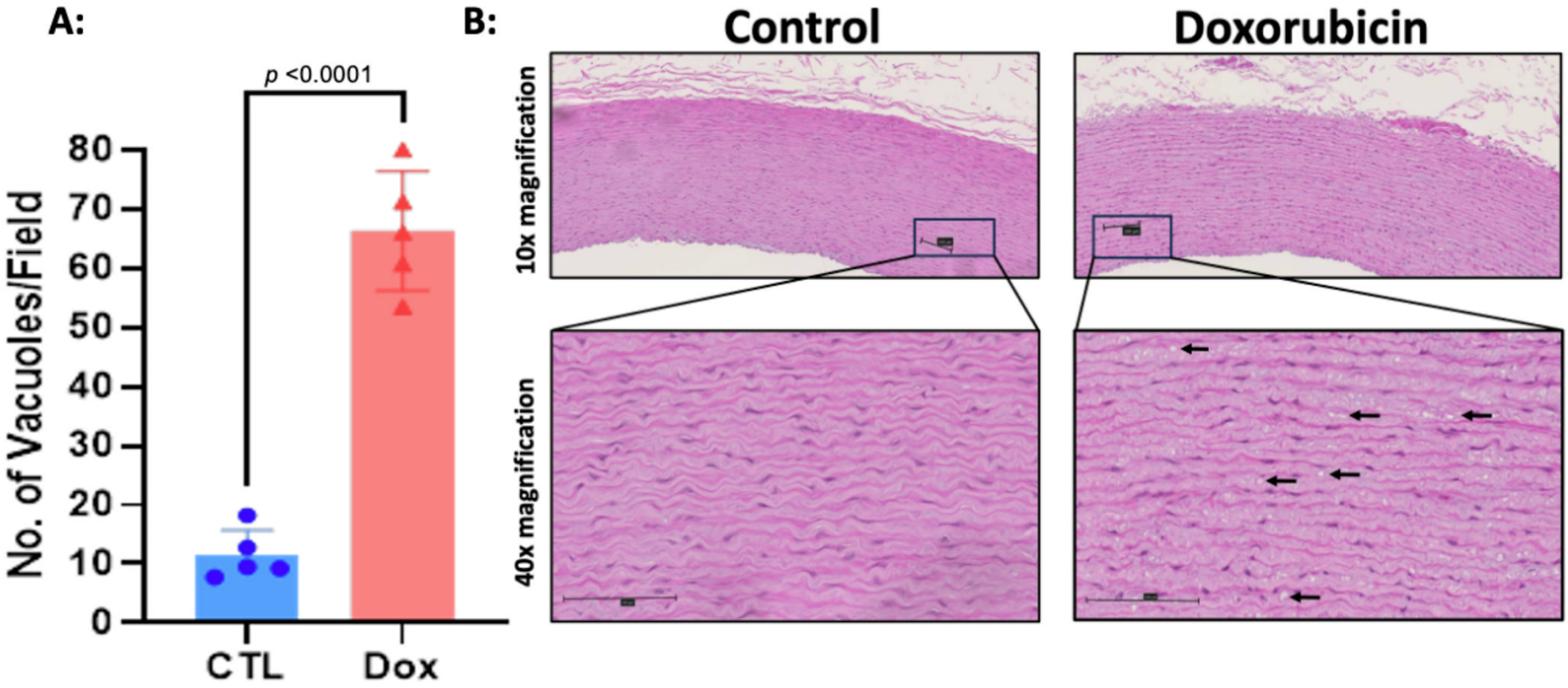

Figure 4-2 Collagen fibre deposition in the aortic media of monkeys exposed to doxorubicin compared with controls. Assessment of ascending aorta media deposition of interstitial collagen. Graphical representation of collagen volume fraction (A) in aortas of untreated controls (blue bar, n=5) and Dox-treated AGMs (red bar, n=5). Representative microphotographs (20X) of aortas of untreated controls (B) and Dox-treated AGMs(C). Collagen is stained blue (highlighted by black arrows), and the cytoplasm of smooth muscle cells is stained red and pink in the microphotographs. All values are mean ± SEM. *analysed by unpaired two tailed t test p=0.01

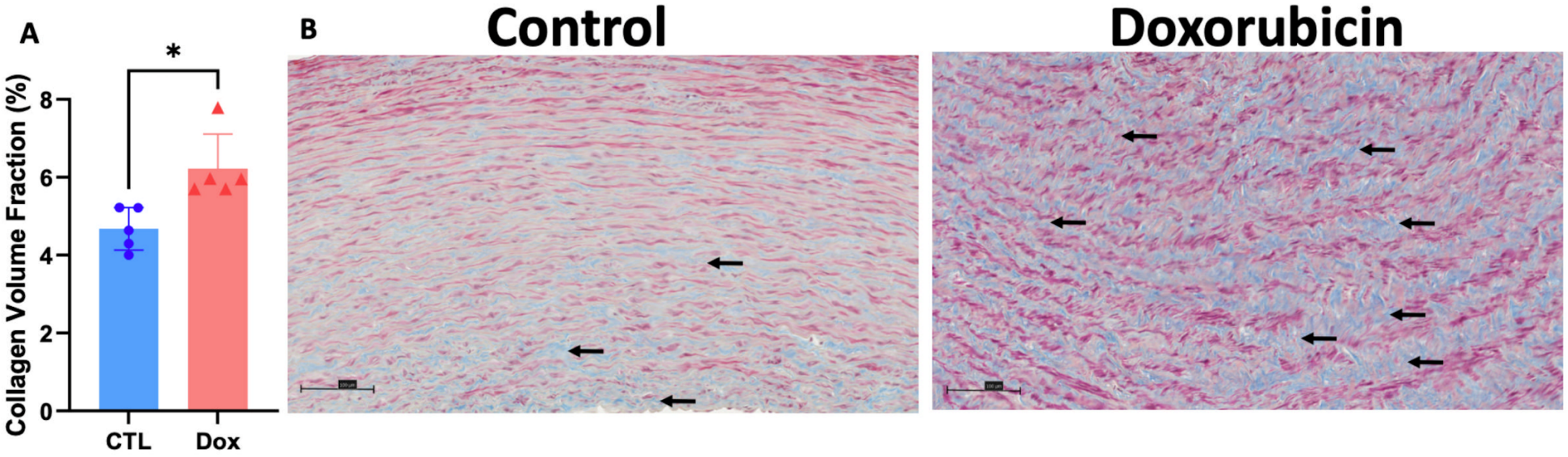

4.3.2 Clinical Study in Patients with Lymphoma

A total of 101 patients were included in the analysis (Figure 4-3) of whom the mean age was 64 ± 12 years and 47 were female. The majority of patients had advanced lymphoma (71% with stage III/IV disease). The median cumulative doxorubicin dose was 300mg/m^2 (IQR 225-300mg/m^2) and 82% of patients received 6 cycles of doxorubicin. There was a high prevalence of cardiovascular risk factors (hypertension, dyslipidaemia, ischemic heart disease, smoking history, diabetes, body mass index ≥35kg/m^2) with 69% of patients having at least one.

On the basis of ESC Cardio-Oncology cardiovascular risk stratification criteria, 55% of patients would be considered to have at least 'medium' cardiovascular risk (36% 'medium', 18% 'high' and 1% 'very high' risk, Table 4-1). The median time from baseline PETCT to starting doxorubicin was 7 days (IQR 4-14 days). The mean time between starting doxorubicin and post-doxorubicin PET/CT was 4.8±0.9 months and the median time from finishing chemotherapy to follow up PET/CT was 1.2 months (IQR 0.9-1.6 months).

Figure 4-3 Consort figure

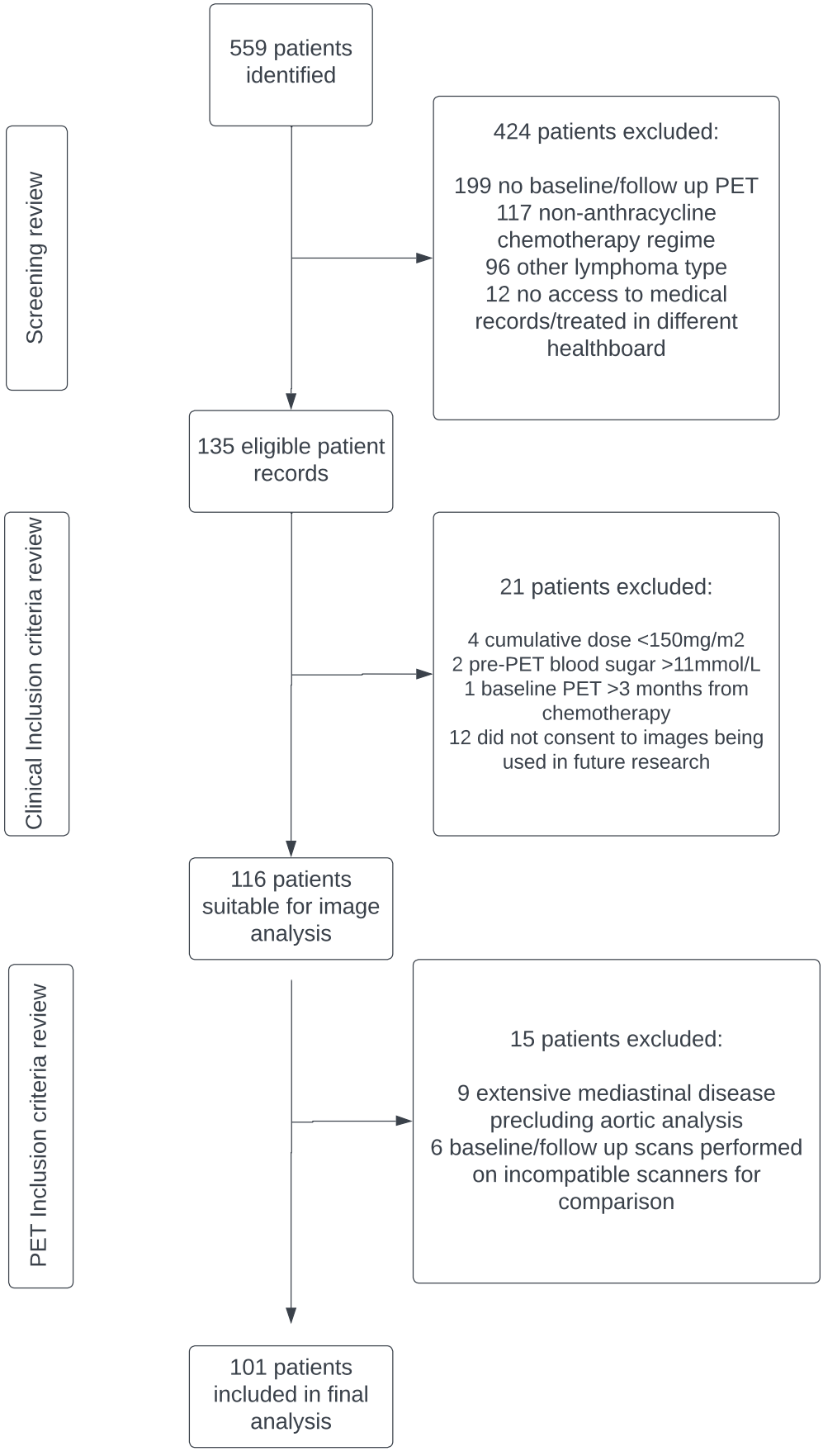

Table 4-1 Baseline demographics of patients with diffuse large B-cell lymphoma (DLBCL), treated with anthracycline-based chemotherapy

Demographics		Total (n=101)
Mean age (years ± SD)		64.3±12
Sex (n/%)		
Male		54 (54)
Female		47 (47)
Mean BMI (kg/m^2 ± SD)		27.8±5.8
Hematological characteristics		
Cancer stage (n/%)		
1		14 (14)
2		16 (16)
3		24 (24)
4		47 (47)
Previous chemotherapy (n/%)	No	86 (86)
Non-anthracycline regimen		10 (10)
Anthracycline regimen		4 (4)
Anthracycline regimen (n/%)	RCHOP	96 (95)
R-CODOX-M-IVAC		5 (5)
Cycles of anthracycline (n/%)	≤3	12 (12)
4-5		5 (5)
≥6		84 (84)
Median doxorubicin cumulative dose (mg/m^2)		300.0 (IQR 225.0-300.0)
Baseline cardiovascular characteristics		
ESC Baseline CV risk stratification (n/%)		
Low risk		46 (46)
Medium risk		36 (36)
High risk		18 (18)
Very high risk		1 (1)
Aortic calcification at baseline (n/%)	Yes	78 (78)
No		23 (23)
Median aortic calcium score		213.0 (IQR 11.0-938.0)
Previous myocardial infarction (n/%)		5 (5)
Previous coronary revascularisation* (n/%)		3 (3)
Angina (n/%)		2 (2)
Previous stroke (n/%)		7 (7)
Previous heart failure (n/%)		1 (1)
History of atrial fibrillation (n/%)		3 (3)
Hypertension (n/%)		35 (35)
Diabetes (n/%)		14 (14)
Smoking history (n/%)		
ex-smoker		27 (27)
current		18 (18)
Antiplatelet therapy (n/%)		12 (12)
ACEI or ARB (n/%)		28 (28)
Diuretic therapy (n/%)		5 (5)
Beta-blocker (n/%)		18 (18)
Rate limiting CCB (n/%)		3 (3)
Non-rate limiting CCB (n/%)		12 (12)
Statin (n/%)		26 (26)

ACEI – Angiotensin-converting enzyme inhibitor, ARB – angiotensin receptor blocker, BMI- Body Mass Index, CCB – calcium channel blocker, CV-cardiovascular, RCHOP- rituximab, cyclophosphamide, doxorubicin, vincristine, prednisolone. R-CODOX-M-IVAC- rituximab, cyclophosphamide, cytarabine, vincristine, doxorubicin, methotrexate, ifosfamide, etoposide, cytarabine *prior percutaneous coronary intervention or coronary artery bypass grafting.

4.3.3 PET analysis

The mean TBRmax of the thoracic aorta at baseline and follow up was 1.46 ± 0.16 vs 1.43 ± 0.14, respectively, p=0.14, Figure 4-4. In comparison to baseline, there was no observed difference in aortic inflammation, measured by mean TBRmax, TBRmean, TBRmax within 'active segments' or 'most diseased segment (MDS)' after doxorubicin exposure, Table 4-2.

Figure 4-4 FDG uptake of the thoracic aorta in patients with lymphoma before and after treatment with anthracycline-based chemotherapy Boxplot of the mean TBRmax (± SD) of the whole aorta pre and post anthracycline exposure in 101 lymphoma patients using a paired two tailed t test, p=0.14.

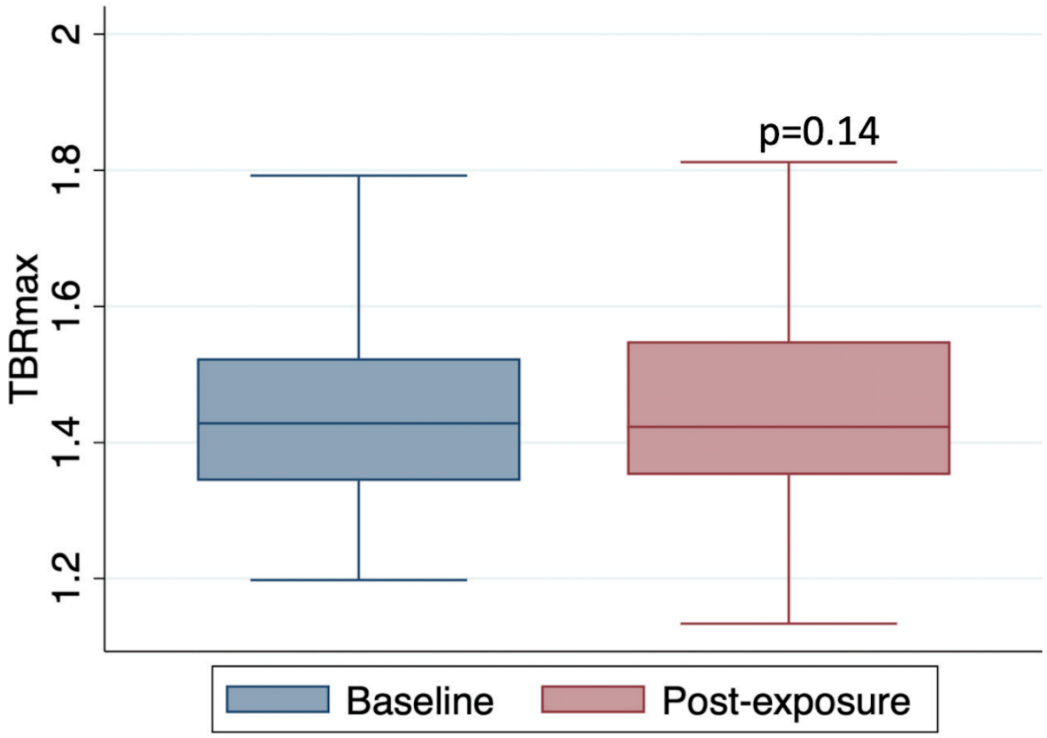

Table 4-2 Aortic TBR and MDS measured by PET, before and after anthracycline-based chemotherapy. Aortic assessments were compared from two PET/CT scans (baseline and post-exposure) for each patient in the study (n=101). Results are presented as the mean ± SD and analysed using paired two-tailed *t* test.

		Mean TBRmax				
Aortic Segment	**PET parameter**	**Pre-dox**	**Post-dox**	**Difference**	**95% CI**	***p***
Whole aorta	TBRmax	1.46 ±0.16	1.44 ±0.14	-0.02 ±0.15	-0.05 to 0.01	0.14
	TBRmean	1.06 ±0.10	1.05 ±0.09	-0.01 ±0.1	-0.03 to 0.01	0.29
	TBR max of active segments	1.71 ±0.08	1.7 ±0.06	-0.01 ±0.08	-0.03 to 0.07	0.18
	MDS	1.65 ±0.22	1.64 ±0.20	-0.01±0.23	-0.06 to 0.03	0.62
Ascending	TBRmax	1.51 ±0.18	1.48 ±0.15	-0.02 ±0.15	-0.05 to 0.01	0.19
	TBRmean	1.07 ±0.11	1.06 ±0.09	-0.01 ±0.1	-0.03 to 0.07	0.19
	TBR max of active segments	1.74 ±0.11	1.70 ±0.07	-0.03 ±0.11	-0.07 to 0.04	0.08
	MDS	1.57 ±0.19	1.55 ±0.17	-0.02 ±0.18	-0.06 to 0.01	0.20
Arch	TBRmax	1.52 ±0.16	1.49 ±0.14	-0.03 ±0.16	-0.65 to 0.00	0.05
	TBRmean	1.07 ±0.08	1.06 ±0.07	-0.01 ±0.08	-0.02 to 0.09	0.36
	TBR max of active segments	1.75 ±0.10	1.71 ±0.12	-0.03 ±0.15	-0.08 to 0.02	0.18
	MDS	1.61 ±0.20	1.57 ±0.18	-0.04 ±0.22	-0.08 to 0.00	0.06
Descending	TBRmax	1.43 ±0.16	1.41 ±0.15	-0.02 ±0.16	-0.05 to 0.01	0.21
	TBRmean	1.05 ±0.12	1.04 ±0.11	-0.01 ±0.11	-0.03 to 0.01	0.33
	TBR max of active segments	1.70 ±0.08	1.70 ±0.07	-0.002 ±0.1	-0.03 to 0.03	0.88
	MDS	1.60 ±0.20	1.59 ±0.22	-0.01 ±0.24	-0.05 to 0.04	0.82

Comparison of [^{18}F]FDG uptake by each aortic segment was similar to that of the whole aorta before and after doxorubicin. There was a very small decrease in mean TBRmax after doxorubicin observed within the aortic arch that was of borderline statistical significance (mean TBRmax pre-doxorubicin: 1.52 vs post-doxorubicin: 1.49; -0.03 difference, 95% CI -0.65-0, p=0.05), Table 2. Intra-observer and inter-observer assessments were highly correlated and demonstrated excellent reproducibility (Table 4-3).

Table 4-3. Inter-observer and intra-observer variability Inter and intra observer agreement was assessed by two-way mixed effect interclass coefficient model in 10% of the cohort (n=10 randomly selected scans)

		(95% confidence interval)	
Aortic Segment	**PET parameter**	**Inter-observer agreement**	**Intra-observer agreement**
Whole aorta	TBRmax	0.95 (0.88-0.98)	0.96 (0.90-0.98)
	TBRmean	0.97 (0.93-0.99)	0.97 (0.93-0.99)
	TBR max of active segments	0.88 (0.64-0.96)	0.86 (0.39-0.87)
	MDS	0.94 (0.86-0.98)	0.90 (0.75-0.96)
Ascending	TBRmax	0.97 (0.93-0.99)	0.97 (0.92-0.99)
	TBRmean	0.97 (0.94-0.99)	0.95 (0.89-0.98)
	TBR max of active segments	0.79 (0.2-0.96)	0.88 (0.38-0.98)
	MDS	0.97 (0.92-0.99)	0.88 (0.71-0.95)
Arch	TBRmax	0.89 (0.75-0.96)	0.94 (0.85-0.97)
	TBRmean	0.95 (0.87-0.98)	0.95 (0.88-0.98)
	TBR max of active segments	0.76 (-0.13-0.97)	0.89 (0.4-0.98)
	MDS	0.78 (0.52-0.91)	0.85 (0.66-0.94)
Descending	TBRmax	0.95 (0.88-0.98)	0.96 (0.91-0.99)
	TBRmean	0.97 (0.93-0.99)	0.98 (0.95-0.99)
	TBR max of active segments	0.85 (0.54-0.96)	0.87 (0.52-0.97)
	MDS	0.93 (0.82-0.97)	0.89 (0.73-0.95)

4.3.4 Baseline aortic Calcification & [^{18}F]FDG uptake

Aortic calcification was present on the baseline PETCT scan in 78 of the 101 patients (calcium score >0, Table 4-1). Aortic calcium scores ranged from 0 to 13566, with a median score of 213 (IQR 11-938). TBRmax remained unchanged from baseline, irrespective of the baseline aortic calcium score: there was no difference in TBRmax when comparing patients grouped by quartile of baseline

aortic calcification, including comparison of the lowest quartile (aortic calcium score range 0-11) with the highest quartile (calcium score range 943-13566), p=0.42, Figure 4-5.

Figure 4-5 Change in mean TBRmax y baseline aortic calcium score in patients with lymphoma before and after treatment with anthracycline-based chemotherapy. The change in aortic TBRmax from before and after anthracycline in 101 lymphoma patients compared with quartiles of aortic calcification, assessed by linear regression between quartiles. There was no difference across any, including the lowest to highest quartile, p=0.42.

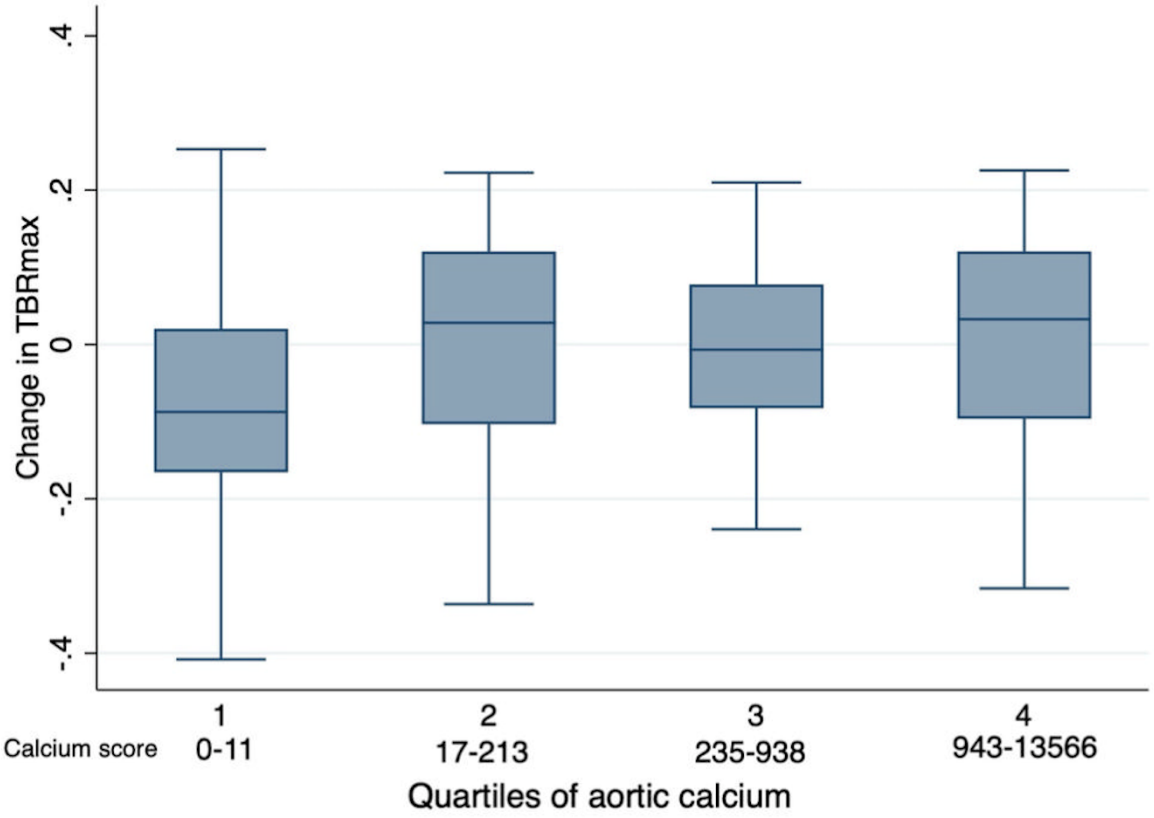

4.3.5 PET analysis by clinical factors

Univariate analysis of baseline demographics and cardiovascular risk factors (hypertension, dyslipidaemia, ischemic heart disease, smoking history, diabetes, body mass index ≥35kg/m^2) did not identify any association between these variables with change in aortic FDG uptake, when assessed by TBRmax, TBRmean, MDS and 'active segments,' after doxorubicin exposure. Baseline CV risk, assessed using the ESC risk stratification tool, was also not associated with change in aortic FDG uptake (Table 4-4).

Table 4-4 Comparison of aortic FDG uptake (assessed by the mean TBRmax of the whole aorta) with the presence or absence of cardiovascular risk factors. Univariate analysis was presumed in 101 patients. Unpaired two-tailed *t* test was performed for univariate analysis with two variable (yes/no) and ANOVA for >2 variables (ESC baseline CV risk).

		Mean TBRmax			
CV risk factor	**N=**	**Baseline**	**Follow up**	**Difference**	***p***
Hypertension					0.47
No	66	1.46	1.45	-0.01	
Yes	35	1.46	1.43	-0.04	
Dyslipidaemia					0.31
No	95	1.46	1.44	-0.03	
Yes	6	1.43	1.46	0.04	
Ischaemic heart disease					0.06
No	95	1.46	1.44	-0.02	
Yes	6	1.52	1.38	-0.14	
Smoking history					0.49
No	56	1.48	1.46	-0.01	
Yes	45	1.44	1.41	-0.03	
Diabetes					0.77
No	87	1.47	1.44	-0.02	
Yes	14	1.42	1.41	-0.01	
Calcium score					0.53
<1000	77	1.47	1.44	-0.03	
≥1000	24	1.43	1.42	-0.01	
Statin					0.26
No	75	1.46	1.45	-0.01	
Yes	26	1.45	1.40	-0.05	
BMI					0.6
<35	91	1.46	1.44	-0.02	
≥35	10	1.46	1.41	-0.05	
ESC Baseline CV risk					
Low risk	46	1.50	1.45	-0.04	0.32
Medium risk	36	1.44	1.45	0.01	
High/Very high risk	19	1.41	1.39	-0.02	

There was no association between the change in aortic activity and cumulative doxorubicin dose, stage of disease at diagnosis, or response to treatment on follow up imaging (Table 4-5).

Table 4-5 Comparison of aortic FDG uptake (assessed by the mean TBRmax of the whole aorta) by baseline demographics and treatment response. Univariate analysis was presumed in 101 patients. Unpaired two-tailed *t* test was performed for univariate analysis with two variable (yes/no) and ANOVA for >2 variables (cancer stage & Deauville score).

		Mean TBRmax			
Group	**N=**	**Baseline**	**Follow up**	**Difference**	***p***
Sex					0.08
Male	54	1.46	1.42	-0.05	
Female	47	1.46	1.46	0.00	
Age					0.19
≤70	63	1.48	1.45	-0.04	
>70	38	1.42	1.43	0.00	
Cancer stage					0.22
1	14	1.45	1.40	-0.05	
2	16	1.40	1.42	0.02	
3	24	1.47	1.48	0.01	
4	47	1.48	1.43	-0.05	
Cumulative dose					
<250mg/m^2	27	1.45	1.42	-0.04	0.5
≥250mg/m^2	74	1.46	1.45	-0.02	
Complete response					
No	32	1.49	1.44	-0.05	0.17
Yes	69	1.45	1.44	-0.01	
Deauville score on follow up scan					
1	4	1.36	1.38	0.01	0.64
2	46	1.44	1.43	-0.01	
3	19	1.48	1.48	0.00	
4	11	1.46	1.43	-0.03	
5	21	1.51	1.44	-0.06	

4.4 Discussion

We investigated the arterial effects of anthracyclines in a non-human primate model and in patients with lymphoma. Doxorubicin, a very commonly used anthracycline drug, was associated with substantial aortic vacuolization and fibrosis in monkeys. In contrast, we did not observe more inflammation in the thoracic aorta of patients exposed to doxorubicin in patients treated for lymphoma. [^{18}F]FDG PETCT, the gold standard imaging modality for arterial inflammation, was used and did not identify inflammation as a pathogenetic mechanism for the anthracycline related fibrosis.

Our non-human primate study provides novel insights into arterial morphologic changes and extracellular matrix remodelling induced by anthracyclines. By employing this unique large animal model that shares similar genetic traits with humans, our results provide valuable and potentially translatable data. Our animal study incorporated a doxorubicin dosing scheme similar to that received by the patients in our clinical study. Anthracycline exposure was associated with substantial histopathological vascular changes including greater deposition of vascular collagen and intracellular vacuolization of the arterial media. We have previously reported that these animals developed cardiac fibrosis and an absolute reduction of left ventricular (LV) ejection fraction of 25%[30]. However, to the best of our knowledge, the effects of anthracyclines on arterial remodelling have not previously been explored in a large animal model. Small animal models consistently demonstrate that inflammation is implicated in the pathophysiology of hypertension- and age-related vascular dysfunction[211,212] and there are overlaps between the structural and functional consequences of these pathologies and anthracycline-associated arterial toxicity, including extracellular matrix remodelling, degradation of elastin, and formation of advanced glycated end products [201,202,211,212]. In animal models of age-related vascular dysfunction, pro-inflammatory pathways are active, including tumour necrosis factor-alpha (TNF-α), interleukins-1ß and -6, with macrophage and T cell infiltration observed in the adventitia and surrounding adipose tissue [213,214]. Similar circulating biomarkers, and in mouse aortic lysates, have been observed in small mouse models of anthracycline vascular toxicity[207]. Other mechanisms, such as, inflammation mediated through Toll-like receptors have been implicated in both anthracycline toxicity and vascular disease[215]. It is also plausible that arterial

inflammation also occurs in the coronary macro- and microvasculature to contribute to myocardial toxic effects of anthracycline. Notably, prior work has demonstrated a link between cardiomyocyte vacuolization and tissue oedema [33] while we and others have demonstrated that cardiac fibrosis is preceded by inflammation and oedema [30,32,33]. Intriguingly, the recent STOP-CA trial demonstrated that atorvastatin prevents anthracycline-associated cardiotoxicity in patients with lymphoma[216]. It has been postulated that this reflects the pleotropic of statins. The mechanism underlying this effect has not been defined but it is possible that the arterial protective effects, including anti-inflammatory, may be at least partially responsible. This treatment effect may be particularly prominent in patients with systemic inflammatory activation, such as is seen in patients with lymphoma[217]. The mechanism underlying this effect has not been defined but it is possible that arterial protective effects, including anti-inflammatory, may be at least partially responsible.

In humans, prior treatment with anthracycline is associated with elevated arterial stiffness and this may be a consequence of arterial fibrosis[17]. Elevated arterial stiffness exacerbates ventriculo-arterial uncoupling which, in turn, contributes to LV pressure overload, adverse remodelling and LV dysfunction[28]. Therefore, understanding the mechanisms via which anthracycline evokes arterial fibrosis and stiffening is of fundamental importance so that patients can receive optimal cancer treatment while preventative strategies are developed to minimise adverse cardiovascular effects.

In light of our pre-clinical data, we hypothesised that inflammation may be central to the development of anthracycline-associated arterial stiffening in humans. We assessed aortic inflammation in a cohort of 101 patients with lymphoma treated with anthracycline. Capitalising upon clinical datasets, we had detailed cardiovascular and oncologic information available. We excluded patients with low-anthracycline dose exposures and the median cumulative doxorubicin dose of 300 mg/m^2 received by these patients was similar to that used in the non-human primate study. The patients included were representative of the 'real world' population of patients with a mean age of 64 years and an almost equal representation of men and women. Cardiovascular disease and risk factors were prevalent at baseline, with over half of patients considered to be at least moderate risk when assessed using the ESC baseline CV

risk stratification assessment tool. Despite these methodological strengths, we observed no change in aortic inflammation when assessed just over a month after the completion of treatment with anthracycline-based chemotherapy. Our primary measure of [^{18F}]FDG PETCT inflammatory activity was mean TBRmax but the lack of change in inflammatory activity also held true when assessed via other analysis methods including TBRmean, TBRmax within 'active segments' and within 'most diseased segments (MDS)'. There was also no association between inflammatory activity and potential hematologic and cardiovascular risk factors, including aortic calcification in 78% of patients, which we used as an objective and quantifiable marker of pre-existing cardiovascular disease.

Previous studies have demonstrated a possible link between inflammatory biomarkers and anthracycline-associated cardiac toxicity. However, there have been conflicting findings and research has primarily focused upon cardiac rather than arterial toxicity[218-222]. A link between inflammatory markers and cardiotoxicity was not seen in a large prospective randomized trial assessing cardiac toxicity[223]. Of studies investigating aortic stiffness in humans after anthracycline exposure, to the best of our knowledge, no study simultaneously investigated inflammatory markers[17].

We assessed the inflammatory effects of anthracycline around one month after completion of anthracycline. Aortic stiffening has been demonstrated to occur within 4 months of anthracycline exposure and we wished to examine this 'high risk' period [224]. A previous smaller retrospective study examined arterial [^{18F}]FDG PETCT in 52 patients following anthracycline treatment for Hodgkin lymphoma at a mean of 65 weeks and found no difference in large artery TBR [210]. The longer time between completion of chemotherapy and PET scanning meant that evidence of ongoing active inflammation would have been considerably less likely. Furthermore, in contrast to our study, the mean age of the patients was only 35 years, with very few cardiovascular risk factors and, of particular relevance to immune-related analyses, 35% were HIV positive. Overall, our findings imply that anthracycline-associated arterial fibrosis and stiffening occurs independently of inflammation.

4.4.1 Limitations

While the animals in the non-human primate study were age- and gender-matched between groups, these animals would be considered to be otherwise healthy and without pre-existing cardiovascular disease or risk factors. Furthermore, although the animals were exposed to clinically relevant doses of anthracycline (as well as using the same agent as received by the patients), they were free of cancer and a potential interaction between anthracycline exposure, active malignancy and the propensity for arterial injury cannot be excluded. Our human study was a retrospective analysis of clinically-indicated imaging and, therefore, the PETCT scans were performed for clinical indications to assess for cancer rather than specifically for vascular assessments. Smaller vessels such as carotids and iliac arteries, which may be more likely to show a signal for FDG uptake, were not assessed. Patients in this cohort were most commonly treated with the 'R-CHOP' chemotherapy regime (rituximab, cyclophosphamide, doxorubicin, vincristine and prednisolone), which contains high-dose pulses of immunosuppression which may attenuate any inflammatory signal. Given the persisting risk of anthracycline cardiotoxicity using these chemotherapy regimens, we feel this cohort still remains a valid group for analysis[225,226].

4.4.2 Conclusion

In conclusion, in our large animal model, anthracycline exposure was associated with aortic fibrosis and increased intracellular vacuolization. In patients with lymphoma, anthracycline exposure was not associated with aortic inflammation assessed by [^{18F}]FDG PETCT. Further research is required to elucidate the mechanisms of anthracycline-related vascular harm and its clinical consequences.

Chapter 5 Image Reconstruction and Analysis of Atherosclerosis Imaging by [^{18}F]FDG PETCT using Digital PET Technology

5.1 Introduction

[^{18}F]Fluorodeoxyglucose (FDG) positron emission tomography computed tomography (PETCT) is a well-established modality for atherosclerosis imaging and is the gold standard method for the assessment of large vessel inflammation[227]. Imaging of aortic atherosclerosis has been used for risk stratification in cardiovascular disease, including acute coronary artery syndromes and ischaemic stroke[135,145,228,229]. In 2016, the European Association of Nuclear Medicine (EANM) published guidance on optimal PETCT reconstruction parameters and methods of assessment for atherosclerotic imaging [227].

Digital PETCT technology offers significant improvements in spatial resolution, improved sensitivity and signal-to-noise ratio, using digital silicon photomultiplier (SiPM)[148,230]. Quantifiable metrics, such as the mean contrast recovery (MCR), traditionally have been used to assess optimal reconstruction parameters[231]. On non-digital scanners, high number of iterations and subsets were required to yield a high MCR, minimise partial volume effects (PVE) of smaller regions of interest and achieve adequate imaging. This is particularly relevant for atherosclerotic assessment and is reflected in EANM guidelines. As digital scanners offer higher sensitivity and better resolution, fewer iterations and subsets may be required than those suggested by EANM. Additional methods of assessing reconstructions include absolute error, coefficient of variation (CoV) and curvature of the contrast recovery vs lesion size curve[231]. These additional metrics may provide valuable insights into atherosclerotic assessment reconstructions in digital scanners.

In addition to image acquisition and reconstruction protocols, EANM suggest methods for analysis using the tissue-to-background ratio (TBR*)* which assesses arterial [^{18}F]FDG uptake corrected for background blood pool activity. To ensure there is scientifically accurate, clinically meaningful and reproducible data with TBR, there must be clear and accurate assessment of both arterial FDG uptake (the numerator of the ratio) and standardised analysis of the blood pool (the

denominator of the ratio). For atherosclerotic imaging, a TBR threshold of 1.6 has previously been suggested as an indicator of 'inflamed disease', and so reconstruction which reflects true activity is important[143,227,232]. EANM also highlights the importance of avoiding other metabolically active structures, such as muscle or malignant tissue, in the assessment of aortic uptake.

For collecting blood pool activity, EANM advise that a vein that is anatomically close to the artery of interest should be used in order to account for any time delay and FDG decay during the scan. For example, internal jugular (IJ) vein, superior vena cava (SVC) and inferior vena cava (IVC) blood pool activity are suggested to be used for blood pool assessment when examining the carotid artery, thoracic and descending aorta, respectively. However, there remains variation in the choice of region used for blood pool assessment, including using SVC alone, subclavian vein, muscle and atria[139,160,227,233,234] and detail of how blood pool data are collected is often lacking[165,232,235]. While the reasons for this heterogeneity are often not clearly stated, there may be practical challenges in obtaining robust data from smaller veins, particularly when these are close to other potentially metabolically active structures. Digital PETCT scanners allow for shorter acquisition time due to their higher sensitivity (and the options for continuous scanning) thus potentially negating the need for multiple blood pool analyses but the impact of digital scanners on the choice of optimal blood pool region has not been formally assessed.

The aims of this study were to evaluate reconstruction parameters recommended by EANM recommendations for atherosclerotic arterial analysis, specifically the number of effective iterations and subsets, and compare these with locally optimised parameters on a digital scanner. We aimed to address the following questions: 1) Are EANM recommended reconstruction parameters optimal for arterial inflammation analysis using digital PET scanners? 2) Does blood pool activity vary across different regions? 3) What is the reproducibility of assessments of these regional blood pools over time and between different assessors? 4) Does the choice of blood pool region affect atherosclerotic analysis? Our analysis involved arterial assessment of patients enrolled in a prospective clinical research study with additional analysis using phantoms to compare the accuracy of measured FDG activity against known 'true' FDG activity.

5.2 Methods

5.2.1 Imaging analysis

5.2.1.1 Patient cohort

Arterial PETCT analysis was performed on the baseline scans of the first twenty patients enrolled in a prospective clinical research study of unselected patients with cancer. The study was approved by the West of Scotland Research Ethics Committee 5 (REC5) in July 2022 REC reference 22/WS/0085 and by the Administration of Radioactive Substances Advisory Committee (ARSAC) for the administration of radioactive substances (ARSAC Ref AA-4580). Inclusion and exclusion criteria are available online (clinicaltrials.gov NCT06597045). The main exclusion were: age <18 years, diabetes, and those who were unable to consent. Baseline demographics of patients included in the analysis are summarised in Table 1.

Table 5-1 Baseline Demographics

Characteristic	N=20
Mean age (years ±SD)	65.9 (10.3)
Sex (n/%)	
Female	6 (30)
Male	14 (70)
Mean BMI (±SD)	30.4 (7.5)
Cancer stage	
3	2 (10)
4	18 (90)
WHO Performance status	
0 (n/%)	14 (70)
1 (n/%)	4 (20)
2 (n/%)	2 (10)
Nephrectomy	14 (70)
History of heart failure (n/%)	1 (5)
Hypertension (n/%)	13 (65)
Previous myocardial infarction(n/%)	1 (5)
Previous coronary revascularisation	1 (5)
Diabetes (n/%)	0
Atrial fibrillation (n/%)	2 (10)
Dyslipidaemia (n/%)	9 (45)
Stroke or TIA (n/%)	4 (20)
Mean blood glucose pre-PET (±SD)	5.1 (0.6)
Haemoglobin g/L (IQR)	140.0 (19.1)
White cell count x10^9/L (IQR)	7.4 (1.9)
Urea mmol/L (IQR)	6.3 (1.5)
Creatinine umol/L (IQR)	102.0 (26.9)
eGFR ml/min (IQR)	55.7 (7.9)
BMI – body mass index, eGFR – estimated glomerular filtration rate, IQR – interquartile range, PET – positron emission tomography , SD – standard deviation	

PETCT Imaging acquisition

[^{18}F]FDG-PETCT scanning was performed on the digital scanner, Biograph Vision 600 (Siemens, Erlangen, Germany). Patients were fasted for a minimum of 6 hours prior to tracer administration and blood glucose levels were checked during patient preparation to ensure concentrations <11mmol/L. Scanning was performed 90 minutes after administration of 4 MBq/kg [^{18}F]FDG. CT images were acquired at 120kV, with automatic tube current modulation and reference mAs of 50 mAs, covering the base of the skull to mid-thigh, reconstructed at 1.5-mm increments. PET images encompassed the same transverse field of view as the CT, scanning craniocaudally. PET acquisition times were 0.7mm/s. PETCT scans were analysed using two reconstructions. Patients were scanned at baseline, prior to anti-cancer therapy, and 24 weeks after baseline. To address the possible impact of circulation time on TBR, we compared the blood pool and descending aorta TBRmax in this cohort with a 90-minute circulation time with matched patients (n=20) from a similar cohort published previously[236], in a retrospective analysis using the same reconstruction parameter (440x440 matrix, voxel size 1.65 x 1.65 x 1.65mm with a filter and 4 iterations (i) 5 subsets, 4i5s) with a 60-minute circulation time. In accordance with EANM, carotid artery assessment was not made due to the retrospective nature of the study.

5.2.1.2 Choice of reconstruction parameters

A matrix size of 440 x 440 was selected to achieve matched PET and CT voxels of 1.65 x 1.65 x 1.65 mm without applying a software zoom, thus minimising interpolation artefacts. This corresponds to the native pixel size for the PET scanner and approximates the EANM suggested voxel size of 1 x 1 x 1mm. In order to maximise SUV recovery, we chose to use an all-pass post-reconstruction filter (equivalent to using no filter), in line with EANM guidelines. EANM guidelines suggest that the optimal choice of iterative reconstruction parameters for ordered subset expectation maximisation (OSEM) is at least 120 effective iterations. The Siemens implementation of the OSEM algorithm limits reconstructions on the Vision to 5 subsets (s), thus the closest match to the effective iterations (i) suggested by EANM was 24 iterations and 5 subsets (24i 5s = 120 effective iterations). Local optimisation work suggested that 4i 5s (20 effective iterations) was likely to be quantitatively more accurate and was

therefore used for the local reconstruction (Figure 8-1 and Table 8-4). We chose to use the 4i5s All Pass reconstruction which had amongst the optimum recovery curve characteristics, but which would also maximise the spatial resolution.

Based upon the above data, we compared two reconstructions: 440x440 matrix, all pass filter 4i 5s ('Local Reconstruction') with the 440x400 matrix, all pass filter 24i 5s ('EANM Reconstruction').

5.2.1.3 PETCT arterial assessment

Arterial [^{18}F]FDG uptake was assessed using FusionQuant v1.21 software (Cedars-Sinai Medical Centre, Los Angeles). The baseline scan only was used for arterial assessment, to ensure no effect from anti-cancer therapy was included in the analysis. For all methods, co-registration between PET signal and CT images was ensured in 3 orthogonal planes. Arterial [^{18}F]FDG PET activity was measured using 4mm thick 3-dimensional (3D) polygonal volumes of interest (VOI) starting at the descending aorta, inferior to the level of the right pulmonary artery to descending aorta passing through the diaphragm (Figure 5-1). [^{18}F]FDG uptake of the artery compared to background uptake was used, giving a target-to-background ratio (TBR), in accordance with EANM recommendations. The right carotid artery was used for smaller arterial assessments, to the level of carotid bifurcation at the cricothyroid cartilage. TBR was calculated for each VOI by dividing the maximal and mean Standardised Uptake Value (SUV) value by the mean blood pool activity (SVC) to calculate TBRmax and TBRmean, respectively. Analysis was performed in concordance with EANM recommendation for arterial activity including TBRmax, TBRmean, TBRmax within 'active segments' (defined as a TBRmax $\geq$1.6) and most diseased segment (MDS, the mean TBRmax of 1.2cm arterial segment centred on the VOI with the highest FDG activity[227].

Figure 5-1 Landmarks for arterial analysis

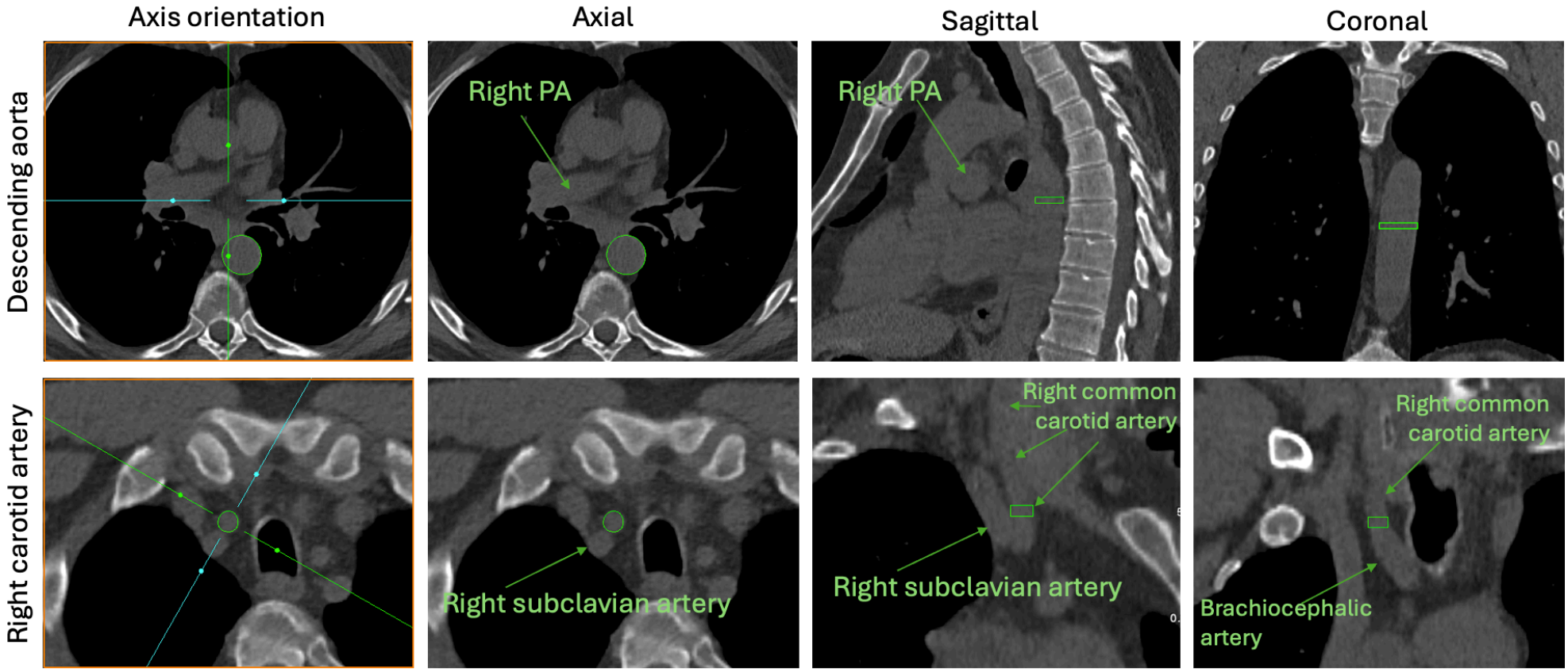

5.2.1.4 Blood pool measurement & analysis

We aimed to assess the blood pool activity in the SVC, IJ and IVC, recommended in EANM for arterial analysis. We also aimed to assess whether the innominate (IN) vein may be more suitable for carotid analysis than the IJ. Blood pool analysis was performed on the same group of patients enrolled in the above study, at baseline and 24 weeks, using both reconstructions in four regions: SVC, IJ, IN & IVC. For all blood pool regions, a total of ten sequential 4mm high cylindrical 3D VOIs with a 3mm radius were collected by two observers (DC & SR). For the SVC, blood pool analysis started at the confluence of the innominate veins, moving caudal to the heart. For the IN, five sequential VOIs were collected in both left and right IN, starting when the left IN had traversed the midline and became circular on axial plane. For the IJ, five sequential VOIs were collected in both left and right IJ, starting at the bifurcation of the brachiocephalic vein, moving cranially. For IVC, 10 sequential VOIs were collected starting at the iliac bifurcation.

Observers also reported whether it was possible to acquire all ten VOIs in each region, due to vessel size or interference from adjacent tissue and we compared the number of missing VOIs from each region at baseline and 24 weeks for reproducibility. We then compared the different arterial TBR measurements using the blood pool closest to the arterial segment, as recommended by EANM (IJ for carotid and IVC for descending aorta), and compared it to the SVC, which we hypothesise is the most suitable blood pool region to use as it is the largest and most central vessel. Finally, we assessed whether the IN, a vein that is larger and more easily identifiable than the IJ but closer to the carotid artery, was suitable for use as a blood pool comparator for carotid arterial analysis.

5.2.1.5 Interference from adjacent tissue

In assessments of aortic activity, avoiding interference from surrounding tissue is crucial. When an area of interference was identified, the adjacent arterial tissue was excluded from that VOI, ensuring a clear margin. If interference affected more than two thirds of the arterial VOI, the 4mm segment was not included in analysis. Reconstruction parameters can affect image quality. We compared the number of arterial segments that were affected by interference from adjacent

structures in both reconstructions to assess if the reconstruction affected interpretation of arterial activity and ability to detect interference.

5.2.2 Phantom analysis

As it is not possible to ascertain which of the two reconstructions was more accurately identifying [^{18}F]FDG activity within the patient group, phantoms were analysed with both reconstructions to compare the observed measured activity of [^{18}F]FDG in each reconstruction and with the known true activity within the phantom by quantitative recovery coefficients (RC, formula in online resource 1) acquired on the digital scanner. RCs were measured using two different phantoms – A National Electrical Manufacturer Association / Internal Electrotechnical Commission (NEMA IEC) body phantom using sphere diameters of 10-37 mm (to approximate larger vessels in the abdomen and chest) and a smaller custom phantom (12x16cm cylinder) to replicate vessels in the neck (five spheres, diameters 5-13 mm). Sphere:background concentrations of approximately 4:1 were achieved using [^{18}F]FDG and the phantoms were scanned at the same speed and parameters outlined above for scans used for arterial assessment. Each phantom was scanned three times with both reconstructions.

Table 5-2 Metrics of PETCT reconstruction parameters. Adapted from Kaalep et al, 2018 [231]

Recovery coefficient	the ratio between image derived and expected activity concentration: $$Activity\ Recovery\ Coefficient\ (RC) = \frac{A}{a}$$ *A=activity concentration measured in sphere* *a=known activity concentration in sphere*
Mean Contrast Recovery	mean RC of all spheres in corresponding reconstruction mode's long duration acquisition. Parameter is indicative of reconstruction mode's overall contrast recovery potential
Absolute error	Long acquisition duration root-mean-square deviation of spheres' RC values from unity. The parameter characterises the reconstruction mode's ability to report accurate activity concentration values.
Coefficient of Variation	Coefficient of Variation (100*SD/mean, %) of a group of MCR values. Parameter is indicative of RC curves' alignment within a group.

To compare the differences between a digital and non-digital scanner, phantoms were analysed using 120 effective iterations on the digital Siemens Vision (24 iterations, 5 subsets), and a non-digital scanner, GE Discovery 710 (5 iterations, 24 subsets). For the non-digital scanner, Time of Flight and Point Spread Function were used with a 3 min/bed scan over multiple scans. 20 effective iterations were not analysed on the non-digital scanner.

Phantom images were analysed using Hermes Hybrid Viewer 6.1 (Hermes Medical Solutions, Stockholm, Sweden), with VOIs created using the nominal sphere diameters and positioned on the co-registered CT images, with results recorded in Bq/ml. RCs from both reconstructions were plotted against sphere diameter and a best-fit curve calculated using a logistic function[237].

5.2.2.1 Additional metrics of reconstruction analysis

PETCT reconstruction performance was also assessed quantitatively using a range of metrics, including MCR, absolute error, and CV, reported previously and summarised in online resource 1[231]. The MCR provides an overall assessment of the corresponding reconstruction by calculating the mean RC of all spheres. Given the variation in size of artery assessed in atherosclerotic imaging, this

gives an indication of the suitability of the corresponding reconstruction for atherosclerotic imaging. The ideal MCR should converge to 1.0. Absolute error is calculated by the standard deviation from the RC values and is indicative of the accuracy of the reconstruction. CV assesses the variation in MCR on repeated assessment of each sphere and reflects the alignment and repeatability of the corresponding reconstruction.

5.2.3 Statistical analysis

Statistical analysis was performed using STATA software (Version 17) and R package with ggplot2[238]. Continuous data with normal distribution are presented as mean ± standard deviation (SD), and skewed data are presented as median and interquartile range (IQR). Between groups comparisons were made using paired t tests or non-parametric equivalents, as appropriate. Comparison of blood pool activity was performed using a repeated measure analysis of variance analysis with Bonferroni correction to account for multiple testing. Correlations were used to assess two continuous variables by Pearson's R correlation coefficient. To assess agreement and observer variability, intra-class correlation (ICC) coefficient and Bland-Altman plots were used. Inter- and intra-observer variability was assessed by absolute agreement ICC using two-way random effects model[239,240]. Due to potential missing data, individual ICC was reported using a mean of values from the VOIs collected in each blood pool region and assessed by an individual ICC. A p value <0.05 was taken to represent statistical significance.

5.3 Results

5.3.1 FDG activity: Maximal and mean

5.3.1.1 Arterial analysis

On assessment of PETCT, EANM reconstruction had significantly higher TBRmax compared with the local reconstruction (p<0.0001), Table 5-3. TBRmax was 2.4-fold higher using the EANM reconstruction in large arteries, with TBRmax 4.26 (IQR 3.8-4.5) in the EANM reconstruction compared to 1.74 (IQR 1.6-2.0) in the local reconstruction, p<0.0001. Carotid TBR was 1.9-fold higher in EANM compared to the local reconstruction, p<0.0001. The difference in TBRmax between the two reconstructions increased with higher values (

Figure S8-2). EANM reconstruction yielded TBRmax values greatly above the threshold of TBRmax 1.6 for active disease defined in EANM recommendations. TBRmean and SUVmean were similar in both reconstructions in arterial analysis. When comparing 60-minute versus 90-minute circulation time in two cohorts with cancer, both scanned on the Siemens Vision digital scanner with the same reconstruction protocol, we observed high TBRmax values in 90 minute circulation due to lower blood pool values and no difference in arterial FDG uptake (Figure 5-2).

Table 5-3 Arterial and blood pool activity by EANM recommended reconstruction vs Local reconstruction.
Both SUVmax and TBRmax are greater in the EANM reconstruction in both large artery (descending aorta) and small artery (carotid artery) with TBR values greatly exceeding the threshold of 1.6 indicating inflammation

	Descending aorta				Carotid artery			
Variable	Mean (±SD)	Median (IQR)	Min	Max	Mean (±SD)	Median (IQR)	Min	Max
SUVmean								
EANM	2.13 ± 0.44	2.09 (2.0-2.2)	1.54	3.39	2.26 ± 0.33	2.19 (2.1-2.5)	1.74	2.96
Local	1.97 ± 0.46	1.88 (1.8-2.0)	1.34	3.31	2.03 ± 0.37	1.94 (1.8-2.2)	1.51	2.96
TBRmean								
EANM	1.17 ± 0.12	1.18 (1.1-1.28)	0.95	1.38	1.26 ± 0.19	1.27 (1.1-1.4)	0.88	1.65
Local	1.13 ± 0.12	1.10 (1.0-1.2)	0.96	1.37	1.18 ± 0.17	1.15 (1.0-1.3)	0.92	1.56
SUVmax								
EANM	7.79 ± 1.82	7.40 (6.4-8.7)	5.64	12.43	5.27 ± 0.99	5.31 (4.3-6.2)	4.01	6.66
Local	3.13 ± 0.76	3.0 (2.7-3.2)	2.22	5.08	2.74 ± 0.53	2.56 (2.4-3.0)	2.02	4.02
TBRmax								
EANM	4.28 ± 0.65	4.26 (3.8-4.5)	3.16	5.64	2.95 ± 0.66	2.71 (2.4-3.5)	1.98	4.26
Local	1.81 ± 0.24	1.74 (1.6-2.0)	1.47	2.25	1.59 ± 0.25	1.54 (1.4-1.8)	1.18	2.22

Figure 5-2 Comparison of 60 minute vs 90 minutes circulation time in patients with cancer (n=40) using the digital PET scanner, Siemens Vision

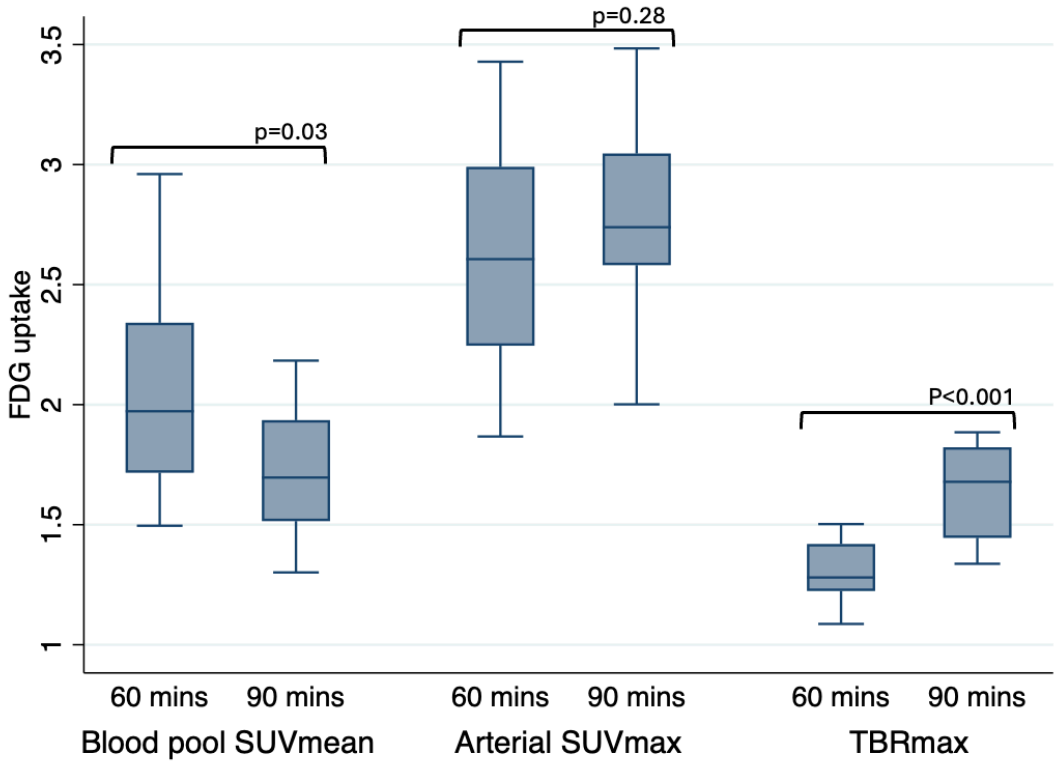

5.3.1.2 Phantom analysis

When comparing the EANM with local reconstruction, phantom data reflected the arterial analysis indicating that EANM reconstruction almost always over-estimated true activity for RCmax. The EANM reconstruction over-estimated the true Bq/ml in both the torso phantom (Figure 5-3A) and neck phantom (Figure 5-3B). In the torso phantom, the MCR was 1.87 in the EANM vs 1.23 with local reconstruction for RCmax (Table 5-4). The RCmean in the phantom data with both reconstructions showed similar trends although it remained consistently less than 1.0 for all sphere sizes (Figure 5-3, Table 5-4). Looking at the smaller spheres alone (<10mm diameter), MCR was 1.18 with 24i5s and 0.6 with 4i5s, however CV was 13.2% vs 3.9%.

Figure 5-3 Recovery coefficient, comparing EANM & Local Reconstruction.
RC max and RCmean for A: torso phantom, B: neck phantom. Error bars: standard deviation on the mean from the 3 repeated scans.

a

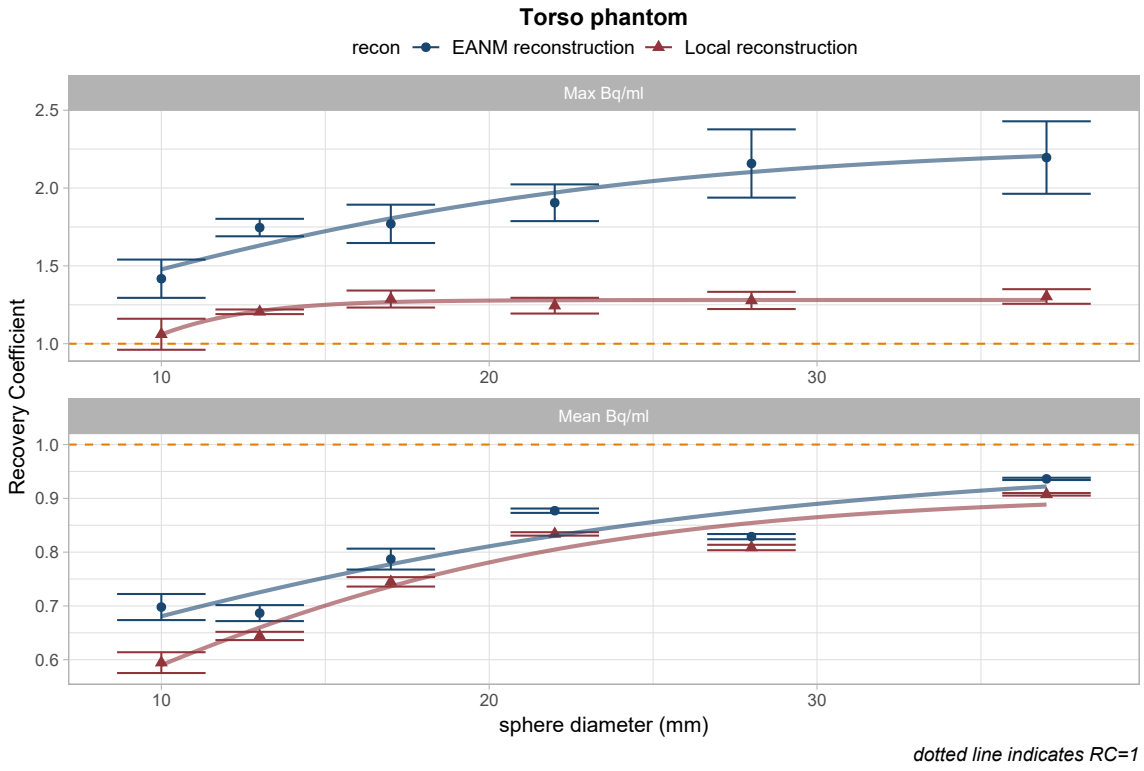

b

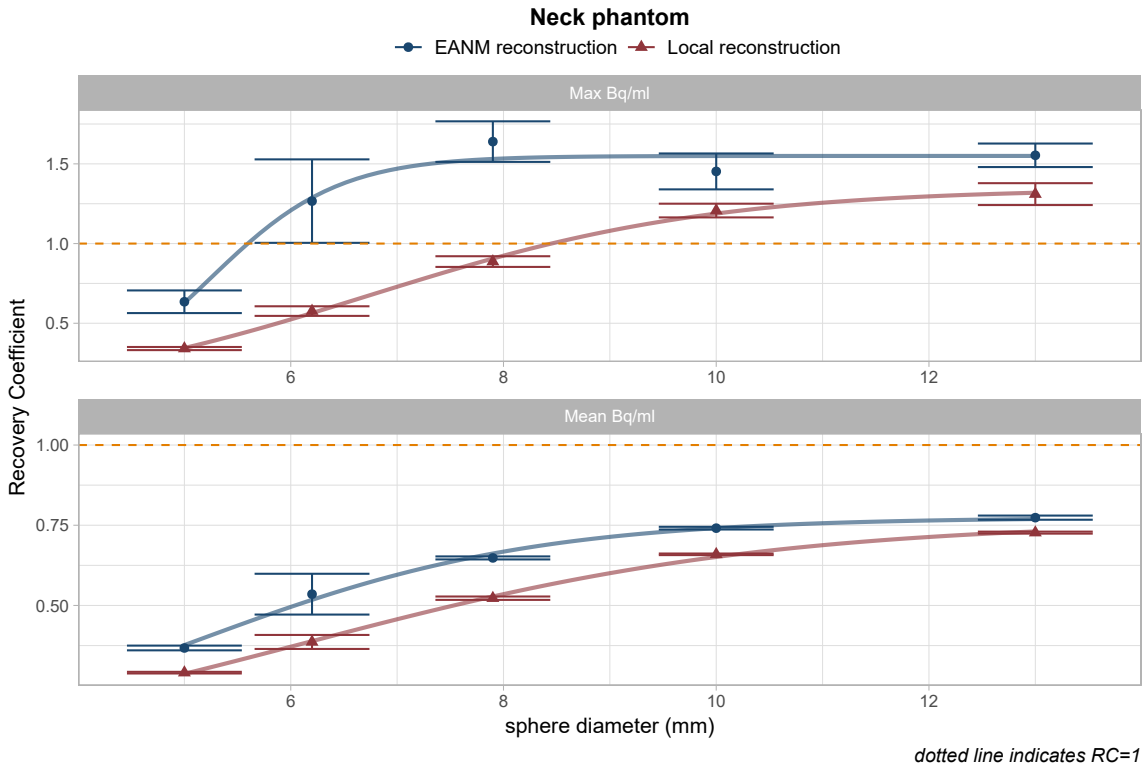

Table 5-4 Quantitative measurements for RCmax and RCmean for torso and neck phantoms MCR - Mean contrast recovery, RC – recovery coefficient, i-iterations, s-subsets, CoV-coefficient of variation

RCmax			
Reconstruction	MCR ± SD	Absolute error ± SD	Average CoV
Torso phantom			
Local	1.23 ± 0.02	0.61 ± 0.03	4.48%
EANM	1.87 ± 0.07	2.24 ± 0.18	7.63%
Neck phantom			
Local	0.86 ± 0.03	0.88 ± 0.02	4.14%
EANM	1.31 ± 0.09	1.08 ± 0.20	10.43%
RCmean			
Torso phantom			
Local	0.76 ± 0.002	0.66 ± 0.008	1.15%
EANM	0.80 ± 0.001	0.53 ± 0.003	1.56%
Neck phantom			
Local	0.52 ± 0.003	1.14 ± 0.010	1.67%
EANM	0.61 ± 0.011	0.93 ± 0.028	3.20%

On both digital and non-digital scanner, we observed that 24i5s had greater overshoot of RC in torso phantoms on both digital and non-digital scanners, compared with 4i5s on the digital scanner (Figure 5-4). On smaller phantoms, more relevant for atherosclerotic assessment, 24i5s reached convergence earlier and with high RCmax compared with 4i5s on a digital scanner. When comparing 24i5s on a non-digital scanner (EANM recommendation), there was an S-shaped curve, with lower RC at spheres <7mm compared to 4i5s digital then overshoot thereafter. 4i5s digital remained closest to 1.0.

Figure 5-4 Comparing digital & non-digital scanners with 20 (local reconstruction) vs 120 iterations (EANM reconstruction.

a

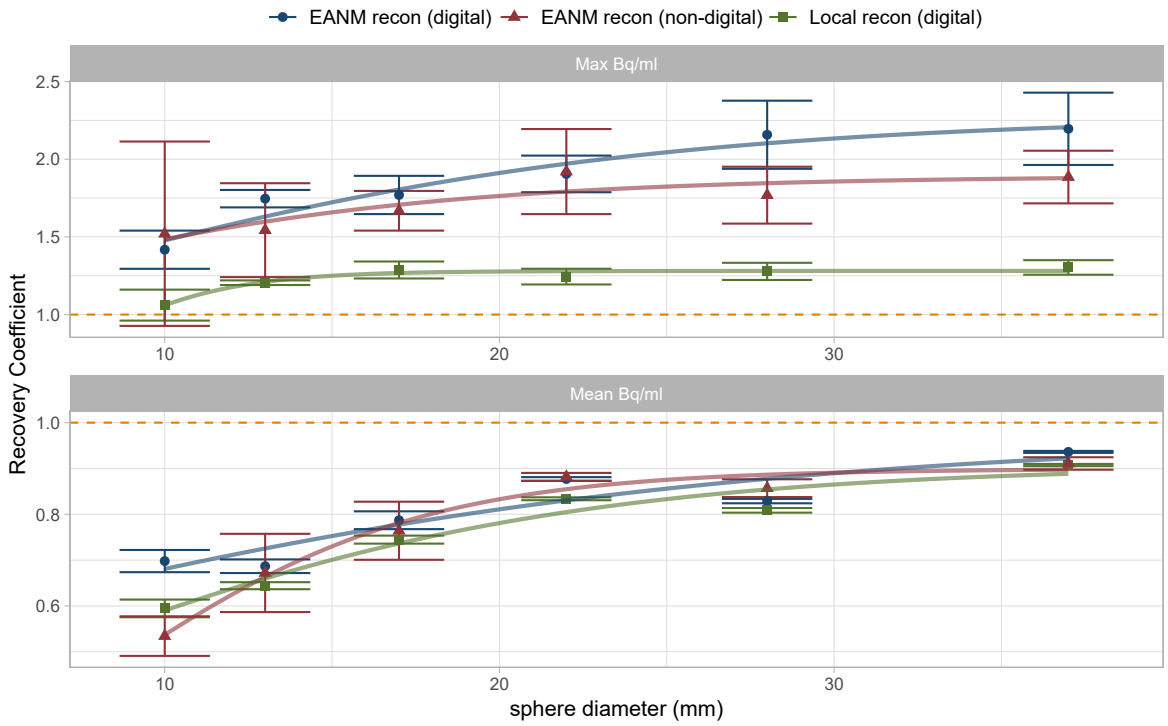

dotted line indicates RC=1

b

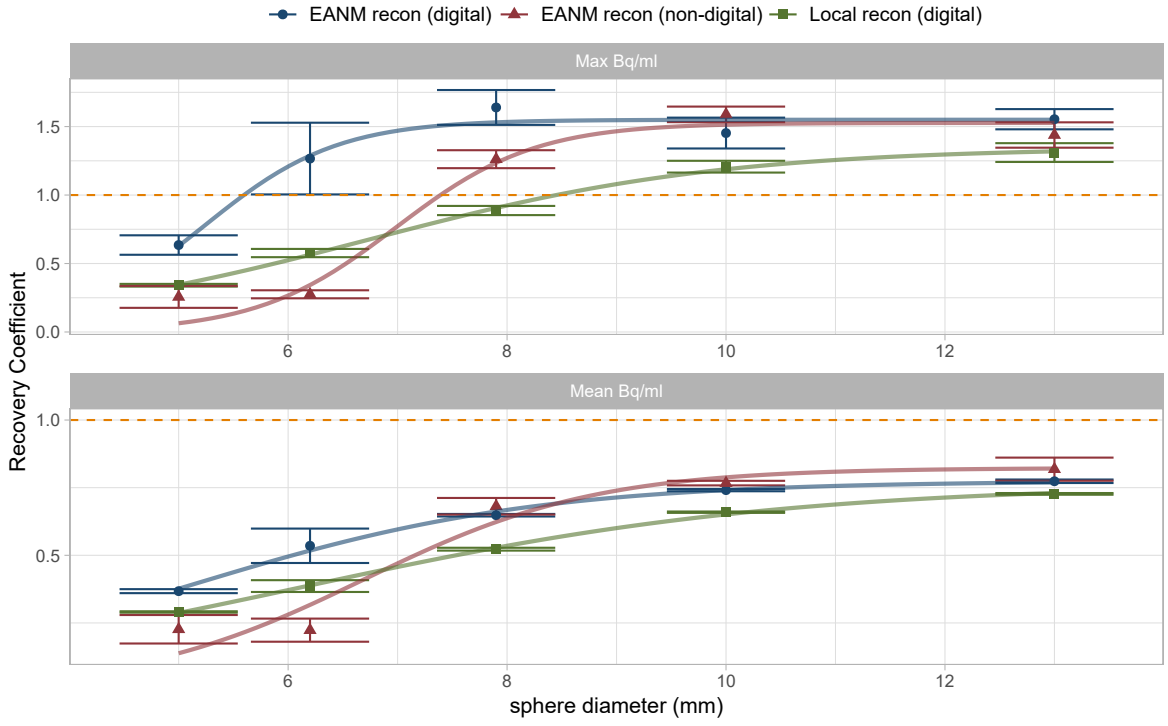

dotted line indicates RC=1

5.3.2 Visual analysis, accuracy & reliability

5.3.2.1 Arterial analysis

In comparison to the local reconstruction, PET image quality using the EANM reconstruction was poor, lacking smooth gradient with higher noise across PET activity with poor differentiation between PET activity and adjacent structures, Figure 5-5. This poorly differentiated image quality had an impact on the assessment of possible areas of interference. When comparing arterial analysis using both reconstructions, 100 (10%) VOI's were modified to avoid interference from adjacent tissue using the local reconstruction. On repeat analysis of the same scans with the EANM reconstruction, 39 (4%) ROIs were modified due to interference.

5.3.2.2 Phantom analysis

Visual assessment of phantom data (Figure 5-5 a,b,d,e) demonstrated increased activity on the outer rim of phantom, in keeping with ring artefact, in the EANM reconstruction in the 13mm sphere (Figure 5-5b & Figure 5-6). Phantom assessment demonstrated poorer repeatability with the EANM reconstruction. The EANM reconstruction had higher absolute error (2.23 vs 0.61) with a CoV of 10.4% compared to 4.14% with the local reconstruction on repeated imaging in torso phantoms, Table 5-4. This was consistent across all sphere size for both SUVmax and SUVmean. Results were similar in neck phantoms.

Figure 5-5 Examples of phantoms and PETCT images using different reconstructions
For each subfigure upper is Local and lower is EANM reconstruction. A: PET axial slice of custom neck phantom to represent distal artery size. B: Colour scale of neck phantom demonstrating Gibbs artefact. C: Representative equivalent axial slice of PET/CT of the carotid arteries. D: PET axial slice of NEMA/IEC torso phantom. E: Axial slice using colour scale of torso phantom F: Representative axial slice of PET/CT. This axial slice also clearly demonstrates interference from high FDG uptake from the oesophagus adjacent to the aorta.

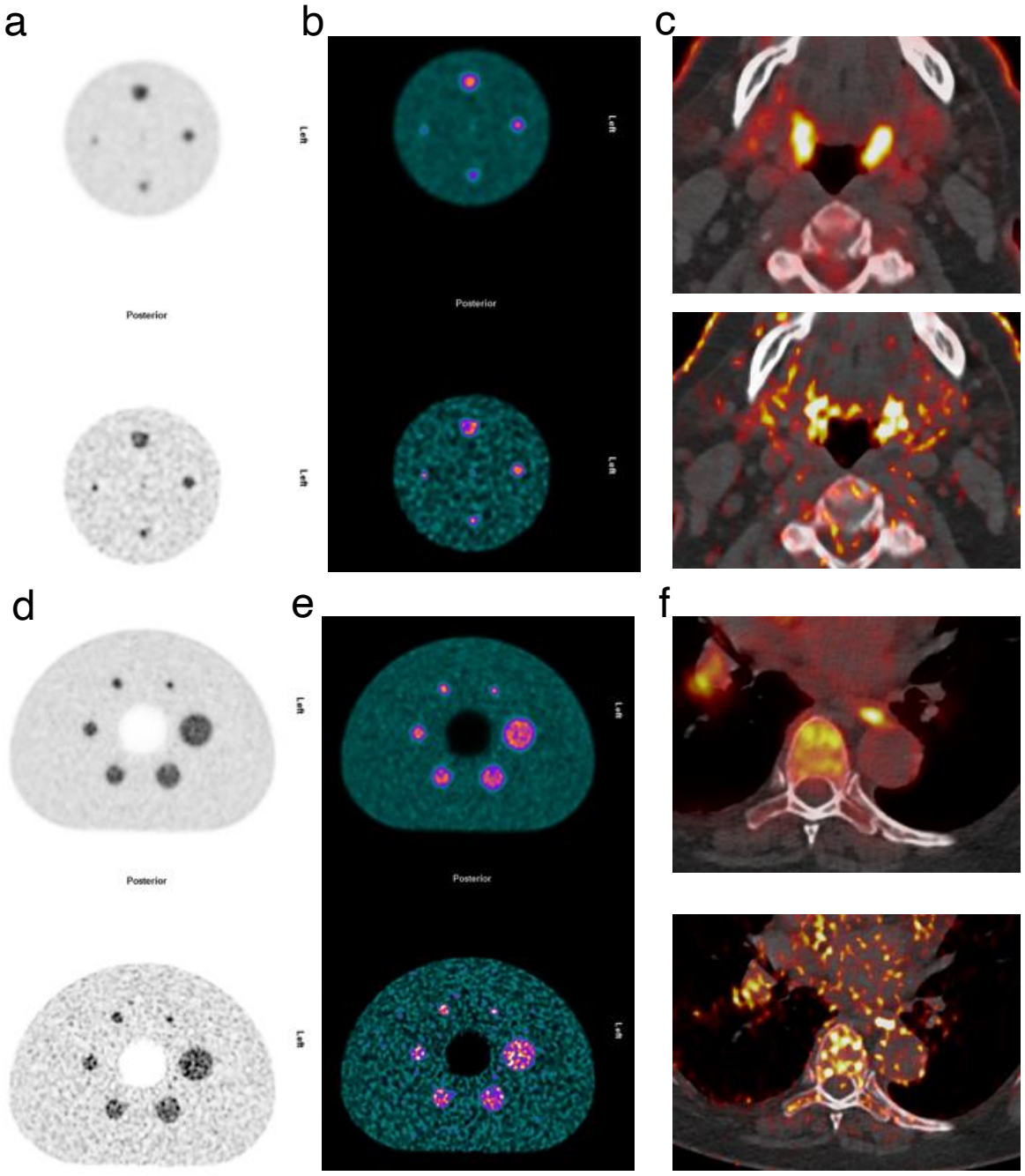

Figure 5-6 Profile of 13mm neck phantom and the presence of Gibbs artefact in EANM reconstruction

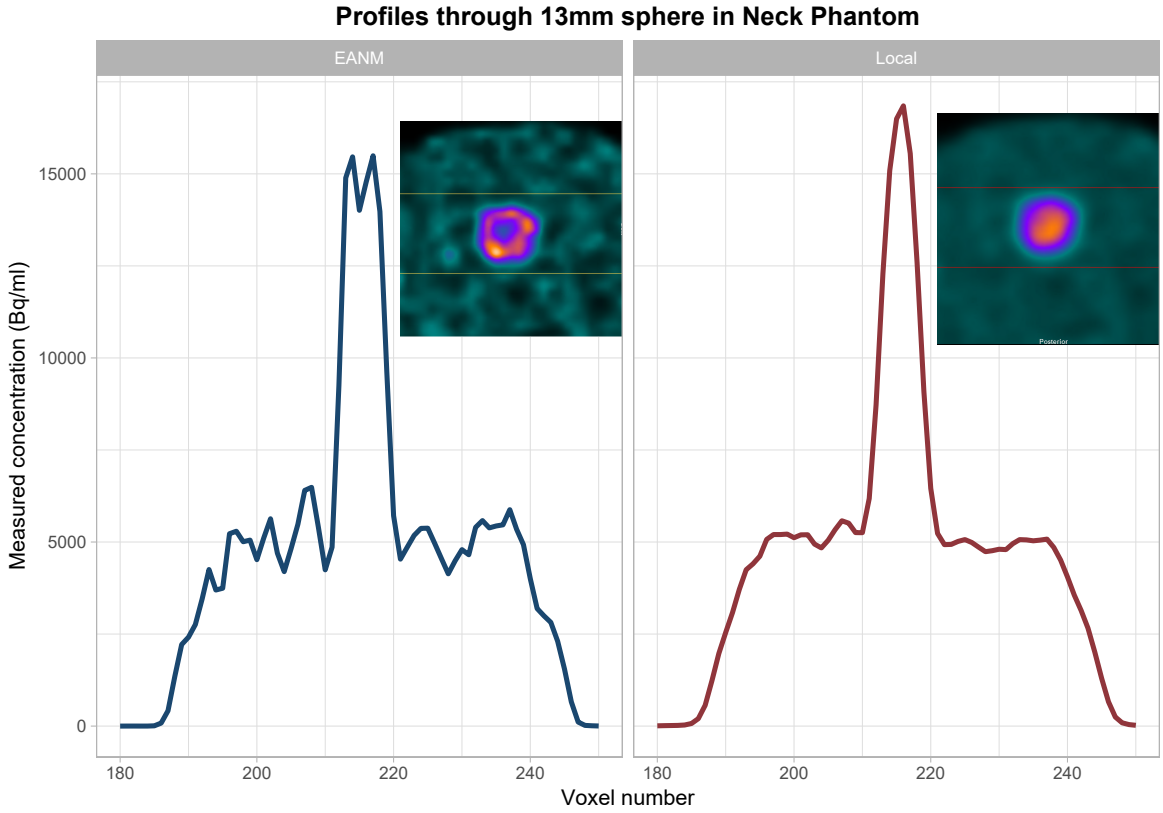

5.3.3 Blood pool assessment

5.3.3.1 Blood pool activity measured in different regions

When assessing blood pool activity by SVC, IN, IJ and IVC, mean blood pool SUVmean was significantly lower when measured in IJ, compared to other regions in local reconstruction (

Figure 5-7). When compared with SVC, both IN and IJ regions had lower SUVmean (SVC: 1.72±0.37 vs IN: 1.58±0.36, estimate -0.14, 95% CI -0.23 to -0.05, p<0.0001, and IJ: 1.36±0.35, estimate -0.36 95% CI -0.45 to -0.27, p<0.0001, respectively). There was no difference in SUVmean between SVC and IVC, 1.72±0.37 vs 1.66±0.37, estimate -0.06 95% CI -0.15 to 0.03, p=0.4. Blood pool data using the EANM reconstruction were similar (

Table S8-5).

Figure 5-7 SUVmean values by different blood pool regions on local reconstruction Blood pool measured in IJ was consistently lower than other regions. While there was variation between blood pool regions, there was little variation within each patient scan.

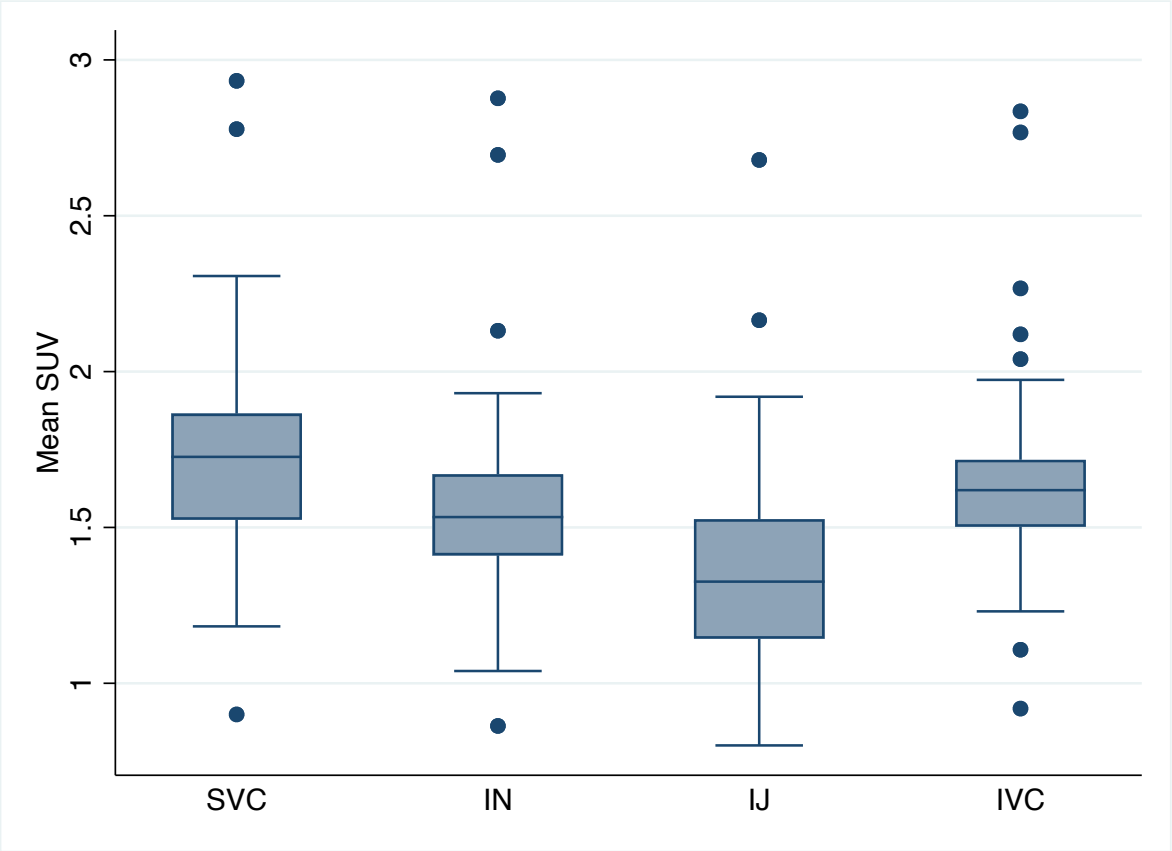

When using SVC as the reference blood pool region, there was good agreement between SVC and the other three regions (Figure 5-9) and good correlation with ICC. Activity within the IJ had the least agreement with SVC with a mean bias of 0.36, 95% LOA -0.08 to 0.79, and the lowest ICC with SVC (0.55 95% CI -0.09 to 0.83). Inter-observer and intra-observer reproducibility was excellent across all blood pool regions (although lower for the IJ),

Table S8-6).

In all scans, all 10 VOIs were successfully collected in SVC and IN for blood pool analysis. Of the 10 VOI's collected per scan, IVC blood pool measurements were missing 2% of VOI's and the IJ missing 5.7% of VOI's. When assessing missing data on repeated scanning, 3.5% of baseline IJ VOIs were missing and this increased to 7.8% at 24 weeks. The most common reason for inability to collect all IJ VOIs was due to the small calibre of IJ making it challenging to track the vessel superiorly (Figure 5-8) and place the VOI within the vessel. Interfering uptake from vocal cords, thyroid tissue and malignant disease also accounted for missing data. IVC data was missed due to adjacent high bowel uptake and malignant disease.

Figure 5-8 An example of carotid artery and jugular veins on repeated imaging. On both scans the left IJ is smaller than the right IJ. The LIJ was smaller than the pre-determined ROI size. The RIJ on baseline scan is smaller on baseline scan compared to 24 weeks.

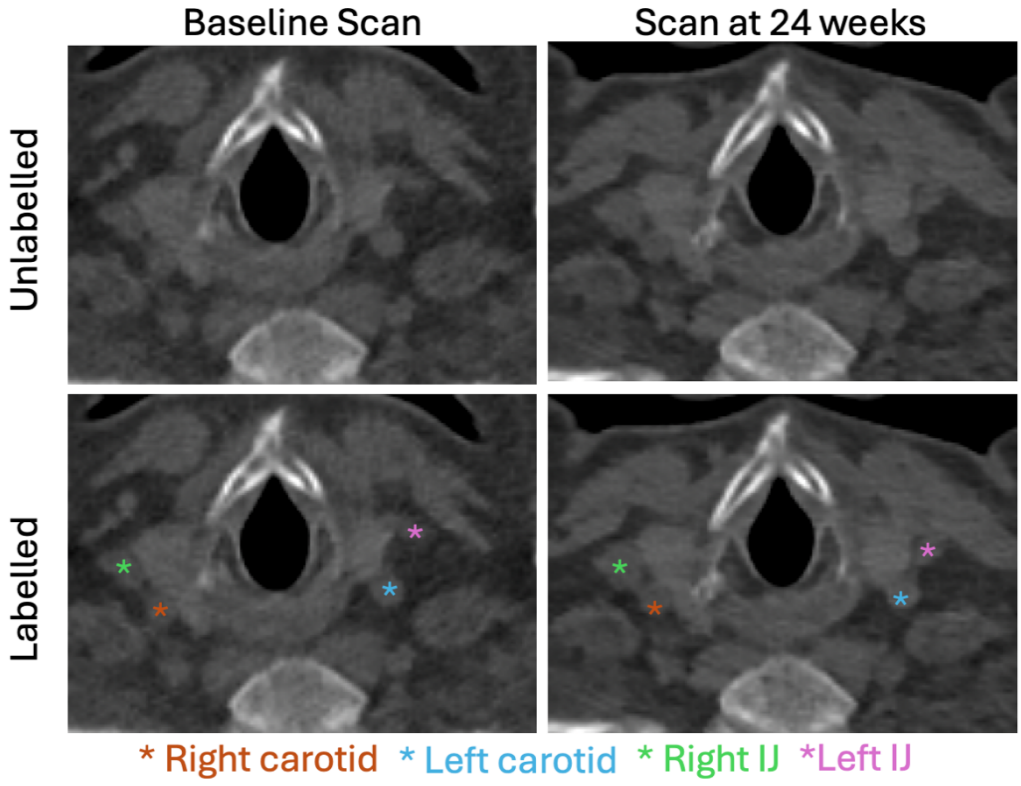

Figure 5-9 Bland-Altman plots comparing blood pool activity in IN, IJ & IVC to SVC A: SVC:IN B: SVC:IJ C: SVC:IVC D: IN:IJ. SVC: Superior vena cava, IN: innominate, IJ: internal jugular, IVC: inferior vena cava. ICC: interclass correlation coefficient, LOA: limits of agreement, 95% CI: 95% confidence interval.

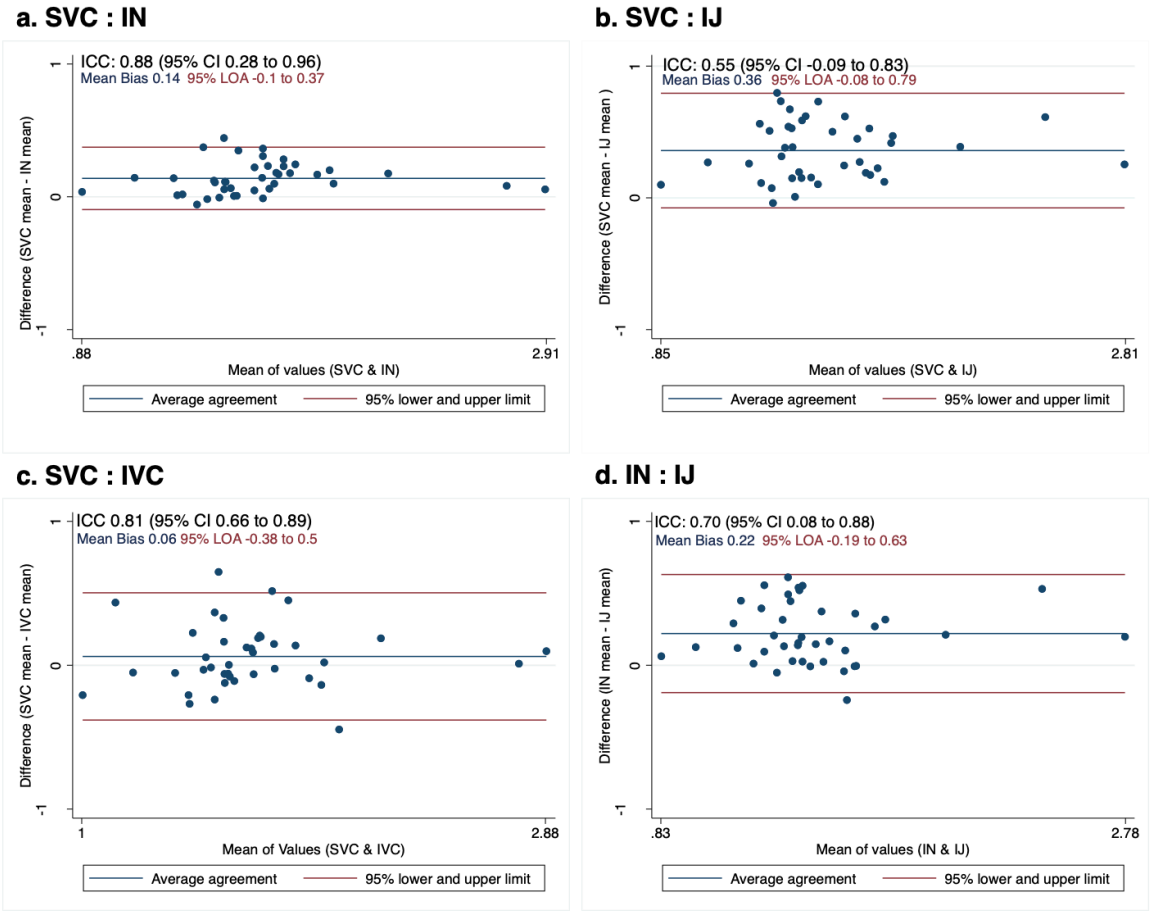

5.3.3.2 Effect of blood pool on TBR calculations using different blood pool regions

When assessing descending aorta by either SVC or IVC using the local reconstruction, there was no evidence of a difference in TBRmax (1.80 vs 1.87, respectively, p=0.5, Table 8-7). Carotid TBRmax levels were statistically higher using both IN and IJ compared to SVC, Figure 5-10. TBRmax increased from 1.58 using SVC to 1.99 using IJ, p=0.0001. There was also wider distribution in TBR values with IJ in comparison to SVC and IN, Figure 8-3.

Figure 5-10 Carotid & Descending aorta [18F]FDG uptake using different blood pool regions to calculate TBRmax
A: boxplot of carotid TBRmax calculated using different blood pool regions. TBRmax calculated using IJ had higher TBRmax and was over the 1.6 threshold for active disease. B: boxplot of TBRmax of the descending aorta calculated using either SVC or IVC. * p=0.0001 **p=0.0002 (comparison made using Wilcoxon sign rank test)

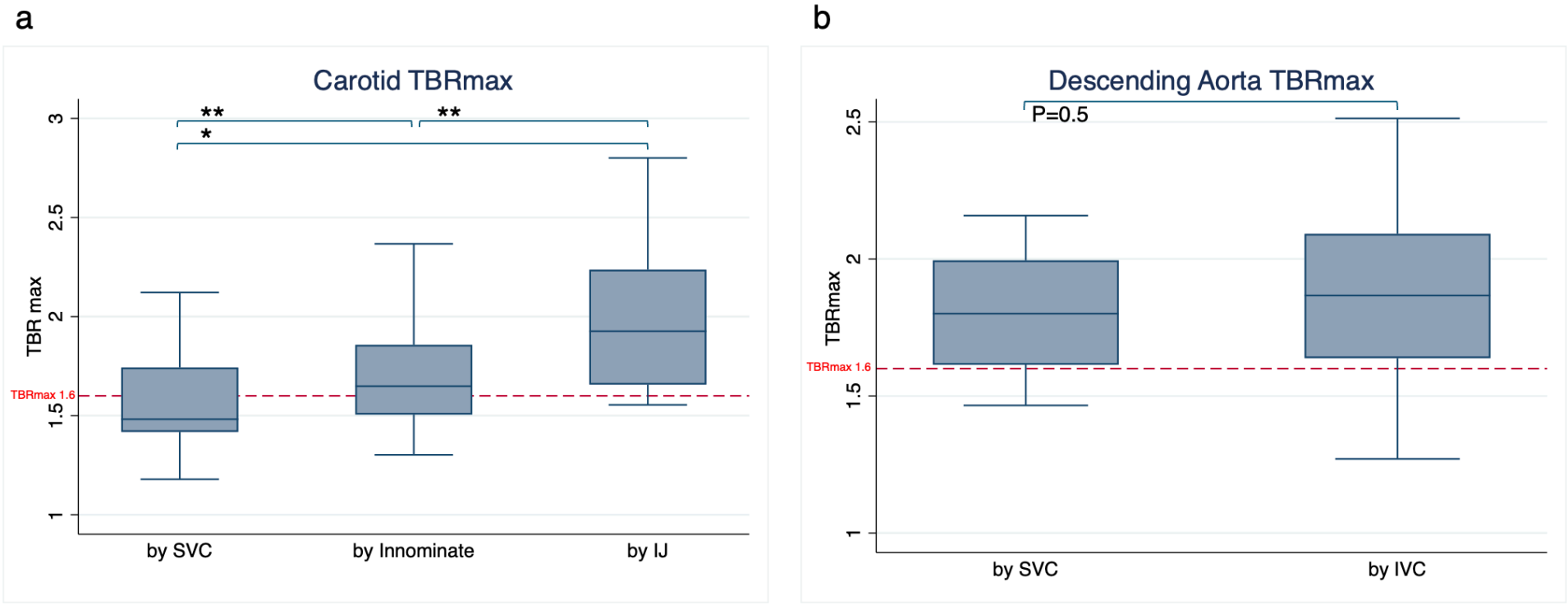

5.4 Discussion

We investigated the use of digital scanners in atherosclerosis imaging by [^{18}F]FDG-PETCT. Digital PET scanners allow for faster scans with better resolution and less PVE[148], therefore fewer effective iterations may be required than non-digital scanners. The improved signal-to-noise ratio yielded from improved timing resolution of digital PET imaging may result in fewer iterations and the need for filters[230]. Using PETCT images from a prospective observational research study, we assessed the impact of reconstruction parameters on imaging analysis and the measurements of different blood pool regions, as recommended by EANM. Using phantoms, we assessed recommended reconstruction parameters provided by EANM recommendations on a digital PET scanner and compared these reconstructions with additional metrics of assessment. We observed that EANM recommended reconstruction parameters yielded substantially higher TBRmax, higher than values reported in the literature[143,145,160,165,229]. We also observed different blood pool activity throughout numerous regions of the body, with IJ yielding lower activity results than other regions. This may be explained by challenges in data collection and PVE. An explanation for the high TBRmax is found in our phantom work. Overshoot of SUV, greater noise, and presence of edge artefact using higher number of effective iterations in the reconstruction led to artificially higher activity readings. Utilising additional metrics, we identified that fewer iterations provided better repeatability (with lower CoV) and more accurate quantification (with lower absolute error and overshoot), than the EANM suggested number of iterations.

5.4.1 TBRmax values & the recommended number of iterations

TBRmax is the most commonly used method of analysis for atherosclerotic assessment. A TBRmax >1.6 is indicative of an inflamed and 'active' arterial segment and used in research and clinical studies[232]. Phantom data using the EANM reconstruction demonstrated higher MCR than local and the presence of ring artefact on the outer rim of the phantom, also known as Gibbs artefact (online resource 7). Edge artefacts cause an apparent overshoot of SUV at sharp transitions of intensity of FDG uptake resulting in overestimation of radioactivity in small regions[241]. This phenomenon poses a challenge in standardisation of PET imaging and is particularly relevant to atherosclerotic assessment. This artefact

and overshooting contributed to falsely high TBRmax values with the EANM reconstruction, which is further confounded by the risk of high [^{18}F]FDG activity from adjacent metabolically active structures being incorrectly included in the arterial analysis due to poor image quality using EANM reconstruction. Artificially high TBRmax values could lead to false-positive diagnoses of 'active inflammation. This analysis was performed in an enriched cohort with a high prevalence of CV risk factors and disease: 65% of patients had hypertension and 30% had a history of atherosclerotic disease. (MI, coronary vascularisation, stroke, peripheral vascular disease) making it a relevant population for the assessment of atherosclerotic imaging.

5.4.2 MCR, absolute error & coefficient of variation

With the improved sensitivity and resolution of digital PET, fewer effective iterations may be required to meet convergence and more accurate MCR. We observed that the greater number of effective iterations led to high MCR, an overshoot in the activity recovery and increased error and variation in SUV. These additional metrics demonstrate variations in PET imaging quality resulting from different reconstructions and offer valuable insights in addition to MCR. The additional metrics utilised in this study may provide a method to standardise and harmonise reconstruction parameters throughout the literature. When assessing smaller spheres alone, 24i5s outperformed 4i5s with a greater MCR, however this was at the cost of greater variation. Overall, we believe 4i5s is a more favourable reconstruction for atherosclerotic imaging.

Data used on the development of EANM recommendations were based on small simulated lesions, the smallest of which was 0.032ml[166]. In our phantom work using a non-digital scanner, we observed a similar finding. Smaller spheres, particularly with 120 effective iterations (24i5s), yielded favourable RC curves, in keeping with EANM recommendations on the non-digital scanner. However, on a digital scanner, the 4i5s reconstruction produced a more a favourable RC curve than the 24i5s.

5.4.3 Partial volume effects

EANM recommend that reconstructions should be optimised to reduce the bias in SUV caused by PVE which can have substantial effects on atherosclerotic imaging, particularly when assessing small lesions which are more prone to PVE. Surrounding tissue activity can influence SUV measurements through PVE. This can dilute the intensity of small atherosclerotic lesions but can also increase blood pool SUVs when measured close to areas with high activity. Despite the improvement in spatial resolution with digital PETCT, PVE is observed in the smallest neck spheres in both reconstructions, as seen in the RC curves. As such, choosing a larger vein may minimise the effects of PVE observed in our RC curves.

5.4.4 Blood pool

Details of where and how blood pool activity is optimally measured are limited in the literature[165,232,242]. These measurements should be consistent and reproducible to minimise variability across studies. We observed excellent inter- and intra-observer reproducibility in blood pool SUVmean in all regions on repeated imaging but found that the IJ was technically more challenging and susceptible to missing data due to small vessel size and interfering tissue. Smaller vessels, such as IN and IJ in the neck, had lower values than more central blood pool activity within the SVC or IVC. While this may support the use of current EANM recommendations for digital PETCT with continuous bed motion scanning capabilities, the technical challenge and consistency of smaller veins, such as IJ, need to be considered. The lower measured blood pool activity within the neck is not secondary to washout as patients were scanned craniocaudally. It is much more likely that these smaller vessels are subject to PVE.

The region used to collect blood pool had a significant effect on TBR values. The lower SUV values within IJ gave higher TBRmax values than with SVC, putting it over the threshold of 1.6, indicating ‘active inflamed’ disease on the local reconstruction.

When considering the optimal area for measuring blood pool activity, the SVC may be the most reliable and reproducible. While there are many options for

area for measuring blood pool and many used, SVC is commonly used, even for carotid imaging[156,164,243]. Arterial TBR using SVC, IVC and IJ have been validated in non-digital scanners[233,244,245]. Direct comparison and validation of blood pools is limited in the literature. When comparing IVC with SVC, SVC was comparable to IVC for detection of large vessel vasculitis on a non-digital scanner [246,247]. Data on other areas, such as IJ vs SVC, is limited, but favours SVC[248]. Comparisons of the vena cava, above and below the diaphragm did not differ between groups on a non-digital scanner[249]. It has been observed that more VOI lead to better accuracy than fewer[250]. The IVC yielded similar SUV readings to the SVC but was susceptible to interference from bowel uptake. Given this, we believe using IVC for abdominal and descending aortic analysis offers no benefit over SVC. We hypothesised that the IN would yield similar blood pool measurements to IJ. IN is a larger vein that is close to the carotid artery, but distant from metabolically active structures within the neck (muscle, lymph nodes, thyroid, trachea). Therefore, it could be a suitable alternative for carotid TBR analysis. We observed that the IN activity was more reflective of the SVC than IJ, with similar levels of agreement, and offered little additional benefit over SVC, as an alternative to IJ. Although SVC has potential to yield lower TBRmax values in the carotid artery, given its lack of missing data and central proximity, this may be the most appropriate blood pool region to use for all arterial regions.

5.4.5 Limitations

There were several limitations to this study, particularly relating to limitations to follow every aspect of EANM guidance, meaning these factors may influence our results. Our circulation time was 90 minutes, rather than 120 minutes, suggested in EANM recommendations. However, literature advocating for longer circulation times were performed on non-digital scanners and may not be applicable[164,165]. As >2 hour circulation time causes increased FDG washout from the circulation, this would likely exacerbate issues with the TBRmax threshold of 1.6 beyond 90 minutes. This was observed in our preliminary data (online resource 6). Circulation times less than 2 hours have been used previously[159,233,235,251], including studies cited in establishing the 1.6 cut off threshold[143,160]. We analysed scans of patients in a prospective clinical study. To minimise variation in the study, scans were only performed on the digital scanner meaning our comparison of digital and non-digital systems is limited to

phantom analysis. Our analysis was performed in a cohort of patients with cancer which can introduce metabolic confounders. We believe this is in part mitigated by performing comparison of reconstructions within the same patients. In this way, they act as their own control and allow adequate comparison of reconstructions. Our phantom data corroborate the human data. The focus of this study was to assess the comparison of reconstructions rather than the absolute TBR values. However, the cancer cohort is a limitation of this study and limits the generalisability of this data to non-cancer populations. Optimisation of acquisition time was limited by pragmatic concerns: a longer scan time increase the possibility of patient motion which would degrade image quality. Whilst the chosen scan speed corresponds to a time/bed shorter than that recommended in the guidelines (non-digital equivalent of 5 mins/bed, compared to EANM recommended 8 mins/bed [227]), shorter acquisition times were found to have a minimal effect on SUV, when comparing 8 mins/bed to 4 mins/bed [166]. We assessed collecting blood pool by methods outlined above. The results and reproducibility of different segments may vary if using different anatomical landmarks are used.

The use of phantom studies to infer suitable acquisition or reconstruction parameters for clinical studies has potential limitations, most notably in that the structure of most common phantoms (including those used in this study) do not adequately replicate patient physiology. More anatomically accurate phantoms design may be possible with advances in 3D printing but have not yet been investigated in atherosclerosis imaging.

5.5 Conclusions

In comparison to EANM guidance, far fewer effective iterations for optimal atherosclerotic assessment are required on contemporary digital scanners. Higher iteration and subset reconstruction parameters result in higher TBRmax, much greater than values reported in the literature, with challenging image quality affecting analysis. Higher iteration and subset reconstruction results in overshoot of recovery coefficients and therefore SUV, greater error and variation on phantom analysis. Additional metrics of assessing reconstructions, such as absolute error and CoV, provide valuable information in addition to traditional assessments which may be relevant for assessing digital scanners.

The use of differing blood pool regions for calculating TBRmax can alter the result of TBRmax and has potential to artificially impact results. As the largest and most central blood vessel, we propose that SVC could be used as the sole area of assessment for blood pool.

These findings provide an opportunity to standardise practice within the literature with the advent of newer, more sophisticated technology, not previously available.

Chapter 6 Biomarker and Imaging Characterisation of Inflammatory Atheroma in Patients Receiving Immunotherapy and Angiogenesis Inhibitors (BIOCAPRI Study)

6.1 Introduction

Immune checkpoint inhibitors (ICI) are a modern anti-cancer drug class used in a number of cancer types with a broad spectrum of indications, including adjuvant treatment for patients who have undergone curative surgery[43,252-255]. ICI exposure may be associated with increased risks of ischemic events such as myocardial infarction (MI) and ischaemic stroke. Data to suggest this are mostly derived from single centre retrospective and registry studies[47,57,61,84] and case reports[72,74,75]. It has been proposed that ICI lead to accelerated atherosclerosis and inflammatory plaque instability due to infiltration of activated T cells and stimulation of inflammatory pathways[47,69,97].

[^{18}F]fluorodeoxyglucose positron emission tomography computed tomography ([^{18}F]FDG-PETCT) is the gold standard imaging modality for assessing large vessel inflammation and is validated for atherosclerosis assessment[137]. [^{18}F]FDG-PETCT may offer valuable insights into the pathophysiological process of ICI-associated atherosclerosis and inflammatory atheroma. There have been six studies to date assessing large vessel atherosclerotic inflammation by [^{18}F]FDG-PETCT in patients on ICI[96,151-153,156,256]. These have produced conflicting results. All were performed retrospectively and therefore used PET imaging protocols optimised for clinical oncological assessment rather than atherosclerosis assessment. Characteristics of PET imaging protocols, such as circulation time and reconstruction parameters, can impact the results and interpretability of atherosclerosis assessment[147]. There has been no prospective assessment of large vessel inflammation in patients on ICI using optimised imaging parameters.

ICI are increasingly used in combination with vascular endothelial growth factor inhibitors (VEGFI) with greater survival benefits than monotherapy in different cancer types[117-119,186,191]. VEGFI are associated with substantial cardiovascular (CV) toxicity including hypertension, heart failure and thrombotic events[99,120,121]. It is unclear if the combination of ICI plus VEGFi is associated with a higher risk

for CV events than associated with either drug used as monotherapy. Pre-clinical data would support the hypothesis that concomitant treatment with VEGFI plus ICI would have a synergistic effect on inflammatory atheroma progression and plaque instability[98,99]. ICI+VEGFI combination therapy may therefore be associated with higher risk for ischaemic events than monotherapy. It is crucial to understand the mechanism of potential arterial injury in both ICI monotherapy and when used in combination with VEGFI in order to identify those at risk and to develop strategies to prevent associated atherothrombotic complications.

In this prospective, longitudinal observational study of patients with cancer I sought to evaluate the effect of ICI on arterial inflammation and to compare arterial inflammatory effects of ICI monotherapy versus those treated with combined ICI+VEGFI, using VEGFI monotherapy as a control.

6.2 Methods

I conducted a prospective, observational study of patients with cancer before and during treatment with VEGFI monotherapy, ICI monotherapy and ICI+VEGFI combination therapy. Patients were recruited from a regional cancer hospital network (West of Scotland Cancer Network, National Health Service, United Kingdom) between August 2022 and June 2024. The study was approved by the West of Scotland Research Ethics Committee 5 (22/WS/0085) and by the Administration of Radioactive Substances Advisory Committee (ARSAC) for the administration of radioactive substances (ARSAC Ref AA-4580). The study was registered on clinicaltrials.gov (NCT06597045). It was performed in accordance with the Declaration of Helsinki and written informed consent was obtained for all patients.

Patients who were 18 years or older were eligible for inclusion if they had cancer and were planned to receive treatment with ICI or VEGFI, either alone or in combination. Patients recruited were required to have ≥6 months predicted survival in the opinion of the clinical oncology team. Those who were unwilling or unable to provide valid consent were excluded, as were patients with a history of diabetes treated with oral or subcutaneous treatment at the time of recruitment. Patients scheduled to receive concurrent thoracic, neck or abdominal radiotherapy were excluded. Patients with active vasculitis were also excluded. Patients on immunosuppression at the time of recruitment, defined as >10mg/day prednisolone, a threshold commonly used in oncological ICI+VEGFI trials[46,257], were excluded.

6.2.1 Study procedures

Patients who consented to participation underwent [^{18F}]FDG-PETCT and blood biomarker analysis at baseline (prior to commencing therapy), and 24 weeks (±2 weeks) after the initiation of therapy. Echocardiography and electrocardiography (ECG) were also taken at baseline and 24 weeks.

6.2.2 [^{18}F]FDG-PETCT imaging

Patients were assessed using [^{18F}]FDG-PETCT, the gold standard imaging modality for large artery inflammation using a digital PETCT scanner (Biograph Vision 600;

Siemens, Erlangen, Germany). They were fasted for a minimum of 6 hours prior to tracer administration and blood glucose levels were checked during patient preparation to ensure concentrations <11mmol/L. Scanning was performed 90 minutes after administration of 4 MBq/kg [^{18}F]FDG using reconstruction parameters outlined previously[137,236,258]. A matrix size of 440x440 was used with an all-pass filter to achieve matched PET and CT voxels of 1.65x1.65x1.65cm without applying a software zoom, which corresponds to a voxel size of 1x1x1mm as recommended by the European Association of Nuclear Medicine (EANM). Scanning was performed with 4 iteration and 5 subsets (4i5s) and Siemens implementation of ordered subset expectation maximisation (OSEM), as described in Chapter 5. CT images were acquired at 120kV, with automatic tube current modulation and reference mAs of 50 mAs, covering the base of the skull to mid-thigh, reconstructed at 1.5-mm increments. PET images encompassed the same transverse field of view as the CT, scanning craniocaudally. PET acquisition times were 0.7mm/s.

6.2.3 [^{18}F]FDG-PETCT arterial analysis

Volumes of interest (VOI) were assessed at baseline and 24 weeks in six arterial segments (thoracic aorta, abdominal aorta, both carotid arteries, and both iliac arteries). Full image analysis methods are described in Chapter 2 and were in accordance with EANM recommendations. In brief, sequential 4mm thick 3-dimensional polygonal VOIs were analysed in each artery. Within each arterial VOI, the maximal and mean standardised uptake value (SUV) of [^{18}F]FDG was corrected to the blood pool activity in the superior vena cava, in order to calculate a tissue-to-background ratio (TBR). Further analyses were also performed including calculation of TBRmean, TBRmax of 'active segments' (defined as a TBR $\geq$1.6) and most diseased segment (MDS), in accordance with EANM[137]. Analysis was performed blinded to both patient and scan timing.

6.2.4 Calcium Scoring

Aortic calcification was assessed using the CT component of the PETCT on a dedicated workstation (Vitrea Advanced, Vital Imaging, Toshiba Systems, Minnesota, USA). A density threshold of 130 Hounsfield units (with a 3-pixel threshold on 3mm slice thickness) was used to define the presence of

calcification. A cumulative calcium score of each arterial segment, and all arterial segments, was calculated as previously described [167].

6.2.5 Analyses for heterogeneity

The [^{18}F]FDG activity change was assessed in both the presence and absence of potential confounding factors and an interaction *p* value between the two analyses were reported. Analyses assessing the interaction between arterial characteristics (large arteries vs medium arteries, calcification above and below the median calcium score for each segment, presence vs absence of pre-existing inflammation in segments at baseline, defined as TBRmax ≥1.6) and FDG uptake were performed. Large arteries were defined as aortic segments and medium arteries were defined as both carotids and iliac arteries. Further analyses to assess for potential interaction between FDG uptake and clinical characteristics were performed. These included analysis stratified based upon: 1) the presence or absence of pre-existing atherosclerotic cardiovascular disease (ASCVD), defined as previous myocardial infarction, chronic coronary syndrome, coronary revascularisation, ischaemic stroke, or symptomatic peripheral arterial disease; 2) chronic kidney disease (CKD), defined as at least two recorded eGFR <60ml/min/1.72m^2 measured 3 months apart in the absence of an acute insult); 3) use of immunosuppression (defined as the use of intravenous methylprednisolone or administration of equivalent to 1mg/kg/day of prednisolone[46,257,259]) and 4) treatment with a statin during cancer therapy.

6.2.6 Biomarkers

High sensitivity troponin T (hsTnT), N-terminal pro B-type natriuretic peptide (NT-proBNP), growth differentiation factor-15 (GDF-15), high sensitivity C-reactive protein (hsCRP), lipoprotein(a) (lp(a)), total cholesterol, triglycerides, high density lipoprotein (HDL-cholesterol), apolipoprotein A (ApoA) and apolipoprotein B (ApoB) were measured using a Roche Cobas autoanalyser (Roche Diagnostics, Rotkreuz, Switzerland). Intracellular-adhesion molecule-1 (ICAM-1), vascular cell adhesion molecule-1 (VCAM-1), myeloperoxidase (MPO), p-selectin, interleukin-6 (IL-6), endothelin-1 (ET-1), tissue necrosing factor-α (TNF-α), VEGF, tissue plasminogen activator (tPA) and plasminogen activator

inhibitor-1 (PAI-1) were measured by ELISA (BioTechne ELLA automated ELISA analyser; Minneapolis, Minnesota, United States).

6.2.7 Clinical events

Demographic data, drug prescriptions and clinical events were recorded by review of electronic patient records. All potential CV adverse events (CVAEs) were classified according to the definitions of the International Cardio-oncology Society (ICOS) definitions [14]. Treatment with immunosuppression with high dose steroids was defined as the use of intravenous methylprednisolone or administration of equivalent to 1mg/kg/day of prednisolone, as described previously[46,257,259].

6.2.8 Statistical analysis and sample size calculation

The primary outcome was the change in TBRmax of all arterial segments in patients receiving ICI+VEGFI combination therapy vs ICI alone or VEGFI alone. Additional analyses were conducted to account for any heterogeneity within the cohort and an interaction p value was reported to demonstrate the presence of heterogeneity. An interaction *p* value <0.05 was chosen to define a significant interaction between FDG uptake and the factor tested in the analysis.

Based on prior studies, using TBRmax as primary outcome, a sample size of 16 patients per group would have 80% power at 5% significance to detect a between groups difference of 10-15%[142,151,160]. Furthermore, given the paired nature of the data, within group assessments would have greater power than this.

Continuous data with normal distribution are presented as mean ± standard deviation (SD) and skewed data are presented as median and interquartile range (IQR). For TBR analysis, to account for potential variation within arterial segments and to correct for baseline activity, a linear mixed effects model was used. The patient identification (ID) number and arterial segment (nested within ID) were specified as random effects, with baseline [^{18}F]FDG uptake as a fixed effect. To compare variance between the groups, analysis of covariance (ANCOVA) was used, correcting for baseline measurements. The change in the

log-transformed biomarker within each group from baseline to 24 weeks were reported as a geometric mean ratio with 95% confidence intervals (CI).

A *p* value <0.05 was taken to represent statistical significance. Statistical analysis was performed using STATA software (Version 17). Figures were designed in STATA and R package with ggplot2[238].

6.3 Results

6.3.1 Patient characteristics

Sixty-one patients were enrolled in the study (VEGFI: 18 ICI: 23 ICI+VEGFI: 20). Six patients did not undergo follow-up assessment (Figure 6-1). A total of 55 patients were included in the final analysis. Their mean age was 66±10 years and 16 (29%) were female. The cohort included patients treated in both the palliative and adjuvant setting. The majority had renal cell carcinoma. ASCVD and risk factors for atherosclerosis were prevalent in each of the treatment groups (

Table 6-1).

Figure 6-1 Consort diagram

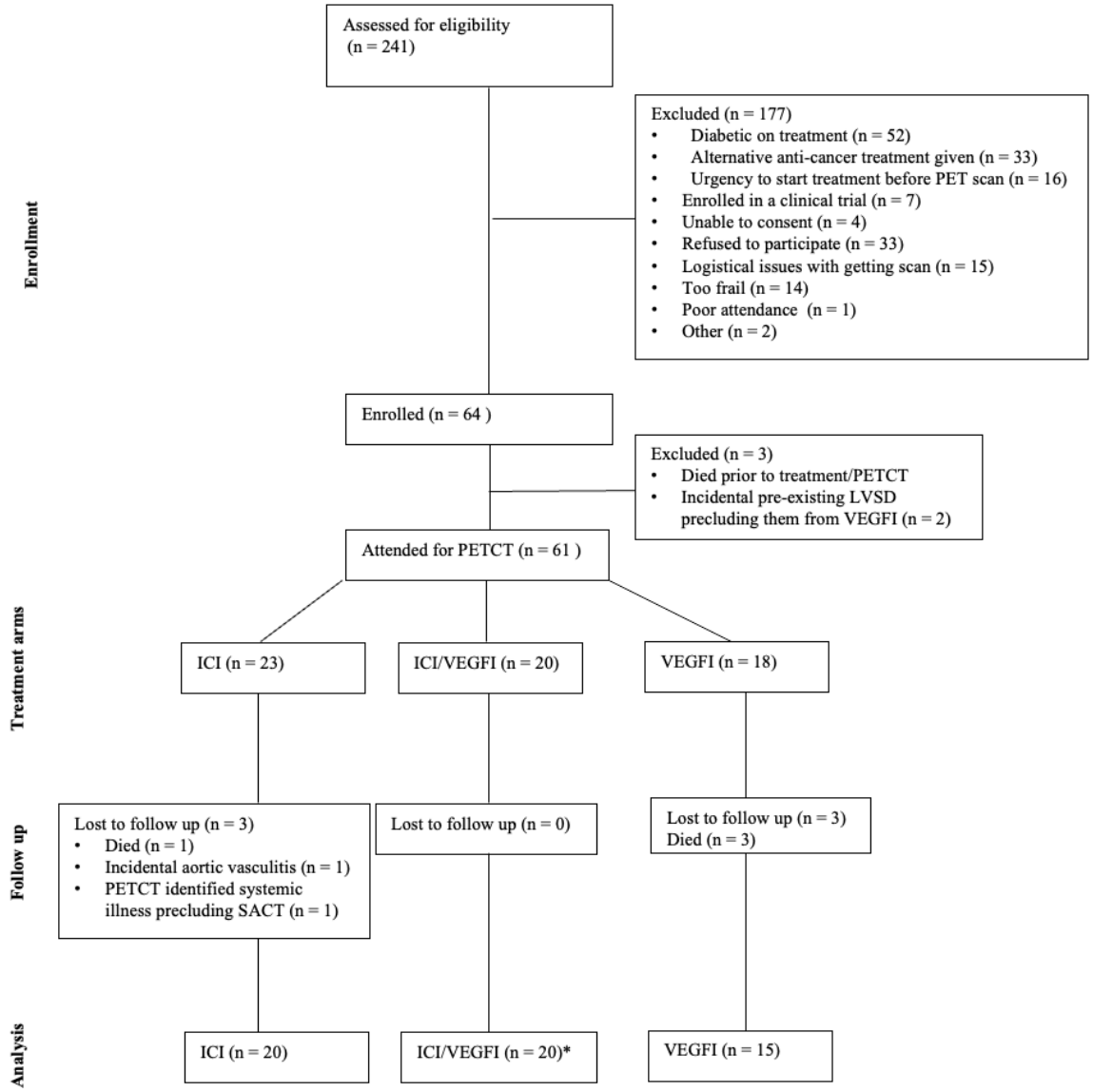

Table 6-1. Baseline Characteristics

	VEGFI (N=15)	ICI (N=20)	ICI+VEGFI (N=20)	p-value
Age (±SD)	66±10	64±10	67±8	0.54
Female sex	3	8	5	0.38
BMI kg/m^2 (±SD)	31±4	30±7	28±6	0.41
Comorbidities				
Smoking history				0.97
No	8	12	12	
Ex	5	5	6	
Current	2	3	2	
Diabetes	3	1	2	0.37
Hypertension	8	7	12	0.27
Chronic kidney disease	8	6	8	0.38
History of cardiovascular disease				
Myocardial infarction	0	1	1	0.68
Coronary revascularisation*	0	2	0	0.16
Stroke	1	1	3	0.51
Peripheral arterial disease	1	1	0	0.26
Atrial fibrillation	1	2	1	0.83
Heart failure hospitalisation	0	1	0	0.41
Noncancer medication				
Anti-platelet	1	3	1	0.51
Warfarin or DOAC	3	2	3	0.71
Statin	7	6	7	0.73
Cancer type				
Renal	14	9	17	<0.001
Hepatocellular	1	0	3	
Melanoma	0	10	0	
Cervical	0	1	0	
Cancer Stage				
2	0	0	1	<0.001
3	1	14	2	
4	14	6	17	
Treatment intent				
Post curative surgery	0	14	0	<0.001
Palliative	15	6	20	
Previous Cancer treatment				
Surgery	1	16	12	0.37
Chemotherapy	0	1	2	0.43
ICI	2	0	0	0.063
VEGFI	2	0	0	0.063
Adverse event during follow up period				
Cardiovascular AE	11	4	15	<0.001
Immune related AE requiring high dose steroids	0	3	2	0.31

Abbreviations: AE – adverse event; DOAC - direct oral anticoagulant; ICI – immune checkpoint inhibitor; VEGFI – vascular endothelial growth factor inhibitor *percutaneous coronary intervention and coronary artery bypass grafting
P value represents the difference between the three treatment groups. Normally distributed data (presented as mean±SD were analysed by one-way ANOVA, skewed data (presented as median and IQR) were analysed by kruskall-wallis test.

6.3.2 Arterial [^{18}F]FDG-PETCT

The median time from baseline PETCT to starting therapy was 5 days (IQR 3-10 days). The median time between starting treatment and follow up PETCT was 24.6 weeks (IQR 23.4-25.6). In 55 patients, 7198 arterial VOIs were assessed at baseline and 24 weeks measured across six arterial segments.

TBRmax did not rise from baseline in any group. TBRmax at baseline and 24 weeks was: VEGFI 1.72±0.22 vs 1.72±0.17; ICI 1.71±0.14 vs 1.67±0.14 and; ICI+VEGFI 1.74±0.18 vs 1.64±0.15, respectively (Fig 1).

Figure 6-2 TBRmax at baseline & 24 weeks: VEGFI, ICI & ICI/VEGFI. ICI – immune checkpoint inhibitor. TBRmax – maximal tissue to background ratio; VEGFI – vascular endothelial growth factor inhibitor

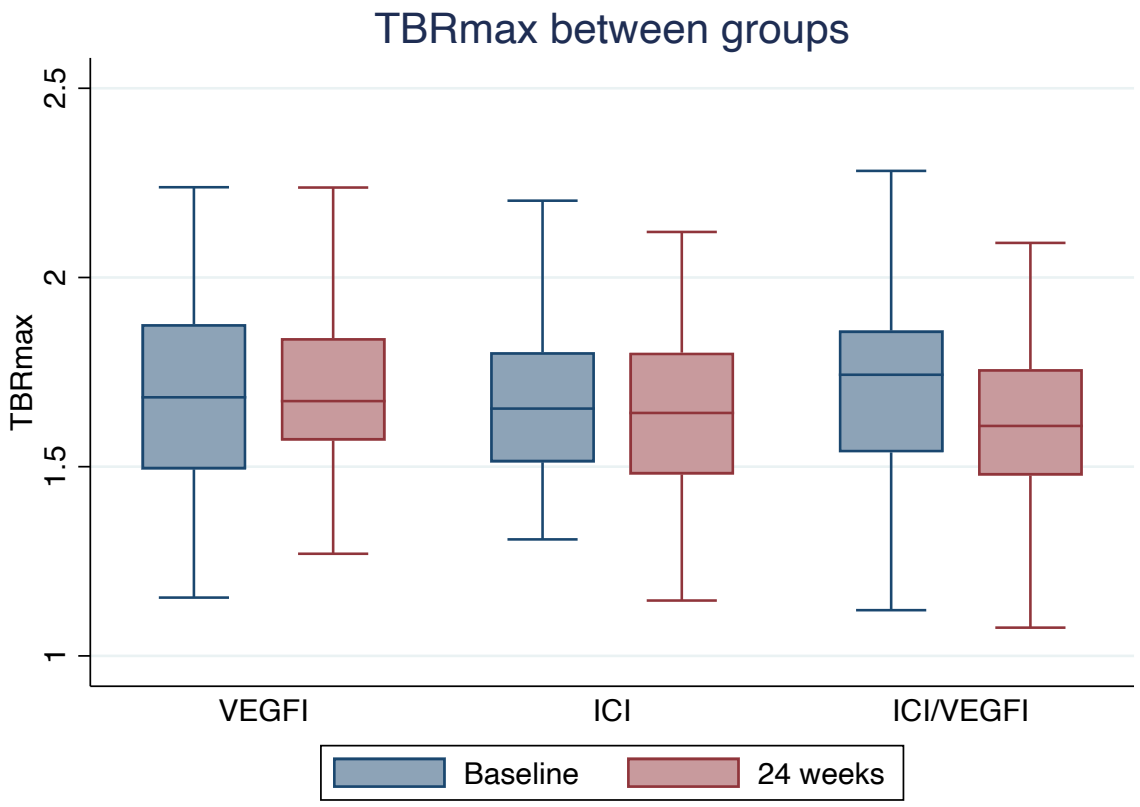

There was also no difference in the change of TBRmax over time when comparing between the three groups and adjusting for baseline activity (p=0.13). These results were consistent when each artery in isolation was assessed. In comparison to those treated with VEGFI monotherapy, TBRmax was not different at 24 weeks in those treated with either ICI monotherapy (β-coefficient -0.05, 95% CI -0.15 to 0.04 *p*=0.28) or the combination of ICI+VEGFI (β-coefficient -0.09, 95% CI -0.18 to 0.003 *p*=0.06). ICI+VEGFI did not have a higher TBRmax at 24 weeks from baseline, in comparison to ICI monotherapy (ICI+VEGFI vs ICI: -0.04, 95% CI -0.12 to 0.04, p=0.34). These results were consistent irrespective of whether they were analysed as TBRmean, TBRmax within 'active segments', MDS, or number of active segments (Table 6-2).

Table 6-2 PETCT Atherosclerotic assessment by SACT group (unadjusted analysis)

	VEGFI	ICI	ICI+VEGFI	p-value
	N=15	N=20	N=20	
TBRmean				
Baseline	1.10 (0.14)	1.13 (0.09)	1.13 (0.11)	0.65
24 weeks	1.11 (0.10)	1.10 (0.10)	1.08 (0.09)	0.66
Difference	0.01 (0.10)	-0.03 (0.09)	-0.05 (0.11)	0.19
Active segments, (TBRmax ≥1.6)				
Baseline	1.86 (0.13)	1.85 (0.10)	1.86 (0.12)	0.90
24 weeks	1.85 (0.13)	1.84 (0.09)	1.81 (0.09)	0.44
Difference	-0.01 (0.11)	-0.01 (0.09)	-0.06 (0.10)	0.23
Most diseased segment (MDS)				
Baseline	2.00 (1.89-2.42)	2.14 (1.95-2.36)	2.13 (1.85-2.38)	0.91
24 weeks	2.06 (1.93-2.44)	2.14 (1.91-2.23)	2.03 (1.94-2.24)	0.81
Difference	-0.03 (0.42)	-0.05 (0.32)	-0.08 (0.29)	0.90
Calcium score				
Baseline	1995 (832-13004)	2162 (144-9263)	2143 (900-4462)	0.82
24 weeks	2144 (866-12103)	2295 (193-10122)	2232 (926-4902)	0.86
Difference	103 (0-194)	144 (30-726)	177 (20-439)	0.56

Abbreviations: ICI: immune checkpoint inhibitor; MDS – most diseased segment; VEGFI: vascular endothelial growth factor inhibitor; TBR: tissue-to-background ratio. Normally distributed data presented as mean (standard deviation); skewed data presented as median (interquartile range). 'Active segments' are defined as TBR≥1.6 as per EANM recommendations

6.3.2.1 Additional analyses

The findings remained consistent in additional analyses evaluating arterial [^{18}F]FDG-PETCT uptake only in medium or large arteries, Figure 6-3. There was no difference in change in TBRmax in those with or without pre-existing inflammation (interaction p value=0.66). In addition, statin exposure and history of CKD had no impact on change of TBRmax over time (interaction *p* for steroid exposure = 0.9; interaction *p* for CKD = 0.36). There was also no interaction observed between the use of any dose of steroid during the study (n=14; interaction p=0.56) nor in the small number (n=5) who received high dose immunosuppression (interaction p=0.42), Figure 6-3.

6.3.2.2 Arterial calcification

Arterial calcification was present on the baseline PETCT scan in 52 (95%) patients and the median calcification score was 2196 (IQR 587-8420). When TBRmax was compared between those with arterial calcification above versus below the median value, the change of TBRmax over time remained the same within and between groups, Figure 6-3. When adjusting for baseline FDG activity and baseline calcium score, this did not affect the overall findings. There remained no change in TBRmax both within group analysis and between group analysis (ICI+VEGFI vs VEGFI: β-coefficient -0.09, 95% CI -0.19 to 0.004, p=0.06; ICI+VEGFI vs ICI: -0.04, 95% CI -0.12 to 0.04, p=0.35; ICI vs VEGFI: -0.05, 95% CI -0.15 to 0.04, p=0.28).

Figure 6-3 Change in TBRmax over time for VEGFI, ICI and ICI+VEGFI by baseline patient & arterial segment characteristics.
P value=interaction between the presence vs absence of characteristic tested and its effect on TBRmax. A) Large arteries: thoracic & abdominal aorta; medium arteries: carotid and iliac arteries b) arterial calcification, defined as above vs below median calcium score for each arterial segment c) ASCVD: atherosclerotic cardiovascular disease (defined as previous myocardial infarction, coronary revascularisation, ischaemic stroke, symptomatic angina or peripheral arterial disease) d) immunosuppression on treatment defined as the use of intravenous methylprednisolone or equivalent to 1mg/kg/day of prednisolone

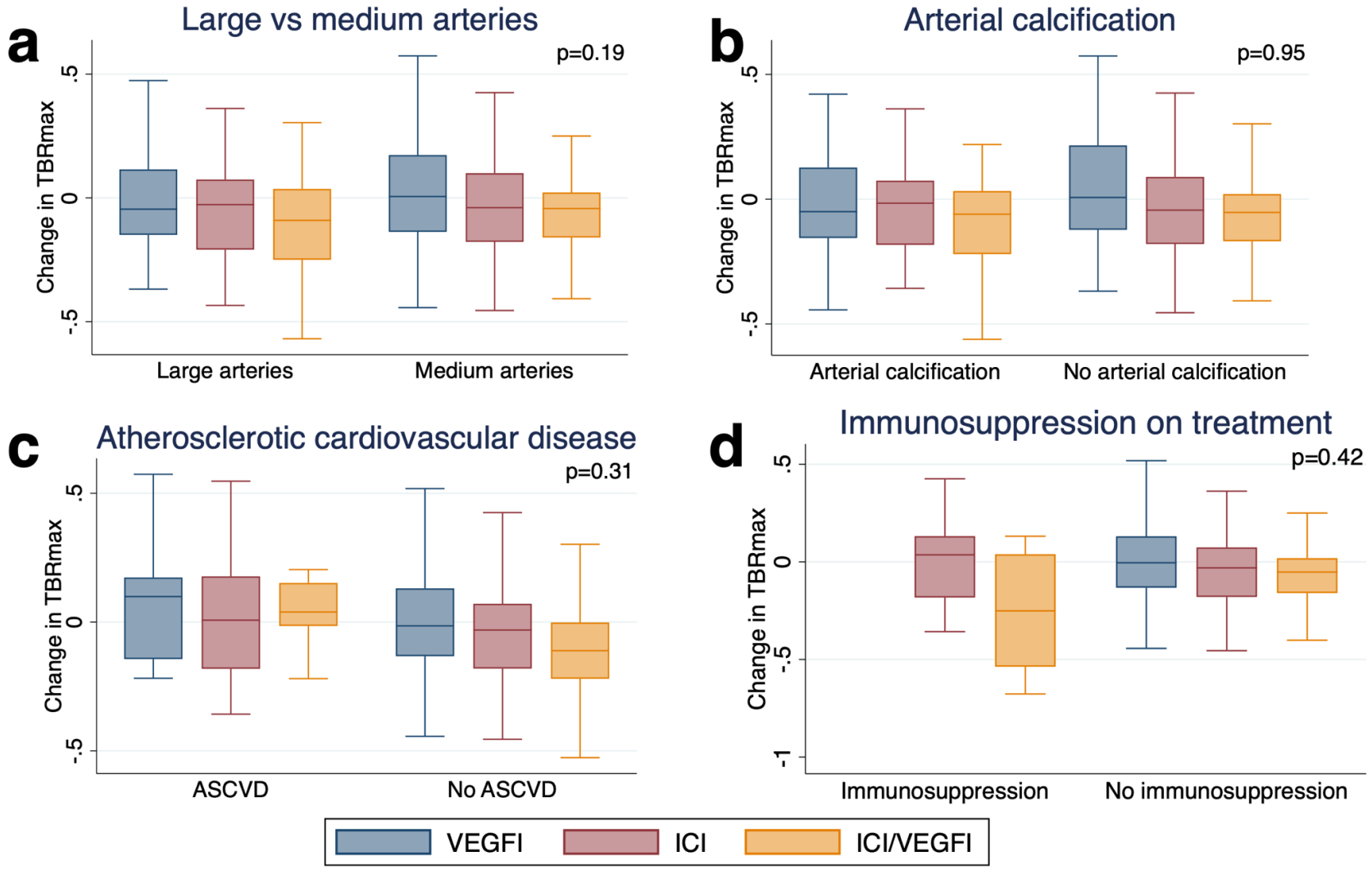

*p value=interaction between presence vs absence of variable tested in sensitivity analyses and its effect on TBRmax

6.3.3 Biomarkers

Baseline biomarkers were similar between groups (

Table 6-3).

Table 6-3 Baseline biomarkers

	VEGFI	ICI	ICI/VEGFI	p-value
	N=15	N=20	N=20	
hsTnT (pg/ml)	10.3 (7.9-15.6)	9.4 (7.0-12.6)	9.3 (8-12.7)	0.68
NT-proBNP (pg/ml)	109.3 (33.3-177.7)	85.4 (32-226.9)	104.9 (54.5-315.5)	0.87
Apolipoprotein A1 (g/l)	1.1 (1-1.2)	1.2 (0.8-1.4)	1.1 (0.9-1.2)	0.95
Apolipoprotein B (g/l)	0.9 (0.5-1)	0.8 (0.6-1.0)	0.7 (0.6-0.9)	0.70
Total cholesterol (mmol/l)	4.3 (2.8-4.9)	4.0 (2.8-5.0)	3.5 (3.2-4.2)	0.61
HDL-cholesterol (mmol/l)	0.9 (0.8-1.0)	1.1 (0.8-1.3)	1.0 (0.8-1.3)	0.89
Triglycerides (mmol/l)	1.6 (0.9-2.7)	1.3 (0.8-1.9)	1.1 (0.7-1.6)	0.24
Lipoprotein(a) (mmol/l)	22.3 (15.0-59.7)	10.5 (3.1-18)	20.9 (8.3-44.3)	0.021
hs-CRP (pmg/l)	2.6 (1.9-6.0)	1.6 (0.5-3.7)	4.6 (1.7-9.0)	0.077
GDF15 (pg/ml)	1993 (1052-2349)	1067 (677-2131)	1499 (1108-2399)	0.16
MPO (ng/ml)	23.8 (21.9-34.9)	19.0 (14.7-23.7)	21.3 (15.0-27.7)	0.051
ICAM-1 (ng/ml)	556 (491-699)	492 (444-576)	476 (419-548)	0.14
VCAM-1 (ng/ml)	1144 (956-1335)	993 (876-1148)	1041 (900-1203)	0.11
TNFα (pg/ml)	13.4 (11.7-17.7)	11.4 (9.7-13.9)	13.1 (11.8-16.1)	0.074
tPA (pg/ml)	1380 (958-1997)	1101 (826-1530)	1261 (889-1463)	0.52
PAI-1 (ng/ml)	2.4 (1.3-3.7)	1.7 (1.2-2.5)	2.0 (1.7-2.6)	0.34
p-selectin (ng/ml)	142 (125-172)	115 (98-143)	117 (100-150)	0.13
ET-1 (pg/ml)	1.5 (1.1-2.0)	2.0 (1.2-2.4)	1.8 (1.2-2.0)	0.43
VEGF (pg/ml)	35.7 (22.6-50.0)	35.2 (19.9-57.0)	41.0 (24.1-63.2)	0.78

Abbreviations: TnT – troponin T; NTproBNP – N-terminal pro-brain natriuretic peptide, hsCRP – high sensitivity C-reactive protein; IL-6 – interleukin 6; GDF15- growth differentiation factor-15; MPO- myeloperoxidase; TNFa – tumour necrosis factor α; ICAM-1 – intracellular adhesion molecule-1; VCAM-1- vascular cell adhesion molecule-1; tPA – tissue plasminogen activator; PAI-1 – plasminogen activator inhibitor-1; ET-1 – endothelin-1; VEGF – vascular endothelial growth factor

ICAM-1 and VCAM-1, markers of endothelial activation and arterial injury, increased in patients treated with ICI (monotherapy and combination VEGFI+ICI), Figure 6-4. ICAM-1 increased by 22% in the ICI monotherapy group (geometric mean ratio: 1.22 95% CI 1.1 to 1.35, p=0.001) and 29% in ICI+VEGFI (geometric mean ratio 1.29, 95% CI 1.09 to 1.52, p=0.005). It decreased by 6% in those treated with VEGFI monotherapy (geometric mean ratio: 0.94, 95% CI 0.83 to 1.06, p=0.3). At 24 weeks, VCAM-1 was higher than baseline in all groups although the magnitude of this was greatest in those treated with ICI (ICI monotherapy geometric mean ratio 1.25, 95% CI 1.09 to 1.45 p=0.004; ICI+VEGFI combination therapy geometric mean ratio: 1.51, 95% CI 1.30 to 1.74, p <0.0001; VEGFI monotherapy geometric mean ratio 1.17, 95% CI 1.0 to 1.38 p=0.06).

At 24 weeks, TNFα was higher than baseline in patients treated with ICI (ICI monotherapy geometric mean ratio 1.28, 95% CI 1.12 to 1.47, p=0.001, and ICI+VEGFI combination therapy 1.29, 95% CI 1.06 to 1.56, p=0.012) but it was not higher in those who were treated with VEGFI monotherapy (geometric mean ratio 1.09, 0.97 to 1.23, p=0.153). Other inflammatory biomarkers did not rise significantly after exposure to ICI, Figure 6-4.

At 24 weeks the pro-fibrolytic factor, t-PA, was higher than baseline in patients treated with VEGFI monotherapy (geometric mean ratio 1.38, 95% CI 1.02 to 1.87, p=0.038) and ICI+VEGFI combination therapy (geometric mean ratio 1.44, 95% CI 1.09 to 1.90, p=0.01) but did not rise in patients treated with ICI alone (geometric mean ratio 1.05, 95% CI 0.82 to 1.36, p=0.67).

VEGF and ET-1 increased in those exposed to VEGFI, both in the monotherapy and combination therapy groups but did not change in the ICI monotherapy group. Cardiac biomarkers (TnT, NTproBNP) and lipids did not change over time.

Figure 6-4 Geometric mean ratio of log-mean biomarker concentration at 24 weeks:log-mean at baseline. Within group significance represented by symbols + p<0.05; * p<0.001; ** p<0.01). Abbreviations: TnT – troponin T; NTproBNP – N-terminal pro-brain natriuretic peptide, ApoA – apolipoprotein A; ApoB – apolipoprotein B; Total chol – total cholesterol, lp(a) – lipoprotein(a); hsCRP – high sensitivity C-reactive protein; IL-6 – interleukin 6; GDF15- growth differentiation factor-15; MPO- myeloperoxidase; TNFa – tumour necrosing factor α; ICAM-1 – intracellular adhesion molecule-1; VCAM-1- vascular cell adhesion molecule-1; tPA – tissue plasminogen activator; PAI-1 – plasminogen activator inhibitor-1; ET-1 – endothelin-1; VEGF – vascular endothelial growth factor; 95% CI – 95% confidence interval

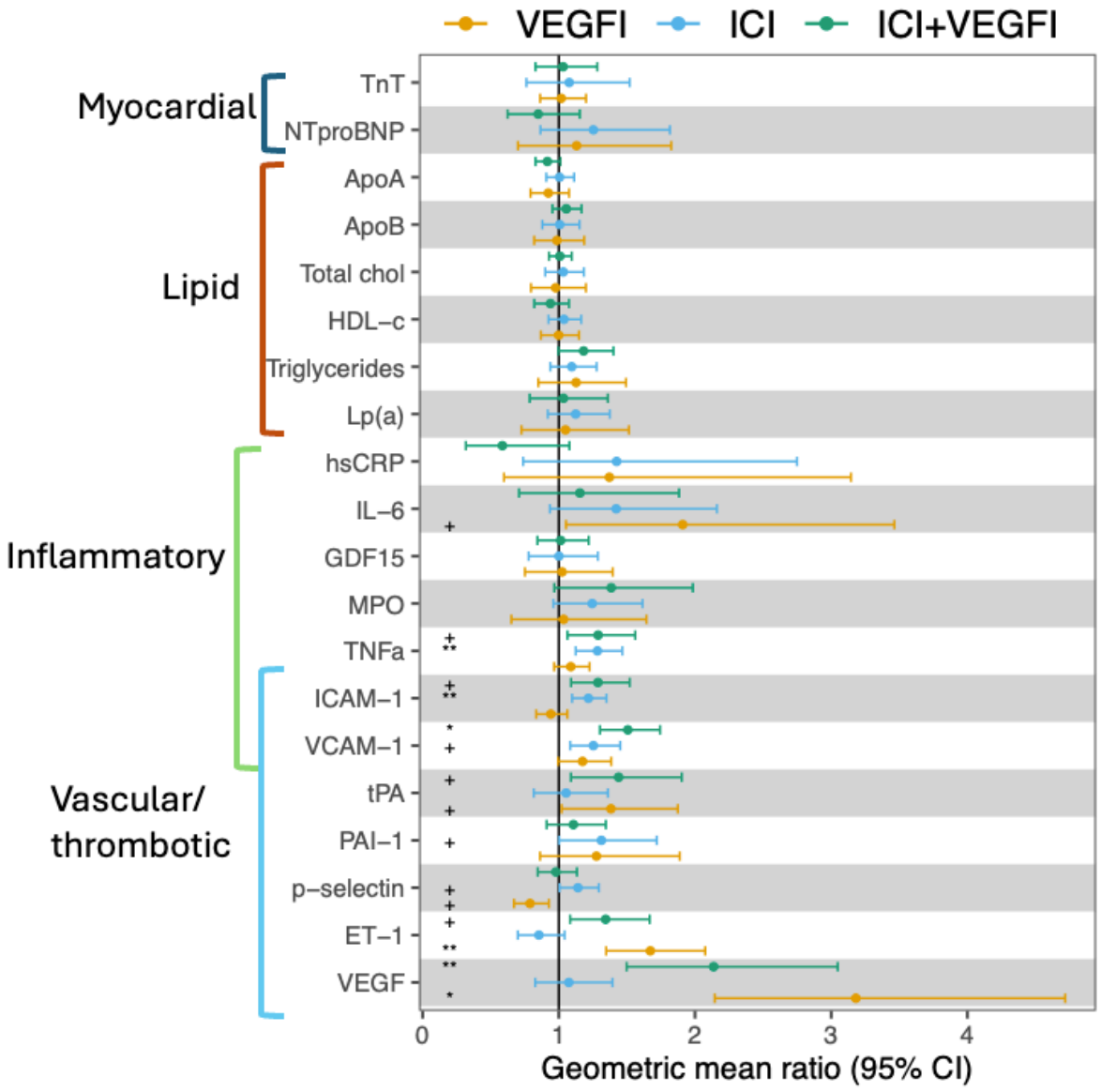

6.3.4 Clinical events

Thirty-two CTCAE grade ≥2 irAEs occurred in 23 patients, Table 6-4. Severe irAE requiring high doses of intravenous methylprednisolone occurred in five patients (two myocarditis, both in the ICI monotherapy group; three colitis, one in the ICI monotherapy group, two in the combination ICI+VEGFI group).

Table 6-4 CTCAE ≥2 adverse events. 32 events occurred in 23 patients

	ICI (n=20)	ICI+VEGFI (n=20)	Total
Myocarditis	2 (10%)	0	2 (10%)
Colitis	1 (5%)	3 (15%)	4 (20%)
Hepatitis	1 (5%)	3 (15%)	4 (20%)
Thyroid	3 (15%)	6 (30%)	9 (45%)
Skin	0	6 (30%)	6 (15%)
Renal	1* (5%)	1** (5%)	2 (10%)
Pancreatitis	0	1 (5%)	1 (5%)
Hypoadrenal	2 (10%)	1 (5%)	3 (8%)
Arthritis	1 (5%)	0	1 (5%)
Total number of AEs	11	21	32

*ICI nephritis **nephrotic syndrome
Abbreviations: AEs – adverse events; ICI – immune checkpoint inhibitor; VEGFI – vascular endothelial growth factor inhibitor

CVAEs occurred in 30 patients: 11 (73%) patients in VEGFI monotherapy, 4 (20%) in the ICI monotherapy group and 15 (75%) of the ICI+VEGFI combination therapy group, Table 6-5. Hypertension was the most common CVAE. No ischaemic events occurred. Five patients (two in VEGFI monotherapy, three in the combination ICI+VEGFI group) developed asymptomatic cancer therapy related cardiac dysfunction.

Table 6-5 CVAEs during the study period

	Asymptomatic CTRCD	Symptomatic CTRCD	Myocarditis	Hypertension	Hypertensive crisis	Arrhythmia
VEGFI (n=15)	2 (13%)	0	0	11 (73%)	0	0
ICI (n=20)	0	0	2 (10%)	2 (10%)	0	1 (5%)
ICI+VEGFI (n=20)	3 (15%)	0	0	14 (70%)	1	1 (5%)
Total (n=55)	5 (9%)	0	2 (4%)	27 (49%)	1 (2%)	2 (4%)

6.4 Discussion

Here, I present the first prospective assessment of large artery inflammation in patients exposed to ICI using dedicated PETCT methods optimised for inflammatory atheroma assessment. I observed no change in arterial inflammation, measured by [^{18}F]FDG-PETCT, in patients receiving ICI. This cohort includes not only those on ICI but also VEGFI, as monotherapy and combination ICI+VEGFI. There was no greater [^{18}F]FDG uptake observed when ICI were used in combination with VEGFI compared to monotherapy. These data were consistent when accounting for baseline demographics, CV risk factors and ASCVD, use of statins and immunosuppression, as well as arterial characteristics, such as calibre of artery and degree of calcification. The results are strengthened by a cohort that is representative of patients seen in routine clinical practice. ICI are eligible for use in 44% of all cancers and are increasingly used in patients who have undergone curative surgery, in whom the balance of risk and benefit may differ than in the palliative setting[48]. Given the enormous number of patients eligible for ICI treatment, even a small risk of ischaemic events could have a substantial impact. This study adds valuable insight to the potential association of ICI and atherothrombotic ischaemic events.

It has been suggested that ICIs accelerate atherosclerosis and cause plaque instability via T cell mediated inflammation, which is supported by pre-clinical models[88,89,95,96,260]. Several meta-analyses of clinical trials have not observed an increase in MI or stroke in patients receiving ICI, either alone or in combination with VEGFI[79,80,122,125]. One meta-analysis specifically assessing CVAEs in 63 randomised controlled trials of ICI found higher risk of MI and ischaemic stroke in patients treated with ICI in comparison to those in control arms, although events were infrequent[82]. Systematic limitations of trial design and heterogenous AE reporting may impair interpretation of CV safety (Chapter 3)[261]. Registry data and AE reporting databases may be more reflective of real-world practice. These studies have observed higher rates of MI and ischaemic stroke in patients receiving ICI compared with non-ICI treated cancer patients and non-cancer controls matched for age, sex and CV comorbidities[47,83,87]. Observational registry data is subject to residual confounding factors and reporting bias. Understanding any pathophysiological process underlying ICI-associated atherothrombosis is key to allow risk stratification and develop prevention strategies.

Characterisation of inflammatory atheroma during ICI exposure has been assessed previously using [^{18}F]FDG-PETCT[96,151–153,156,256]. Each of these six studies have been retrospective and yielded conflicting results. Positive findings were usually only observed when analyses were made when stratifying by sub-group. In many of the studies, the reported imaging acquisition and analyses methods are unclear, without clear description of how arterial segments were identified, defined and chosen for analysis[96,151–153,156] despite recommendations by EANM on how to perform atherosclerosis assessment[137]. I consistently observed no signal of ICI associated arterial inflammation. The data from my study presented here is strengthened by their prospective nature, optimised imaging acquisition protocol and robust methods for analysis.

There are several potential reasons as to why I observed no association between ICI and arterial inflammation. Firstly, one might question whether the sensitivity of [^{18}F]FDG-PETCT and assessment at 24-week time point present risks that a 'true' inflammatory signal may be missed. [^{18}F]FDG-PETCT is a well-validated assessment of atherosclerosis inflammation and is the gold standard method of assessing large artery inflammation[137,258] and prior studies reported increased arterial inflammation evident on [^{18}F]FDG-PETCT after more than one year from initiation of ICI[156,256] as well as from 2.5 to 10 months from initiation in other studies [151–153]. The technical limitations described above and heterogeneity of the methods of used in these retrospective studies impairs the interpretation and confidence of their results. Case reports observe ACS occurring early, after the first or second cycle, and single centre cohort studies observe an association with ICI and ischaemic events starts within the first six months of therapy[47,74]. I believe if there was an inflammatory signal as a result of ICI, this would have been apparent by 24 weeks in my study. Secondly, It has been proposed that [^{18}F]FDG-PETCT predominantly assesses macrophage activity and therefore may not be sensitive to T-cell mediated processes. Although ICI have a very specific mechanism for T-cell activation, the consequent inflammatory process incorporates both adaptive and innate immunity, with recruitment of macrophage and cytotoxic T-cells. This is supported by the clinical utility of [^{18}F]FDG-PETCT for the assessment of ICI-induced non-cardiovascular irAE[150]. In my study, [^{18}F]FDG-PETCT identified multiple irAEs, including thyroiditis, pancreatitis and four cases of ICI related sarcoidosis. Thirdly, there remains a

possibility that ICIs are not associated with ischaemic events and that, consistent with my findings, atheromatous plaque inflammation is not caused by ICI. Indeed, inherent limitations with trial adverse event reporting and potential over-attribution of non-specific symptoms or biomarker changes to ACS may mean that a potential link to ACS has been over-stated. Retrospective analyses and pharmacovigilance analyses are prone to substantial reporting biases and residual confounding factors. Further prospective studies with standardised CVAE definitions with robust comparator groups are required to truly understand the association between ICI and atherothrombotic events.

Finally, it is possible that other non-inflammatory mechanisms, such as direct pro-thrombotic effects or direct arterial injury, are responsible for ICI-associated atherothrombosis. These effects would not be expected to be seen by [^{18}F]FDG-PETCT. My data may suggest that ICI are associated with direct arterial activation and injury. Adhesion molecules ICAM-1 and VCAM-1 were elevated at 24 weeks compared to baseline in those treated with ICI. Higher ICAM-1 levels correlate with ICI responsiveness[262]. TNFα was also elevated at 24 weeks compared to baseline in patients treated with ICI. ICAM-1, VCAM-1 and TNFα are crucial for infiltration of immune cells into cancer tissue and facilitate the anti-cancer effect of ICI. Therefore, increases in these biomarkers with ICI is not surprising. While ICI have a very specific mechanism of action, an 'off-target' activation of endothelial cells may promote infiltration into atheroma with upregulation of the proximal inflammatory cytokine, TNFα, promoting inflammation. ICIs are associated with increased expression of VCAM-1 in the aortic plaque of mice, with increased necrotic core and T cell infiltration into plaque, compared to controls[96]. Similar to my results, there was no increase in [^{18}F]FDG in the aortic plaque within that mouse model. All three biomarkers are implicated in CVD and CV risk[90,92,263,264]. These circulating biomarkers may be a more sensitive measure of arterial inflammation and allow for risk stratification in the future. Assessing changes in biomarkers, in the context of cancer and its treatment, is challenging and other complex and competing physiological and pathophysiological processes may be occurring in addition to arterial injury.

6.4.1 ICI+VEGFI combination therapy

This study also explores whether the combination of ICI+VEGFI modulates inflammatory plaque activity. It has been proposed that additional anticancer benefits of combining ICI with VEGFI lie in the immunomodulatory effects of VEGFI occurring via mechanisms such as augmentation of T cell infiltration, reduction of regulatory T cell function and downregulation of PD-1 expression within cancer cells[42,129]. While these mechanisms may enhance anticancer efficacy, it is unclear whether they also enhance plaque instability and ischaemic events. Despite reassuring (but sub-optimal) CV safety data from trials, observational data and AE reporting databases suggest that there is an increased risk of CVAEs, particularly thrombotic events, in patients treated with ICI+VEGFI combination therapy compared with ICI alone[125,126] and VEGFI alone[127]. Despite this, I observed no change in TBRmax over time in patients exposed to VEGFI, when used as monotherapy or in combination. VEGFI exposure was associated with elevated vascular and thrombotic biomarkers, such as VEGF and ET-1. These changes, in conjunction with the elevated biomarkers observed with ICI, may lead to accelerated atherosclerosis that is not seen by [^{18}F]FDG-PET assessment of arterial inflammation.

ICI+VEGFI may exert a greater anticancer effect than monotherapy via immunomodulation by VEGFI. VEGFI stimulates immune cell infiltration by increasing expression of adhesion molecules, such as ICAM-1 and VCAM-1[99]. It has been hypothesised that the enhanced expression of adhesion molecules exerts a greater atherothrombotic effect than monotherapy[99]. In all of the biomarkers assessed, including adhesion molecules, the combination of ICI+VEGFI was not associated with a greater increase over 24 weeks from baseline in comparison to monotherapy.

6.4.2 Heterogeneity within sub-groups

6.4.2.1 Statins & immunosuppression

Statins reduce arterial inflammation in patients with CVD in the absence of cancer [142,159]. Two prior PETCT studies observed that statins and immunosuppression attenuated increased arterial FDG uptake in patients receiving ICI[156,256]. It is important to note, however, that these two studies found

no increase arterial uptake with ICI based on their primary outcome analysis and this positive association was only seen in a sub-group analysis. I observed no association between [^{18}F]FDG uptake and statin use or immunosuppression use across the three anticancer treatment groups. I believe that my inclusion of patients on immunosuppression and statins was important to ensure the study had a population that was representative of clinical practice.

6.4.2.2 Arterial calcification

The prevalence of arterial calcification was high in this cohort but was comparable to the existing literature[156,256]. It has previously been hypothesised that plaque inflammation does not occur in 'burnt out', established calcified atheroma[154]. Data from studies assessing arterial inflammation and calcification are conflicting and other studies refute this hypothesis, both in the context of ICI-associated inflammation as well as in non-cancer cohorts[151–153,155]. My analysis revealed no change in TBRmax in any of the three treatment groups, irrespective of calcium burden. It does remain possible that the high burden of pre-existing calcification in patients in my cohort could have attenuated any potential signal for ICI-inflammation.

6.4.2.3 Pre-existing inflammation

It has been proposed that ICI-associated inflammation only occurs in arterial segments without pre-existing inflammation. The majority of studies have only found an increase in arterial inflammation after ICI in segments without pre-existing inflammation[152,153,155,156]. One study did find an increase in TBRmax after ICI in lesions with TBR >1.6.[151] Two neutral studies did not dichotomise arterial segments based on a baseline TBR threshold[96,256]. On first impression, my cohort might be considered as having 'high' baseline TBR. While a TBRmax threshold of ≥1.6 has traditionally been used as a threshold for 'active inflamed disease', these data are derived from historic studies using older PET scanners in contrast to the contemporary digital scanners used for this study[137,138,144]. As outlined in Chapter 5, it is most probable that the 'high' TBR values reflect the reconstruction parameters and circulation times used to optimise imaging for atherosclerotic assessment, rather than being representative of truly active inflammation. Importantly, the primary measure of interest in my study was the

change in TBR from baseline to follow-up which minimises the relevance of absolute TBR values. I observed no change in arterial TBRmax in segments irrespective of the presence of absence of 'pre-existing inflammation' at baseline.

6.4.3 Limitations

There are limitations to this study. It enrolled a relatively heterogenous population with a small sample size. The cohort contained patients with different cancer types and a range of ages and comorbidities. However, this also means that the cohort is a clinically-representative group and my results were consistent when accounting for this heterogeneity. The ICI group also contained patients treated in the adjuvant setting, after curative surgery. These patients had a range of cancer types, age and comorbidities. It is essential to study the adjuvant treated population as this is the group where the use of ICI is most likely to extend in the near future and in this group the risk to benefit ratio may differ to those treated palliatively.

The inclusion of patients on statins at baseline and not excluding those requiring immunosuppression during the study may have diluted the signal of arterial inflammation by PETCT. I believed it was important that my cohort was representative of patients seen in clinical practice. Assessing any interaction between these factors and PET activity was limited by the small numbers in the additional analyses.

I used VEGFI as a comparator group and it might be argued that this cannot be considered as a true control group. However, the inclusion of a 'no cancer, no anticancer therapy' control group would have been ethically challenging in the context of radiation exposure. Furthermore, by including such a group the absence of cancer would have further confounded true comparisons. I therefore firmly believe that the comparator groups in this study are appropriate and pragmatic. Given the complex interplay between CVD, cancer and its treatment, establishing a clear link between biomarkers is challenging. My biomarker findings should be considered as hypothesis-generating. PET scans were performed at 90 minutes after [^{18}F]FDG administration, rather than at 120-minutes, as recommended by the EANM. A 90-minute circulation time was based

on optimal assessment of reconstruction parameters using digital PET scanners, (Chapter 5). The recommendation of a 120-minute circulation time predates the advent of digital scanners. Based on my data, I anticipated 120 minutes would only increase TBR further without improving arterial uptake.

6.4.4 Conclusion

Using gold standard PET imaging methods, I found no evidence that ICI and VEGFI (alone or in combination) are associated with arterial inflammation. This is the first prospective, controlled PET study in patients treated with ICI and the first to make clinically relevant assessments in patients treated in combination with VEGFI. In patients treated with ICI, the circulating biomarkers, ICAM-1, VCAM-1 and TNFα both increased at 24 weeks from baseline. It remains possible that ICI provoke direct arterial activation and arterial injury. Further prospective controlled studies with standardised CV definitions are required to understand the risk of ischaemic events in the context of ICI therapy. The results within this study suggest biomarkers may help understand the process of ICI-associated atherothrombosis to inform early risk stratification as well as to develop therapeutic strategies for prevention and management of ICI-associated ischaemic events.

Chapter 7 Discussion

7.1 Summary of findings

The main findings within this thesis are:

In a systematic review of 17 ICI+VEGFI combination trials with 10313 patients, I assessed to what extent patients with CVD were excluded and represented, and how CVD and CVAE were defined and reported (Chapter 3). I found:

- Broad and heterogenous definitions are used for CV eligibility criteria and CVAE reporting within ICI+VEGFI oncology trials.

- Limitations in trial design, such as incidence thresholds of AE reporting impair the ability to understand the CV safety of ICI+VEGFI.

In a retrospective analysis of clinically-indicated PETCT scans of patients with lymphoma undergoing anthracycline chemotherapy regimens I assessed whether there was an inflammatory response in large arteries with anthracyclines (Chapter 4) and found:

- Anthracyclines were not associated with large artery inflammation, assessed by [^{18}F]FDG-PETCT, in patients with lymphoma at end of treatment, compared to baseline.

- This finding was consistent, irrespective of baseline characteristics, CV history or haematological history.

In a detailed comparison and validation of vascular PET methods, I assessed the validity of current recommendations for atherosclerosis assessment by PETCT in modern state of the art digital PET scanners (Chapter 5) and showed:

- Using modern digital PETCT, fewer iterations and subsets (4i 5s) are required to achieve optimal imaging on a digital PET scanner for atherosclerosis assessment than using the method recommended by EANM (24i 5s). Use of the EANM recommendations results in over-estimation of

[^{18}F]FDG uptake compared to our locally optimised protocol, with greater variability and error.

- Novel metrics of analysis, such as mean contrast recovery (MCR), coefficient of variation (CoV) and error provide additional information to allow robust comparison of imaging acquisition protocols within PETCT to develop a locally optimised protocol.

- SVC offered the best and most reliable data for blood pool collection. IJ was the least reliable and most difficult blood pool data to obtain.

In a comprehensive, prospective study of patients with cancer receiving VEGFI, ICI and ICI+VEGFI (Chapter 6), I demonstrated that:

- ICIs were not associated with higher levels of large artery inflammation at 24 weeks, when assessed by [^{18}F]FDG-PETCT, compared to baseline.

- There was no evidence of greater arterial inflammation when ICI was used in combination with VEGFI, compared to ICI or VEGFI monotherapy.

- Markers of arterial injury and endothelial activation, ICAM-1 and VCAM-1, were elevated in patients treated with ICI. TNFα was elevated in patients treated with ICI at 24 weeks, compared to baseline.

The use of ICIs and their licensed indications over the last decade has been rising rapidly and continues to expand. Their introduction has been associated with the most remarkable improvements in cancer-specific outcomes. In recent years, the indications for ICIs have moved from the palliative setting to use in the adjuvant setting, after potentially 'curative' surgery. ICI are also now increasingly used in combination with VEGFI, a drug class associated with numerous CVAEs.

The hypothesis that ICI are associated with atherothrombotic events is supported by pre-clinical models and these events have been described in observational studies and clinical registries[47,57,61,84]. This association has not been rigorously assessed in randomised controlled trials (RCTs). Despite the supporting evidence, it is still unclear whether ICI are associated with ischaemic events and, if so, the

true magnitude of the risk. In order to understand this better, RCTs with appropriate endpoints must be performed. Mechanistic studies, using robust methods with prospective assessments, are highly important.

Prior to investigating potential arterial inflammatory effects, I wished to understand why the association of ICI and atherothrombosis has been so hard to establish in the existing literature. In Chapter 3, I assessed oncology efficacy trials of ICI+VEGFI to explore how eligibility criteria, definitions of pre-existing CV conditions and AE reporting may impact our understanding of the CV safety of these treatment regimens. I found that potential trial participants are subject to broad and heterogeneously defined CV eligibility criteria. This means that trial populations are likely to be unrepresentative of patients seen in routine clinical practice. Due to a lack of reporting of baseline CV characteristics, it is not possible to accurately understand baseline CV risk or the presence of established CV disease in trial populations. CVAE reporting is heterogenous and often only done when the incidence crosses a pre-defined threshold. Centralised adjudication of potential CVAEs is not performed in cancer trials. CVAE reporting is not based on methods that have been standardised for use in CV trials, including the use of defined clinical CV endpoints. No trial specifically reported the absence of CVAEs. Without clear and transparent data on the characteristics of the patients included in the trials and standardised definitions of CVD and CVAE, the CV risk of these drugs may be under-appreciated. The limitations I have identified mean that it is not possible to perform robust trial meta-analysis to gather truly meaningful insights about the incidence of CVAEs associated with these important drugs. While the limitations in methods and data capture are more likely to under report events, it is also possible that over-reporting of events could occur from incorrect definitions of CVAEs[198].

In Chapter 4, I assessed the potential arterial toxic effect of anthracyclines using [^{18}F]FDG-PETCT. While anthracycline cardiotoxicity has been extensively investigated, arterial toxicity of anthracyclines has been largely unexplored. Anthracycline arterial toxicity has potential to result in CV conditions such as hypertension and atherothrombotic events. It is also possible that anthracycline-associated arterial toxicity contributes to the development of anthracycline-associated cardiotoxicity via effects on peripheral vascular resistance and

ventriculo-arterial uncoupling[28]. My study was performed in collaboration with colleagues at Wake Forest University (North Carolina, USA), by Ms Caitlin Fountain and Dr Giselle Meléndez, who provided histopathological insights to structural arterial changes following exposure to clinically relevant doses of anthracycline in a large animal model. The data from the animal model revealed increased collagen deposition (a marker of fibrosis) and increased intracellular vacuolisation (a marker of oedema) in the arterial walls of monkeys treated with anthracyclines in comparison to matched controls. The structural changes observed in the aorta of these monkeys was similar to the changes seen in anthracycline-associated myocardial toxicity in the same model[30,208]. Indeed, inflammation and cardiac infiltration by leukocytes have previously been implicated in anthracycline cardiotoxicity[30,32,33]. I hypothesised that an inflammatory process was occurring within the aorta of monkeys exposed to anthracyclines. The unique insight from this large animal study prompted me to corroborate arterial PET imaging data obtained from humans treated with anthracyclines.

I performed a retrospective analysis of patients with lymphoma being treated with anthracycline chemotherapy to understand whether this inflammatory effect was apparent when comparing clinically-indicated baseline pre-treatment [^{18}F]FDG-PETCT staging scans and end-of-treatment PETCT imaging. In this analysis of 101 patients, I observed no change in arterial inflammation after anthracycline exposure, compared to baseline. I therefore concluded that anthracycline exposure is not associated with substantial arterial inflammation. The analysis was performed in patients with diffuse large B-cell lymphoma (DLBCL). This subtype of lymphoma was chosen for a number of reasons. Due to the retrospective nature of the study, I required a cohort of patients who were treated with anthracyclines and had clinically-indicated PETCT imaging for both staging and assessing response to treatment. Many breast cancer patients receive anthracyclines but the use of PETCT in imaging in breast cancer is limited. Within Scotland, PETCT is used in other types of lymphoma, such as Hodgkin's lymphoma, but only for staging purposes and not for assessing treatment response. PETCT imaging is used for both staging and response to treatment in DLBCL. DLBCL is typically treated with R-CHOP chemotherapy which typically includes higher doses of anthracycline than used in current

practice for the treatment of other cancers, such as breast cancer. In addition to these practical and logistical reasons, patients with DLBCL are typically older with a high prevalence of CV RFs. I hypothesised that this cohort would therefore be enriched to demonstrate any potential arterial inflammatory signal due to a higher burden of pre-existing atheromatous plaque disease. The absence of an inflammatory signal even in this 'enriched' population lends further weight to my observation that anthracycline exposure was not associated with substantial arterial inflammation when assessed after a mean of 4.8 months. One prior study had assessed arterial [^{18}F]FDG-PETCT activity in patients with Hodgkin's lymphoma and observed no change in arterial inflammation after anthracyclines[210]. The mean age of participants in that study was 34 years and pre-existing CV RFs were uncommon. Furthermore, there was a high prevalence of HIV (35%) and follow up scans were performed at 65 weeks. These factors had the potential to confound the interpretation of their results but my own findings in a higher risk group are congruent.

The scans assessed in Chapter 4 were analysed retrospectively and had originally been performed as part of routine clinical assessment. As such, the imaging protocol was not optimised for atherosclerosis assessment, as recommended by EANM[137]. The BioCAPRI study (Chapter 6) was designed as a dedicated, prospective assessment of the potential arterial inflammatory effects of ICI and VEGFI. No atherosclerosis research using [^{18}F]FDG-PETCT had been performed in Glasgow prior to my PhD. Therefore, in collaboration with the team at The West of Scotland PET Centre (Gartnavel Hospital, Glasgow, UK), I developed a robust PET imaging protocol for the assessment of arterial inflammation. I reviewed the existing literature to inform atherosclerosis assessment by [^{18}F]FDG-PETCT and international recommendations in order to create an optimised imaging protocol for atherosclerosis assessment. In doing so, this highlighted challenges and limitations of [^{18}F]FDG-PETCT and led me to question some of the current dogma in PET research (Chapter 5).

In the BioCAPRI Study, all the scans were performed on a state-of-the-art digital SiPM PETCT scanner, as opposed to traditional analogue photomultiplier PET scanner. This added further weight to the need to optimise imaging and analysis protocols for this prospective component of my research. While digital PETCT

scanners offer higher sensitivity and better resolution, this meant that the recommended parameters in PET reconstruction for atherosclerosis assessment may not be optimal for digital PET scanning. I compared the EANM recommended reconstruction parameters with a locally optimised reconstruction protocol on the first twenty patients scanned in the BioCAPRI study. This work was performed with the incorporation of data from studies using phantoms (performed by Mr Alastair Gemmell) and using traditional and novel metrics to assess reconstruction parameters and compare imaging protocols. The interpretation of phantom data to develop the PET protocol was performed by myself in addition to Mr Gemmell and the team at the PET Centre, with supervision from Dr Sandy Small and Prof Dave Colville. I observed that EANM recommended parameters were not optimal for use with contemporary digital PET scanners. Use of the EANM-recommended number of iterations and subsets (24i 5s) led to over-estimation of SUV and MCR, with greater variability, unrealistic TBR values and poorer image quality. Metrics such as MCR, CoV and error added valuable information to compare and assess imaging protocols. Using locally optimised parameters with fewer iterations and subsets (4i 5s), I observed more reliable SUV values and MCR with better variability and reliability, compared to EANM parameters.

In addition to recommended reconstruction parameters for image acquisition, EANM make recommendations on image analysis, including methods for the collection of blood pool data for TBR analysis[137]. These recommendations are not supported by strong evidence and data comparing the use of different blood pool regions for this analysis is lacking. Practice within the existing literature varies and there is usually sparse information relating to methods used for blood pool data collection[139,160,229,233,235]. I compared different blood pool regions for TBR analysis. I compared their repeatability and reliability over time in order to understand the potential impact this may have on TBR analysis. I observed that the use of blood pool regions near to the artery of interest for TBR is not required on digital PET scanners with continuous bed motion scanning as heterogeneity in circulation time is minimised with this quicker technique.

Between all four blood pool regions (SVC, IJ, IN, IVC), there was only 0.36 absolute difference in mean SUV between the highest (SVC) and lowest (IJ)

region. Although a small absolute difference, as blood pool is the denominator of the TBR ratio, this had an impact on TBR. IJ yielded lower blood pool readings resulting in higher TBR values. This meant that in the carotid artery analysis, carotid TBR was >1.6 when using IJ, but not when using other blood pool regions. A TBR ≥1.6 has traditionally been used as the threshold for being indicative of 'active' inflamed disease and has been used an endpoint in clinical trials[137,142,143,146]. This means that choice of blood pool region could change the result of a study using this threshold as an endpoint from negative to positive. This is particularly relevant to IJ specifically, as it was the most challenging and least reproducible blood pool region to obtain data for. This highlights the need for clear and transparent description of the methods within the literature. The IJ is the smallest blood vessel assessed and is therefore most susceptible to inherent errors within PET imaging, such as partial volume error. SVC, being the larger vessel, offered the best and most reliable data for blood pool collection.

There is need for standardisation within PETCT research regarding imaging protocols, reporting and analysis. This may be challenging to implement, due to the heterogeneity within protocols and scanners used. PETCT is also often used at the forefront of hypothesis generating research, where no gold standard exists. These reasons also highlight the need to minimise any other areas of heterogeneity. Methods should be standardised within PET research. Routine use, and publication of, metrics like the RCmax, CoV and error of the imaging protocol used within a study is easy to interpret and helps build transparency and consistency in PET research. I believe this would be a helpful way to improve the robustness of PET research.

In Chapter 6, the BIOCAPRI study, I compared large artery inflammation at 24 weeks in patients receiving ICI monotherapy, VEGFI monotherapy and ICI+VEGFI combination therapy. In this first prospective assessment of large artery inflammation, assessed by [^{18}F]FDG-PETCT, ICIs were not associated with large artery inflammation at 24 weeks, compared to baseline. The combination of ICI+VEGFI did not result in greater change in large artery inflammation at 24 weeks from baseline, compared to ICI or VEGFI monotherapy. These findings were consistent across all methods of arterial analysis irrespective of clinical CV

and oncological characteristics, and arterial characteristics, such as calibre of artery and degree of calcification.

Biomarker analysis yielded interesting, hypothesis generating results. In agreement with the PETCT data, there was no consistent inflammatory signal, in biomarkers such as hsCRP and IL-6. The inflammatory cytokine, TNFα was modestly elevated at 24 weeks in patients in ICI. Markers of arterial injury and endothelial activation, ICAM-1 and VCAM-1, were elevated in patients treated with ICI, which may suggest that ICI associated atherothrombosis occurs through a mechanism of direct arterial activation (Chapter 6). It has been previously suggested that accelerated dyslipidaemia as a result of ICI may be a mechanism for ischaemic events associated with ICI[82]. There was no change in lipids over time in patients treated with ICI in my study.

The current evidence base relating to ICI-associated large artery inflammation, assessed by [^{18}F]FDG-PETCT, yields conflicting results. Frequently, the description of PETCT imaging and analysis methods are somewhat unclear and this has been a challenge in the interpretation of findings. The BioCAPRI study adds clarity and valuable insights into this area with robust, validated and transparent methods for image acquisition and analysis. In several prior studies, only arterial lesions without pre-existing inflammation, demonstrated a rise in arterial uptake. I consistently found no signal of increased arterial inflammation, irrespective of the presence or absence of any characteristic assessed, including calcification and pre-existing inflammation. I also performed a number of additional analyses to account for potential heterogeneity within the cohort and found no difference.

My thesis focused on only using [^{18}F]FDG as a tracer to analyse arterial uptake. This decision was taken because [^{18}F]FDG has been validated in numerous clinical settings and corroborated with histopathological samples as a surrogate for inflammatory atheroma. It is also the tracer used in all six of the other studies used to assess ICI and large artery inflammation. The tracer [^{18}F]NaF is much more specific to atherosclerotic processes through NaF uptake by binding to calcium phosphate in microcalcification, produced by smooth muscle cell-derived osteoblast-like cells in response to inflammatory cytokines[155,265]. There

are several reasons why I chose not to use this tracer. Firstly, [^{18}F]FDG is the gold standard tracer for assessing large artery inflammation. [^{18}F]NaF also has the potential to miss a primary vasculitic process in the large arteries. This has been proposed as a mechanism for ICI-associated atherothrombosis[69]. From a more practical and pragmatic perspective, with this study I needed to prove CV PET research is deliverable in Glasgow in a complex cohort. Throughout the completion of the study, I have identified and overcome numerous challenges. Patients undergoing anticancer treatment are under time pressure to initiate therapy. This combined with the clinical pressures of the PET department would have made using novel tracers much more challenging. [^{18}F]FDG is made on site in Glasgow. [^{18}F]NaF is bought and would be transferred from another city. With a half-life of 110 minutes, this makes delivering PET research more challenging.

The sensitivity of [^{18}F]FDG-PETCT and 24-week time point may mean an inflammatory signal was missed. Despite the advances in PETCT technology, the spatial resolution is a limiting factor, particularly in smaller lesions (as seen in Chapter 5). Previous studies of ICI arterial inflammation have reported evidence of arterial inflammation acutely (2.5-10 months[151–153]) and more than a year after initiation[156,256]. Clinical observational studies have observed an early association of ICI with ACS, even after the first cycle[47,74]. With this information, I believe that if there was an inflammatory signal within atheroma it would occur early. In addition, with the marked sustained anticancer response observed with ICI, I would expect that if there were an inflammatory signal, it would remain positive for months after exposure.

Lastly, I believe [^{18}F]FDG-PETCT's use for oncological assessment makes the tracer an attractive one for the world in cardio-oncology. It has the potential to provide both oncological and CV assessment within the one scan. [^{18}F]FDG-PETCT has already been shown to be associated with risk stratification in both cancer and non-cancer populations for CV events. There is an association between aortic TBR and CV events in patients with and without cancer[145,229]. The incorporation of [^{18}F]FDG arterial activity with the Framingham risk score (FRS) for CVD has previously been shown to improve risk prediction for CV events over 4 years [145]. Despite this appeal, my study does not provide strong support for the

use of [^{18}F]FDG-PETCT for assessment of ICI or VEGFI arterial toxicity in the relatively short-term (24 weeks).

7.2 Strengths

A main strength of this thesis was the BioCAPRI study: its robust methods of analysis and prospective design to assess patients on ICI. These data were strengthened by granular data and comprehensive assessment by echocardiography and ECG. This allowed for characterisation of baseline CV risk as well as the use of standardised definitions for CV toxicity, such as the IC-OS definitions. The strong methods I used in this study help bring clarity and, I believe, provide more definitive answers than prior retrospective assessments of arterial inflammation in patients exposed to ICI. The impact and relevance of this study was further strengthened by the assessment of patients also on VEGFI. I compared against VEGFI monotherapy (as a valid control group). I compared the combination of ICI+VEGFI in comparison to monotherapy, which has never been assessed by [^{18}F]FDG-PETCT imaging. This increases the scope of my results to clinically relevant treatment regimens.

My drive to challenge accepted methods with this field extended to trial design and safety data collection within trials. By critically appraising and assessing trial design of clinical oncological trials, I gave insight into how our understanding of ischaemic risk with ICI may be impaired. I also critiqued aspects of PET. I did not take recommendations and previous practice as acceptable methods of analysis. Without my desire to understand why recommendations were made, the evidence used to support them and their potential impact on my results, I would not have been able to interpret and explain my data nor draw clear conclusions from them. It also allowed me to have confidence in my work and reduced the amount of potential error introduced into the results through suboptimal imaging. I believe the work presented in this thesis could be used a benchmark for how to develop and deliver successful arterial [^{18}F]FDG PET research.

7.3 Limitations

In Chapter 3, I chose to focus on publicly available data in my review. Had I chosen to delve into clinical trial report data, I may have found higher rates of CVAEs. However, the accuracy of these investigator-reported events would still impair the ability to accurately assess CV safety profile of these drugs. The landmark trials included in my analysis are the main point of reference and source of information for clinicians in day to day practice. A limitation of the results of Chapter 4 lies in the retrospective nature of the scans and use of non-optimised imaging protocols. While my data was paired with histopathological arterial assessment in an animal model, I was unable to link my PET data to any histopathological or functional arterial assessment.

In BIOCAPRI, I included a relatively large population size for prospective PET research[139,142,151,152,160,266]. In other contexts, the sample size may appear small. The study included patients with different cancer types, treated in both palliative and adjuvant settings, and with several different drugs within each class. Assessing the impact of this heterogeneity is limited by the small sample size. Reassuringly, the results within the BioCAPRI study were consistent despite the heterogeneity within the groups. The biomarker data are hypothesis generating. It is not possible to determine the source of these biomarkers; whether changes seen in the biomarkers reflect changes relevant to CV and arterial disease, versus cancer and response to anticancer treatment.

There are many limitations relating to PETCT which are relevant to this body of work. Aspects of PETCT, such as cost, radiation and time to patients must be taken into consideration. It must be acknowledged that the spatial resolution of PET limits its ability to perform inflammatory atherosclerosis assessment of small lesions, even in large arteries. Caution must be exercised in any research stating otherwise. The spatial resolution of PET is 3-4mm. Even with the improved resolution and sensitivity with digital PET, I observed RCmax of <0.5 in phantom spheres with diameters of 5mm (Chapter 5). These small lesions are much more susceptible to errors such as partial volume error (PVE). Although total artery TBR can be used as a surrogate for inflammatory atheroma, the spatial resolution of PET impairs its ability to make assessment on small lesions. This is relevant to atherosclerosis assessment. Patients with diabetes on

treatment were excluded from enrolment to BioCAPRI. Insulin increases [^{18}F]FDG uptake into muscle tissue which impairs analysis and increases variability. Metformin causes a markedly increased uptake within the bowel which may impair analysis within the abdomen. For this reason, despite diabetes being highly prevalent globally and an important CV risk factor, I felt it was important to exclude diabetic patients on treatment to minimise variability in PETCT analysis.

[^{18}F]FDG uptake within the arterial wall has been used as a surrogate for inflammatory atheroma. In this study I was unable to confirm the presence of atheroma. Intravenous CT contrast can be used to aid in the identification atheroma and may have strengthened my analysis. This is not without consequences. Intravenous contrast interferes with the PET scanner's ability to create accurate data. Contrast interferes with corrective algorithms, such as attenuation correction. If contrast is to be given, an additional arterial phase CT scan must be performed after the PET scan and markedly increases the amount of radiation. Given this, and the predicted high prevalence of CKD in a renal cancer population, I did not perform an additional arterial phase contrast CT scan. In an attempt to mitigate this, I performed calcium scoring analysis on the arterial tree which would act as a surrogate for the presence of atherosclerotic disease and corroborated my PET data with granular clinical data relating to CV history and risk profile.

Despite the limitations discussed above, I believe that my study design was the most appropriate, achievable and safe method to answer the questions set out.

7.4 Areas of future research

In clinical practice, cardio-oncology has moved from being a niche, subspecialist area of cardiology to part of everyday practice for all cardiologists. The publication of European Society of Cardiology's cardio-oncology guidelines created a benchmark and standard to work to[1]. The robustness of evidence supporting the guideline, however, is lacking. The future of cardio-oncology must focus on improving the evidence base within the field. The results presented within my thesis offer strong foundations to develop different areas within CV imaging and cardio-oncology.

7.4.1 Standardisation of trial endpoints & PET research methods

Within oncology trials, there needs to be clear capture of CV events within cancer trials. Adjudication of CV endpoints could be mandated by regulators in cancer trials. This could be done by utilising existing CV endpoint definitions, such as Hick's criteria[183], updating CTCAE for CV specific conditions, or integrating IC-OS definitions in AE reporting[14]. Transparent and standardised reporting of CV baseline characteristics are essential to adequately perform meta-analysis. Other specific, clinically relevant cardio-oncology endpoints that should be implemented could include unscheduled interruption, or permanent discontinuation, of anticancer therapy for a CV reason. Lastly, it is important that any RCT within cardio-oncology assesses the potential impact upon oncological efficacy and safety.

PET research is an exciting and rapidly progressing field. With the scope of radiotracers, PET research can give vital understanding to underlying mechanisms and metabolic assessments in a number of areas, including cardio-oncology. While TBR assessment (using the whole vessel for TBRmax, TBRmean, active segments and MDS) is the most comprehensive for the assessment of arterial inflammatory activity, it is also the most time consuming and labour intensive. In an attempt to make analysis quicker and easier, two prior ICI studies only assessed specific areas within the arteries[156,256]. While this is appealing, there is no head-to-head comparison of these methods with the EANM gold-standard recommended method (used in my thesis). For these methods to be adopted, comparison and assessment of the validity, repeatability and reproducibility with these methods must occur. A prospective study using both digital and nondigital PET scanners should be undertaken to compare imaging protocols, and different arterial analysis methods, ideally being compared to histopathological data.

7.4.2 Mechanistic research

Randomised mechanistic trials of cardiac and vascular effects of ICI and other cancer therapies should be performed. PET and biomarker analysis may offer valuable insights into the mechanisms underlying potential arterial injury of

anticancer treatments so that, where present, mechanism-based preventative strategies and treatment strategies can be refined.

PET research can offer a great deal to increase the understanding of ICI and arterial injury, particularly with the use of other radiotracers. Performing prospective assessment of patients treated with ICI using [^{18}F]NaF as a radiotracer is a next logical step from the BioCAPRI study. If ICI are indeed associated with ischaemic events from atherosclerotic plaque rupture, using a tracer that looks more specifically at atherosclerosis may add value. Using a true cancer control group could add value but there are practical challenges to recruiting this cohort. Many patients who are eligible for adjuvant ICI, in renal cell carcinoma and melanoma, decline ICI. These patients would be suitable controls. However, they may be challenging to recruit and may reflect a different cohort. Often those that refuse ICI do so for reasons such as to minimise hospital visits, pressures with work or caring for family members or have other comorbidities (including previous autoimmune conditions or on immunosuppression). A cancer free population could also be of value but with cancer being such a competing comorbidity, I believe having a cancer control group is a more comparable group. An alternative could be to perform the study in an enriched population, such as those who had a CVAE compared with those who did not.

Fibroblast activation protein inhibitor ([^{68}Ga]FAPI) is a PET radiotracer that detects fibrosis. FAPI has been used to assess myocardial and arterial fibrosis[267,268]. [^{68}Ga]FAPI has been used for the early detection of ICI myocarditis and may offer valuable insights into arterial changes in ICI patients[269]. This could be prospectively used in patients, including those treated with anthracyclines or ICI. Assessing [^{68}Ga]FAPI, before and after exposure to anthracyclines, may confirm the histopathological changes seen in the animal model, described in Chapter 4. These PET data could then be paired with longitudinal assessment of arterial stiffness, blood pressure monitoring, assessments of endothelial function and cardiac function. Assessment of [^{68}Ga]FAPI arterial uptake at baseline and changes in serial imaging may predict those most at risk of CV toxicity from anticancer treatment.

As [^{68}Ga]FAPI has little uptake within healthy myocardium, unlike FDG, [^{68}Ga]FAPI could also be used for assessment of myocardial toxicity as well as arterial toxicity, in the same prospective study assessing arterial toxicity. Animal model data suggests that both anthracycline arterial toxicity and myocardial toxicity occur via similar processes (Chapter 4)[30]. Assessment of both myocardial uptake and arterial uptake could confirm or refute this hypothesis. If a signal is observed by PET imaging, this could be targeted in a mechanistic RCTs of drugs used in clinical practice for preventative strategies. Medications used for protection of CV toxicity from anticancer treatment, including β-blockers, angiotensin receptor blockers and statins, also have an effect on arteries. These drugs could offer protection for both arterial and myocardial toxicity from anticancer treatment.

Other tracers may soon be available that offer valuable information into the inflammatory process of ICI and arterial toxicity. Exploratory tracers have been used in mouse models treated with PD-1 inhibitors showing accelerated atherosclerosis using [^{64}Cu]-DOTA-extracellular loop 1 inverso, which is a cysteine-cysteine motif chemokine receptor 2+ radiotracer; a receptor recognised on pro-inflammatory macrophages[270]. The scope of inflammatory PET radiotracers is vast, including CD80 radiotracers for shear-stress associated atherosclerosis[271], radio labelled CD80/86-targeting fusion protein belatacept (Indium^{111}-DOTA-belatacept)[272] Zirconium-89 labelled antibody for CD40, a co-stimulatory molecule present plaque and associated with plaque vulnerability[266], Somatostatin receptor subtype 2 (SSR-2) is expressed on activated macrophages and has been labelled with 68Ga-DOTATATE (DOTA-octreotide)[265]. The majority of these radiotracers have not been used in humans. There is concern regarding fitness for clinical application due to long half-life, non-specific uptake and concerns with immunogenicity of some of these proteins[272]. One particular radiotracer that may be relevant to ICI arterial injury is radiolabelled anti-VCAM-1 nanobody which has been used in mouse models with expression of VCAM-1 in atherosclerotic plaques[273,274]. My biomarker data may suggest that ICI may be associated with direct arterial activation and these adhesion molecule radiotracers may in the future be able to further investigate this hypothesis.

The data generated from biomarker analysis are hypothesis generating and further research in a larger number of patients with serial measurements is required. With greater patient numbers, it may be easier to extrapolate how changes in biomarkers may relate to CV toxicity of these drug regimens. Biomarker data could be corroborated with baseline CV and oncological characteristic, oncological treatment regimens as well as CV events and oncological response. Deeper immunophenotyping and proteomics analysis may give new insights into CV toxicity and risk stratification.

7.4.3 Therapeutic targets

The identification of potential therapeutic targets is one of the key aims of mechanistic research. An aim of the BioCAPRI study was to assess an inflammatory signal in ICI-associated arterial injury. Had an inflammatory signal been found, anti-inflammatory drugs could be candidates for RCTs for therapeutic and preventative strategies. Anti-inflammatory drugs have been effective in reducing CV events in atherosclerotic disease in non-cancer populations[204,206]. Statins are widely used in atherosclerotic disease. If ICIs are found to have an association with atherothrombotic events, statins may be helpful. Statins have anti-inflammatory properties and some evidence suggests they may reduce arterial inflammation, measured by [^{18}F]FDG, in patients with cancer and without[47,142,156]. Despite the lack of an inflammatory signal seen in BioCAPRI study, statins may still offer benefit in prevention in atherothrombotic events with their reduction in LDL-cholesterol and slowing of rate of atherosclerosis. Statin therapy is relevant not only in the context of ICI and VEGFI therapy but also for patients treated with anthracyclines. Statins may reduce anthracycline-associated cardiotoxicity, although the data within the literature is conflicting[216,275,276]. If indeed, the arterial toxic effects of anthracyclines occur via a similar mechanism as cardiotoxicity, statins may reduce the risk of arterial toxicity. If changes of the fibrotic marker, FAPI, are observed in either the myocardium or arteries after anthracycline, statins could be trialled to assess the attenuation of anthracycline associated fibrosis.

My biomarker data may offer some insight into potential therapeutic targets, however, prospective large scale assessment of serial biomarkers are required first. TNFα inhibitors, such as infliximab, are sometimes used in the treatment

of ICI induced irAEs[277]. This could be assessed in arterial toxicity and prevention of CV ischaemic events. TNFα inhibitors are also appealing as they may also have an anticancer effect and are being trialled in melanoma in conjunction with ICI in a phase I study[278]. A therapy that could both reduce CVAEs and increase anticancer efficacy would be the ideal therapeutic target for cardio-oncology. TNFα inhibitors application may be limited however as they are contra-indicated in patients with HF[1].

7.4.4 Prospective randomised controlled trials

I believe a prospective RCT comparing conventional lipid-lowering therapies for atherosclerotic disease against placebo in patients receiving ICI is deliverable and achievable. With both anti-inflammatory properties, and offering protection from atherosclerotic disease, I believe lipid-lowering therapies should be trialled for reducing arterial injury from anticancer treatments. Using statins would be the most obvious choice of lipid lowering therapy; although many patients may already be on a statin prior to enrolment. This may impact enrolment and preclude those most at risk of ischaemic events from enrolling. As such, other therapies such as propotein convertase subtilisin/kexin type 9 (PSCK9) inhibitors may be of more value.

Prior to undertaking this study, I would first perform a prospective observational PET imaging study assessing [^{18}F]NaF uptake in the arteries of patients receiving ICI at 4 weeks, 24 weeks and 52 weeks from baseline. Serial imaging over one year would be of importance to ensure no accelerated atherosclerotic process, measured by PET, was missed. I would use a cancer free population (or a similar cancer cohort not receiving anticancer therapy) as a control. This control group would be matched by sex, age and CV risk factors. If this study demonstrated increased [^{18}F]NaF arterial uptake from baseline after ICI, compared to controls, suggesting an active atherosclerotic process, this would give further mechanistic support for performing a subsequent RCT. The primary objective of the RCT would be to assess the effect of lipid lowering therapies on [^{18}F]NaF arterial uptake vs placebo, in patients receiving ICI and in a control group. I believe having two groups (ICI and control) being randomised to treatment and placebo would offer the most robust data. It would allow assessment of atherosclerosis in ICI vs control, in the placebo group. It would also be able to show if any change

seen in the treatment arm was specific to ICIs or whether a reduction in [^{18}F]NaF was seen with PSCK9 inhibition. During this RCT, CVAE (defined by IC-OS definitions), and CV endpoints (defined by Hick's criteria) could be collected. BP monitoring, ECG, echocardiography and assessment of endothelial dysfunction, such as endoPAT, could be performed. Recruited patients could be then be enrolled into a registry for prospective longitudinal monitoring for CV events and oncological progress. Though ambitious, I believe this proposed study could provide the most robust assessment of atherothrombosis in association with ICIs and evidence for therapeutic strategies.

7.5 Conclusions

In this thesis I have shown that current trial data are not sufficient to draw adequate conclusions on CV safety of ICI+VEGFI regimens. This may limit our appreciation of CV risk in ICI with VEGFI. Arterial toxicity occurs in association with anthracycline exposure, as seen in a large animal model, but this does not appear to occur through large artery inflammation when assessed using [^{18}F]FDG-PETCT in patients with lymphoma. I have provided robust evidence supporting the development and implementation of a protocol for prospective atherosclerosis assessment. Digital PETCT offers improved spatial resolution and sensitivity meaning that fewer reconstruction parameters are required for optimal arterial inflammation imaging using [^{18}F]FDG-PETCT. Imaging acquisition and analysis of PETCT can result in substantial changes in PETCT data. I have demonstrated that methods, such as MCR, CoV and error, provide valuable information to quantifiably assess PETCT protocols. Using and publishing these methods in PET research may aid transparency and standardisation within the field. In the first prospective assessment of ICI associated large artery inflammation by [^{18}F]FDG-PETCT using robust and comprehensive methods, ICI were not associated with increased large artery inflammation at 24 weeks compared to baseline. Treatment with combination ICI+VEGFI was not associated with greater large artery inflammation at 24 weeks from baseline in comparison to ICI monotherapy or VEGFI monotherapy. The results of my thesis could be used as a benchmark and means of assessment of future research within cardio-oncology and PET research. The results of the BioCAPRI study have added clarity in an area of research with conflicting results. This work is important to aid our ability to perform risk stratification and to give informed consent to our

patients. The study has set strong foundations to continue research in arterial toxicity associated with anticancer therapy. This research could help risk stratify and develop therapeutics in prevention and management of arterial toxicity of anticancer therapy.

Chapter 8 Appendices

8.1 Appendix I. Outcomes of interest using PICO framework and data points of interest

Population	Inclusion criteria: - adult population with cancer, - all solid organ tumour sites (including lymphoma). Exclusion criteria: - animal studies.
Intervention	Inclusion criteria: - trials that included the use of a VEGF-inhibitors (VEGFI), and/or in combination with immune checkpoint inhibitors (ICIs) class of drugs for the treatment of cancer, - VEGFI with or without ICI used as either control arm or intervention arm of study, - phase II, III and IV trials, - randomised studies, - published in English language, - completed enrolment, The specific intervention exclusion criteria are listed below: - single dosing, - sequential therapy rather than concurrent therapy, - population of treatment group of <20 patients, -non-randomised trials - meta-analysis, - review articles or commentaries, - subsequent therapy analysis, - cost-effective analysis, - published abstracts, - patient reported outcomes, - subgroup analysis, - duplications, - retrospective analysis. Trials that have incomplete protocol and text will be included in the results as part of our objective is to identify the representation of patients with kidney disease in trial data.
Comparison	Not applicable
Outcome	We will collect the following data points from the extracted articles regarding the exclusion and representation of patients with cardiovascular disease: 1. Were patients excluded with cardiovascular disease? 2. Were patients excluded with the following diagnosis: - Hypertension - Coronary artery disease (CAD) - Heart failure - Cardiomyopathy - Arrhythmia

	- Valvular disease - Thromboembolic disease - Cerebrovascular disease - Abnormal ECG - Myocarditis - Pericarditis - Vasculitis 3. Are the diagnosis of cardiovascular disease of trial population available in baseline characteristics or supplementary materials? 4. Are cardiovascular adverse events reported in the published clinical trial or supplement? We will also collect the following information about the trial characteristics to analysis if this had an influence on the trial design or patient enrolment: 1. Is the trial ID number identifiable? 2. Is the trial name identifiable? 3. What is the trial design? 4. Was this a randomised control design? 5. Was this intervention or control? 6. Was there an active comparator? 7. Trial year published 8. Trial population size 9. Funding source 10. Cancer diagnosis 11. Is trial protocol available? 12. How were adverse events defined and were they adjudicated? 13. Is there a clear safety follow up period specified in the protocol? 14. Is data collected on adverse events of special interest? 15. Are adverse events of special interest defined in the protocol?

8.2 Appendix II. Pre-PET scan checklist

PET-CT PRE SCAN CHECKLIST	WoS PET Centre

Name : _____

Address: _____

Date of Birth: _____ Contact phone no.:

Did you arrive by **Hospital Transport**?	Y	N
Have you had **Radiotherapy** in the past **8 weeks**?	Y	N
Have you had **Surgery** in the past **6 weeks**?	Y	N
Have you had a **Biopsy** in the past **2 weeks**?	Y	N
Have you had **Chemotherapy** in the past **2 weeks**?	Y	N
Have you had any **Scans** in the last **24 hours**?	Y	N
Do you have any current complaints e.g. **Injury, Infection, Recent Vaccination**? If yes give details_____	Y	N
Are you **Diabetic**?	Y	N
• If **Yes**, controlled by: Insulin ☐ Tablets ☐ Diet ☐		
• If **Yes** and **Insulin controlled**: Did you take your insulin and eat as normal?	Y	N
If yes, when? _____	Y	N
What was your last Blood Glucose reading if known _____		
• If **Yes** and **Tablet controlled**: Have you fasted for **4 hours**?	Y	N
Have you taken your tablets today?	Y	N
• If **No**: Have you had anything to eat or drink (except plain water) in the past **6 Hours**? If yes, what and when? _____	Y	N
If you were given **Special Fasting instructions**, did you bring your food diary?	Y	N
Have you done any **Strenuous exercise** in the past **24 hours**?	Y	N
Have you eaten any **Chewing gum** in the past **24 hours**?	Y	N
Do you have any issues with **Continence**?	Y	N
Do you currently stay in a **Nursing / Care home**?	Y	N
Do you consider yourself to have a **carer**?	Y	N
We may wish to use your anonymised data from this test for teaching or research purposes. Do you consent to this?	Y	N

The above information was completed by:

Patient's signature: _____ DATE:_

Checked by signature: _____ DATE:

8.3 Appendix III. Local validation of FusionQuant

Aims

To compare the non-commercial FusionQuant software with the commercial ISBI-approved Hermes software for assessment of [^{18}F]FDG.

Methods

Phantom analysis

Uniform phantoms containing ^{18}F were acquired on two PET scanners, one digital (Siemens Biograph Vision 600) and one non-digital (GE 710 Discovery) following calibration of each of the PET scanners. A 10cm diameter sphere volume of interest was analysed on the phantom using both Hermes and FusionQuant software. Both SUV measurements and Bq measurements were then compared using the coefficient of variation (CoV). The formula for CoV is presented below.

Equation 3. Coefficient of Variation

$$Coefficient\ of\ Variation\ (CoV)(\%) = \frac{Standard\ Deviation}{SUV_{mean}} \times 100$$

PET analysis of clinical scans

In addition to phantom analysis, a measurement of uptake in the liver was used to assess the two software. A 3 cm diameter spherical VOI was placed in the right upper lobe of the liver in ten patients from the cohort of chapter 4, as recommended in EANM guidelines[279]. Assuming that organ boundaries and any pathological features are avoided, the SUV_{mean} should lie within the range of 1.3 and 3.0[280,281]. Analysis was performed by assessing the percentage difference in FDG uptake, Equation 4.

Equation 4 Percentage difference in SUV measurements in two software systems

$$Difference\ in\ System's\ SUV\ measurment\ (\%)$$

$$= \frac{Fusion\ Quant\ SUV - Hermes\ SUV}{Hermes\ SUV} \times 100$$

Results

Phantom analysis

In local validation analysis, I found that FusionQuant performed well and was comparable to Hermes. The results are summarised in Table S8-1 and Table 8-2

Table S8-1 SUV measurements of phantom data comparing Hermes and FusionQuant software

Scanner	Hermes SUVmean			FusionQuant SUVmean			SUV_{mean} difference
	SUV_{mean}	Std. Dev.	CoV	SUV_{mean}	Std. Dev.	CoV	
GE 710	1.07	0.14	13.084	1.07	0.12	11.2	0
Siemens Vision (GE phantom)	0.99	0.10	10.1	0.99	0.09	9.09	0

Table 8-2 Bq measurements of phantom data comparing Hermes and FusionQuant software

Scanner	Hermes Bq mean			FusionQuant Bq mean			Bq mean difference
	Bq mean	Std. Dev.	CoV	Bq mean	Std. Dev.	CoV	
GE 710	3065	406.99	13.27	3063.91	350.55	11.44	-0.036%
Siemens Vision	3946.35	405.23	10.27	3941.55	353.2	8.96	-0.12%

PET analysis

The measured uptake within the liver of the ten patients, using two scanners, with FusionQuant was comparable to Hermes with very little difference between the two software systems, Table S8-3.

Table S8-3 Assessment of 18F-FDG uptake within the liver of ten patients with lymphoma using FusionQuant & Hermes software

710							
Patient (PET number)	**Hermes SUVmean**			**FusionQuant SUVmean**			**SUV_{mean} difference**
	SUV_{mean}	**Std. Dev.**	**CoV**	**SUV_{mean}**	**Std. Dev.**	**CoV**	**(FQ-H)/H**
85 Y	1.97	0.19	9.64	1.99	0.19	9.55	1.02
90 Y	2.38	0.23	9.66	2.44	0.20	8.20	2.52
34 Y	2.45	0.21	8.57	2.45	0.18	7.35	0.00
4 Y	1.73	0.16	9.25	1.72	0.14	8.14	-0.58
45 Z	2.3	0.26	11.30	2.31	0.22	9.52	0.43
						average	**0.68**
Vision							
Patient (PET number)	**Hermes SUVmean**			**FusionQuant SUVmean**			**SUV_{mean} difference**
	SUV_{mean}	**Std. Dev.**	**CoV**	**SUV_{mean}**	**Std. Dev.**	**CoV**	**(FQ-H)/H**
60 Z	2.6	0.39	15.00	2.67	0.39	14.61	2.69
41 Y	2.31	0.23	9.96	2.31	0.21	9.09	0.00
56 Y	2.01	0.2	9.95	2.07	0.17	8.21	2.99
25 Z	3.06	0.28	9.15	3.02	0.27	8.94	-1.31
81 Z	1.88	0.16	8.51	1.88	0.14	7.45	0.00
						average	**0.87**

Conclusion

FusionQuant is a suitable software system for PET analysis and matches performance of ISBI-approved software, Hermes.

8.4 Appendix IV. BioCAPRI Consent Form

BHF Glasgow Cardiovascular Research Centre
126 University Place
Glasgow
G12 8TA

Enquiries to: Dr Stephen Rankin
Telephone: 0141 301 7000
E-mail Stephen.rankin3@nhs.scot

PATIENT CONSENT FORM

STUDY TITLE: Characterisation of inflammatory atheroma due to Immunotherapy and VEGF inhibitors

Dr Ninian Lang, Prof Mark Petrie and Dr Stephen Rankin

Patient ID:_____ ***Please initial***

I confirm that I have read and understand the information sheet dated 09/01/024 (version 1.3) for the above study. I have had the opportunity to consider the information, ask questions and I am satisfied these have been answered. ☐

I understand that my participation is voluntary and that I am free to withdraw at any time without giving any reason, without my medical care or legal rights being affected. ☐

I agree that if I withdraw from the study for any reason, data and samples obtained up to that point will be retained by NHS Greater Glasgow and Clyde and the University of Glasgow and included in the study. ☐

I agree to undergo blood and urine tests, an electrocardiogram, echocardiogram, 18F-FDG PET/CT and EndoPAT tests as described in the Patient Information Sheet. ☐

I agree to a small volume of anonymised blood being sent to laboratories outside of the University of Glasgow, including laboratories abroad, for analysis. ☐

I agree to have my blood and urine samples stored and used in future ethically approved studies. ☐

I agree to allow a small volume of my anonymised stored blood samples and anonymous data to be shared with Roche Diagnostics, Germany, for research purposes. ☐

I understand that sections of my medical notes may be looked at by the research team and by representatives of the Sponsor, NHS Greater Glasgow and Clyde, where it is relevant to my taking part in the research. I give permission for these people to have access to my records. ☐

I agree to my electronic records and images being reviewed for up to 10 years for long-term follow up in order to collect data on my clinical progress and possible future events. ☐

I agree to my GP being informed of my participation in the study and of any clinically relevant findings that arise. ☐

I agree to take part in the above study. ☐

---	---	---
Name of Participant	Signature	Date
---	---	---
Name of Researcher	Signature	Date

8.5 Appendix V – GP information Letter

BHF Glasgow Cardiovascular Research Centre
126 University Place
Glasgow
G12 8TA

Enquiries to: Dr Stephen Rankin
Telephone: 0141 301 7000
E-mail: Stephen.rankin3@nhs.scot
Date:

GP INFORMATION LETTER
STUDY TITLE: Characterisation of inflammatory atheroma due to Immunotherapy and VEGF inhibitors
Dr Ninian Lang, Prof Mark Petrie and Dr Stephen Rankin

Dear Doctor,
I am conducting a research project involving patients with cancer before and during treatment with immune checkpoint inhibitors (ICIs) and vascular endothelial growth factor inhibitors (VEGFIs). Examples of immune checkpoint inhibitor drugs include nivolumab, pembrolizumab, atezolizumab, ipilimumab and others. Examples of VEGF inhibitor drugs include axitinib, lenvatinib, sunitinib, sorafenib and others.
Your patient has been recruited via the oncology clinic at the Beatson West of Scotland Oncology Centre and has kindly agreed to take part in the study.

Patient name: **CHI number:**

The aim of the study is to improve understanding of the vascular and myocardial effects of immune checkpoint inhibitors and VEGF inhibitors. We wish to understand how, and how often, these drugs cause vascular toxicity and impaired cardiac function. In doing so we hope to identify markers that are associated with an increased risk for cardiovascular toxicity.

Your patient will undergo a series of non-invasive vascular assessments and imaging procedures including echocardiography. All patients will also undergo a PET/CT scan. These assessments are described in the patient information leaflet enclosed.
Your patient will be involved for 6 months. Patients will be invited to attend for research visits intended to coincide with routine clinical appointments on two occasions. The study does not involve taking any additional medications. We will notify the patient's Consultant Oncologist should any clinically significant information from their participation in this study, who may arrange further investigation, treatment and will inform you if appropriate.
If you have any questions or require any further information, please do not hesitate to contact me on the above telephone number or e-mail address.
Yours sincerely,

Dr Stephen Rankin
Clinical Research Fellow
University of Glasgow

8.6 Appendix VI – BioCAPRI echocardiography protocol

View	Modality	Doppler	2D/M-mode	Post-processing measurements	Notes
Baseline measurement				-Height -Weight -blood pressure -heart rate/rhythm -BSA	
Parasternal					
Long axis	2D (plain) LVOT zoom	Colour on AV + MV	-IVSd -LVIDd -LVIDd (indexed) -LVPWd -LVIDs -LVIDs (index) LVOTd		*LVIDd/s taken for clinical report but not collected at time of echo*
PLAX: RV inflow	cine (plain)	TV CW Colour on TV			
Short axis	AV/TV/PV cine (plain) MV: cine (plain) LV papillary level: cine (plain) LV apex: cine (plain)	Colour on AV PW Doppler RVOT Doppler colour CW PV			*Sweep speed 100mm/s*
Apical Views					
4AC (atria)	2D (plain) for atria assessment		-LA area -RA area	-LA volume -LA volume (indexed) -LA r strain	*Image optimised to demonstrate maximal LA length and volume at end-systole.*
A4C	cine (plain) Zoom LV	colour on MV Doppler PW MV inflow Doppler CW MV TDI lateral mitral annulus TDI septal mitral annulus	E wave velocity A wave velocity E/A ratio E deceleration time MV lateral e' -MV septal e' -Average E/e'	A4C LVEF Simpson's Biplane -LVEDV (indexed) -LVESV (indexed) -LVSV (indexed) -Cardiac output -Stroke volume (VTI) -segmental strain -GLS -valve assessment -WMA assessment	*-LVEDV (indexed)* *-LVESV (indexed)* *-LVSV (indexed) taken at time for clinical report but not collected for analysis at time of echo*

A4C RV view	cine (plain)	Colour on TV Doppler CW TV TDI lateral	M Mode-TAPSE RVEDD (basal RVEDD2 (mid) RVEDD3 (apical)	TR Vmax /TR maxPG/Estimated RVSP TAPSE rS' RV-FWLS RV strain	*>40 fps for RV strain, lowest cut off is 37fps*
A5C	Cine (plain)	Colour on AV Doppler PW LVOT Doppler CW AV		LVOT VTI AVA VTI AVA (VTI) AV PeakPG AV meanPG DI	
A2C	cine (plain) – including LA	Colour on MV Zoom LV		A2C LVEF Simpson's Biplane Segmental strain GLS	*Collect two sets of A4C, A2C and A3C for Biplane assessment*
A3C	cine (plain) LV zoom			GLS	
Subcostal					
Subcostal	cine (plain) colour on IAS M-Mode IVC with respiration			IVC diameter (inspiration/expiration)	
Strain					
GLS	Take cine of A4C, A2C and A3C sequentially (two sets)			18 segment segmental strain GLS Myocardial work	*If more than 2 segments in any one view are not adequately tracked then GLS should be avoided. quarter of LA in view. FPS 40-90 with stable heart rate (<30% variation between cine*
4D					
	4D LV volumes on multi slice (8 or 12 slice)			LV volumes and EF	

In AF, an average of measurements will be taken from 5-10 beats.

Number of cardiac cycles in a loop = 2 if sinus rhythm, 3 if AF

8.7 Appendix VII. Supplementary analyses of Chapter 5

Figure 8-1. (supplementary) Comparison of RCmax in torso phantom with varying iterative reconstructions on the digital scanner (Siemens Vision)

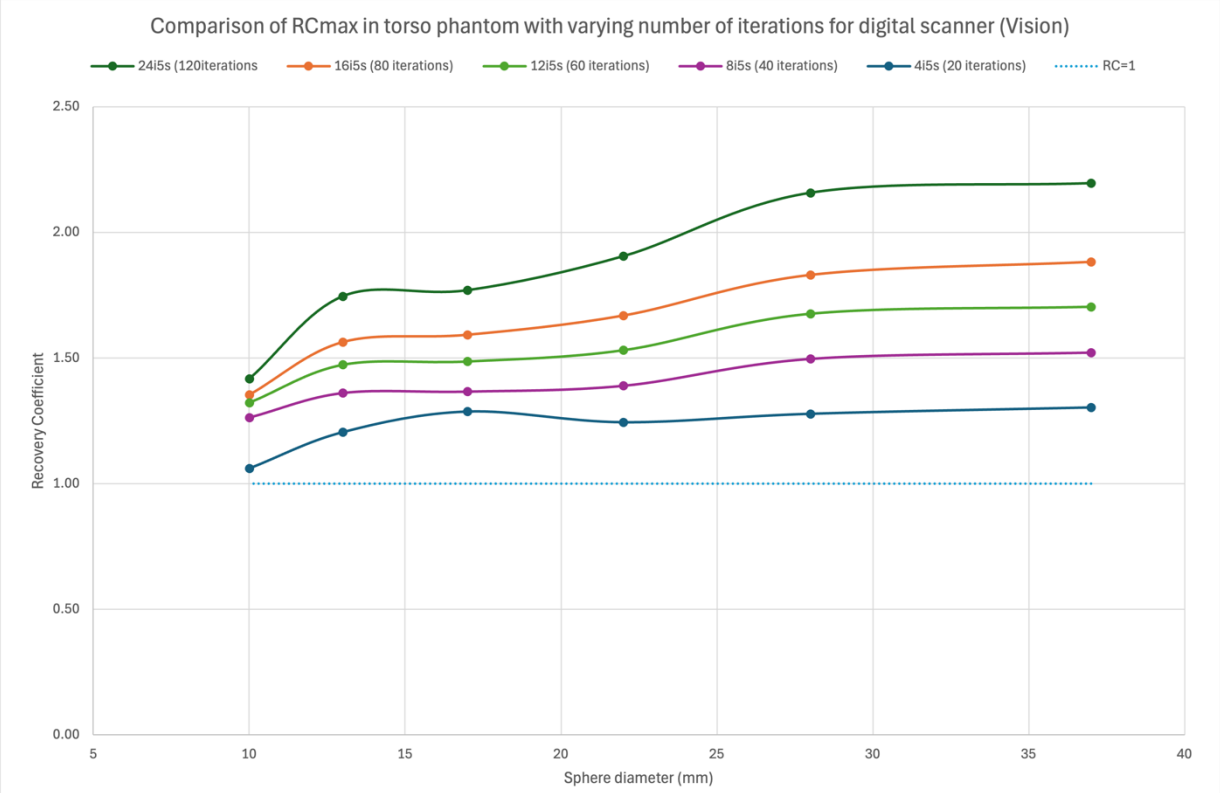

Table 8-4 (supplementary) Quantitative measurements for RCmax and RCmean using torso phantom

		RCmax (torso)		RCmax (neck)	
Reconstruction	**Filter**	**MCR**	**Absolute error**	**MCR**	**Absolute error**
4i 5s	2mm	1.17	0.47	0.80	0.90
4i 5s	All Pass	1.23	0.61	0.86	0.88
24i 5s	1mm	1.86	2.23	1.31	1.08
24i 5s	2mm	1.54	1.40	1.09	0.73
24i 5s	4mm	1.10	0.37	0.74	0.80
24i 5s	6mm	0.95	0.37	0.56	1.10
24i 5s	All Pass	1.87	2.23	1.31	1.08
		RCmax (torso)		**RCmax (neck)**	
Reconstruction	**Filter**	**MCR**	**Absolute error**	**MCR**	**Absolute error**
4i 5s	2mm	0.74	0.69	0.51	1.15
4i 5s	All Pass	0.76	0.66	0.52	1.14
24i 5s	1mm	0.80	0.53	0.65	0.84
24i 5s	2mm	0.78	0.58	0.61	0.92
24i 5s	4mm	0.73	0.71	0.51	1.13
24i 5s	6mm	0.67	0.86	0.43	1.31
24i 5s	All Pass	0.80	0.53	0.61	0.93

Figure S8-2 (supplementary) Comparison of TBR by EANM vs Local reconstruction

A: Descending TBRmean B: Descending TBRmax C: Carotid TBRmean D: Carotid TBRmax (LOA: limits of agreement). There is an upward trend in the difference of TBRmax between the two reconstructions.

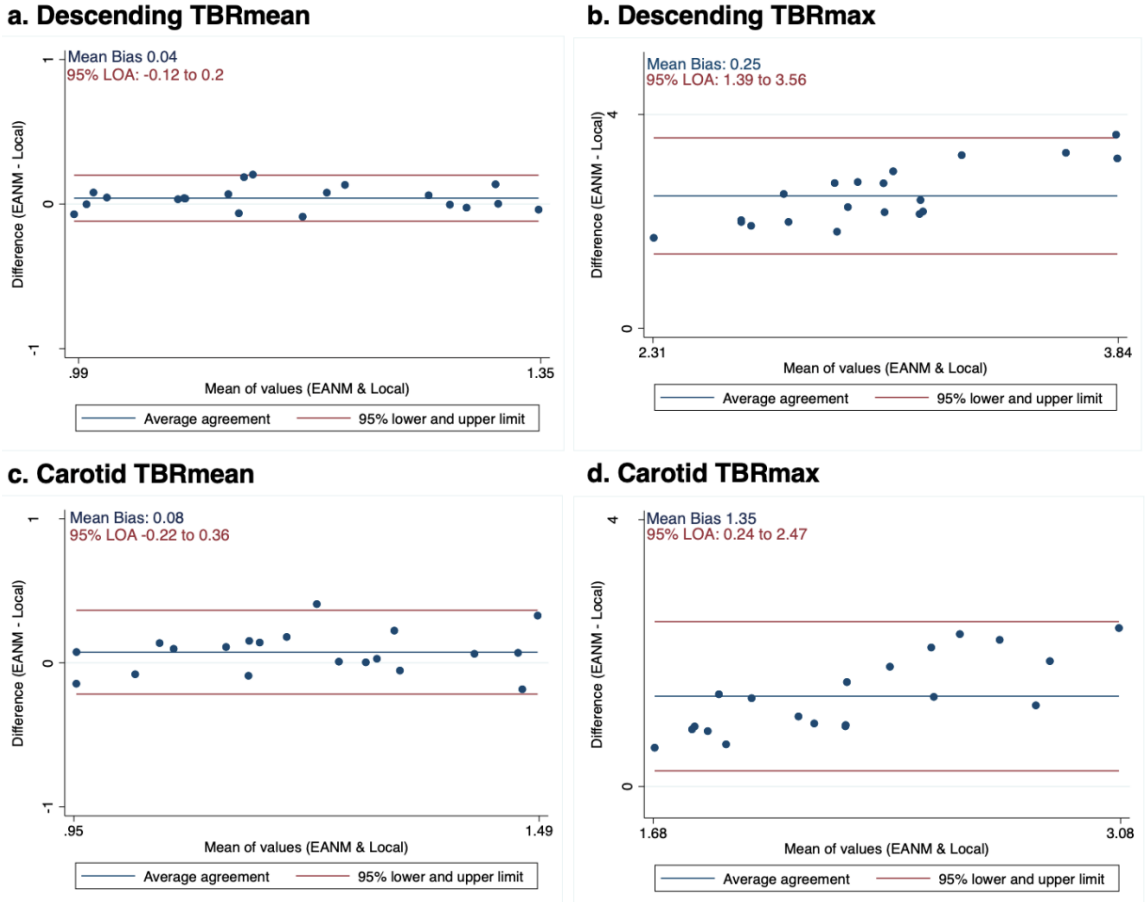

Table S8-5 (supplementary) Blood pool SUVmean values using Glasgow & EANM reconstruction.

	Mean		Min		Max	
	EANM	Local	EANM	Local	EANM	Local
SVC	1.76 ± 0.44	1.73 ± 0.37	0.96	0.90	3.3	2.9
IN	1.70 ± 0.42	1.58 ± 0.57	0.92	0.86	3.1	2.88
IJ	1.47 ± 0.44	1.36 ± 0.36	0.92	0.80	3.06	2.68
IVC	1.76 ± 0.45	1.66 ± 0.37	0.99	0.92	3.32	2.84

Table S8-6 (supplementary) Intra- & inter-observer variability on repeated testing of blood pool collection.
ICC: intraclass correlation coefficient. CI: confidence interval. LOA: limits of agreement.

Vessel	Test	ICC	95% CI Lower LOA	95% CI Upper LOA
SVC	intra-observer	0.97	0.93	0.98
	inter-observer	0.95	0.75	0.98
IN	intra-observer	0.97	0.95	0.98
	inter-observer	0.97	0.94	0.98
IJ	intra-observer	0.92	0.81	0.96
	inter-observer	0.90	0.81	0.94
IVC	intra-observer	0.96	0.92	0.98
	inter-observer	0.92	0.71	0.97

Table 8-7 (supplementary) TBR values of large artery (descending aorta) and small artery (carotid) when calculated by different blood pool regions

Carotid artery				
	Region	Mean	Min	Max
TBRmax	SVC	1.58±0.24	1.18	2.12
	IN	1.69±0.26	1.30	2.37
	IJ	1.99±0.37	1.55	2.80
TBRmean	SVC	1.15±0.17	0.89	1.51
	IN	1.23±0.18	0.98	1.69
	IJ	1.46±0.26	1.12	2.02
Mean TBR max of active segments	SVC	1.80±0.12	1.63	2.12
	IN	1.86±0.16	1.69	2.37
	IJ	2.06±0.33	1.69	2.80
Most diseased segment	SVC	1.83±0.34	1.27	2.51
	IN	1.96±0.37	1.41	2.80
	IJ	2.32±0.51	1.59	3.63
Descending aorta				
	Region	Mean	Min	Max
TBRmax	SVC	1.80±0.21	1.47	2.16
	IVC	1.87±0.31	1.27	2.51
TBRmean	SVC	1.14±0.11	0.98	1.33
	IVC	1.18±0.17	0.84	1.56
Mean TBR max of active segments	SVC	1.86±0.16	1.63	2.18
	IVC	1.93±0.25	1.62	2.51
Most diseased segment	SVC	1.98±0.24	1.60	2.35
	IVC	2.06±0.38	1.35	2.85

Figure 8-3 (supplementary) Carotid TBR by SVC compared to TBR by IN & IJ using A: TBRmax B: TBRmean, C: TBRmax of 'active segments', D: Most diseased segment
these figures show that overall the trend arterial analysis is similar across the blood pools. TBRmax calculated by SVC activity is on the x axis and the y axis has the same artery being assess by TBRmax using IN (in red) and using IJ (in blue). This demonstrates that IN is closely correlated with SVC, whereas IJ has much wider spread compared to SVC. Red: TBR calculated by innominate vein as denominator, blue: TBR calculated by IJ as denominator

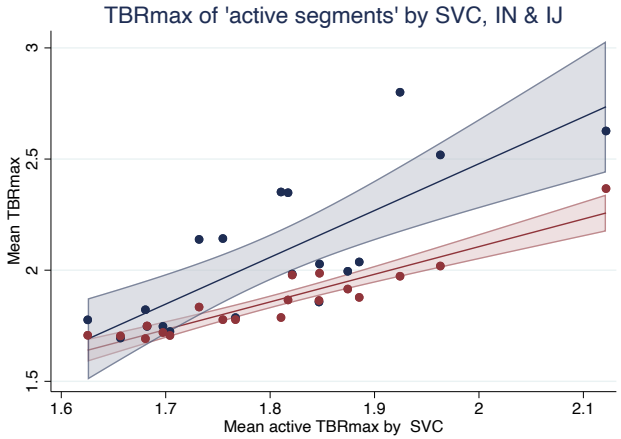

a

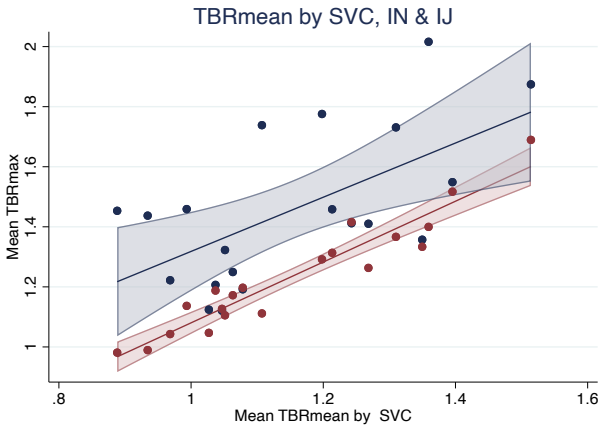

b

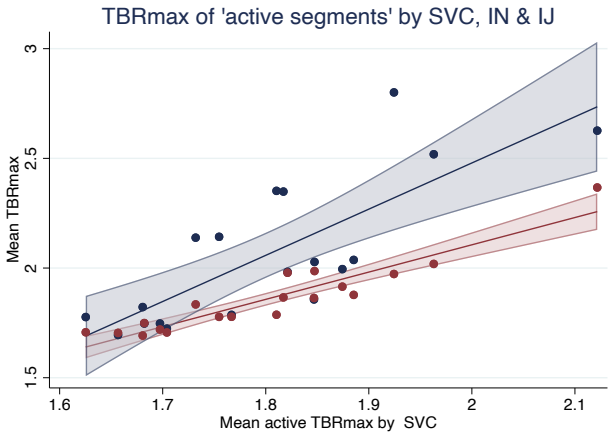
TBRmax of 'active segments' by SVC, IN & IJ
Mean TBRmax
1.5
2
2.5
3
1.6
1.7
1.8
1.9
2
2.1
Mean active TBRmax by SVC

c

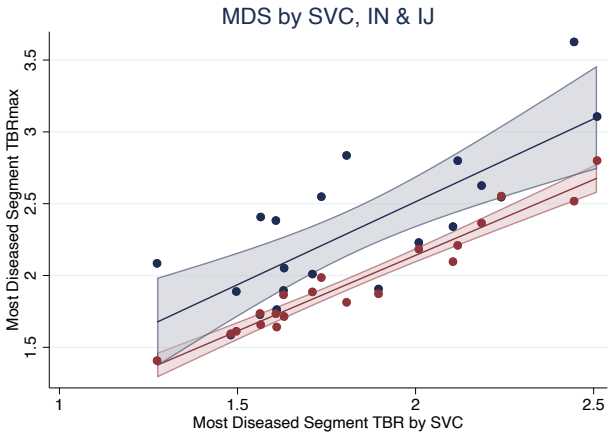
MDS by SVC, IN & IJ
Most Diseased Segment TBRmax
1.5
2
2.5
3
3.5
1
1.5
2
2.5
Most Diseased Segment TBR by SVC

d

Chapter 9 References

1. Lyon AR, López-Fernández T, Couch LS, Asteggiano R, Aznar MC, Bergler-Klein J, et al. 2022 ESC Guidelines on cardio-oncology developed in collaboration with the European Hematology Association (EHA), the European Society for Therapeutic Radiology and Oncology (ESTRO) and the International Cardio-Oncology Society (IC-OS): Developed by the task force on cardio-oncology of the European Society of Cardiology (ESC). European Heart Journal [Internet]. 2022 Nov 1 [cited 2025 Feb 11];43(41):4229–361. Available from: https://doi.org/10.1093/eurheartj/ehac244

2. Quaresma M, Coleman MP, Rachet B. 40-year trends in an index of survival for all cancers combined and survival adjusted for age and sex for each cancer in England and Wales, 1971–2011: a population-based study. The Lancet. 2015 Mar;385(9974):1206–18.

3. de Boer RA, Hulot JS, Tocchetti CG, Aboumsallem JP, Ameri P, Anker SD, et al. Common mechanistic pathways in cancer and heart failure. A scientific roadmap on behalf of the Translational Research Committee of the Heart Failure Association (HFA) of the European Society of Cardiology (ESC). European Journal of Heart Failure [Internet]. 2020 [cited 2025 Feb 26];22(12):2272–89. Available from: https://onlinelibrary.wiley.com/doi/abs/10.1002/ejhf.2029

4. Florido R, Daya NR, Ndumele CE, Koton S, Russell SD, Prizment A, et al. Cardiovascular Disease Risk Among Cancer Survivors. Journal of the American College of Cardiology. 2022 July;80(1):22–32.

5. Battisti NML, Welch CA, Sweeting M, de Belder M, Deanfield J, Weston C, et al. Prevalence of Cardiovascular Disease in Patients With Potentially Curable Malignancies. JACC: CardioOncology. 2022 June;4(2):238–53.

6. Miller KD, Nogueira L, Mariotto AB, Rowland JH, Yabroff KR, Alfano CM, et al. Cancer treatment and survivorship statistics, 2019. CA: A Cancer Journal for Clinicians. 2019 Sept 11;69(5):363–85.

7. Armenian SH, Xu L, Ky B, Sun C, Farol LT, Pal SK, et al. Cardiovascular Disease Among Survivors of Adult-Onset Cancer: A Community-Based Retrospective Cohort Study. Journal of Clinical Oncology. 2016 Apr 1;34(10):1122–30.

8. de Wit S, Glen C, de Boer RA, Lang NN. Mechanisms shared between cancer, heart failure, and targeted anti-cancer therapies. Cardiovascular Research. 2022 Aug 25;

9. Zaorsky NG, Churilla TM, Egleston BL, Fisher SG, Ridge JA, Horwitz EM, et al. Causes of death among cancer patients. Annals of Oncology. 2017 Feb;28(2):400–7.

10. Paterson DI, Wiebe N, Cheung WY, Mackey JR, Pituskin E, Reiman A, et al. Incident Cardiovascular Disease Among Adults With Cancer. JACC: CardioOncology. 2022 Mar;4(1):85–94.

11. Abdel-Qadir H, Austin PC, Lee DS, Amir E, Tu JV, Thavendiranathan P, et al. A Population-Based Study of Cardiovascular Mortality Following Early-Stage Breast Cancer. JAMA Cardiology. 2017 Jan 1;2(1):88.

12. Navi BB, Reiner AS, Kamel H, Iadecola C, Okin PM, Elkind MSV, et al. Risk of Arterial Thromboembolism in Patients With Cancer. Journal of the American College of Cardiology. 2017 Aug;70(8):926–38.

13. National Cancer Institute. Common Terminology Criteria for Adverse Events (CTCAE). [Internet]. Cancer Therapy Evaluation Program. 2023 [cited 2023 Mar 16]. Available from: https://ctep.cancer.gov/protocoldevelopment/electronic_applications/ctc.htm

14. Herrmann J, Lenihan D, Armenian S, Barac A, Blaes A, Cardinale D, et al. Defining cardiovascular toxicities of cancer therapies: an International Cardio-Oncology Society (IC-OS) consensus statement. European Heart Journal. 2022 Jan 31;43(4):280–99.

15. Tan TC, Neilan TG, Francis S, Plana JC, Scherrer-Crosbie M. Anthracycline-Induced Cardiomyopathy in Adults. In: Comprehensive Physiology. Wiley; 2015. p. 1517–40.

16. Ewer MS, Lippman SM. Type II Chemotherapy-Related Cardiac Dysfunction: Time to Recognize a New Entity. Journal of Clinical Oncology. 2005 May 1;23(13):2900–2.

17. Parr SK, Liang J, Schadler KL, Gilchrist SC, Steele CC, Ade CJ. Anticancer Therapy–Related Increases in Arterial Stiffness: A Systematic Review and Meta-Analysis. JAHA [Internet]. 2020 July 21 [cited 2024 Apr 25];9(14):e015598. Available from: https://www.ahajournals.org/doi/10.1161/JAHA.119.015598

18. Schneider C, González-Jaramillo N, Marcin T, Campbell KL, Suter T, Bano A, et al. Time-Dependent Effect of Anthracycline-Based Chemotherapy on Central Arterial Stiffness: A Systematic Review and Meta-Analysis. Front Cardiovasc Med [Internet]. 2022 July 5 [cited 2025 Apr 28];9. Available from: https://www.frontiersin.orghttps://www.frontiersin.org/journals/cardiovascular-medicine/articles/10.3389/fcvm.2022.873898/full

19. Prasad PK, Signorello LB, Friedman DL, Boice Jr. JD, Pukkala E. Long-term non-cancer mortality in pediatric and young adult cancer survivors in Finland. Pediatric Blood & Cancer [Internet]. 2012 [cited 2025 Apr 16];58(3):421–7. Available from: https://onlinelibrary.wiley.com/doi/abs/10.1002/pbc.23296

20. Oeffinger KC, Mertens AC, Sklar CA, Kawashima T, Hudson MM, Meadows AT, et al. Chronic Health Conditions in Adult Survivors of Childhood Cancer. New England Journal of Medicine [Internet]. 2006 Oct 12 [cited 2025 Apr 16];355(15):1572–82. Available from: https://www.nejm.org/doi/full/10.1056/NEJMsa060185

21. Vo JB, Ramin C, Veiga LHS, Brandt C, Curtis RE, Bodelon C, et al. Long-term cardiovascular disease risk after anthracycline and trastuzumab treatments in US breast cancer survivors. J Natl Cancer Inst [Internet]. 2024 May 8 [cited 2025 Apr 16];116(8):1384–94. Available from: https://www.ncbi.nlm.nih.gov/pmc/articles/PMC11308182/

22. Bhakta N, Liu Q, Yeo F, Baassiri M, Ehrhardt MJ, Srivastava DK, et al. Cumulative burden of cardiovascular morbidity in paediatric, adolescent, and young adult survivors of Hodgkin's lymphoma: an analysis from the St Jude Lifetime Cohort Study. The Lancet Oncology. 2016 Sept;17(9):1325–34.

23. Rugbjerg K, Mellemkjær L, Boice JD, Køber L, Ewertz M, Olsen JH. Cardiovascular Disease in Survivors of Adolescent and Young Adult Cancer: A Danish Cohort Study, 1943–2009. JNCI: Journal of the National Cancer Institute. 2014 June;106(6).

24. Swerdlow AJ, Higgins CD, Smith P, Cunningham D, Hancock BW, Horwich A, et al. Myocardial Infarction Mortality Risk After Treatment for Hodgkin Disease: A Collaborative British Cohort Study. JNCI: Journal of the National Cancer Institute. 2007 Feb 7;99(3):206–14.

25. Mulrooney DA, Yeazel MW, Kawashima T, Mertens AC, Mitby P, Stovall M, et al. Cardiac outcomes in a cohort of adult survivors of childhood and adolescent cancer: retrospective analysis of the Childhood Cancer Survivor Study cohort. BMJ. 2009 Dec 8;339:b4606.

26. De Bruin ML, Dorresteijn LDA, van't Veer MB, Krol ADG, van der Pal HJ, Kappelle AC, et al. Increased Risk of Stroke and Transient Ischemic Attack in 5-Year Survivors of Hodgkin Lymphoma. JNCI: Journal of the National Cancer Institute [Internet]. 2009 July 1 [cited 2025 Apr 16];101(13):928–37. Available from: https://doi.org/10.1093/jnci/djp147

27. Aleman BMP, van den Belt-Dusebout AW, De Bruin ML, van 't Veer MB, Baaijens MHA, Boer JP de, et al. Late cardiotoxicity after treatment for Hodgkin lymphoma. Blood [Internet]. 2006 Nov 21 [cited 2025 Apr 16];109(5):1878–86. Available from: https://doi.org/10.1182/blood-2006-07-034405

28. Narayan HK, French B, Khan AM, Plappert T, Hyman D, Bajulaiye A, et al. Noninvasive Measures of Ventricular-Arterial Coupling and Circumferential Strain Predict Cancer Therapeutics–Related Cardiac Dysfunction. JACC: Cardiovascular Imaging [Internet]. 2016 Oct [cited 2024 Mar 26];9(10):1131–41. Available from: https://linkinghub.elsevier.com/retrieve/pii/S1936878X16300353

29. van den Belt-Dusebout AW, Nuver J, de Wit R, Gietema JA, ten Bokkel Huinink WW, Rodrigus PTR, et al. Long-Term Risk of Cardiovascular Disease in 5-Year Survivors of Testicular Cancer. JCO [Internet]. 2006 Jan 20 [cited 2025 Apr 16];24(3):467–75. Available from: https://ascopubs.org/doi/10.1200/JCO.2005.02.7193

30. Meléndez GC, Vasu S, Lesnefsky EJ, Kaplan JR, Appt S, D'Agostino RB, et al. Myocardial Extracellular and Cardiomyocyte Volume Expand After

Doxorubicin Treatment Similar to Adjuvant Breast Cancer Therapy. JACC: Cardiovascular Imaging [Internet]. 2020 Apr [cited 2024 Mar 5];13(4):1084–5. Available from: https://linkinghub.elsevier.com/retrieve/pii/S1936878X19310204

31. Zeiss CJ, Gatti DM, Toro-Salazar O, Davis C, Lutz CM, Spinale F, et al. Doxorubicin-Induced Cardiotoxicity in Collaborative Cross (CC) Mice Recapitulates Individual Cardiotoxicity in Humans. G3 (Bethesda) [Internet]. 2019 July 1 [cited 2024 Mar 6];9(8):2637–46. Available from: https://www.ncbi.nlm.nih.gov/pmc/articles/PMC6686936/

32. Farhad H, Staziaki PV, Addison D, Coelho-Filho OR, Shah RV, Mitchell RN, et al. Characterization of the Changes in Cardiac Structure and Function in Mice Treated With Anthracyclines Using Serial Cardiac Magnetic Resonance Imaging. Circ: Cardiovascular Imaging [Internet]. 2016 Dec [cited 2024 May 7];9(12):e003584. Available from: https://www.ahajournals.org/doi/10.1161/CIRCIMAGING.115.003584

33. Galán-Arriola C, Lobo M, Vílchez-Tschischke JP, López GJ, De Molina-Iracheta A, Pérez-Martínez C, et al. Serial Magnetic Resonance Imaging to Identify Early Stages of Anthracycline-Induced Cardiotoxicity. Journal of the American College of Cardiology [Internet]. 2019 Feb [cited 2024 Apr 25];73(7):779–91. Available from: https://linkinghub.elsevier.com/retrieve/pii/S0735109718395366

34. Theofilis P, Sagris M, Oikonomou E, Antonopoulos AS, Siasos G, Tsioufis C, et al. Inflammatory Mechanisms Contributing to Endothelial Dysfunction. Biomedicines. 2021 July 6;9(7):781.

35. Castellon X, Bogdanova V. Chronic Inflammatory Diseases and Endothelial Dysfunction. Aging and disease. 2016;7(1):81.

36. Netea MG, Schlitzer A, Placek K, Joosten LAB, Schultze JL. Innate and Adaptive Immune Memory: an Evolutionary Continuum in the Host's Response to Pathogens. Cell Host & Microbe [Internet]. 2019 Jan 9 [cited 2025 Feb 27];25(1):13–26. Available from: https://www.sciencedirect.com/science/article/pii/S1931312818306334

37. Charles A Janeway J, Travers P, Walport M, Shlomchik MJ. Principles of innate and adaptive immunity. In: Immunobiology: The Immune System in Health and Disease 5th edition [Internet]. Garland Science; 2001 [cited 2025 Feb 27]. Available from: https://www.ncbi.nlm.nih.gov/books/NBK27090/

38. Pardoll DM. The blockade of immune checkpoints in cancer immunotherapy. Nat Rev Cancer [Internet]. 2012 Mar 22 [cited 2025 Feb 27];12(4):252–64. Available from: https://www.ncbi.nlm.nih.gov/pmc/articles/PMC4856023/

39. Chen DS, Mellman I. Oncology Meets Immunology: The Cancer-Immunity Cycle. Immunity [Internet]. 2013 July 25 [cited 2025 Feb 25];39(1):1–10. Available from: https://www.sciencedirect.com/science/article/pii/S1074761313002963

40. Michel L, Rassaf T, Totzeck M. Cardiotoxicity from immune checkpoint inhibitors. IJC Heart & Vasculature. 2019 Dec;25:100420.

41. Johnson DB, Nebhan CA, Moslehi JJ, Balko JM. Immune-checkpoint inhibitors: long-term implications of toxicity. Nature Reviews Clinical Oncology. 2022 Apr 26;19(4):254–67.

42. Varricchi G, Galdiero MR, Marone G, Criscuolo G, Triassi M, Bonaduce D, et al. Cardiotoxicity of immune checkpoint inhibitors. ESMO Open. 2017;2(4):e000247.

43. Topalian SL, Hodi FS, Brahmer JR, Gettinger SN, Smith DC, McDermott DF, et al. Five-Year Survival and Correlates Among Patients With Advanced Melanoma, Renal Cell Carcinoma, or Non–Small Cell Lung Cancer Treated With Nivolumab. JAMA Oncology. 2019 Oct 1;5(10):1411.

44. Wolchok JD, Chiarion-Sileni V, Rutkowski P, Cowey CL, Schadendorf D, Wagstaff J, et al. Final, 10-Year Outcomes with Nivolumab plus Ipilimumab in Advanced Melanoma. New England Journal of Medicine [Internet]. 2025 Jan 1 [cited 2025 Mar 3];392(1):11–22. Available from: https://www.nejm.org/doi/full/10.1056/NEJMoa2407417

45. Onoi K, Chihara Y, Uchino J, Shimamoto T, Morimoto Y, Iwasaku M, et al. Immune Checkpoint Inhibitors for Lung Cancer Treatment: A Review. J Clin Med [Internet]. 2020 May 6 [cited 2025 Apr 15];9(5):1362. Available from: https://www.ncbi.nlm.nih.gov/pmc/articles/PMC7290914/

46. Motzer RJ, Tannir NM, McDermott DF, Frontera OA, Melichar B, Choueiri TK, et al. Nivolumab plus Ipilimumab versus Sunitinib in Advanced Renal-Cell Carcinoma. New England Journal of Medicine [Internet]. 2018 Apr 5 [cited 2025 Mar 5];378(14):1277–90. Available from: https://www.nejm.org/doi/full/10.1056/NEJMoa1712126

47. Drobni ZD, Alvi RM, Taron J, Zafar A, Murphy SP, Rambarat PK, et al. Association Between Immune Checkpoint Inhibitors With Cardiovascular Events and Atherosclerotic Plaque. Circulation. 2020 Dec 15;142(24):2299–311.

48. Haslam A, Prasad V. Estimation of the Percentage of US Patients With Cancer Who Are Eligible for and Respond to Checkpoint Inhibitor Immunotherapy Drugs. JAMA Network Open. 2019 May 3;2(5):e192535.

49. Joint Formulary Committee. British National Formulary (BNF) [Internet]. National Institute for Health and Care Excellence; 2025 Apr. Available from: https://bnf.nice.org.uk/drugs/

50. Baxi S, Yang A, Gennarelli RL, Khan N, Wang Z, Boyce L, et al. Immune-related adverse events for anti-PD-1 and anti-PD-L1 drugs: systematic review and meta-analysis. BMJ [Internet]. 2018 Mar 14 [cited 2025 Feb 25];360:k793. Available from: https://www.bmj.com/content/360/bmj.k793

51. Tarhini AA, Lee SJ, Hodi FS, Rao UNM, Cohen GI, Hamid O, et al. Phase III Study of Adjuvant Ipilimumab (3 or 10 mg/kg) Versus High-Dose Interferon

Alfa-2b for Resected High-Risk Melanoma: North American Intergroup E1609. J Clin Oncol. 2020 Feb 20;38(6):567–75.

52. Johnson DB, Balko JM, Compton ML, Chalkias S, Gorham J, Xu Y, et al. Fulminant Myocarditis with Combination Immune Checkpoint Blockade. New England Journal of Medicine. 2016 Nov 3;375(18):1749–55.

53. Nso N, Antwi-Amoabeng D, Beutler BD, Ulanja MB, Ghuman J, Hanfy A, et al. Cardiac adverse events of immune checkpoint inhibitors in oncology patients: A systematic review and meta-analysis. World Journal of Cardiology [Internet]. 2020 Nov 26 [cited 2025 July 14];12(11):584–98. Available from: https://www.wjgnet.com/1949-8462/full/v12/i11/584.htm

54. Amiri-Kordestani L, Moslehi J, Cheng J, Tang S, Schroeder R, Sridhara R, et al. Cardiovascular adverse events in immune checkpoint inhibitor clinical trials: A U.S. Food and Drug Administration pooled analysis. Journal of Clinical Oncology. 2018 May 20;36(15_suppl):3009–3009.

55. Salem JE, Manouchehri A, Moey M, Lebrun-Vignes B, Bastarache L, Pariente A, et al. Cardiovascular toxicities associated with immune checkpoint inhibitors: an observational, retrospective, pharmacovigilance study. The Lancet Oncology. 2018 Dec;19(12):1579–89.

56. Mahmood SS, Fradley MG, Cohen JV, Nohria A, Reynolds KL, Heinzerling LM, et al. Myocarditis in Patients Treated With Immune Checkpoint Inhibitors. Journal of the American College of Cardiology. 2018 Apr;71(16):1755–64.

57. Oren O, Yang EH, Molina JR, Bailey KR, Blumenthal RS, Kopecky SL. Cardiovascular Health and Outcomes in Cancer Patients Receiving Immune Checkpoint Inhibitors. The American Journal of Cardiology. 2020 June;125(12):1920–6.

58. Jain P, Bugarin JG, Guha A, Jain C, Shen T, Stanevich I, et al. Risk factors for myocarditis associated with immune checkpoint inhibitors using real-world clinical data. JCO [Internet]. 2020 May 20 [cited 2025 Apr 28];38(15_suppl):e15100–e15100. Available from: https://ascopubs.org/doi/10.1200/JCO.2020.38.15_suppl.e15100

59. Asnani A. Cardiotoxicity of Immunotherapy: Incidence, Diagnosis, and Management. Curr Oncol Rep [Internet]. 2018 Apr 11 [cited 2025 Feb 25];20(6):44. Available from: https://doi.org/10.1007/s11912-018-0690-1

60. Norwood TG, Westbrook BC, Johnson DB, Litovsky SH, Terry NL, McKee SB, et al. Smoldering myocarditis following immune checkpoint blockade. J Immunother Cancer. 2017 Nov 21;5(1):91.

61. Rubio-Infante N, Ramírez-Flores YA, Castillo EC, Lozano O, García-Rivas G, Torre-Amione G. Cardiotoxicity associated with immune checkpoint inhibitor therapy: a meta-analysis. European Journal of Heart Failure. 2021 Oct 29;23(10):1739–47.

62. van der Wal AC, Becker AE, van der Loos CM, Das PK. Site of intimal rupture or erosion of thrombosed coronary atherosclerotic plaques is characterized

by an inflammatory process irrespective of the dominant plaque morphology. Circulation [Internet]. 1994 Jan [cited 2025 Feb 27];89(1):36–44. Available from: https://www.ahajournals.org/doi/10.1161/01.cir.89.1.36

63. Hansson GK. Inflammation, Atherosclerosis, and Coronary Artery Disease. New England Journal of Medicine [Internet]. 2005 Apr 21 [cited 2025 Feb 27];352(16):1685–95. Available from: https://www.nejm.org/doi/full/10.1056/NEJMra043430

64. Orbay H, Hong H, Zhang Y, Cai W. Positron Emission Tomography Imaging of Atherosclerosis. Theranostics [Internet]. 2013 Nov 2 [cited 2025 Apr 27];3(11):894–902. Available from: https://www.ncbi.nlm.nih.gov/pmc/articles/PMC3841339/

65. Eriksson EE, Xie X, Werr J, Thoren P, Lindbom L. Importance of Primary Capture and L-Selectin–Dependent Secondary Capture in Leukocyte Accumulation in Inflammation and Atherosclerosis in Vivo. J Exp Med [Internet]. 2001 July 16 [cited 2025 Feb 27];194(2):205–18. Available from: https://www.ncbi.nlm.nih.gov/pmc/articles/PMC2193449/

66. Delves PJ. Roitt's Essential Immunology. Wiley-Blackwell; 2016.

67. Szabo SJ, Sullivan BM, Peng SL, Glimcher LH. Molecular Mechanisms RegulatinG Th1 Immune Responses. Annual Review of Immunology [Internet]. 2003 Apr 1 [cited 2025 Feb 27];21(Volume 21, 2003):713–58. Available from: https://www.annualreviews.org/content/journals/10.1146/annurev.immunol.21.120601.140942

68. Mach F, Schönbeck U, Bonnefoy JY, Pober JS, Libby P. Activation of Monocyte/Macrophage Functions Related to Acute Atheroma Complication by Ligation of CD40. Circulation [Internet]. 1997 July 15 [cited 2025 Feb 27];96(2):396–9. Available from: https://www.ahajournals.org/doi/10.1161/01.cir.96.2.396

69. Lyon AR, Yousaf N, Battisti NML, Moslehi J, Larkin J. Immune checkpoint inhibitors and cardiovascular toxicity. The Lancet Oncology. 2018 Sept;19(9):e447–58.

70. Daxini A, Cronin K, Sreih AG. Vasculitis associated with immune checkpoint inhibitors-a systematic review. Clin Rheumatol. 2018 Sept;37(9):2579–84.

71. Dobbin SJH, Petrie MC, Myles RC, Touyz RM, Lang NN. Cardiotoxic effects of angiogenesis inhibitors. Clinical Science. 2021 Jan 15;135(1):71–100.

72. Nykl R, Fischer O, Vykoupil K, Taborsky M. A unique reason for coronary spasm causing temporary ST elevation myocardial infarction (inferior STEMI) - systemic inflammatory response syndrome after use of pembrolizumab. Arch Med Sci Atheroscler Dis. 2017;2:e100–2.

73. Zhou YW, Zhu YJ, Wang MN, Xie Y, Chen CY, Zhang T, et al. Immune Checkpoint Inhibitor-Associated Cardiotoxicity: Current Understanding on Its Mechanism, Diagnosis and Management. Front Pharmacol [Internet].

2019 Nov 29 [cited 2025 Feb 27];10. Available from: https://www.frontiersin.org/journals/pharmacology/articles/10.3389/fphar.2019.01350/full

74. Agrawal N, Khunger A, Vachhani P, Colvin TA, Hattoum A, Spangenthal E, et al. Cardiac Toxicity Associated with Immune Checkpoint Inhibitors: Case Series and Review of the Literature. Case Reports in Oncology [Internet]. 2019 Mar 21 [cited 2025 Feb 27];12(1):260–76. Available from: https://doi.org/10.1159/000498985

75. Geisler BP, Raad RA, Esaian D, Sharon E, Schwartz DR. Apical ballooning and cardiomyopathy in a melanoma patient treated with ipilimumab: a case of takotsubo-like syndrome. J Immunother Cancer [Internet]. 2015 Dec 1 [cited 2025 Feb 27];3(1):4. Available from: https://jitc.bmj.com/content/3/1/4

76. Anderson RD, Brooks M. Apical takotsubo syndrome in a patient with metastatic breast carcinoma on novel immunotherapy. International Journal of Cardiology [Internet]. 2016 Nov 1 [cited 2025 Feb 27];222:760–1. Available from: https://www.internationaljournalofcardiology.com/article/S0167-5273(16)31687-4/abstract

77. Chen DY, Huang WK, Chien-Chia Wu V, Chang WC, Chen JS, Chuang CK, et al. Cardiovascular toxicity of immune checkpoint inhibitors in cancer patients: A review when cardiology meets immuno-oncology. Journal of the Formosan Medical Association [Internet]. 2020 Oct 1 [cited 2025 Feb 26];119(10):1461–75. Available from: https://www.sciencedirect.com/science/article/pii/S0929664619304085

78. Newman JL, Stone JR. Immune checkpoint inhibition alters the inflammatory cell composition of human coronary artery atherosclerosis. Cardiovasc Pathol. 2019;43:107148.

79. Hu YB, Zhang Q, Li HJ, Michot JM, Liu HB, Zhan P, et al. Evaluation of rare but severe immune related adverse effects in PD-1 and PD-L1 inhibitors in non-small cell lung cancer: a meta-analysis. Transl Lung Cancer Res. 2017 Dec;6(Suppl 1):S8–20.

80. Agostinetto E, Eiger D, Lambertini M, Ceppi M, Bruzzone M, Pondé N, et al. Cardiotoxicity of immune checkpoint inhibitors: A systematic review and meta-analysis of randomised clinical trials. Eur J Cancer. 2021 May;148:76–91.

81. Salem JE, Ederhy S, Dechartres A. Re: Cardiotoxicity of immune checkpoint inhibitors: A systematic review and meta-analysis of randomised clinical trials: An enigmatic discordance resolved. European Journal of Cancer [Internet]. 2021 Sept 1 [cited 2025 July 13];155:299–302. Available from: https://www.ejcancer.com/article/S0959-8049(21)00326-9/fulltext

82. C D, J A, Pm M, A D, E E, M S, et al. Cardiovascular immunotoxicities associated with immune checkpoint inhibitors: a safety meta-analysis. European heart journal [Internet]. 2021 Dec 21 [cited 2025 July 12];42(48). Available from: https://pubmed.ncbi.nlm.nih.gov/34529770/

83. D'Souza M, Nielsen D, Svane IM, Iversen K, Rasmussen PV, Madelaire C, et al. The risk of cardiac events in patients receiving immune checkpoint inhibitors: a nationwide Danish study. European Heart Journal. 2021 Apr 21;42(16):1621–31.

84. Bar J, Markel G, Gottfried T, Percik R, Leibowitz-Amit R, Berger R, et al. Acute vascular events as a possibly related adverse event of immunotherapy: a single-institute retrospective study. European Journal of Cancer. 2019 Oct;120:122–31.

85. Naqash AR, Moey MYY, Cherie Tan XW, Laharwal M, Hill V, Moka N, et al. Major Adverse Cardiac Events With Immune Checkpoint Inhibitors: A Pooled Analysis of Trials Sponsored by the National Cancer Institute—Cancer Therapy Evaluation Program. Journal of Clinical Oncology. 2022 Oct 10;40(29):3439–52.

86. Wang C, Zoungas S, Yan M, Wolfe R, Haydon A, Shackleton M, et al. Immune checkpoint inhibitors and the risk of major atherosclerotic cardiovascular events in patients with high-risk or advanced melanoma: a retrospective cohort study. Cardio-Oncology. 2022 Dec 2;8(1):23.

87. Laenens D, Yu Y, Santens B, Jacobs J, Beuselinck B, Bechter O, et al. Incidence of Cardiovascular Events in Patients Treated With Immune Checkpoint Inhibitors. JCO [Internet]. 2022 Oct 10 [cited 2025 July 11];40(29):3430–8. Available from: https://ascopubs.org/doi/10.1200/JCO.21.01808

88. Kusters PJH, Lutgens E, Seijkens TTP. Exploring immune checkpoints as potential therapeutic targets in atherosclerosis. Cardiovascular Research. 2018 Mar 1;114(3):368–77.

89. Bu D xiu, Tarrio M, Maganto-Garcia E, Stavrakis G, Tajima G, Lederer J, et al. Impairment of the Programmed Cell Death-1 Pathway Increases Atherosclerotic Lesion Development and Inflammation. Arteriosclerosis, Thrombosis, and Vascular Biology. 2011 May;31(5):1100–7.

90. Rolski F, Błyszczuk P. Complexity of TNF-α Signaling in Heart Disease. J Clin Med [Internet]. 2020 Oct 12 [cited 2025 July 14];9(10):3267. Available from: https://www.ncbi.nlm.nih.gov/pmc/articles/PMC7601316/

91. Suero-Abreu GA, Zanni MV, Neilan TG. Atherosclerosis With Immune Checkpoint Inhibitor Therapy. JACC CardioOncol [Internet]. 2022 Dec 20 [cited 2025 July 7];4(5):598–615. Available from: https://www.ncbi.nlm.nih.gov/pmc/articles/PMC9830225/

92. McKellar GE, McCarey DW, Sattar N, McInnes IB. Role for TNF in atherosclerosis? Lessons from autoimmune disease. Nat Rev Cardiol [Internet]. 2009 June [cited 2025 July 7];6(6):410–7. Available from: https://www.nature.com/articles/nrcardio.2009.57

93. Kim CW, Oh ET, Park HJ. A strategy to prevent atherosclerosis via TNF receptor regulation. FASEB J. 2021 Mar;35(3):e21391.

94. Boesten LSM, Zadelaar ASM, van Nieuwkoop A, Gijbels MJJ, de Winther MPJ, Havekes LM, et al. Tumor necrosis factor-α promotes atherosclerotic lesion progression in APOE*3-leiden transgenic mice. Cardiovascular Research [Internet]. 2005 Apr 1 [cited 2025 July 13];66(1):179–85. Available from: https://doi.org/10.1016/j.cardiores.2005.01.001

95. Fernandez DM, Rahman AH, Fernandez NF, Chudnovskiy A, Amir EAD, Amadori L, et al. Single-cell immune landscape of human atherosclerotic plaques. Nat Med. 2019 Oct;25(10):1576–88.

96. Poels K, Van Leent MMT, Boutros C, Tissot H, Roy S, Meerwaldt AE, et al. Immune Checkpoint Inhibitor Therapy Aggravates T Cell–Driven Plaque Inflammation in Atherosclerosis. JACC: CardioOncology [Internet]. 2020 Nov [cited 2024 Mar 26];2(4):599–610. Available from: https://linkinghub.elsevier.com/retrieve/pii/S266608732030212X

97. Drobni ZD, Gongora C, Taron J, Suero-Abreu GA, Karady J, Gilman HK, et al. Impact of immune checkpoint inhibitors on atherosclerosis progression in patients with lung cancer. J Immunother Cancer [Internet]. 2023 July [cited 2025 Mar 3];11(7):e007307. Available from: https://jitc.bmj.com/lookup/doi/10.1136/jitc-2023-007307

98. Dorst DCH van, Doorn L van, Mirabito Colafella KM, Manintveld OC, Hassing HC, Danser AHJ, et al. Cardiovascular toxicity of angiogenesis inhibitors and immune checkpoint inhibitors: synergistic anti-tumour effects at the cost of increased cardiovascular risk? Clinical Science. 2021 July 30;135(14):1649–68.

99. Huinen ZR, Huijbers EJM, van Beijnum JR, Nowak-Sliwinska P, Griffioen AW. Anti-angiogenic agents — overcoming tumour endothelial cell anergy and improving immunotherapy outcomes. Nature Reviews Clinical Oncology. 2021 Aug 8;18(8):527–40.

100. Food and Drug Administration. Drugs@FDA: FDA Approved Drugs [Internet]. https://www.fda.gov/media/151146/download. [cited 2023 Mar 28]. Available from: Available from https://www.accessdata.fda.gov/scripts/cder/daf/index.cfm

101. Dobbin SJH, Mangion K, Berry C, Roditi G, Basak S, Sourbron S, et al. Cardiotoxicity and myocardial hypoperfusion associated with anti-vascular endothelial growth factor therapies: prospective cardiac magnetic resonance imaging in patients with cancer. European Journal of Heart Failure. 2020 July 7;22(7):1276–7.

102. Chen XL, Lei YH, Liu CF, Yang QF, Zuo PY, Liu CY, et al. Angiogenesis Inhibitor Bevacizumab Increases the Risk of Ischemic Heart Disease Associated with Chemotherapy: A Meta-Analysis. PLoS ONE. 2013 June 20;8(6):e66721.

103. Ghatalia P, Morgan CJ, Je Y, Nguyen PL, Trinh QD, Choueiri TK, et al. Congestive heart failure with vascular endothelial growth factor receptor tyrosine kinase inhibitors. Critical Reviews in Oncology/Hematology. 2015 May;94(2):228–37.

104. Winnik S, Lohmann C, Siciliani G, von Lukowicz T, Kuschnerus K, Kraenkel N, et al. Systemic VEGF inhibition accelerates experimental atherosclerosis and disrupts endothelial homeostasis – implications for cardiovascular safety. International Journal of Cardiology. 2013 Oct;168(3):2453–61.

105. Dobbin SJH, Mangion K, Berry C, Roditi G, Basak S, McClure JD, et al. Vascular endothelial growth factor inhibitor-induced cardiotoxicity: prospective multimodality assessment incorporating cardiovascular magnetic resonance imaging. Heart [Internet]. 2025 Apr 3 [cited 2025 May 2]; Available from: https://heart.bmj.com/content/early/2025/04/03/heartjnl-2024-325535

106. Pantaleo MA, Mandrioli A, Saponara M, Nannini M, Erente G, Lolli C, et al. Development of coronary artery stenosis in a patient with metastatic renal cell carcinoma treated with sorafenib. BMC Cancer [Internet]. 2012 June 11 [cited 2025 Apr 29];12(1):231. Available from: https://doi.org/10.1186/1471-2407-12-231

107. Naib T, Steingart RM, Chen CL. Sorafenib-associated multivessel coronary artery vasospasm. Herz. 2011 June;36(4):348–51.

108. Arima Y, Oshima S, Noda K, Fukushima H, Taniguchi I, Nakamura S, et al. Sorafenib-induced acute myocardial infarction due to coronary artery spasm. Journal of Cardiology [Internet]. 2009 Dec 1 [cited 2025 Apr 29];54(3):512–5. Available from: https://www.sciencedirect.com/science/article/pii/S0914508709001191

109. Celletti FL, Waugh JM, Amabile PG, Brendolan A, Hilfiker PR, Dake MD. Vascular endothelial growth factor enhances atherosclerotic plaque progression. Nature Medicine. 2001 Apr 1;7(4):425–9.

110. Ropert S, Vignaux O, Mir O, Goldwasser F. VEGF pathway inhibition by anticancer agent sunitinib and susceptibility to atherosclerosis plaque disruption. Invest New Drugs. 2011 Dec;29(6):1497–9.

111. Neves KB, Rios FJ, Jones R, Evans TRJ, Montezano AC, Touyz RM. Microparticles from vascular endothelial growth factor pathway inhibitor-treated cancer patients mediate endothelial cell injury. Cardiovascular Research. 2019 Apr 15;115(5):978–88.

112. Faruque LI, Lin M, Battistella M, Wiebe N, Reiman T, Hemmelgarn B, et al. Systematic Review of the Risk of Adverse Outcomes Associated with Vascular Endothelial Growth Factor Inhibitors for the Treatment of Cancer. PLoS ONE. 2014 July 2;9(7):e101145.

113. Choueiri TK, Schutz FAB, Je Y, Rosenberg JE, Bellmunt J. Risk of Arterial Thromboembolic Events With Sunitinib and Sorafenib: A Systematic Review and Meta-Analysis of Clinical Trials. Journal of Clinical Oncology. 2010 May 1;28(13):2280–5.

114. Ranpura V, Hapani S, Chuang J, Wu S. Risk of cardiac ischemia and arterial thromboembolic events with the angiogenesis inhibitor bevacizumab in cancer patients: A meta-analysis of randomized controlled trials. Acta Oncologica. 2010 Jan 16;49(3):287–97.

115. Abdel-Qadir H, Ethier JL, Lee DS, Thavendiranathan P, Amir E. Cardiovascular toxicity of angiogenesis inhibitors in treatment of malignancy: A systematic review and meta-analysis. Cancer Treatment Reviews. 2017 Feb;53:120–7.

116. Scappaticci FA, Skillings JR, Holden SN, Gerber HP, Miller K, Kabbinavar F, et al. Arterial Thromboembolic Events in Patients with Metastatic Carcinoma Treated with Chemotherapy and Bevacizumab. JNCI Journal of the National Cancer Institute. 2007 Aug 15;99(16):1232–9.

117. Motzer R, Alekseev B, Rha SY, Porta C, Eto M, Powles T, et al. Lenvatinib plus Pembrolizumab or Everolimus for Advanced Renal Cell Carcinoma. New England Journal of Medicine. 2021 Apr 8;384(14):1289–300.

118. Rini BI, Plimack ER, Stus V, Gafanov R, Hawkins R, Nosov D, et al. Pembrolizumab plus Axitinib versus Sunitinib for Advanced Renal-Cell Carcinoma. New England Journal of Medicine. 2019 Mar 21;380(12):1116–27.

119. Finn RS, Qin S, Ikeda M, Galle PR, Ducreux M, Kim TY, et al. Atezolizumab plus Bevacizumab in Unresectable Hepatocellular Carcinoma. New England Journal of Medicine. 2020 May 14;382(20):1894–905.

120. Heo JH, Park C, Ghosh S, Park S, Zivkovic M, Rascati KL. A network meta-analysis of efficacy and safety of first-line and second-line therapies for the management of metastatic renal cell carcinoma. Journal of Clinical Pharmacy and Therapeutics. 2021 Feb 28;46(1):35–49.

121. Zheng Y, Dong H, Yu Y, Hu Z, Xue C, Zhang X, et al. Treatment-related adverse events of immune checkpoint inhibitors combined with angiogenesis inhibitors in advanced lung cancer: A systematic review and meta-analysis. International Immunopharmacology [Internet]. 2023 Oct 1 [cited 2025 Feb 28];123:110785. Available from: https://www.sciencedirect.com/science/article/pii/S1567576923011104

122. Inno A, Veccia A, Madonia G, Berti A, Bortolotti R, Incorvaia L, et al. Risk of cardiovascular toxicity with combination of immune-checkpoint inhibitors and angiogenesis inhibitors: a meta-analysis. Front Cardiovasc Med [Internet]. 2024 Feb 2 [cited 2025 May 11];11. Available from: https://www.frontiersin.orghttps://www.frontiersin.org/journals/cardiovascular-medicine/articles/10.3389/fcvm.2024.1309100/full

123. Crocetto F, Ferro M, Buonerba C, Bardi L, Dolce P, Scafuri L, et al. Comparing cardiovascular adverse events in cancer patients: A meta-analysis of combination therapy with angiogenesis inhibitors and immune checkpoint inhibitors versus angiogenesis inhibitors alone. Critical Reviews in Oncology/Hematology [Internet]. 2023 Aug 1 [cited 2025 May 11];188:104059. Available from: https://www.sciencedirect.com/science/article/pii/S1040842823001476

124. Rini BI, Moslehi JJ, Bonaca M, Schmidinger M, Albiges L, Choueiri TK, et al. Prospective Cardiovascular Surveillance of Immune Checkpoint Inhibitor–Based Combination Therapy in Patients With Advanced Renal Cell Cancer:

Data From the Phase III JAVELIN Renal 101 Trial. Journal of Clinical Oncology. 2022 June 10;40(17):1929–38.

125. Chitturi KR, Xu J, Araujo-Gutierrez R, Bhimaraj A, Guha A, Hussain I, et al. Immune Checkpoint Inhibitor–Related Adverse Cardiovascular Events in Patients With Lung Cancer. JACC: CardioOncology. 2019 Dec;1(2):182–92.

126. Wang Y, Cui C, Deng L, Wang L, Ren X. Cardiovascular toxicity profiles of immune checkpoint inhibitors with or without angiogenesis inhibitors: a real-world pharmacovigilance analysis based on the FAERS database from 2014 to 2022. Front Immunol. 2023;14:1127128.

127. Ren X, Deng L, Dong X, Bai Y, Li G, Wang Y. Adverse reactions of immune checkpoint inhibitors combined with angiogenesis inhibitors: A pharmacovigilance analysis of drug-drug interactions. Int J Immunopathol Pharmacol. 2024;38:3946320241305390.

128. Grover-Páez F, Zavalza-Gómez AB. Endothelial dysfunction and cardiovascular risk factors. Diabetes Research and Clinical Practice [Internet]. 2009 Apr 1 [cited 2025 July 5];84(1):1–10. Available from: https://www.sciencedirect.com/science/article/pii/S0168822708006384

129. Motz GT, Coukos G. Deciphering and Reversing Tumor Immune Suppression. Immunity [Internet]. 2013 July 25 [cited 2025 Feb 26];39(1):61–73. Available from: https://www.ncbi.nlm.nih.gov/pmc/articles/PMC3782392/

130. Gabrilovich DI, Ishida T, Nadaf S, Ohm JE, Carbone DP. Antibodies to vascular endothelial growth factor enhance the efficacy of cancer immunotherapy by improving endogenous dendritic cell function. Clin Cancer Res. 1999 Oct;5(10):2963–70.

131. Manzoni M, Rovati B, Ronzoni M, Loupakis F, Mariucci S, Ricci V, et al. Immunological effects of bevacizumab-based treatment in metastatic colorectal cancer. Oncology. 2010;79(3–4):187–96.

132. Ozao-Choy J, Ma G, Kao J, Wang GX, Meseck M, Sung M, et al. The novel role of tyrosine kinase inhibitor in the reversal of immune suppression and modulation of tumor microenvironment for immune-based cancer therapies. Cancer Res. 2009 Mar 15;69(6):2514–22.

133. Sriranjan RS, Tarkin JM, Evans NR, Le EPV, Chowdhury MM, Rudd JHF. Atherosclerosis imaging using PET: Insights and applications. Br J Pharmacol. 2021 June;178(11):2186–203.

134. Cherry SR. Fundamentals of positron emission tomography and applications in preclinical drug development. J Clin Pharmacol. 2001 May;41(5):482–91.

135. Rudd JHF, Narula J, Strauss HW, Virmani R, Machac J, Klimas M, et al. Imaging Atherosclerotic Plaque Inflammation by Fluorodeoxyglucose With Positron Emission Tomography. Journal of the American College of Cardiology. 2010 June;55(23):2527–35.

136. Slart RHJA, Glaudemans AWJM, Gheysens O, Lubberink M, Kero T, Dweck MR, et al. Procedural recommendations of cardiac PET/CT imaging:

standardization in inflammatory-, infective-, infiltrative-, and innervation (4Is)-related cardiovascular diseases: a joint collaboration of the EACVI and the EANM. European Journal of Nuclear Medicine and Molecular Imaging. 2021 Apr 27;48(4):1016–39.

137. Bucerius J, Hyafil F, Verberne HJ, Slart RHJA, Lindner O, Sciagra R, et al. Position paper of the Cardiovascular Committee of the European Association of Nuclear Medicine (EANM) on PET imaging of atherosclerosis. European Journal of Nuclear Medicine and Molecular Imaging. 2016 Apr 17;43(4):780–92.

138. Rudd JHF, Warburton EA, Fryer TD, Jones HA, Clark JC, Antoun N, et al. Imaging atherosclerotic plaque inflammation with [18F]-fluorodeoxyglucose positron emission tomography. Circulation. 2002 June 11;105(23):2708–11.

139. Vesey AT, Jenkins WSA, Irkle Agnese, Moss A, Sng Greg, Forsythe RO, et al. ^{18} F-Fluoride and ^{18} F-Fluorodeoxyglucose Positron Emission Tomography After Transient Ischemic Attack or Minor Ischemic Stroke. Circulation: Cardiovascular Imaging. 2017 Mar;10(3).

140. Rogers IS, Nasir K, Figueroa AL, Cury RC, Hoffmann U, Vermylen DA, et al. Feasibility of FDG Imaging of the Coronary Arteries. JACC: Cardiovascular Imaging. 2010 Apr;3(4):388–97.

141. Ulaner GA. Chapter 2 - FDG PET/CT Performance and Reporting. In: Ulaner GA, editor. Fundamentals of Oncologic PET/CT [Internet]. Elsevier; 2019 [cited 2025 Mar 3]. p. 5–8. Available from: https://www.sciencedirect.com/science/article/pii/B978032356869200002 8

142. Tawakol A, Fayad ZA, Mogg R, Alon A, Klimas MT, Dansky H, et al. Intensification of Statin Therapy Results in a Rapid Reduction in Atherosclerotic Inflammation. Journal of the American College of Cardiology. 2013 Sept;62(10):909–17.

143. Elkhawad M, Rudd JHF, Sarov-Blat L, Cai G, Wells R, Davies LC, et al. Effects of p38 Mitogen-Activated Protein Kinase Inhibition on Vascular and Systemic Inflammation in Patients With Atherosclerosis. JACC: Cardiovascular Imaging. 2012 Sept;5(9):911–22.

144. Tawakol A, Migrino RQ, Bashian GG, Bedri S, Vermylen D, Cury RC, et al. In Vivo 18F-Fluorodeoxyglucose Positron Emission Tomography Imaging Provides a Noninvasive Measure of Carotid Plaque Inflammation in Patients. Journal of the American College of Cardiology. 2006 Nov;48(9):1818–24.

145. Rominger A, Saam T, Wolpers S, Cyran CC, Schmidt M, Foerster S, et al. ^{18} F-FDG PET/CT Identifies Patients at Risk for Future Vascular Events in an Otherwise Asymptomatic Cohort with Neoplastic Disease. Journal of Nuclear Medicine. 2009 Oct;50(10):1611–20.

146. Emami H, Singh P, Macnabb M, Vucic E, Lavender Z, Rudd JHF, et al. Splenic Metabolic Activity Predicts Risk of Future Cardiovascular Events:

Demonstration of a Cardiosplenic Axis in Humans. JACC: Cardiovascular Imaging. 2015 Feb 1;8(2):121–30.

147. Hatt M, Krizsan AK, Rahmim A, Bradshaw TJ, Costa PF, Forgacs A, et al. Joint EANM/SNMMI guideline on radiomics in nuclear medicine. Eur J Nucl Med Mol Imaging [Internet]. 2023 Jan 1 [cited 2025 Apr 6];50(2):352–75. Available from: https://doi.org/10.1007/s00259-022-06001-6

148. Singh MK. A review of digital PET-CT technology: Comparing performance parameters in SiPM integrated digital PET-CT systems. Radiography [Internet]. 2024 Jan [cited 2024 Dec 16];30(1):13–20. Available from: https://linkinghub.elsevier.com/retrieve/pii/S1078817423001864

149. Kaneko K, Baba S, Isoda T, Ishioka H. Compared to conventional PET/CT scanners, silicon-photomultiplier-based PET/CT scanners show higher arterial 18F-FDG uptake in whole-body 18F-FDG-PET/CT. Nuclear Medicine Communications. 2021 Dec 3;42(12):1361–8.

150. Schierz JH, Sarikaya I, Wollina U, Unger L, Sarikaya A. Immune Checkpoint Inhibitor–Related Adverse Effects and 18F-FDG PET/CT Findings. Journal of Nuclear Medicine Technology [Internet]. 2021 Dec 1 [cited 2025 Mar 4];49(4):324–9. Available from: https://tech.snmjournals.org/content/49/4/324

151. Calabretta R, Hoeller C, Pichler V, Mitterhauser M, Karanikas G, Haug A, et al. Immune Checkpoint Inhibitor Therapy Induces Inflammatory Activity in Large Arteries. Circulation. 2020 Dec 15;142(24):2396–8.

152. Calabretta R, Staber PB, Kornauth C, Lu X, Binder P, Pichler V, et al. Immune Checkpoint Inhibitor Therapy Induces Inflammatory Activity in the Large Arteries of Lymphoma Patients under 50 Years of Age. Biology. 2021 Nov 19;10(11):1206.

153. Calabretta R, Beer L, Prosch H, Kifjak D, Zisser L, Binder P, et al. Induction of Arterial Inflammation by Immune Checkpoint Inhibitor Therapy in Lung Cancer Patients as Measured by 2-[18F]FDG Positron Emission Tomography/Computed Tomography Depends on Pre-Existing Vascular Inflammation. Life (Basel). 2024 Jan 19;14(1):146.

154. Rudd JHF, Myers KS, Bansilal S, Machac J, Woodward M, Fuster V, et al. Relationships Among Regional Arterial Inflammation, Calcification, Risk Factors, and Biomarkers. Circulation: Cardiovascular Imaging. 2009 Mar;2(2):107–15.

155. Li X, Heber D, Gonzalez JC, Karanikas G, Mayerhoefer ME, Rasul S, et al. Association Between Osteogenesis and Inflammation During the Progression of Calcified Plaque Evaluated by ^{18}F-Fluoride and ^{18}F-FDG. Journal of Nuclear Medicine. 2017 June;58(6):968–74.

156. Polomski EAS, Kapiteijn EW, Heemelaar JC, van der Kolk AV, Kalisvaart TM, van de Burgt A, et al. Arterial inflammation on [18F]FDG PET/CT in melanoma patients treated with and without immune checkpoint inhibitors: CHECK-FLAME I. Atherosclerosis. 2024 Nov;398:118595.

157. Kinahan PE, Fletcher JW. PET/CT Standardized Uptake Values (SUVs) in Clinical Practice and Assessing Response to Therapy. Semin Ultrasound CT MR [Internet]. 2010 Dec [cited 2025 Apr 7];31(6):496–505. Available from: https://www.ncbi.nlm.nih.gov/pmc/articles/PMC3026294/

158. Rudd JHF, Myers KS, Bansilal S, Machac J, Pinto CA, Tong C, et al. Atherosclerosis Inflammation Imaging with ^{18}F-FDG PET: Carotid, Iliac, and Femoral Uptake Reproducibility, Quantification Methods, and Recommendations. Journal of Nuclear Medicine. 2008 June;49(6):871–8.

159. Tahara N, Kai H, Ishibashi M, Nakaura H, Kaida H, Baba K, et al. Simvastatin Attenuates Plaque Inflammation. Journal of the American College of Cardiology. 2006 Nov;48(9):1825–31.

160. Tawakol A, Singh P, Rudd JHF, Soffer J, Cai G, Vucic E, et al. Effect of Treatment for 12 Weeks With Rilapladib, a Lipoprotein-Associated Phospholipase A2 Inhibitor, on Arterial Inflammation as Assessed With 18F-Fluorodeoxyglucose-Positron Emission Tomography Imaging. Journal of the American College of Cardiology [Internet]. 2014 Jan [cited 2024 Nov 14];63(1):86–8. Available from: https://linkinghub.elsevier.com/retrieve/pii/S0735109713030817

161. López-Mora DA, Carrió I, Flotats A. Digital PET vs Analog PET: Clinical Implications? Seminars in Nuclear Medicine [Internet]. 2022 May 1 [cited 2025 Apr 5];52(3):302–11. Available from: https://www.sciencedirect.com/science/article/pii/S0001299821000805

162. López-Mora DA, Carrió I, Flotats A. Digital PET vs Analog PET: Clinical Implications? Seminars in Nuclear Medicine. 2022;52(3):302–11.

163. Turkington TG. Introduction to PET Instrumentation. Journal of Nuclear Medicine Technology [Internet]. 2001 Mar 1 [cited 2025 Apr 10];29(1):4–11. Available from: https://tech.snmjournals.org/content/29/1/4

164. Bucerius J, Mani V, Moncrieff C, Machac J, Fuster V, Farkouh ME, et al. Optimizing 18F-FDG PET/CT imaging of vessel wall inflammation: the impact of 18F-FDG circulation time, injected dose, uptake parameters, and fasting blood glucose levels. Eur J Nucl Med Mol Imaging [Internet]. 2014 Feb [cited 2024 Nov 14];41(2):369–83. Available from: http://link.springer.com/10.1007/s00259-013-2569-6

165. Blomberg BA, Thomassen A, Takx RAP, Hildebrandt MG, Simonsen JA, Buch-Olsen KM, et al. Delayed 18F-fluorodeoxyglucose PET/CT imaging improves quantitation of atherosclerotic plaque inflammation: Results from the CAMONA study. Journal of Nuclear Cardiology. 2014 June 15;21(3):588–97.

166. Huet P, Burg S, Le Guludec D, Hyafil F, Buvat I. Variability and uncertainty of 18F-FDG PET imaging protocols for assessing inflammation in atherosclerosis: Suggestions for improvement. Journal of Nuclear Medicine. 2015;56(4):552–9.

167. Agatston AS, Janowitz WR, Hildner FJ, Zusmer NR, Viamonte M, Detrano R. Quantification of coronary artery calcium using ultrafast computed

tomography. Journal of the American College of Cardiology. 1990 Mar;15(4):827–32.

168. National Institute for Health Research (NIHR) Centre for Reviews and Dissemination University of York. International Prospective Register of Systematic Reviews (PROSPERO). 2023. [Internet]. [cited 2023 May 3]. Available from: Available from https://www.crd.york.ac.uk/prospero/

169. Martelli M, Ferreri AJM, Agostinelli C, Di Rocco A, Pfreundschuh M, Pileri SA. Diffuse large B-cell lymphoma. Critical Reviews in Oncology/Hematology [Internet]. 2013 Aug 1 [cited 2025 Apr 7];87(2):146–71. Available from: https://www.sciencedirect.com/science/article/pii/S1040842813000024

170. Lyon AR, Dent S, Stanway S, Earl H, Brezden-Masley C, Cohen-Solal A, et al. Baseline cardiovascular risk assessment in cancer patients scheduled to receive cardiotoxic cancer therapies: a position statement and new risk assessment tools from the Cardio-Oncology Study Group of the Heart Failure Association of the European Society of Cardiology in collaboration with the International Society. European Journal of Heart Failure. 2020 Nov 6;22(11):1945–60.

171. Barrington SF, Mikhaeel NG, Kostakoglu L, Meignan M, Hutchings M, Müeller SP, et al. Role of imaging in the staging and response assessment of lymphoma: Consensus of the international conference on malignant lymphomas imaging working group. Journal of Clinical Oncology. 2014;32(27):3048–58.

172. 2024 ESC Guidelines for the management of elevated blood pressure and hypertension | European Heart Journal | Oxford Academic [Internet]. [cited 2025 Apr 4]. Available from: https://academic.oup.com/eurheartj/article/45/38/3912/7741010?login=false

173. Lu S, Zhang P, Li C, Sun J, Liu W, Zhang P. A NIM PET/CT phantom for evaluating the PET image quality of micro-lesions and the performance parameters of CT. BMC Medical Imaging [Internet]. 2021 Nov 8 [cited 2025 Apr 4];21(1):165. Available from: https://doi.org/10.1186/s12880-021-00683-4

174. Peters SMB, van der Werf NR, Segbers M, van Velden FHP, Wierts R, Blokland K (J). AK, et al. Towards standardization of absolute SPECT/CT quantification: a multi-center and multi-vendor phantom study. EJNMMI Physics. 2019;6(1).

175. Gear JI, Cox MG, Gustafsson J, Gleisner KS, Murray I, Glatting G, et al. EANM practical guidance on uncertainty analysis for molecular radiotherapy absorbed dose calculations. European Journal of Nuclear Medicine and Molecular Imaging. 2018;45(13):2456–74.

176. Kaalep A, Sera T, Rijnsdorp S, Yaqub M, Talsma A, Lodge MA, et al. Feasibility of state of the art PET/CT systems performance harmonisation. European Journal of Nuclear Medicine and Molecular Imaging. 2018;45(8):1344–61.

177. Schaefferkoetter J, Ouyang J, Rakvongthai Y, Nappi C, El Fakhri G. Effect of time-of-flight and point spread function modeling on detectability of myocardial defects in PET. Med Phys [Internet]. 2014 June [cited 2025 Apr 7];41(6):062502. Available from: https://www.ncbi.nlm.nih.gov/pmc/articles/PMC4032408/

178. Soret M, Bacharach SL, Buvat I. Partial-volume effect in PET tumor imaging. J Nucl Med. 2007 June;48(6):932–45.

179. Westerterp M, Pruim J, Oyen W, Hoekstra O, Paans A, Visser E, et al. Quantification of FDG PET studies using standardised uptake values in multi-centre trials: Effects of image reconstruction, resolution and ROI definition parameters. European Journal of Nuclear Medicine and Molecular Imaging. 2007;34(3):392–404.

180. Witkowska-Patena E, Budzyńska A, Giżewska A, Dziuk M, Walęcka-Mazur A. Ordered subset expectation maximisation vs Bayesian penalised likelihood reconstruction algorithm in 18F-PSMA-1007 PET/CT. Ann Nucl Med [Internet]. 2020 [cited 2025 Apr 6];34(3):192–9. Available from: https://www.ncbi.nlm.nih.gov/pmc/articles/PMC7033087/

181. Chen DY, Liu JR, Tseng CN, Hsieh MJ, Chuang CK, Pang ST, et al. Major Adverse Cardiovascular Events in Patients With Renal Cell Carcinoma Treated With Targeted Therapies. JACC: CardioOncology. 2022 June;4(2):223–34.

182. Elyan BMP, Rankin S, Jones R, Lang NN, Mark PB, Lees JS. Kidney Disease Patient Representation in Trials of Combination Therapy With VEGF-Signaling Pathway Inhibitors and Immune Checkpoint Inhibitors: A Systematic Review. Kidney Medicine. 2023 July;5(7):100672.

183. Hicks KA, Mahaffey KW, Mehran R, Nissen SE, Wiviott SD, Dunn B, et al. 2017 Cardiovascular and Stroke Endpoint Definitions for Clinical Trials. Circulation. 2018 Feb 27;137(9):961–72.

184. André T, Shiu KK, Kim TW, Jensen BV, Jensen LH, Punt C, et al. Pembrolizumab in Microsatellite-Instability–High Advanced Colorectal Cancer. New England Journal of Medicine. 2020 Dec 3;383(23):2207–18.

185. Choueiri TK, Powles T, Burotto M, Escudier B, Bourlon MT, Zurawski B, et al. Nivolumab plus Cabozantinib versus Sunitinib for Advanced Renal-Cell Carcinoma. New England Journal of Medicine. 2021 Mar 4;384(9):829–41.

186. Colombo N, Dubot C, Lorusso D, Caceres MV, Hasegawa K, Shapira-Frommer R, et al. Pembrolizumab for Persistent, Recurrent, or Metastatic Cervical Cancer. New England Journal of Medicine. 2021 Nov 11;385(20):1856–67.

187. Makker V, Colombo N, Casado Herráez A, Santin AD, Colomba E, Miller DS, et al. Lenvatinib plus Pembrolizumab for Advanced Endometrial Cancer. New England Journal of Medicine. 2022 Feb 3;386(5):437–48.

188. Moore KN, Bookman M, Sehouli J, Miller A, Anderson C, Scambia G, et al. Atezolizumab, Bevacizumab, and Chemotherapy for Newly Diagnosed Stage

III or IV Ovarian Cancer: Placebo-Controlled Randomized Phase III Trial (IMagyn050/GOG 3015/ENGOT-OV39). Journal of Clinical Oncology. 2021 June 10;39(17):1842–55.

189. Motzer RJ, Penkov K, Haanen J, Rini B, Albiges L, Campbell MT, et al. Avelumab plus Axitinib versus Sunitinib for Advanced Renal-Cell Carcinoma. New England Journal of Medicine. 2019 Mar 21;380(12):1103–15.

190. Rini BI, Powles T, Atkins MB, Escudier B, McDermott DF, Suarez C, et al. Atezolizumab plus bevacizumab versus sunitinib in patients with previously untreated metastatic renal cell carcinoma (IMmotion151): a multicentre, open-label, phase 3, randomised controlled trial. The Lancet. 2019 June;393(10189):2404–15.

191. Socinski MA, Jotte RM, Cappuzzo F, Orlandi F, Stroyakovskiy D, Nogami N, et al. Atezolizumab for First-Line Treatment of Metastatic Nonsquamous NSCLC. New England Journal of Medicine. 2018 June 14;378(24):2288–301.

192. Sugawara S, Lee JS, Kang JH, Kim HR, Inui N, Hida T, et al. Nivolumab with carboplatin, paclitaxel, and bevacizumab for first-line treatment of advanced nonsquamous non-small-cell lung cancer. Annals of Oncology. 2021 Sept;32(9):1137–47.

193. Lheureux S, Matei DE, Konstantinopoulos PA, Wang BX, Gadalla R, Block MS, et al. Translational randomized phase II trial of cabozantinib in combination with nivolumab in advanced, recurrent, or metastatic endometrial cancer. Journal for ImmunoTherapy of Cancer. 2022 Mar;10(3):e004233.

194. McDermott DF, Huseni MA, Atkins MB, Motzer RJ, Rini BI, Escudier B, et al. Clinical activity and molecular correlates of response to atezolizumab alone or in combination with bevacizumab versus sunitinib in renal cell carcinoma. Nature Medicine. 2018 June 4;24(6):749–57.

195. Mettu NB, Ou FS, Zemla TJ, Halfdanarson TR, Lenz HJ, Breakstone RA, et al. Assessment of Capecitabine and Bevacizumab With or Without Atezolizumab for the Treatment of Refractory Metastatic Colorectal Cancer. JAMA Network Open. 2022 Feb 18;5(2):e2149040.

196. Nayak L, Molinaro AM, Peters K, Clarke JL, Jordan JT, de Groot J, et al. Randomized Phase II and Biomarker Study of Pembrolizumab plus Bevacizumab versus Pembrolizumab Alone for Patients with Recurrent Glioblastoma. Clinical Cancer Research. 2021 Feb 15;27(4):1048–57.

197. Redman JM, Tsai YT, Weinberg BA, Donahue RN, Gandhy S, Gatti-Mays ME, et al. A Randomized Phase II Trial of mFOLFOX6 + Bevacizumab Alone or with AdCEA Vaccine + Avelumab Immunotherapy for Untreated Metastatic Colorectal Cancer. The Oncologist. 2022 Mar 11;27(3):198–209.

198. Bonsu JM, Guha A, Charles L, Yildiz VO, Wei L, Baker B, et al. Reporting of Cardiovascular Events in Clinical Trials Supporting FDA Approval of Contemporary Cancer Therapies. Journal of the American College of Cardiology. 2020 Feb;75(6):620–8.

199. Food and Drug Administration. Cancer Clinical Trial Eligibility Criteria: Patients with Organ Dysfunction or Prior or Concurrent Malignancies Guidance for Industry [Internet]. [cited 2022 Dec 14]. Available from: Available from: https://www.fda.gov/media/123745/

200. Hanlon P, Butterly E, Shah ASV, Hannigan LJ, Wild SH, Guthrie B, et al. Assessing trial representativeness using serious adverse events: an observational analysis using aggregate and individual-level data from clinical trials and routine healthcare data. BMC Medicine. 2022 Oct 28;20(1):410.

201. Clayton ZS, Ade CJ, Dieli-Conwright CM, Mathelier HM. A bench to bedside perspective on anthracycline chemotherapy-mediated cardiovascular dysfunction: challenges and opportunities. A symposium review. Journal of Applied Physiology. 2022 Dec 1;133(6):1415–29.

202. Clayton ZS, Hutton DA, Mahoney SA, Seals DR. Anthracycline chemotherapy-mediated vascular dysfunction as a model of accelerated vascular aging. Aging and Cancer. 2021 June 22;2(1–2):45–69.

203. Rinaldi B, Romagnoli P, Bacci S, Carnuccio R, Maiuri MC, Donniacuo M, et al. Inflammatory events in a vascular remodeling model induced by surgical injury to the rat carotid artery. British Journal of Pharmacology. 2006 Jan;147(2):175–82.

204. Ridker PM, Everett BM, Thuren T, MacFadyen JG, Chang WH, Ballantyne C, et al. Antiinflammatory Therapy with Canakinumab for Atherosclerotic Disease. N Engl J Med [Internet]. 2017 Sept 21 [cited 2024 Mar 26];377(12):1119–31. Available from: http://www.nejm.org/doi/10.1056/NEJMoa1707914

205. Henriksen PA, Rankin S, Lang NN. Cardioprotection in Patients at High Risk of Anthracycline-Induced Cardiotoxicity. JACC: CardioOncology [Internet]. 2023 June [cited 2024 Mar 26];5(3):292–7. Available from: https://linkinghub.elsevier.com/retrieve/pii/S2666087323001254

206. Nidorf SM, Fiolet ATL, Mosterd A, Eikelboom JW, Schut A, Opstal TSJ, et al. Colchicine in Patients with Chronic Coronary Disease. N Engl J Med [Internet]. 2020 Nov 5 [cited 2024 Mar 26];383(19):1838–47. Available from: http://www.nejm.org/doi/10.1056/NEJMoa2021372

207. Clayton ZS, Brunt VE, Hutton DA, Casso AG, Ziemba BP, Melov S, et al. Tumor Necrosis Factor Alpha-Mediated Inflammation and Remodeling of the Extracellular Matrix Underlies Aortic Stiffening Induced by the Common Chemotherapeutic Agent Doxorubicin. Hypertension. 2021 May;77(5):1581–90.

208. Bodziock GM, Meléndez GC. Long-term QT prolongation in monkeys after doxorubicin administration at doses similar to breast cancer therapy. Front Cardiovasc Med [Internet]. 2023 Dec 12 [cited 2024 Mar 5];10:1247273. Available from: https://www.frontiersin.org/articles/10.3389/fcvm.2023.1247273/full

209. Ito S, Amioka N, Franklin MK, Wang P, Liang CL, Katsumata Y, et al. Association of NOTCH3 with Elastic Fiber Dispersion in the Infrarenal Abdominal Aorta of Cynomolgus Monkeys [Internet]. Pathology; 2023 Mar [cited 2024 Mar 5]. Available from: http://biorxiv.org/lookup/doi/10.1101/2023.03.04.530901

210. Lawal IO, Orunmuyi AT, Popoola GO, Lengana T, Mokoala KMG, Ankrah AO, et al. FDG PET/CT for evaluating systemic arterial inflammation induced by anthracycline-based chemotherapy of Hodgkin lymphoma. Medicine. 2020 Nov 25;99(48):e23259.

211. Guzik TJ, Touyz RM. Oxidative Stress, Inflammation, and Vascular Aging in Hypertension. Hypertension. 2017 Oct;70(4):660–7.

212. Guzik TJ, Hoch NE, Brown KA, McCann LA, Rahman A, Dikalov S, et al. Role of the T cell in the genesis of angiotensin II–induced hypertension and vascular dysfunction. Journal of Experimental Medicine. 2007 Oct 1;204(10):2449–60.

213. Fleenor BS. Large elastic artery stiffness with aging: novel translational mechanisms and interventions. Aging and disease. 2013 Apr;4(2):76–83.

214. Lesniewski LA, Durrant JR, Connell ML, Henson GD, Black AD, Donato AJ, et al. Aerobic exercise reverses arterial inflammation with aging in mice. American Journal of Physiology-Heart and Circulatory Physiology. 2011 Sept;301(3):H1025–32.

215. Rocca C, Pasqua T, Cerra MC, Angelone T. Cardiac Damage in Anthracyclines Therapy: Focus on Oxidative Stress and Inflammation. Antioxidants & Redox Signaling [Internet]. 2020 May 20 [cited 2024 Dec 2];32(15):1081–97. Available from: https://www.liebertpub.com/doi/10.1089/ars.2020.8016

216. Neilan TG, Quinaglia T, Onoue T, Mahmood SS, Drobni ZD, Gilman HK, et al. Atorvastatin for Anthracycline-Associated Cardiac Dysfunction: The STOP-CA Randomized Clinical Trial. JAMA [Internet]. 2023 Aug 8 [cited 2024 Apr 9];330(6):528. Available from: https://jamanetwork.com/journals/jama/fullarticle/2807988

217. Camilli M, Cipolla CM, Dent S, Minotti G, Cardinale DM. Anthracycline Cardiotoxicity in Adult Cancer Patients. JACC: CardioOncology [Internet]. 2024 Oct [cited 2024 Dec 2];6(5):655–77. Available from: https://linkinghub.elsevier.com/retrieve/pii/S2666087324002758

218. Murtagh G, Januzzi JL, Scherrer-Crosbie M, Neilan TG, Dent S, Ho JE, et al. Circulating Cardiovascular Biomarkers in Cancer Therapeutics-Related Cardiotoxicity: Review of Critical Challenges, Solutions, and Future Directions. JAHA [Internet]. 2023 Nov 7 [cited 2024 Dec 2];12(21):e029574. Available from: https://www.ahajournals.org/doi/10.1161/JAHA.123.029574

219. Ky B, Putt M, Sawaya H, French B, Januzzi JL, Sebag IA, et al. Early Increases in Multiple Biomarkers Predict Subsequent Cardiotoxicity in Patients With Breast Cancer Treated With Doxorubicin, Taxanes, and

Trastuzumab. Journal of the American College of Cardiology [Internet]. 2014 Mar [cited 2024 Dec 2];63(8):809–16. Available from: https://linkinghub.elsevier.com/retrieve/pii/S0735109713061573

220. Yu LR, Cao Z, Makhoul I, Daniels JR, Klimberg S, Wei JY, et al. Immune response proteins as predictive biomarkers of doxorubicin-induced cardiotoxicity in breast cancer patients. Exp Biol Med (Maywood) [Internet]. 2018 Feb [cited 2024 Dec 2];243(3):248–55. Available from: http://journals.sagepub.com/doi/10.1177/1535370217746383

221. Mercuro G, Cadeddu C, Piras A, Dessì M, Madeddu C, Deidda M, et al. Early Epirubicin-Induced Myocardial Dysfunction Revealed by Serial Tissue Doppler Echocardiography: Correlation with Inflammatory and Oxidative Stress Markers. The Oncologist [Internet]. 2007 Sept 1 [cited 2024 Dec 2];12(9):1124–33. Available from: https://academic.oup.com/oncolo/article/12/9/1124/6398794

222. Grover S, Leong DP, Chakrabarty A, Joerg L, Kotasek D, Cheong K, et al. Left and right ventricular effects of anthracycline and trastuzumab chemotherapy: A prospective study using novel cardiac imaging and biochemical markers. International Journal of Cardiology [Internet]. 2013 Oct [cited 2024 Dec 2];168(6):5465–7. Available from: https://linkinghub.elsevier.com/retrieve/pii/S016752731301471X

223. Gulati G, Heck SL, Røsjø H, Ree AH, Hoffmann P, Hagve T, et al. Neurohormonal Blockade and Circulating Cardiovascular Biomarkers During Anthracycline Therapy in Breast Cancer Patients: Results From the PRADA (Prevention of Cardiac Dysfunction During Adjuvant Breast Cancer Therapy) Study. JAHA [Internet]. 2017 Nov [cited 2024 Dec 3];6(11):e006513. Available from: https://www.ahajournals.org/doi/10.1161/JAHA.117.006513

224. Chaosuwannakit N, D'Agostino R, Hamilton CA, Lane KS, Ntim WO, Lawrence J, et al. Aortic Stiffness Increases Upon Receipt of Anthracycline Chemotherapy. Journal of Clinical Oncology. 2010 Jan 1;28(1):166–72.

225. Limat S, Daguindau E, Cahn JY, Nerich V, Brion A, Perrin S, et al. Incidence and risk-factors of CHOP/R-CHOP-related cardiotoxicity in patients with aggressive non-Hodgkin's lymphoma. Journal of Clinical Pharmacy and Therapeutics. 2014 Apr;39(2):168–74.

226. Szmit S, Jurczak W, Zaucha JM, Drozd-Sokołowska J, Spychałowicz W, Joks M, et al. Pre-existing arterial hypertension as a risk factor for early left ventricular systolic dysfunction following (R)-CHOP chemotherapy in patients with lymphoma. Journal of the American Society of Hypertension. 2014 Nov;8(11):791–9.

227. Bucerius J, Hyafil F, Verberne HJ, Slart RHJA, Lindner O, Sciagra R, et al. Position paper of the Cardiovascular Committee of the European Association of Nuclear Medicine (EANM) on PET imaging of atherosclerosis. European Journal of Nuclear Medicine and Molecular Imaging. 2016;43(4):780–92.

228. Joshi NV, Vesey AT, Williams MC, Shah ASV, Calvert PA, Craighead FHM, et al. 18F-fluoride positron emission tomography for identification of ruptured and high-risk coronary atherosclerotic plaques: a prospective clinical trial. The Lancet. 2014 Feb;383(9918):705–13.

229. Figueroa AL, Abdelbaky A, Truong QA, Corsini E, MacNabb MH, Lavender ZR, et al. Measurement of Arterial Activity on Routine FDG PET/CT Images Improves Prediction of Risk of Future CV Events. JACC: Cardiovascular Imaging. 2013 Dec;6(12):1250–9.

230. Salvadori J, Odille F, Verger A, Olivier P, Karcher G, Marie PY, et al. Head-to-head comparison between digital and analog PET of human and phantom images when optimized for maximizing the signal-to-noise ratio from small lesions. EJNMMI Physics [Internet]. 2020 Feb 21 [cited 2025 Mar 18];7(1):11. Available from: https://doi.org/10.1186/s40658-020-0281-8

231. Kaalep A, Sera T, Rijnsdorp S, Yaqub M, Talsma A, Lodge MA, et al. Feasibility of state of the art PET/CT systems performance harmonisation. Eur J Nucl Med Mol Imaging [Internet]. 2018 July [cited 2024 Aug 26];45(8):1344–61. Available from: http://link.springer.com/10.1007/s00259-018-3977-4

232. Emami H, Vucic E, Subramanian S, Abdelbaky A, Fayad ZA, Du S, et al. The effect of BMS-582949, a P38 mitogen-activated protein kinase (P38 MAPK) inhibitor on arterial inflammation: A multicenter FDG-PET trial. Atherosclerosis [Internet]. 2015 June [cited 2024 Nov 14];240(2):490–6. Available from: https://linkinghub.elsevier.com/retrieve/pii/S0021915015001999

233. Rudd JHF, Myers KS, Bansilal S, Machac J, Rafique A, Farkouh M, et al. 18Fluorodeoxyglucose Positron Emission Tomography Imaging of Atherosclerotic Plaque Inflammation Is Highly Reproducible. Journal of the American College of Cardiology. 2007 Aug;50(9):892–6.

234. Figueroa AL, Subramanian SS, Cury RC, Truong QA, Gardecki JA, Tearney GJ, et al. Distribution of Inflammation Within Carotid Atherosclerotic Plaques With High-Risk Morphological Features: A Comparison Between Positron Emission Tomography Activity, Plaque Morphology, and Histopathology. Circ: Cardiovascular Imaging [Internet]. 2012 Jan [cited 2024 Dec 11];5(1):69–77. Available from: https://www.ahajournals.org/doi/10.1161/CIRCIMAGING.110.959478

235. Fifer KM, Qadir S, Subramanian S, Vijayakumar J, Figueroa AL, Truong QA, et al. Positron Emission Tomography Measurement of Periodontal 18F-Fluorodeoxyglucose Uptake Is Associated With Histologically Determined Carotid Plaque Inflammation. Journal of the American College of Cardiology [Internet]. 2011 Feb [cited 2024 Nov 14];57(8):971–6. Available from: https://linkinghub.elsevier.com/retrieve/pii/S0735109710048059

236. Rankin S, Fountain C, Gemmell AJ, Quinn D, Henderson A, McClure J, et al. Arterial effects of anthracycline: structural and inflammatory assessments in non-human primates and lymphoma patients. Clin Sci (Lond). 2025 Jan 15;139(1):29–41.

237. Gear JI, Cox MG, Gustafsson J, Gleisner KS, Murray I, Glatting G, et al. EANM practical guidance on uncertainty analysis for molecular radiotherapy absorbed dose calculations. Eur J Nucl Med Mol Imaging [Internet]. 2018 Dec [cited 2024 Aug 26];45(13):2456–74. Available from: http://link.springer.com/10.1007/s00259-018-4136-7

238. Wickham H. ggplot2: Elegant Graphics for Data Analysis. Springer-Verlag New York ISBN 978-3-319-24277-4,. 2016;

239. Koo TK, Li MY. A Guideline of Selecting and Reporting Intraclass Correlation Coefficients for Reliability Research. J Chiropr Med. 2016 June;15(2):155–63.

240. Bland JM, Altman D. STATISTICAL METHODS FOR ASSESSING AGREEMENT BETWEEN TWO METHODS OF CLINICAL MEASUREMENT. The Lancet [Internet]. 1986 Feb 8 [cited 2025 Jan 30];327(8476):307–10. Available from: https://www.thelancet.com/journals/lancet/article/PIIS0140-6736(86)90837-8/fulltext

241. Tsutsui Y, Awamoto S, Himuro K, Umezu Y, Baba S, Sasaki M. Edge Artifacts in Point Spread Function-based PET Reconstruction in Relation to Object Size and Reconstruction Parameters. AOJNMB [Internet]. 2017 May [cited 2024 Dec 10];(Online First). Available from: https://doi.org/10.22038/aojnmb.2017.8802

242. Kaneko K, Baba S, Isoda T, Ishioka H. Compared to conventional PET/CT scanners, silicon-photomultiplier-based PET/CT scanners show higher arterial 18F-FDG uptake in whole-body 18F-FDG-PET/CT. Nuclear medicine communications. 2021;42(12):1361–8.

243. Ryu J, Han SA, Han S, Choi S, Moon DH, Oh M. Comparison of SUVA/V and SUVA-V for Evaluating Atherosclerotic Inflammation in 18F-FDG PET/CT. Nucl Med Mol Imaging [Internet]. 2024 Feb [cited 2025 Mar 26];58(1):25–31. Available from: https://www.ncbi.nlm.nih.gov/pmc/articles/PMC10796899/

244. Gholami S, Salavati A, Houshmand S, Werner TJ, Alavi A. Assessment of atherosclerosis in large vessel walls: A comprehensive review of FDG-PET/CT image acquisition protocols and methods for uptake quantification. J Nucl Cardiol. 2015 June;22(3):468–79.

245. Lawal IO, Mokoala KG, Popoola GO, Lengana T, Ankrah AO, Stoltz AC, et al. Impact of optimized PET imaging conditions on 18F-FDG uptake quantification in patients with apparently normal aortas. J Nucl Cardiol. 2021 Aug;28(4):1349–59.

246. Stellingwerff MD, Brouwer E, Lensen KJDF, Rutgers A, Arends S, van der Geest KSM, et al. Different Scoring Methods of FDG PET/CT in Giant Cell Arteritis. Medicine (Baltimore) [Internet]. 2015 Sept 18 [cited 2025 Mar 26];94(37):e1542. Available from: https://www.ncbi.nlm.nih.gov/pmc/articles/PMC4635818/

247. Gheysens O, Jamar F, Glaudemans AWJM, Yildiz H, van der Geest KSM. Semi-Quantitative and Quantitative [18F]FDG-PET/CT Indices for

Diagnosing Large Vessel Vasculitis: A Critical Review. Diagnostics (Basel) [Internet]. 2021 Dec 14 [cited 2025 Mar 26];11(12):2355. Available from: https://www.ncbi.nlm.nih.gov/pmc/articles/PMC8700698/

248. Saboury B, Salavati A, Hatami M, Werner T, Delbello C, Cheng G, et al. Superior vena cava as the most optimal site for background correction in quantification of atherosclerosis. Journal of Nuclear Medicine [Internet]. 2013 May 1 [cited 2025 Mar 26];54(supplement 2):2082–2082. Available from: https://jnm.snmjournals.org/content/54/supplement_2/2082

249. Lensen KJDF, Sijl AM van, Voskuyl AE, Laken CJ van der, Heymans MW, Comans EFI, et al. Variability in quantitative analysis of atherosclerotic plaque inflammation using 18F-FDG PET/CT. PLOS ONE [Internet]. 2017 Aug 11 [cited 2025 Mar 26];12(8):e0181847. Available from: https://journals.plos.org/plosone/article?id=10.1371/journal.pone.0181847

250. Johnsrud K, Seierstad T, Russell D, Revheim ME. Inter-reader agreement of 18F-FDG PET/CT for the quantification of carotid artery plaque inflammation. JRSM Cardiovascular Disease [Internet]. 2020 Jan 1 [cited 2025 Mar 26];9:2048004020980941. Available from: https://doi.org/10.1177/2048004020980941

251. Johnsrud K, Skagen K, Seierstad T, Skjelland M, Russell D, Revheim ME. 18F-FDG PET/CT for the quantification of inflammation in large carotid artery plaques. Journal of Nuclear Cardiology [Internet]. 2019 June [cited 2024 Nov 14];26(3):883–93. Available from: https://linkinghub.elsevier.com/retrieve/pii/S1071358123061883

252. Ugurel S, Röhmel J, Ascierto PA, Flaherty KT, Grob JJ, Hauschild A, et al. Survival of patients with advanced metastatic melanoma: the impact of novel therapies–update 2017. European Journal of Cancer. 2017 Sept;83:247–57.

253. Rathmell WK, Rumble RB, Van Veldhuizen PJ, Al-Ahmadie H, Emamekhoo H, Hauke RJ, et al. Management of Metastatic Clear Cell Renal Cell Carcinoma: ASCO Guideline. JCO [Internet]. 2022 Sept [cited 2025 Mar 5];40(25):2957–95. Available from: https://ascopubs.org/doi/full/10.1200/JCO.22.00868

254. Eggermont AMM, Blank CU, Mandala M, Long GV, Atkinson V, Dalle S, et al. Adjuvant Pembrolizumab versus Placebo in Resected Stage III Melanoma. New England Journal of Medicine [Internet]. 2018 May 10 [cited 2025 Mar 5];378(19):1789–801. Available from: https://www.nejm.org/doi/full/10.1056/NEJMoa1802357

255. Choueiri TK, Tomczak P, Park SH, Venugopal B, Ferguson T, Chang YH, et al. Adjuvant Pembrolizumab after Nephrectomy in Renal-Cell Carcinoma. New England Journal of Medicine. 2021 Aug 19;385(8):683–94.

256. Bacmeister L, Hempfling N, Maier A, Weber S, Buellesbach A, Heidenreich A, et al. Longitudinal Assessment of Subclinical Arterial Inflammation in Patients Receiving Immune Checkpoint Inhibitors by Sequential [18F]FDG PET Scans. Circ Cardiovasc Imaging. 2025 Feb;18(2):e016851.

257. Powles T, Tomczak P, Park SH, Venugopal B, Ferguson T, Symeonides SN, et al. Pembrolizumab versus placebo as post-nephrectomy adjuvant therapy for clear cell renal cell carcinoma (KEYNOTE-564): 30-month follow-up analysis of a multicentre, randomised, double-blind, placebo-controlled, phase 3 trial. Lancet Oncol. 2022 Sept;23(9):1133–44.

258. Slart RHJA, Slart RHJA, Glaudemans AWJM, Chareonthaitawee P, Treglia G, Besson FL, et al. FDG-PET/CT(A) imaging in large vessel vasculitis and polymyalgia rheumatica: joint procedural recommendation of the EANM, SNMMI, and the PET Interest Group (PIG), and endorsed by the ASNC. Eur J Nucl Med Mol Imaging [Internet]. 2018 July 1 [cited 2025 Jan 31];45(7):1250–69. Available from: https://doi.org/10.1007/s00259-018-3973-8

259. Management of Immune-Related Adverse Events in Patients Treated With Immune Checkpoint Inhibitor Therapy: ASCO Guideline Update | Journal of Clinical Oncology [Internet]. [cited 2025 Mar 12]. Available from: https://ascopubs.org/doi/10.1200/JCO.21.01440

260. Gotsman I, Grabie N, Dacosta R, Sukhova G, Sharpe A, Lichtman AH. Proatherogenic immune responses are regulated by the PD-1/PD-L pathway in mice. Journal of Clinical Investigation. 2007 Oct 1;117(10):2974–82.

261. Rankin S, Elyan B, Jones R, Venugopal B, Mark PB, Lees JS, et al. Cardiovascular Eligibility Criteria and Adverse Event Reporting in Combined Immune Checkpoint and VEGF Inhibitor Trials. JACC: CardioOncology [Internet]. 2024 Apr [cited 2025 May 18];6(2):267–79. Available from: https://www.jacc.org/doi/10.1016/j.jaccao.2023.12.010

262. Lee S, Kim Y, Jeon B, Kim G, Sohn J, Yoon Y, et al. Intracellular Adhesion Molecule-1 Improves Responsiveness to Immune Checkpoint Inhibitor by Activating CD8+ T Cells. Adv Sci (Weinh) [Internet]. 2023 Apr 25 [cited 2025 July 7];10(17):2204378. Available from: https://www.ncbi.nlm.nih.gov/pmc/articles/PMC10265102/

263. Troncoso MF, Ortiz-Quintero J, Garrido-Moreno V, Sanhueza-Olivares F, Guerrero-Moncayo A, Chiong M, et al. VCAM-1 as a predictor biomarker in cardiovascular disease. Biochimica et Biophysica Acta (BBA) - Molecular Basis of Disease [Internet]. 2021 Sept 1 [cited 2025 Apr 3];1867(9):166170. Available from: https://www.sciencedirect.com/science/article/pii/S0925443921001034

264. Yu J, Liu Y, Peng W, Xu Z. Serum VCAM-1 and ICAM-1 measurement assists for MACE risk estimation in ST-segment elevation myocardial infarction patients. Journal of Clinical Laboratory Analysis [Internet]. 2022 [cited 2025 Apr 4];36(10):e24685. Available from: https://onlinelibrary.wiley.com/doi/abs/10.1002/jcla.24685

265. Pérez-Medina C, Fayad ZA, Mulder WJM. Atherosclerosis Immunoimaging by Positron Emission Tomography. ATVB [Internet]. 2020 Apr [cited 2025 July 14];40(4):865–73. Available from: https://www.ahajournals.org/doi/10.1161/ATVBAHA.119.313455

266. Poels K, Schreurs M, Jansen M, Vugts DJ, Seijkens TTP, van Dongen GAMS, et al. Immuno-PET Imaging of Atherosclerotic Plaques with [89Zr]Zr-Anti-CD40 mAb—Proof of Concept. Biology [Internet]. 2022 Mar [cited 2025 July 14];11(3):408. Available from: https://www.mdpi.com/2079-7737/11/3/408

267. Kosmala A, Serfling SE, Michalski K, Lindner T, Schirbel A, Higuchi T, et al. Molecular imaging of arterial fibroblast activation protein: association with calcified plaque burden and cardiovascular risk factors. Eur J Nucl Med Mol Imaging [Internet]. 2023 Aug 1 [cited 2025 Aug 6];50(10):3011–21. Available from: https://doi.org/10.1007/s00259-023-06245-w

268. Liang S, Hou P, Chen H, Zhao R, Guo W, Hong C, et al. FAPI PET/CT Evaluation of Pulmonary Vascular and Myocardial Fibrosis in Pulmonary Arterial Hypertension. Journal of Nuclear Medicine [Internet]. 2024 June 1 [cited 2025 Aug 6];65(supplement 2):241412–241412. Available from: https://jnm.snmjournals.org/content/65/supplement_2/241412

269. Finke D, Heckmann MB, Herpel E, Katus HA, Haberkorn U, Leuschner F, et al. Early Detection of Checkpoint Inhibitor-Associated Myocarditis Using 68Ga-FAPI PET/CT. Front Cardiovasc Med [Internet]. 2021 Feb 25 [cited 2025 Feb 25];8:614997. Available from: https://www.ncbi.nlm.nih.gov/pmc/articles/PMC7946849/

270. Lou L, Detering L, Luehmann H, Amrute JM, Sultan D, Ma P, et al. Visualizing Immune Checkpoint Inhibitors Derived Inflammation in Atherosclerosis. Circ Res. 2024 Oct 25;135(10):990–1003.

271. Meletta R, Steier L, Borel N, Mu L, Keller C, Chiotellis A, et al. CD80 Is Upregulated in a Mouse Model with Shear Stress-Induced Atherosclerosis and Allows for Evaluating CD80-Targeting PET Tracers. Mol Imaging Biol [Internet]. 2017 Feb 1 [cited 2025 July 14];19(1):90–9. Available from: https://doi.org/10.1007/s11307-016-0987-0

272. Meletta R, Müller Herde A, Dennler P, Fischer E, Schibli R, Krämer SD. Preclinical imaging of the co-stimulatory molecules CD80 and CD86 with indium-111-labeled belatacept in atherosclerosis. EJNMMI Research [Internet]. 2016 Jan 4 [cited 2025 July 14];6(1):1. Available from: https://doi.org/10.1186/s13550-015-0157-4

273. Bala G, Blykers A, Xavier C, Descamps B, Broisat A, Ghezzi C, et al. Targeting of vascular cell adhesion molecule-1 by 18F-labelled nanobodies for PET/CT imaging of inflamed atherosclerotic plaques. Eur Heart J Cardiovasc Imaging. 2016 Sept;17(9):1001–8.

274. Broisat A, Hernot S, Toczek J, De Vos J, Riou LM, Martin S, et al. Nanobodies targeting mouse/human VCAM1 for the nuclear imaging of atherosclerotic lesions. Circ Res. 2012 Mar 30;110(7):927–37.

275. Thavendiranathan P, Houbois C, Marwick TH, Kei T, Saha S, Runeckles K, et al. Statins to prevent early cardiac dysfunction in cancer patients at increased cardiotoxicity risk receiving anthracyclines. Eur Heart J Cardiovasc Pharmacother [Internet]. 2023 Apr 29 [cited 2025 Aug

1];9(6):515–25. Available from: https://www.ncbi.nlm.nih.gov/pmc/articles/PMC10509566/

276. Hundley WG, D'Agostino R, Crotts T, Craver K, Hackney MH, Jordan JH, et al. Statins and Left Ventricular Ejection Fraction Following Doxorubicin Treatment. NEJM Evid [Internet]. 2022 Sept [cited 2025 Aug 1];1(9):10.1056/evidoa2200097. Available from: https://www.ncbi.nlm.nih.gov/pmc/articles/PMC9997095/

277. Chen AY, Wolchok JD, Bass AR. TNF in the era of immune checkpoint inhibitors: friend or foe? Nat Rev Rheumatol [Internet]. 2021 Apr [cited 2025 July 6];17(4):213–23. Available from: https://www.ncbi.nlm.nih.gov/pmc/articles/PMC8366509/

278. Meyer N, Lusque A, Virazels M, Filleron T, Colacios C, Montfort A, et al. 846P Triple combination of ipilimumab + nivolumab + anti-TNF in treatment naive melanoma patients: Final analysis of TICIMEL, a phase Ib prospective clinical trial. Annals of Oncology [Internet]. 2022 Sept 1 [cited 2025 July 27];33:S936–7. Available from: https://www.annalsofoncology.org/article/S0923-7534(22)02823-X/fulltext

279. Boellaard R, Delgado-Bolton R, Oyen WJG, Giammarile F, Tatsch K, Eschner W, et al. FDG PET/CT: EANM procedure guidelines for tumour imaging: version 2.0. Eur J Nucl Med Mol Imaging. 2015 Feb;42(2):328–54.

280. Boktor RR, Walker G, Stacey R, Gledhill S, Pitman AG. Reference range for intrapatient variability in blood-pool and liver SUV for 18F-FDG PET. J Nucl Med. 2013 May;54(5):677–82.

281. Wahl RL, Jacene H, Kasamon Y, Lodge MA. From RECIST to PERCIST: Evolving Considerations for PET response criteria in solid tumors. J Nucl Med. 2009 May;50 Suppl 1(Suppl 1):122S-50S.